



TECHNISCHE UNIVERSITÄT MÜNCHEN

Lehrstuhl für Experimentelle Genetik

Analyses of metabolic pathways of cellular processes in apoptosis and adipogenesis

Anna Maria Halama

Vollständiger Abdruck der von der Fakultät Wissenschaftszentrum Weihenstephan für Ernährung, Landnutzung und Umwelt der Technischen Universität München zur Erlangung des akademischen Grades eines

Doktors der Naturwissenschaften

genehmigten Dissertation.

Vorsitzende(r): Univ.-Prof. Dr. M. Klingenspor

Prüfer der Dissertation: 1. apl. Prof. Dr. J. Adamski
2. Univ.-Prof. Dr. J. J. Hauner
3. Univ.-Prof. Dr. K. Suhre (Weill Cornell Medical College in Qatar)

Die Dissertation wurde am 20.06.2013 bei der Technischen Universität München eingereicht und durch die Fakultät Wissenschaftszentrum Weihenstephan für Ernährung, Landnutzung und Umwelt am 10.10.2013 angenommen.

TABLE OF CONTENTS

| | |
|--|-----------|
| Abstract | 1 |
| Zusammenfassung | 3 |
| 1 INTRODUCTION | 6 |
| 1.1 COMPLEX DISEASES: OBESITY AND CANCER – TWENTY-FIRST CENTURY ISSUE | 6 |
| 1.1.1 <i>Obesity</i> | 6 |
| 1.1.2 <i>Cancer</i> | 9 |
| 1.1.3 <i>Apoptosis - way to cancer treatment</i> | 11 |
| 1.2 OMICS TECHNOLOGIES TOWARD RAPID DETECTION AND SUCCESSFUL PREVENTION OF COMPLEX DISEASES..... | 11 |
| 1.3 METABOLOMICS – AN OVERVIEW | 14 |
| 1.3.1 <i>Significance of ex vivo metabolic studies</i> | 15 |
| 1.3.2 <i>Challenges of metabolomics in cell culture model</i> | 16 |
| 1.4 AIM OF THE THESIS | 17 |
| 1.4.1 <i>Development of protocols for metabolite measurements in adherently growing cells</i> | 17 |
| 1.4.2 <i>Metabolic biomarkers of apoptotic cancer cell lines</i> | 18 |
| 1.4.3 <i>Adipogenesis “pathfinding” - first step toward novel biomarkers in development of obesity..</i> | 18 |
| 2 MATERIALS AND METHODS | 19 |
| 2.1 CHEMICALS AND REAGENTS | 19 |
| 2.2 KITS | 20 |
| 2.3 EQUIPMENT..... | 20 |
| 2.4 CELL CULTURE | 21 |
| 2.5 PREPARATION OF CELL CULTURE SAMPLES FOR MASS SPECTROMETRY (MS)..... | 22 |
| 2.5.1 <i>Cell preparation for new born screening assay</i> | 22 |
| 2.5.2 <i>Cell preparation for Absolute IDQ assay</i> | 22 |
| 2.6 IMPLEMENTATION OF MASS SPECTROMETRY-BASED METHODS FOR CELL CULTURE..... | 24 |
| 2.6.1 <i>Adaptation of newborn screening assay for cell culture</i> | 24 |
| 2.6.2 <i>Absolute IDQ assay for metabolite measurements in cells</i> | 25 |
| 2.7 STUDIES ON APOPTOSIS..... | 26 |
| 2.7.1 <i>Stimulation of apoptosis or necrosis</i> | 26 |
| 2.7.2 <i>Determination of cell viability my MTT assay</i> | 27 |
| 2.7.3 <i>Apoptosis detection by Caspase 3/7 assay</i> | 27 |
| 2.7.4 <i>Metabolite detection</i> | 28 |
| 2.8 STUDIES ON ADIPOGENESIS | 28 |
| 2.8.1 <i>Stimulation of adipogenesis</i> | 28 |
| 2.8.2 <i>Oil Red O assay - examination of lipid droplet accumulation</i> | 30 |

Table of contents

| | | |
|----------|---|------------|
| 2.8.3 | <i>DAPI staining – determination of cell proliferation during adipogenesis</i> | 30 |
| 2.8.4 | <i>Transcriptional analysis of adipogenesis</i> | 31 |
| 2.8.5 | <i>Analysis of adipogenesis by Western Blot</i> | 35 |
| 2.8.6 | <i>Characterization of adipogenesis by metabolomics</i> | 37 |
| 2.8.7 | <i>Characterization of adipogenesis by transcriptomics</i> | 38 |
| 2.9 | PATHWAY ANALYSIS..... | 39 |
| 3 | RESULTS | 41 |
| 3.1 | METABOLITE MEASUREMENT IN CELLS – PROTOCOLS DEVELOPMENT..... | 41 |
| 3.1.1 | <i>Optimization of new born screening assay for cell culture</i> | 41 |
| 3.1.2 | <i>Optimization of Absolute IDQ assay for cell culture approaches</i> | 43 |
| 3.1.3 | <i>Evaluation of harvesting and extraction procedures for metabolite measurements in adherent growing cells lines</i> | 45 |
| 3.2 | METABOLIC SIGNATURES OF APOPTOTIC HUMAN CANCER CELL LINES | 49 |
| 3.2.1 | <i>Staurosporine as apoptotic agent</i> | 49 |
| 3.2.2 | <i>Etoposide and 5-Fluorouracil as proapoptotic agents</i> | 58 |
| 3.2.3 | <i>Alanine and glutamate distinguish apoptotic cells regardless of treatment</i> | 62 |
| 3.3 | ADIPOGENESIS “PATHFINDING” - FIRST STEP TOWARD NOVEL BIOMARKERS IN DEVELOPMENT OF OBESITY | 63 |
| 3.3.1 | <i>Monitoring of adipogenesis by Oil Red O assay</i> | 65 |
| 3.3.2 | <i>Verification of adipogenesis by monitoring of crucial transcription factors promoting adipogenesis</i> | 67 |
| 3.3.3 | <i>Monitoring of adipogenesis by metabolomics</i> | 68 |
| 3.3.4 | <i>Monitoring of adipogenesis by transcriptomics</i> | 72 |
| 3.3.5 | <i>Pathway interferences: where metabolomics meet transcriptomics</i> | 78 |
| 3.3.6 | <i>Changes in glycerophospholipids metabolism as consequence of adipogenesis</i> | 87 |
| 4 | DISCUSSION | 102 |
| 4.1 | METABOLOMICS FOR CELL CULTURE APPROACH – ASSAY DEVELOPMENT AND OPTIMIZATION | 102 |
| 4.1.1 | <i>Adaptation of human targeted metabolomics assays for cell culture approaches</i> | 102 |
| 4.1.2 | <i>Harvesting and extraction protocols for adherently growing cells – in search for golden standard</i> | 105 |
| 4.2 | NOVEL BIOMARKERS OF APOPTOSIS DEPICTED BY METABOLOMICS – A STEP TOWARDS PERSONALIZED MEDICINE | 106 |
| 4.2.1 | <i>Staurosporine, 5-Fluorouracil and Etoposide – representatives for pro-apoptotic agents in cancer treatment</i> | 107 |
| 4.2.2 | <i>Staurosporine, 5-Fluorouracil and Etoposide affect cell viability by apoptosis induction</i> | 108 |
| 4.2.3 | <i>Newborn screening assay promising tool for metabolomics study in cancer cell line</i> | 109 |
| 4.3 | FACING ADIPOGENESIS – A STEP FORWARD IN OBESITY PREVENTION. (ADIPOGENESIS BLAMED FOR | |

| | |
|--|------------|
| OBESITY – WOULD METABOLOMICS BE A JUDGE?) | 115 |
| 4.3.1 3T3-L1 cell culture model for the study of obesity development on the metabolic level | 115 |
| 4.3.2 Adipogenesis validation | 117 |
| 4.3.3 Metabolomics reflect different stages of adipogenesis..... | 118 |
| 4.3.4 Transcriptomics reflect adipogenesis progression | 120 |
| 4.3.5 Global metabolic pathways are regulated during adipogenesis – highlighted after merging metabolomics and transcriptomics data. | 122 |
| 4.3.6 BCAA degradation is crucial for adipogenesis progression – in searching for a link to obesity 123 | |
| 4.3.7 Biogenic amines as potential biomarkers of different stages of adipogenesis..... | 125 |
| 4.3.8 Lipid metabolism and adipogenesis | 125 |
| 5 APPENDIX | 132 |
| 5.1 ABBREVIATIONS | 132 |
| 5.2 PUBLICATIONS AND PRESENTATIONS | 135 |
| 5.2.1 Original papers | 135 |
| 5.2.2 Manuscripts in preparation | 136 |
| 5.2.3 Reviews | 136 |
| 5.2.4 Poster presentations..... | 136 |
| 5.2.5 Oral presentations | 137 |
| 6 REFERENCES | 138 |
| 7 ACKNOWLEDGEMENTS | 157 |
| 8 LEBENSLAUF..... | 159 |

Abstract

Timely detection of complex chronic diseases like cancer or obesity, emerging in consequence of the interplay between genetic and environmental factors, is of great importance in patient therapy, since late diagnosis still correlates with aggravated prognosis. Therefore, technologies offering early detection, monitoring of disease progression or response to treatment are urgently required. Among all, the “omics” technology metabolomics provides a new perspective in the field of complex diseases due to its sensitivity in depicting responses of living systems to the environmental or pathophysiological stimuli. However, the metabolic profile of whole organisms, tissues or body fluids can be often influenced by several factors e. g. health conditions, aging, or life habits, and therefore metabolic studies in cell culture model could be a beneficial alternative to complement human studies.

In this work, novel applications of existing analytical methods were introduced in metabolomics to study apoptosis and adipogenesis, extending present knowledge in the field of cancer and obesity.

Apoptosis, one of the frequent targets in cancer therapies, was examined in several cancer cell lines to facilitate drug development for potential treatment. Three different pro-apoptotic agents were applied. Apoptosis was validated with detection of Caspase 3/7, known hallmark of apoptosis. The newborn screening (NBS) assay, originally used in the clinics to screen infants for inherited disorders, was adapted in this study for metabolite measurements in cell culture. Among all 42 measured metabolites, only alanine and glutamate were regulated independent of the pro-apoptotic agent used and in this study are introduced as potential novel biomarkers of apoptosis. Furthermore, changes in these metabolites may be biologically relevant because they can be connected to taurine metabolism, known to be strongly affected in apoptosis. In conclusion, novel implementation of the NBS assay for metabolomics studies in cells may provide promising strategies to improve drug screening and development, especially regarding its robustness and simplicity facilitating further application beside studies in human biofluids.

Differentiation from preadipocytes to fat cells known as adipogenesis, was analyzed in the mouse 3T3-L1 cell culture model, using transcriptomics and

metabolomics, to learn about the fundamental mechanisms of adipogenesis development and to determine potential biomarkers for obesity risk. In the study, accumulation of lipid droplets as well as a strong regulation of the transcription factors promoting adipogenesis (C/EBP α , C/EBP β and PPAR γ) was observed and proofed the adipogenic differentiation process. In the course of adipogenesis, several metabolites affiliated to different metabolic classes were found to be significantly regulated. Moreover, significantly regulated metabolites correlated with significantly regulated genes, and exhibited characteristic patterns for different stages of adipogenesis. Features with highest score were further analyzed and were linked to glycolysis, citrate cycle, steroid biosynthesis as well as the metabolism of branched chain amino acids (BCAAs), fatty acids and glycerophospholipids. Decrease of BCAAs was connected to increased expression of genes involved in the BCAA catabolic pathway. Valine and isoleucine degradation products were linked to the citrate cycle and the products of leucine catabolism to cholesterol synthesis. Among examined total fatty acids, a majority of odd chain fatty acids were found and it was hypothesized to be due to an excess of propionyl-CoA or enhanced alpha-oxidation. Fatty acid chains are further incorporated into phosphatidylcholines (PCs). Data suggested an incorporation of fatty acids chains into PCs characterized by increasing saturation levels in case of acyl-acyl side chains or by increased chain length in case of acyl-ether side chains. Decrease in phosphatidylcholines and lysophosphatidylcholines containing very long unsaturated fatty acids were connected with mead, arachidonic, and eicosapentaenoic acid, which are known as precursors of fatty acids that mediate inflammatory responses. In conclusion, metabolic pathways and molecules highlighted in this thesis, as characteristic for adipogenesis, might be potential biomarkers for obesity development and drug targets for its prevention. Moreover, identification of obesity risk in early stages of human life and its effective treatment may reduce subsequent health complications

Zusammenfassung

Die frühzeitige Erkennung komplexer chronischer Krankheiten, wie Krebs oder Fettleibigkeit, die aus dem Zusammenspiel genetischer Faktoren und Umweltfaktoren hervorgehen, ist für die Therapie von Patienten von großem Interesse. Nicht zuletzt da eine späte Diagnose immer noch mit einer schlechten Prognose einhergeht. Deswegen sind Technologien, die eine Früherkennung zulassen oder eine Kontrolle des Krankheits- oder des Behandlungsverlauf beobachten lassen, dringend notwendig. Dabei stellen die "omic"-Technologien einen neuen Ansatz im Bereich chronischer Erkrankungen dar und dabei insbesondere die Metabolomik aufgrund ihrer Sensitivität bezüglich Umwelt- oder pathophysiologischen Stimuli in lebenden Organismen. Allerdings kann das metabolische Profil eines gesamten Organismus durch verschiedenste Faktoren verfälscht werden, wie beispielsweise durch den Gesundheitszustand, das Altern oder die Lebensgewohnheiten, weswegen die Studie des Metabolismus in einem Zellkulturmodell eine nützliche Alternative zu komplementären Studien im Menschen bietet.

In dieser Arbeit wurden neuartige Anwendungen existierender Analysemethoden in der Metabolomik eingeführt, um Apoptose und Adipogenese zu untersuchen. Auf diese Weise wird der derzeitige Kenntnisstand in den Bereichen Krebs und Fettleibigkeit erweitert.

Um beispielsweise die Entwicklung eines Medikaments für eine potentielle Krebstherapie zu ermöglichen, wurde die Apoptose, eine inzwischen häufige Therapieform, in mehreren Krebszelllinien untersucht. Drei verschiedene pro-apoptotische Agenzien wurden eingesetzt. Apoptose wurde mit dem Caspase 3/7-Assay, einem anerkannten Test auf Apoptose, bestimmt. Das "newborn screening" (NBS), das in der Klinik zum Screening für Erbkrankheiten bei Kindern genutzt wird, wurde in dieser Studie dafür verwendet, um Metabolitenmessungen in der Zellkultur durchzuführen. Unter allen 42 gemessenen Metaboliten, waren nur Alanin und Glutaminsäure unabhängig vom pro-apoptotischen Agenz reguliert. Veränderungen in diesen Metaboliten könnten biologisch relevant sein, da sie mit dem Taurinstoffwechsel verbunden werden können, welcher in der Apoptose beeinträchtigt wird. Alanin und Glutaminsäure, könnten somit als potentielle Kandidaten für metabolische Biomarker in

der Apoptoseerkennung dienen.

Die neuartige Anwendung des NBS-Tests für metabolische Studien in Zellen, zeigt vielversprechende Strategien auf, um ein Medikamentenscreening und die Entwicklung eines Medikamentes zu verbessern, insbesondere im Bezug auf die leichte, spätere Anwendung in menschlichen biologischen Flüssigkeiten.

Die Differenzierung von Präadipozyten zu Fettzellen, die sogenannte Adipogenese, wurde in der Mauszelllinienmodell 3T3-L1 analysiert. Um fundamentale Mechanismen der Adipogenese zu erforschen und potentielle Biomarker für Fettleibigkeit zu identifizieren wurden transkriptomische und metabolische Technologien verwendet, Durch Nachweis der Anreicherung von Fetttröpfchen sowie eine starke Regulation der Transkriptionsfaktoren C/EBP α , C/EBP β und PPAR γ , wurde die Adipogenese verifiziert. Während der Adipogenese wurden signifikant regulierte Metabolite identifiziert, die zu unterschiedlichen metabolischen Klassen gehören. Darüberhinaus konnten diese Metabolite mit signifikant regulierten Genen korreliert werden. und wiesen charakteristische Muster für unterschiedliche Stadien der Lipogenese auf. Befunde mit höchster Signifikanz wurden nähergehend analysiert und mit der Glykolyse, dem Zitronensäurezyklus, der Steroidbiosynthese oder dem Metabolismus verzweigtkettiger Aminosäuren (BCAA), gesättigter Fettsäuren und Glykophospholipiden in Zusammenhang gebracht. Die Abnahme verzweigtkettiger Aminosäuren korrelierte mit ansteigender Expression von Genen, die in den BCAA-Katabolismus eingebunden sind. Des Weiteren konnten die Abbauprodukte von Valin und Isoleucin mit dem Zitronensäurezyklus, und das Produkt des Leucinabbaus mit der Cholesterinsynthese in Verbindung gebracht werden. Unter den gesättigten Fettsäuren wurde ein Großteil ungerader Fettsäuren gefunden und es wird angenommen, dass diese durch einen Überschuss an Propionyl-CoA oder durch Alpha-Oxidation resultieren. Fettsäureketten werden darüber hinaus in Phosphatidycholinen (PCs) eingebaut. Die Daten ließen vermuten, dass sich im Laufe der Adipogenese PCs mit niedrig gesättigten Acyl-acyl-Seitenketten und PCs mit Acylether-Seitenketten höherer Kettenlänge anreichern. Eine Abnahme von Phosphatidylcholinen und Lysophosphatidylcholinen, die sehr lange ungesättigte Fettsäure enthalten, wurden mit

Mead-, Arachidon- und Eicosapentaensäure in Verbindung gebracht, die als Vorstufen solcher Fettsäuren gelten, die den Entzündungsprozess vermitteln. Zusammenfassend lässt sich sagen, dass die metabolischen Signalwege und Moleküle, die in dieser Arbeit als Charakteristika für die Adipogenese erarbeitet wurden, als potentielle Biomarker bei der Entstehung von Fettleibigkeit gesehen werden können, ebenso wie sie als Medikamentenzielscheiben genommen werden können, um vor Fettleibigkeit zu schützen. Die Feststellung des Risikos von Fettleibigkeit in frühen Stadien und deren effektive Behandlung könnte helfen, Folgeschäden zu reduzieren.

1 INTRODUCTION

1.1 Complex diseases: obesity and cancer – twenty-first century issue

Condition of human health is a consequence of several factors including not only discrete genetic and environmental effects but also the interplay between them. The multifactorial etiology of diseases like cancer (Knox 2010), Alzheimer (Williamson, Goldman et al. 2009), obesity or type 2 diabetes (Bell, Finer et al. 2010), mostly caused by interactions between genes and factors, e.g. poor diet, lack of exercise, smoking or hazardous chemicals (Schork 1997), allows to define them as complex diseases (Schork 1997).

1.1.1 Obesity

Obesity, defined by the World Health Organization (WHO) as abnormal or excessive fat accumulation that represents a risk of health (Consultation 2000), recently reached an epidemic level by affecting nearly half a billion of the world's population (Rossner 2002), and becomes a challenge of the twenty-first century. The body mass index (BMI) is the most widely used weight-for-height measure (function of body mass and body height) (Calle and Thun 2004) for classifying and reporting human fatness (fat mass). Standard values described by the WHO, defining underweight, normal weight range, overweight, and obesity are presented in **Table 1**. Generally, overweight, obesity, and morbid obesity, characterized by the BMI ranges 25-29.9, 30.0-39.9, and ≥ 40 , respectively, are consequences of chronic imbalance between energy (calories) intake and expenditure/consumption leading to increased fat mass. The fat mass is regulated by the change of fat cell (adipocyte) size (hypertrophy) and/or number (hyperplasia). In the past, obesity was ignored as a medical issue and minimized to aesthetic and cosmetic difficulties.

Table 1 Human fatness specified in BMI described by WHO.

| BMI (kg/m ²) | WHO classification |
|--------------------------|--------------------|
| 18.5 | Underweight |
| 18.5–24.9 | Normal range |
| 25.0–29.9 | Overweight |
| 30.0–39.9 | Obesity |
| ≥ 40.0 | Morbid obesity |

However, recent studies uncover obesity as a major risk factor of chronic diseases like cardiovascular disease, hypertension, dyslipidemia, hyperglycemia, (Lavie, Milani et al. 2009) type 2 diabetes, insulin resistance (Flier 2004), (Guilherme, Virbasius et al. 2008), some cancers (Calle and Thun 2004) (colon cancer (Ma, Yang et al. 2013), breast cancer (Ligibel 2011), prostate cancer (Amling 2005)) as well as increased risk of early death (Calle, Thun et al. 1999). The epidemic of obesity was frequently connected with an “obesogenic lifestyle” based on high-energy diet and reduced physical activity. However, Stunkard *et al.* demonstrated already in 1986 in an adoption study that obesity can be also determined by genetics (Stunkard, Sorensen et al. 1986). Their study was based on 540 Danish adopted children, which were divided into four weight classes: thin, median weight, overweight and obese. The authors found strong correlation between the body-mass index of the biological parents and the children in contrast to their adoptive parents, where body-mass index relation was not observed (Stunkard, Sorensen et al. 1986). Those studies demonstrated significant contribution of genetics and marginal impact of environment to human fatness in adults. Moreover, those findings were supported by a twin study on human obesity which also showed correlation between human fatness and genetics (Stunkard, Foch et al. 1986). To summarize, obesity is caused by a disrupted energy balance determined by both genetic predisposition and environmental factors like nutrition, life style or social factors which place it into the complex diseases family (Yang, Kelly et al. 2007).

1.1.1.1 Regulation of adipogenesis – a step toward obesity comprehension

Since the explosion of global epidemic of obesity, specified by excess accumulation of white adipose tissue (WAT), has become a fact, studies on adipocyte biology began and initiated an emerging field of research (de Ferranti and Mozaffarian 2008). The number of fat cells present in an organism is mostly determined by adipogenesis (Camp, Ren et al. 2002), (Hirsch and Batchelor 1976) – a process of cell transformation from preadipocytes to fat cells. Adipogenic cell differentiation was frequently studied *ex vivo* in murine cell culture models ((Green and Meuth 1974), (Casimir, Miller et al. 1996), (Ntambi and Young-Cheul 2000)) (3T3-L1 or 3T3-F442 A) where pro-adipogenic and anti-adipogenic molecules were determined (Rosen and MacDougald 2006). **Figure 1** presents the transformation of fibroblast-like cells (preadipocytes) to mature adipocytes containing large lipid droplets and underlying transcriptional cascade, consisting of genes categorized into early, intermediate and late markers of adipogenesis. Generally a hormonal mixture serves as a stimuli for adipogenic cell differentiation, starting with an increased expression of pro-adipogenic genes including C/EBP β , C/EBP δ , and Krüppel-like factors (KLF) which further induce the expression of PPAR γ and C/EBP α present in the intermediate and late phase of cell differentiation (MacDougald and Lane 1995, Rosen and MacDougald 2006), (White and Stephens 2010). WAT primarily consisting of mature adipocytes, plays a crucial role in systemic glucose and lipid homeostasis (Rosen and Spiegelman 2006). Moreover, WAT secretes several molecules including cytokines (leptin, TNF α , and IL-6), enzymes involved in steroid metabolism (e.g. hydroxysteroid dehydrogenases like 17 β HSDs and 11 β HSD1), molecules for lipid metabolism or transport (e.g. lipoprotein lipase (LPL)), and cholesterol ester transfer protein (CETP) regulating metabolism in other tissues (Kershaw and Flier 2004). Thus, fat tissue is recently considered as endocrine organ involved in inflammation or immune response (Saltiel 2001, Desai, Beall et al. 2013). Besides, resistin, a protein secreted by adipose tissue, was pointed out as crosslink between obesity and diabetes (Steppan, Bailey et al. 2001). Therefore, studies on adipogenesis and fat cells itself could be beneficial for patients, considering development of methods for early detection of risk

and novel therapies for obesity.

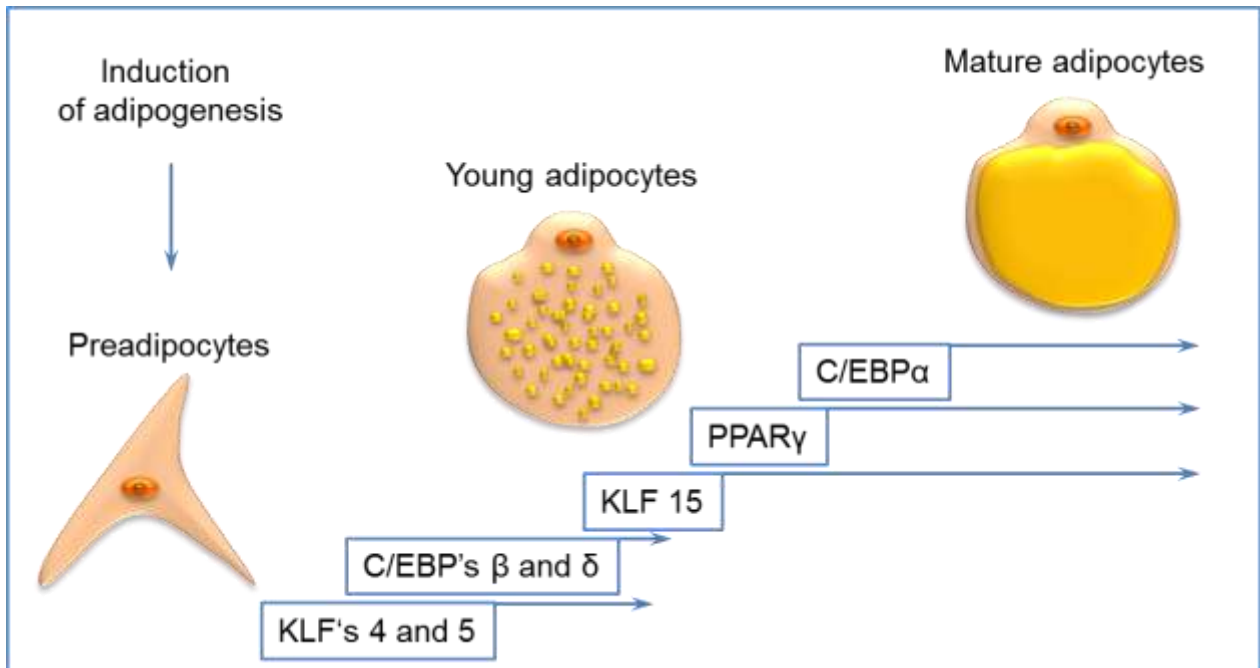


Figure 1 Fat cell development - from preadipocytes to mature adipocytes. Stimulation of preadipocytes with a hormonal mixture containing glucocorticoids and insulin (induction of apoptosis) activates transcriptional cascade promoting adipogenesis. The transcription factors including KLF' (4 and 5) and C/EBP's (β and δ) are up-regulated at the early stage of adipogenesis to activate other pro-apoptotic molecules. In turn, KLF15, PPARγ and C/EBPα once activated (at intermediate and late phase) remain expressed.

1.1.2 Cancer

Cancer is referred to as uncontrolled cell hyperproliferation with simultaneous resistance to apoptosis, can appear in any part of the body and was denoted by the WHO as a major cause of death in Europe after cardiovascular diseases (<http://www.euro.who.int/en/what-we-do/health-topics/noncommunicable-diseases/cancer>). Trends in cancer mortality estimated for 2012 are presented in **Figure 2**. Lung, intestine, and prostate cancer in men and breast, lung, and intestine cancer in women are expected to cause almost half of the total cancer deaths. Cancer development and progression occurs in dysfunctional system corrupted through interactions with environmental, immunologic, genetic, viral, or behavioral factors (Knox 2010). The complexity of cancer can be demonstrated by the example of lung cancer because the risk factors are well known. In this case tobacco smoking is the

documented factor for 90% of lung cancer incidences. However, only 10 – 15% of current or former smokers develop lung cancer (Alberg and Samet 2003).

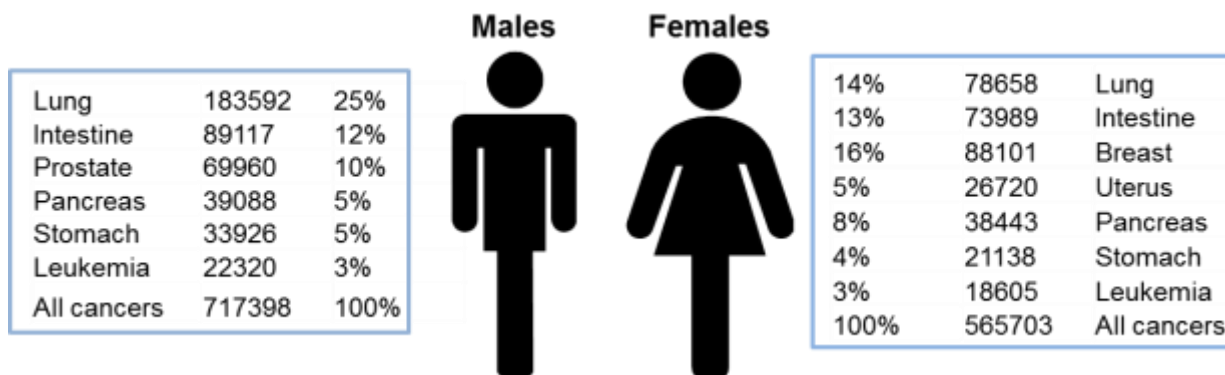


Figure 2 Number of predicted deaths caused by leading cancer types in the European Union for the year 2012 (Malvezzi, Bertuccio et al. 2012).

Paradoxically, never-smokers of all lung cancer patients, about 15% of the male and 53% of the female patients, can be also affected and develop this disease. Hence, lung cancer could be induced by other factors including “at risk” genotypes, low socioeconomic status, poor diet, arsenic exposure, or other chemical carcinogens (Knox 2010).

The hallmarks of cancer including sustained proliferative signaling, evaded growth suppressors, activated invasion and metastasis, enabled replicative immortality, induced angiogenesis, resisted cell death, avoided immune destruction, and deregulated cellular energetics, were recently reviewed by Hanahan and Weinberg (Hanahan and Weinberg 2011). Considering cancer complexity and the fact that it is a “part of the body”, it is not surprising that drug development still remains a challenge. The anticancer drug should ideally target between essential and non-essential cellular functions (Kamb, Wee et al. 2006) to be effective but not destructive. Compounds affecting essential functions, like traditional cytotoxic agents, result in high efficiency but simultaneously can damage healthy cells (Kamb, Wee et al. 2006). In contrast, drugs like the estrogen-receptor modulator tamoxifen, are better tolerated, however, limited in their efficiency (Knox 2010). Recent strategies toward novel drug development attempt to target several cellular processes including primarily apoptosis, angiogenesis, stress response or metabolism (Kamb, Wee et al. 2006).

1.1.3 Apoptosis - way to cancer treatment

Apoptosis also known as programmed cell death (PCD) or cell suicide can be induced by several exogenous or endogenous stimuli including radiation, oxidative stress, replication or recombination errors as well as environmental or therapeutic genotoxins (Rastogi and Sinha 2010). The apoptotic process is required in life cycle of healthy organisms eliminate damaged cells and to ensure diversity and unequivocal lineage development in embryogenesis (Alberts 2008). For example, in humans in average 50 – 70 billion cells undergo apoptosis daily (Li and Martin 2009). Because failure in PCD was pointed out as one of the hallmarks of cancer, apoptosis serves as a natural barrier for cancer development (Hanahan and Weinberg 2011). Hence, targeted induction of apoptosis in cancer cells, according to the phrase “the only good cancer cell is a dead cancer cell” (Gerl and Vaux 2005), is a perspective for successful therapy. Recently, molecules inducing apoptosis by inhibiting B-cell lymphoma-2 (Bcl-2) family member proteins, whose expression protects cancer cells from apoptosis (Gerl and Vaux 2005, Kang and Reynolds 2009) were applied for cancer therapies (Kang and Reynolds 2009). However, apoptosis-inducing drugs may simultaneously provoke hyperactive mitogenic signaling (critical for cell proliferation) and thereby prevent apoptosis (Hanahan and Weinberg 2011).

1.2 Omics technologies toward rapid detection and successful prevention of complex diseases

Despite increased knowledge in complex disease etiologies, early detection and effective treatment of these diseases remain 21st-century issues. Cancer pharmacology get weakest records for investigational drugs in clinic development (Kamb, Wee et al. 2006). Moreover, obesity and its co-morbidities burden the health care budgets with 2 – 8 % of the costs, which could be avoided by early detection (Zimmet, Alberti et al. 2001). Thus prospective strategies should involve technologies which could focus not only on the single gene or pathway but on the global context. Recent significant increase in development of omics technologies, referred to as large scale screening for molecules including genes (genomics), proteins (proteomics) and metabolites (metabolomics),

serves to facilitate medical science and clinical pharmacology in understanding of disease complexity, its early detection and proper treatment. A schematic general overview on omics coverage is presented in **Figure 3**.

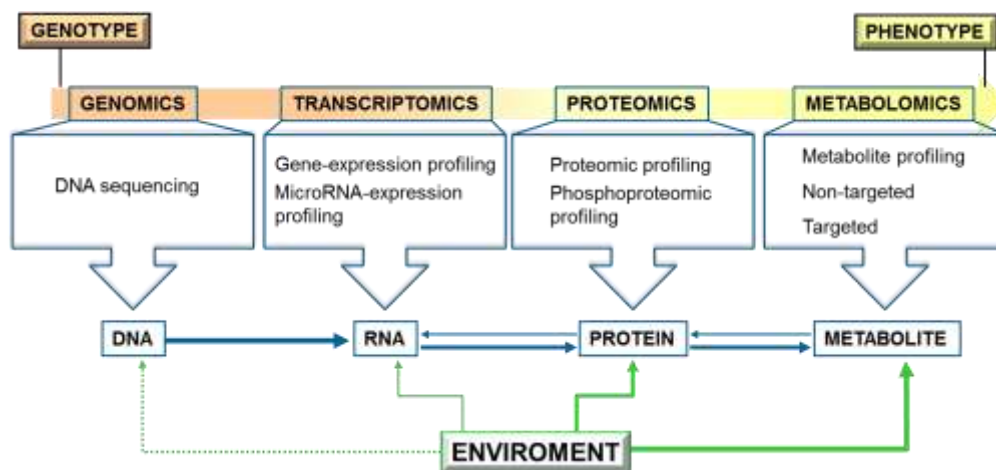


Figure 3 Coverage of omics technologies. Influence of environment on different molecule classes (DNA, RNA, protein and metabolite) is proportional to the green arrow intensity. Methods of detection required for each of the molecules are presented in the big boxes and the technologies enabling detection of a large number of these molecules are depicted above. The relation of “omics” levels is represented by colors. For example genomics is stronger related to genotype (depicted in orange) and metabolomics to phenotype (depicted in yellow).

Genomics, a systemic study of the genome (total DNA of a given species), addresses analyzes of gene functions, relationships and their combined influence on the organism’s growth and development (Griffiths 2000). DNA sequencing, a technology used by genomics, enables the identification of gene sequences but can be used also to find genetic variations between people (copy number variation (CNV), deletions and insertions (indels) and single nucleotide polymorphisms (SNP’s) (Adamski 2012)), associated with diversity in population and different predisposition to diseases. The SNP’s are most frequently implemented for homogeneity testing, pharmacogenetic studies, or detection of diseases (Shastry 2002, Altshuler, Daly et al. 2008). However, genomics is mostly limited by a fixed genome (except mutations) and identical genetic information presented by each cell composing an organism independent of physiological and developmental conditions (static nature of the genome). In turn transcriptomics, the study on the transcriptome (complete set of RNA transcripts in the organism), enables monitoring of actively expressed genes (gene expression patterns) under given

conditions. Transcriptomics, until lately preliminary based on microarray technology, is broadly implemented to study gene functions, regulatory pathways and disease mechanisms crucial for the determination and validation of novel drug targets (Skena, Shalon et al. 1995, Asyali, Colak et al. 2006). Nevertheless, the mRNA is not the final product and it's further translated into proteins. Furthermore, each transcript can be differently spliced and lead to various proteins. Hence, the proteins, key structural and functional compounds of each living system, can provide additional information on the state of an organism. Comprehensive analyzes of proteins concerning their chemical modifications (phosphorylation, acylation or methylation) after synthesis, can be achieved with proteomics, the study on the proteome (complete set of proteins in the examined system) (Yanagida 2002). Proteomics facilitated by X-ray crystallography, nuclear magnetic resonance (NMR), mass spectrometry or two-dimensional gel electrophoresis can determine proteins structure, networks and functions (Liebler 2002). Small molecule composition (metabolites below 1500 Da) of biological system is determined by the sum of its genetic features, regulation of gene expression, protein abundance and environmental influence (Artati, Prehn et al. 2012). Therefore, metabolomics (global study on metabolites) has its value in the proximity to the molecular phenotype of a biological sample (Fiehn, Kopka et al. 2000). Metabolomics enables metabolic characterization of an organism due to the monitoring of variable biochemical pathways under specific conditions (Roux, Lison et al. 2011, Imaizumi February 10, 2012). Its implementation in clinical setups for the identification of disease states or for monitoring of therapy efficiency was found to be beneficial (Hunter 2009, Spratlin, Serkova et al. 2009).

Nucleic acids as well as proteins and metabolites could be used to determine conditions of an organism and therefore can serve as biomarkers indicating disease progression or response to the treatment (Goodacre 2005). Implementation of omics technologies has so far beneficial impact on the understanding and monitoring of complex diseases. Genome wide association studies (GWAS), profitably contributing in the complex diseases field since 8 years (Ku, Loy et al. 2010), enables determination of hundreds of disease risk loci (Hindorff, Sethupathy et al. 2009). However, gene-environment interactions are poorly detected by GWAS and in consequence result in a gap between

a genotype and a phenotype (Gieger, Geistlinger et al. 2008). Recently, Adamski (Adamski 2012) suggested to overcome the limitations of GWAS by adding metabolomics information to the studies (mGWAS). Genomics, proteomics and metabolomics were implemented in medical practice regarding diagnosis, prevention and perspectives. For example, proteomics was successfully implicated in neurodegenerative diseases like Alzheimer (Rodolfo, Ciccocanti et al. 2010) or breast cancer (Misek and Kim 2011). In the recent years, metabolomics alone reached a strong position in diagnosis and prevention through its involvement in infants screening for inborn errors with more than 3 million infants screened worldwide and 500 confirmed disorders (Chace, Kalas et al. 2003). Moreover, recent studies suggest distinct relevance of metabolomics in type 2 diabetes (Ferrannini, Natali et al. 2012) and obesity (Wahl, Yu et al. 2012) research.

1.3 Metabolomics – an overview

The term metabolome (Oliver, Winson et al. 1998) covers all low molecular mass compounds (metabolites) in a biological system (cell, tissue, and organism). The dynamic changes in metabolome composition, a result of environmental stimuli or pharmaceutical treatment, are studied by metabolomics. For metabolite detection and quantification several technologies were applied. In the early stages, metabolite measurements were performed without previous fractionation (direct analysis) with nuclear magnetic resonance (NMR), Fourier transform infrared (FT-IR) spectroscopy, Raman spectroscopy or mass spectrometry (MS) (Artati, Prehn et al. 2012). However, direct analysis provide low resolution and was later improved by implementation of separation steps including gas chromatography (GC), multidimensional gas chromatography (GC x GC), liquid chromatography (LC), high performance liquid chromatography (HPLC) or ultra-high performance liquid chromatography (UPLC).

Metabolomics can be variously applied to target the aim of the studies. Metabolic profiling provides insight into metabolite composition with simultaneous identification of novel compounds. This approach, based mostly on GC-MS, NMR, LC-FT-ICR or UPLC-MS techniques, results in a very high mass resolution but low sample throughput (Griffiths, Karu et al. 2007). The non-targeted metabolomics, frequently based on both

GC-MS and LC-MS, provides information on the global metabolic composition. High sample throughput with relative large number of quantified metabolites can be achieved (Artati, Prehn et al. 2012). In turn, targeted-metabolomics, reaching very high sample throughput, is applied to determine and quantify changes in pre-selected metabolites (Griffiths, Koal et al. 2010). Targeted-metabolomics can be specified toward the study of particular component classes like lipids (lipidomics) (Wenk 2005, Griffiths and Wang 2009), glycome (carbohydrates in cells) (glycomics) (Ajit, Richard et al. 2009, Service 2012, Fujitani, Furukawa et al. 2013) or steroids (steromics) (Ceglarek, Shackleton et al. 2010). This approach is used preliminary in diagnostics and is based on LC-MS, GC-MS or flow injection analysis (FIA)-MS (Weljie, Newton et al. 2006).

1.3.1 Significance of *ex vivo* metabolic studies

Despite successful implementation of metabolomics in human population studies (Beckonert, Keun et al. 2007), (Wang-Sattler, Yu et al. 2008), (Suhre, Meisinger et al. 2010) resulting in the discovery of novel biomarkers for numerous diseases (Sreekumar, Poisson et al. 2009), (Tukiainen, Tynkkynen et al. 2008), several questions regarding properties and functions of different cell types under different conditions, remain open. This issue cannot be solved solely by metabolic analysis of human bio fluids (urine, plasma or serum) due to their complexity and therefore *ex vivo* experiments are required (Cuperlovic-Culf, Barnett et al. 2010). Metabolomics of cultured cells is essential for comprehensive understanding of cellular processes. For example metabolite monitoring of adipogenesis can be beneficial for understanding development of obesity, or analyzing apoptotic and necrotic cells can be valuable for anti-cancer drug development. Moreover, cellular metabolomics complement human studies in term of understanding the mechanism of many diseases and enables appropriate pharmacology for their treatment (Khoo and Al-Rubeai 2007). The advantages of the implementation of cultured cells as models for metabolic studies are presented **Figure 4** (Cuperlovic-Culf, Barnett et al. 2010)).

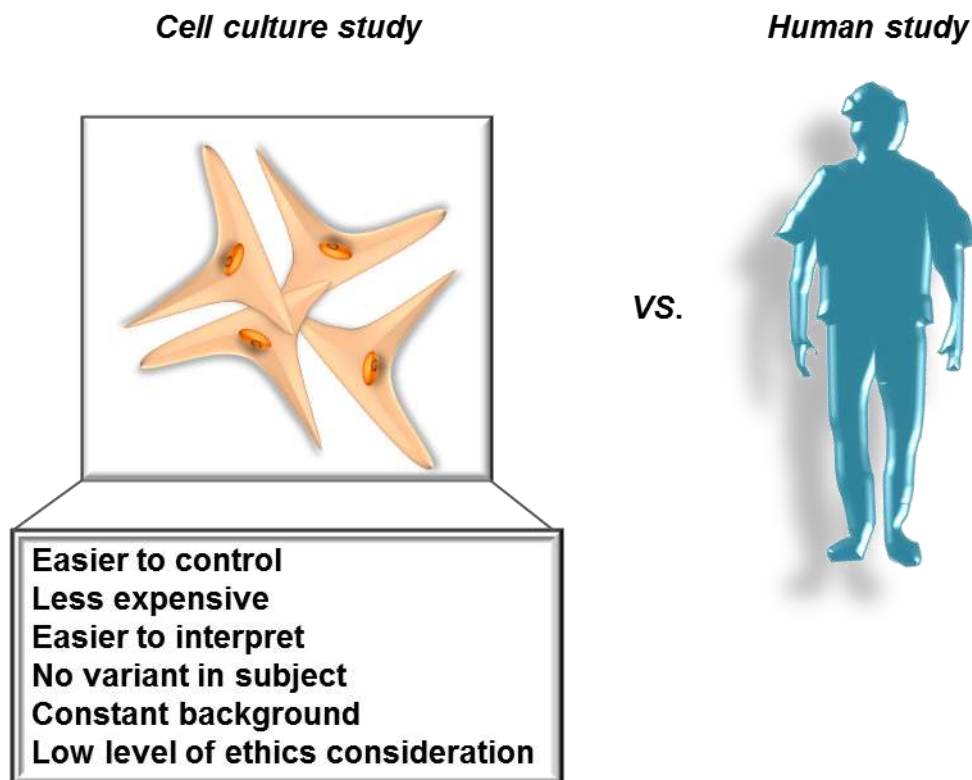


Figure 4 Advantages of implementation of cell culture as model for metabolomics studies.

1.3.2 Challenges of metabolomics in cell culture model

Metabolomics of human bodily fluids have to deal with determination of indicative metabolites (biomarkers) for given process, analysis and prediction of metabolic pathways and cross-talks between them as well as determination of drug action and mechanisms of diseases (Artati, Prehn et al. 2012). Studies on cell culture metabolism should additionally reflect cell quenching (Sellick, Hansen et al. 2009), (Teng, Huang et al. 2009), harvesting (Danielsson, Moritz et al. 2010), extraction (Ritter, Genzel et al. 2008), variability of growth medium and differential rates of cell proliferation (Cuperlovic-Culf, Barnett et al. 2010). Cell quenching (arresting of cellular metabolic activity) is essential for both evaluation of cellular background and distinguishing between samples. Hence, optimal quenching methods should rapidly stop the cellular process without affecting of cellular metabolites at the same time. Cell harvesting is more complex in case of adherent growing cells, where cell detachment is a challenging issue.

Application of trypsin as a standard method results in cell membrane damage and leakage of metabolites (Danielsson, Moritz et al. 2010). Furthermore, the appropriate selection of extraction solvents creates difficulties concerning their selectivity towards certain molecule classes like, e.g. polar solvents badly extract lipids. Thus, all of those factors have influence on the variance in the parameters of interest and therefore are fundamental considerations for each experimental design using cell culture for metabolomics study (Cuperlovic-Culf, Barnett et al. 2010).

1.4 Aim of the thesis

The overarching aim of this thesis was to extend the knowledge in the research area of complex diseases like cancer and obesity by studying metabolic pathways affected during apoptosis and adipogenesis, which are crucial cellular processes in the pathogenesis of referred diseases. To reach the aim, a specific assay for studying metabolomics in cell culture should be developed in the first step. Subsequently, the assay should be used to analyze the metabolic patterns of apoptotic cancer cell lines to determine novel biomarkers of apoptosis. In another aim, the process of adipogenic cell differentiation should be examined by combining metabolomic and transcriptomic techniques to find characteristically regulated metabolic pathways, which may lead to understanding of an interplay between adipogenesis, obesity and its co-mortalities and facilitate their prevention. A more detailed description of the single aims is given in the following text.

1.4.1 Development of protocols for metabolite measurements in adherently growing cells

Although sample preparation is crucial for metabolomics, little is known about the processing of adherently growing cells for the study of small molecules composition with LC/MS techniques. The main objective of this part of the work was therefore to develop and standardize an affordable system for studying metabolomics in adherently growing cells. The harvesting and extraction protocols should be developed and optimized to be compatible with two different targeted metabolomics assays, the newborn screen (NBS)

assay of Chromsystems and the Absolute IDQ kit assays of Biocrates. Both, the NBS assay, originally used in diagnostics for metabolite measurements in blood spots samples (Rashed, Bucknall et al. 1997, Baumgartner, Bohm et al. 2004), as well as the Absolute IDQ p180 kit, up to now used for metabolites measurement in human bodily fluids and tissues (Gieger, Geistlinger et al. 2008, Römisch-Margl, Prehn et al. 2012), should be applied on cell culture samples.

1.4.2 Metabolic biomarkers of apoptotic cancer cell lines

Considering the mortality rate caused by cancer and the poor records of drugs in clinical development (Kamb, Wee et al. 2006), the evaluation of novel diagnostic tools for drug screening in cell culture, based on metabolomics, should be investigated. Because programmed cell death is one of the frequent targets in cancer therapies, the main goal of this project was to determine novel biomarkers of apoptosis using robust analytical assays to facilitate cancer diagnostic and drug treatment monitoring. To find metabolic alterations indicative for apoptosis, known pro-apoptotic drugs (staurosporine, etoposide and 5-fluorouracil), commonly used in cancer therapies, should be applied to induce apoptosis in different cell lines. Changes in small molecules levels should be monitored with the NBS assay.

1.4.3 Adipogenesis “pathfinding” - first step toward novel biomarkers in development of obesity

Up to now, obesity is diagnosed *post factum*, when the patient’s body mass index is already higher than 30 kg/m². Development and adipogenesis progression cannot be monitored with present technologies. Therefore, to prevent overweight, biomarkers indicating obesity risk already at an early stage are desired. This part of the study aimed to examine adipogenesis processes in a cell culture model by applying metabolomics and transcriptomics as analysis tools. Combining the data of both omics technologies in the data evaluation should lead to new findings on adipogenesis pathways and finally to identification of biomarker candidates for patients with obesity risk.

2 MATERIALS AND METHODS

2.1 Chemicals and reagents

| Substance | Manufacturer |
|--|--------------------|
| 0.5% Trypsin EDTA | GIBCO Invitrogen |
| 3-Isobutyl-1-methylxanthine (IBMX) | Sigma |
| 5-Fluorouracil | Sigma |
| Agarose | Biozym Scientific |
| DAPI | Sigma |
| Dexamethasone | Sigma |
| DMEM High Glucose (4.5 g/L) | PAA |
| Ethanol | Merck |
| Ethylenediaminetetraacetic acid (EDTA) | Promega |
| Etoposide | Sigma |
| Fetal Bovine Serum (FBS) | PAA |
| Formaldehyde 37% | Sigma |
| Glycerol | Applichem |
| Insulin | Sigma |
| Isopropanol | Merck |
| Methanol | Merck |
| MgCl ₂ | Roth |
| Milchpulver | Roth |
| MilliQ H ₂ O | Millipore |
| Oil Red O | Sigma |
| Penicillin/Streptomycin | GibcoBRL |
| Power SYBR Green PCR Mastermix | Applied Biosystems |
| RPMI | PAA |
| SDS | Serva |

| Substance | Manufacturer |
|---------------------|--------------|
| Staurosporine | Sigma |
| TEMED | Sigma |
| Thiazolylblau (MTT) | Roth |
| Tris | AppliChem |

2.2 Kits

| Kits | Manufacturer |
|-------------------------------------|---------------------------|
| 5500 MassChro® (NBS assay) | Chromsystems |
| Absolute IDQ P150 & P180 | Biocrates Life Science AG |
| Caspase 3/7 | Promega |
| Expression BeadChip MouseRef-8 v2.0 | Illumina |
| First strand cDNA synthesis | Fermentas |
| RNeasy Mini kit | Qiagen |

2.3 Equipment

| Hardware/Material | Manufacturer |
|------------------------------------|---------------|
| API 4000 Qtrap | AB Sciex |
| Filter paper | Whatman |
| 10% TGX Precast gel | Bio-Rad |
| BioVision gel documentation system | PeqLab |
| Cell scraper | Sarstedt |
| Centrifuge | Rotolavit |
| CO2 incubator | SANYO |
| Cryolys, cooling system | PeqLab |
| DGU-20A3 degasser | Shimadzu |
| DGU-20A5 degasser | Shimadzu |
| FCV-12AH switching valve | Shimadzu |
| Fusion FX7 | VilberLourmat |
| GENiosPro plate reader | Tecan |

| Hardware/Material | Manufacturer |
|--|----------------------------|
| Hamilton ML Star robotics system | Hamilton Bonaduz AG |
| HiScan reader | Illumina |
| Horizontal electrophoresis system | Bio-Rad |
| Laminar flow safety cabinet | Microflow |
| Microscope Axiovert 40 CFL | Zeiss |
| Mini PROTEAN III electrophoresis cell | Bio-Rad |
| NanoDrop ND-1000 spectrophotometer | PeqLab |
| Plate reader SAFIRE II | Tecan |
| Plate Rotors Centrifuge Rotana 46 RSC | Hettich |
| Precell lysing kit glass VK01 | PeqLab |
| Precell lysing kit glass/ceramic SK38 | PeqLab |
| Precellys24 homogenizer | PeqLab |
| SIL-20AC autosampler | Shimadzu |
| TaqMan 7900HT cycler | Applied Biosystems |
| Trans-Blot SD - Semi Dry Transfer Cell | Bio-Rad |
| Ultravap nitrogen evaporator | Porvair Sciences |
| Uniequip speed-vac | Laborgerätebau Martinsried |
| UV/Vis spectrophotometer DU530 | Beckman Coulter |

2.4 Cell culture

All cultured cells were grown at 37°C and 5% CO₂ in a humidified atmosphere in SANYO Electric Biomedical incubators. All laboratory works involving cell cultures was performed in a laminar flow safety cabinet. HEK 293 (human embryonic kidney) and HepG2 (human hepatocellular carcinoma) cells purchased from the German collection of microorganisms and cell culture (DSMZ), and 3T3-L1 (murine preadipocytes) from the American Type Culture Collection (ATCC) were grown in DMEM medium supplemented with 10% fetal bovine serum (FBS), 100 IU / mL penicillin and 100 µg / mL streptomycin. Human prostate adenocarcinoma PC3 (DSMZ) and human breast adenocarcinoma MCF7 cells (kindly provided by Dr. T. Penning, Department of Pharmacology, University of Pennsylvania, Philadelphia, USA) were cultivated in growth medium RPMI 1640 supplemented with 10% fetal bovine serum (FBS), 100 IU / mL penicillin and

100 µg / mL streptomycin. Cells sub-cultured not higher than passage 12 were used for all experiments.

2.5 Preparation of cell culture samples for mass spectrometry (MS)

2.5.1 Cell preparation for new born screening assay

HEK 293, HepG2, PC3 and MCF7 cells were seeded at a density of 2×10^5 cells/ well in 12-well plates. Adherent cells were washed twice with phosphate-buffered saline (PBS) and scraped off the plate wells (floating cells were collected from medium by centrifugation and washed as well twice with PBS. For quenching and metabolite extraction combined cells were mixed with 300 µL of 20% MetOH at -20 °C, pipetted into 4 °C precooled vials containing glass beads (Precellys) and homogenized three times for 20 s at 5500rpm with the homogenizer Precellys24 (PeqLab) at 4 °C. Procedures for metabolite extraction from tissue samples were previously described (Römisch-Margl, Prehn et al. 2012). Homogenized samples were further centrifuged for 10 min at 10 °C at 18,000 x g and the supernatants were used for determination of metabolite composition with the Newborn Screen (NBS) assay (see subsection 2.6.1)

2.5.2 Cell preparation for Absolute IDQ assay

The Absolute IDQ assay (Biocrates AG) was used for both: optimization of protocols for metabolite measurements in cultured cells (p150) and metabolomics studies of adipogenesis (p180). The optimization of protocols was carried out after cells were seeded at a density of 1×10^6 cells/ well in 6-well plates, grown for indicated periods and harvested by trypsinization or scraping off the plate wells.

Trypsinized cells: after growth medium was removed from the well, cells were washed twice with PBS and incubated for 1 min with 0.5 mL trypsin / well at 37 °C. Detached

cells were resuspended in 1.5 mL of growth medium and centrifuged. The supernatant was removed and cell pellet was washed twice with 2 mL PBS. After PBS was aspirated, the cell pellet was mixed with 350 μ L of ice-cold extraction solvents (water or 40% MeOH or 80% MeOH). Extraction and homogenization procedures were carry out in homogenizer Precellys24 (PeqLab) at 4 °C (cells homogenized three times for 20 s at 5500 rpm) after cells were placed into precooled vials containing glass - ceramic beads (Precellys). Homogenized samples were further centrifuged for 10 min at 10 °C at 18,000 x g and the supernatant was used for determination of metabolite composition with Absolute IDQ assay (see subsection **2.6.2**).

Scraped cells: after growth medium was removed from the well, cells were washed twice with PBS. The PBS was aspirated and cells were scraped of the well with 350 μ L of ice cold extraction solvent (water or 40% MeOH or 80% MeOH) and transferred into precooled vials containing glass - ceramic beads (Peqlab). Extraction and homogenization procedure was performed like in case of trypsinized cells.

Metabolomics studies of adipogenesis were performed after cells were seeded at a density of 0.8×10^5 cells/ well in 6-well plates in 2 mL medium and grown for indicated periods. Cell quenching and extraction was performed subsequently by cell scrapping with 350 μ L of 80% MeOH (at -20 °C) after conditioned medium was removed and cells were washed twice with PBS buffer (37 °C). The suspension was transferred into precooled vials containing glass - ceramic beads (Peqlab) and were subsequently extracted and homogenized in homogenizer Precellys24 (PeqLab) at 4 °C (cells homogenized three times for 20 s at 5500 rpm). After homogenization samples were centrifuged for 10 min at 10 °C at 18,000 x g and the supernatant was used for determination of metabolite composition with Absolute IDQ assay (see subsection **2.6.2**).

2.6 Implementation of mass spectrometry-based methods for cell culture

2.6.1 Adaptation of newborn screening assay for cell culture

The Newborn screening (NBS) assay kit from Chromsystems, developed for the quantification of 42 metabolites (amino acids and acylcarnitines) from blood samples was adapted for cell culture approaches. The optimization procedures were performed using cell culture growth medium DMEM, for which amino acid concentrations were declared by manufacturer. In the first experiment, according to the standard NBS assay procedure, 1 mL of DMEM was spotted onto filter paper (Whatman 10538018) and left until dry. Disks with diameter of 3 mm (corresponds to about 3.5 μ L of sample) were cut out of the spot center and placed into 96 well plate cavities. In simultaneous experiment, blank filter paper disks (with diameter of 3 mm) were placed into the 96 well plates. 3.5 μ L of DMEM samples were applied directly onto the blank filter papers and left until dry. Monitoring of metabolite composition in cell extracts was performed with the NBS assay after 3.5 μ L of the extracts (prepared as described in subsection **2.5.1**) were applied onto blank filter paper spots in 96 well plates as previously described. This procedure is already published (Halama, Moller et al. 2011).

Metabolite detection was performed according to the 5500 MassChro® (NBS assay) instructions. Briefly, the dried filter paper spots were extracted for 20 minutes with 200 μ L MeOH containing isotopically labeled amino acids and acylcarnitines as internal standards. The extraction solvent was evaporated at 60 °C and samples were derivatized for 18 minutes at 72 °C with 60 μ L of derivatization reagent. The reconstitution solvent (100 μ L) was added, after evaporation of derivatization reagent, and mixed with samples for 10 minutes at room temperature (RT). The concentration of amino acids and acylcarnitines was measured using FIA - MS/MS on a 4000 QTRAP, (AB Sciex). The reconstituted samples were directly injected (10 μ L) using flow injection analysis (FIA) into the mass spectrometer and 42 metabolites were assayed in total analysis time of 1.7 min per sample. Derivatized amino acids were assayed by neutral

loss scan. Other amino acids include glycine, ornithine, arginine and citrulline were detected by multiple reaction monitoring (MRM) and the carnitines by precursor ion ($m/z = 85+$) scan. All metabolites were analyzed in positive ion mode. Data evaluation was performed with ChemoView software (AB Sciex). Concentration of metabolites in cell extracts is given in μM .

2.6.2 Absolute IDQ assay for metabolite measurements in cells

Adaptation of the Absolute IDQ assay, originally developed for metabolite measurements in human plasma (Griffin and Kauppinen 2007, Altmaier, Ramsay et al. 2008, Bogumil, Koal et al. 2008), for metabolite measurements in cells was performed by applying different volumes (20 μL , 40 μL and 60 μL) of 3T3-L1 cell extracts (prepared as described in subsection 2.5.2) into a Absolute IDQ p150 kit plate.

Metabolite alteration during adipogenesis was monitored with Absolute IDQ p180 after application of 20 μL of cell extracts (obtained after 80% MeOH extraction) or 10 μL of conditioned medium onto the kit plate. Sample preparation and metabolite detection was performed according to the Absolute IDQ assay kit instructions (Biocrates AG) as previously described (Römisch-Margl, Prehn et al. 2012). Briefly, samples (cellular extracts and conditioned medium) were manually pipetted onto the kit plate and the all further steps including: a) sample drying under a nitrogen stream, b) amino acid derivatization with derivatization reagent contain 5% phenylisothiocyanate (PITC), c) second sample drying under a nitrogen stream, d) metabolite and internal standards extraction using 5mM ammonium acetate in methanol, e) filtration by centrifugation, and f) dilution with running solvent were performed on a Hamilton ML Star robotics system (Hamilton Bonaduz AG). Metabolite detection was performed by FIA – MS/MS (for carnitines and lipids) and LC – MS/MS (for amino acid and biogenic amines) on an API 4000 (AB Sciex). Data evaluation was performed with MetIDQ software package (integral part of the Absolute IDQ assay). The intracellular and conditioned medium metabolite concentrations are given in μM . The Absolute IDQ p180 assay enables the detection of 186 metabolites including: 40 acylcarnitines (free carnitine – C0 and acylcarnitines – Cx:y), 21 amino acids, 19 biogenic amines, 90 glycerophospholipids

including lysophosphatidylcholines (LysoPC a Cx:y) and phosphatidylcholines with acyl (PC aa Cx:y) or ether (PC.ae.Cx:y) side chain, 1 hexose (sum of hexoses – H1) and 15 sphingolipids (SM.Cx:y). As previously described (Römisch-Margl, Prehn et al. 2012), the nomenclature used for lipid metabolites refers to the Lipid Maps comprehensive classification system (Fahy, Sud et al. 2007). This method enables only the detection of the total carbon number of the fatty acid chains in case of LysoPCs and PCs without the information regarding the exact side chain composition, chain saturation, substitutions, or region- and stereochemistry. The nomenclature for lipids is as follows: Cx:y, where “x” denotes the number of carbons (C) and “y” represents the number of double bonds (Römisch-Margl, Prehn et al. 2012).

2.7 Studies on apoptosis

2.7.1 Stimulation of apoptosis or necrosis

HEK293, HepG2, MCF7 and PC3 cells were seeded at a density of 2×10^5 cells / well in 12-well plate in 1mL medium for examinations of apoptosis on the metabolite level (see **2.7.4**) and at 0.2×10^5 cell / well in 96 well plate in 100 μ L medium for MTT assays (see **2.7.2**) and Caspase 3/7 assays (see **2.7.3**). Apoptosis or necrosis was induced 24 hours after cells were seeded at a confluence of the cells of ~80 %. Apoptosis was induced by replacement of growth medium for fresh one containing pro-apoptotic agent: staurosporine (4 or 2 μ M) in all used cell lines and etoposide or 5-fluorouracil “5-Fu experiment” (100 and 500 μ M) in HEK293 and HepG2. The whole experimental setups (containing control, vehicle treated, apoptotic and necrotic cells) were nominated according to pro-apoptotic agents: staurosporine - “stauro experiment”, etoposide - “eto experiment” and 5-fluorouracil - “5-Fu experiment”. In the stauro experiment necrosis was induced by cell heating on a hot plate for 20 min at 57 °C after medium replacement for fresh growth medium. The necrosis in the eto and 5-Fu experiments was induced by cell heating on a hot plate for 20 min at 57 °C after medium replacement for fresh growth medium containing DMSO (vehicle). The control group for apoptotic cells was treated with fresh growth medium containing DMSO (vehicle) in all experimental setups. All cells

belonging to the stauro experiment were incubated for 4, 12 and 24 hours after each treatment. Cells belonging to the eto or 5-Fu experiments were incubated for 18, 24, 48 and 72h after treatment in all cases. After incubation times cells were harvested and stored at -80 °C until use or further processed according to the subsequent analyzes.

2.7.2 Determination of cell viability by MTT assay

Cell viability was monitored by MTT (3-(4,5-Dimethylthiazol-2-yl)-2,5-diphenyltetrazolium bromide) assay based on the absorbance measurements after reduction of MTT (yellow tetrazole) into purple formazan in the living cells (Mosmann 1983, Liu, Peterson et al. 1997). The MTT assay was performed in 96 well plates format on treated cells (apoptotic, necrotic and control). Cells were incubated with 10 µL of MTT dissolved in PBS buffer (5 mg /mL) for 2 h at 37 °C. After the incubation time medium was completely removed and samples were frozen at - 80 °C for at least 1h. Plates were removed from the freezer, thawed and to each well 100 µL of DMSO was added. Samples were incubated for another 40 min at RT under constant shaking to dissolve the formazan crystals. Optical absorbance was measured at 590 nm (reference wavelength 630) using a GENiosPro plate reader (Tecan). Cell viability was expressed relative to the MTT value for untreated cells (in stauro experiment) or DMSO (vehicle) treated cells (in eto and 5-Fu experiments) which were taken as 100% viability.

2.7.3 Apoptosis detection by Caspase 3/7 assay

Apoptosis was determined by the measurement of caspase 3 and 7 activity, enzymes primarily involved in apoptosis, using Caspase-Glo 3/7 assay (Promega). The activity of caspase 3/7 was detected in cells grown in 96 well plates after complex treatment described in chapter **2.7.1**. To each well 100 µL of Caspase-Glo reagent was added (according to manufacturer's instruction) and samples were incubated for 30 minutes at RT under constant shaking. Luminescence, being directly proportional to the caspase activity, was measured using a GENiosPro plate reader (Tecan). Data were normalized to the caspase 3/7 activity of non-treated (in case of stauro experiments) or DMSO

treated (in case of eto or 5-Fu experiments) cells taken as controls.

2.7.4 Metabolite detection

Amino acid and acylcarnitine concentrations of intracellular extracts from apoptotic, necrotic and control (untreated or DMSO treated) cells were performed with the NBS assay (see **2.6.1**). Cells were grown in 12 well plates and after complex treatment cells were harvested according to procedure described in chapter **2.5.1**. Briefly, cells were washed with PBS, scraped off the plate, mixed with 350 μL of 20% MeOH and homogenized with Precellys24 homogenizator. After centrifugation cell extracts were applied onto blank filter paper placed in 96 well plates and the procedure according to the NBS assay (Chromsystems) was performed (for detailed description see **2.6.1** section). For direct comparison metabolite concentrations were normalized to the cell number (4×10^5) (in case of stauro experiment) or total protein concentration (in case of eto or 5-Fu experiments) which were determined in a parallel assay. To determine the cell number, cells were cultivated and treated as for the metabolite analysis experiment but harvested by trypsinization and counted with a counting chamber under the microscope. To determine total protein concentration cells were scraped off the wells with 300 μL of lysis buffer (Cell Signaling) contain protease and phosphatase inhibitor. Total protein concentration was assayed by the Pierce BCA protein assay kit (Thermo Scientific) according to the manufacturer's protocol using bovine serum albumin as standard. Briefly, 50 μL of cell lysate or 50 μL of standard solution (BSA - bovine serum albumin) was transferred into a 96-well and incubated for 30 min at 37 °C with kit working solution containing bicinchoninic acid. Optical absorbance was determined at 562 nm (reference wavelength 590) using SAFIRE II plate reader (Tecan).

2.8 Studies on adipogenesis

2.8.1 Stimulation of adipogenesis

Stimulation of adipogenesis was performed with the mouse cell line 3T3-L1 in three

independent experiments. Adipogenesis was monitored at 8 different time points by several tools including Oil Red O assay, DAPI staining, microarray based gene expression analysis, qPCR, metabolite measurements and Western blot. The numbers in **Figure 5** reflect the 22 days of the experimental procedure.



Figure 5 Stimulation of adipogenesis in the cell line, 3T3-L1. Cells were seeded 4 days before the first harvesting. Numbers indicate the day of cell differentiation. Black numbers indicate days at which cells were collected. White numbers indicate days on which no cells were harvested. Colors of numbered boxes represent stages of adipogenesis: dark blue – preadipocytes, light blue – post-confluent preadipocytes, yellow – differentiation and orange – maturation. Medium was changed every second day (indicated by stars): blue star - regular growth medium (DMEM); yellow star - differentiation medium; orange star - maturation medium

Black numbers indicate days at which harvesting was performed. Colored background of the numbers reflect different stages of adipogenic cell differentiation: dark blue – preadipocytes (day -4 to -2) seeded four days before first harvesting; light blue – cells in post-confluence phase (day 0); yellow – cells in differentiation stage (day two to four); orange – maturation stage (days from 6 to 18). Stars above numbers represent points at which medium was changed (every 48h (2 days)) and the different medium composition are indicated in colors: blue – standard growth medium (DMEM), yellow - differentiation medium: DMEM containing dexamethasone (1 μ M), 3-Isobutyl-1-methylxanthine (IBMX; 0.5 mM) and insulin (10 mg/mL) added at day zero, and orange – maturation medium: DMEM containing 10 mg/mL of insulin added at day four. For each experiment and harvesting time point four 6-well plates were prepared and cells were seeded in 2 mL of DMEM growth medium at a density of 0.8×10^5 cells /well (at day -4). Metabolomics studies (**2.6.2**) and DAPI staining (**2.8.3**) were performed out of three single wells, and Oil Red O assay out of two single wells. Cells for protein analysis (total protein; for

Western blotting) and RNA analysis (quantitative PCR) were collected from two double wells and three double wells respectively. Gene expression profiling assays (**2.8.6**) were performed with RNA isolated from the whole plate (6 wells). All assays were performed in three independent experiments.

2.8.2 Oil Red O assay - examination of lipid droplet accumulation

The cytoplasmic accumulation of lipid droplets was determined in 3T3-L1 cells, cultivated as describe above, at each harvesting day (day 0, 2 4, 6, 8, 10, 14 and 18) with Oil Red O dye. The Oil Red O working solution was prepared directly before staining by mixing 6 parts of Oil Red O stock solution (8.58 mM in isopropanol) with 4 parts of water. Before staining, medium was completely removed and cells were incubated with 3 mL of 10% formaldehyde in PBS for 5 min at RT. The formaldehyde was then replaced by 3 mL of fresh 10% formaldehyde and cells were incubated at least 1 h (covered with parafilm and aluminum foil cells can even be incubated for a couple of days). Formalin was completely removed and cells were washed with 3 mL of 60% isopropanol. Oil Red O working solution (1 mL) was added to the dried wells (after isopropanol was removed and evaporate) and cells were incubated for 10 min at RT. The Oil Red O solution was removed and wells were washed 4 times with ddH₂O, to eliminate traces of staining solution. Lipid droplet accumulation was assessed by microscopic inspection (Axiovert, Zeiss) and each well was photographed 3 times. For quantification, water was completely removed and the Oil Red O was extracted by addition of 3.5 mL of 100% isopropanol. Samples were incubated for 10 min at RT by constant shaking and 1 mL of samples were transferred into a cuvette. Optical density was determined at 520 nm using the spectrophotometer DU 530 (Beckman, Coulter). 100% isopropanol was used as blank.

2.8.3 DAPI staining – determination of cell proliferation during adipogenesis

The number of cells at different stages of adipogenesis was monitored by cell imaging

after the nuclei were stained with DAPI. At each day of harvesting, after medium was completely removed, cells were washed with 2 mL of PBS and incubated with 1 mL of ice-cold methanol for 10 min at RT. After removal of methanol cells were washed twice with 2 mL of PBS and incubated in darkness for 5 minutes at RT with 0.5 mL of DAPI (5.7 μ M) dissolved in methanol. DAPI was removed and samples were washed three times with ddH₂O to eliminate staining traces. Stained cellular nuclei were viewed in a microscope and four photos of different well areas were taken (tiff. format). Cells were counted using ImageJ, a free public domain Java program for image processing and analysis.

Transcriptional analysis of adipogenesis

2.8.3.1 Cell preparation and RNA isolation

Cell harvesting for gene expression profiling and qPCR was performed according to the following steps: conditioned medium was removed and cells were washed twice with PBS, to each well Trizol (0.5 mL/well) was added and cells were scraped off the well. Samples were placed into the Eppendorf tubes and stored at – 80 °C until further processing. For gene expression analysis cells were collected out of 6 wells and for qPCR out of two wells pro sample. The RNA isolation was performed with RNeasy Midi Kit (Qiagen) following the manufacturer's protocol. Briefly, samples were thawed, vortexed for 15 sec and to each tube 0.2 mL of chloroform per 1 mL of Trizol were added. The chloroform/Trizol samples were mixed for 15 sec and incubated for 3 min at RT. The colorless upper aqueous phase, obtain after 15 min centrifugation at 4 °C, 4500 rpm, was transferred into a new tube and mixed with the same volume of 100% ethanol. Samples were applied onto an RNeasy midi column and centrifuged 5 min at RT. Upon flow-throw removal 2 mL of RW1 buffer was added, centrifuged and digestion of DNA (on column) was carry out by incubation with 160 μ L of DNase for 10 min at RT. After DNA digestion samples were incubated with 2 mL of RW1 buffer at RT for 5 minutes. After centrifugation flow-throw was removed and RPI buffer (2.5 mL) was placed on the column and samples were centrifuged. The column was transferred onto a new collection tube and RNA was collected after elution with 150 μ L of RNase-free water

from the column. Concentration and quality of RNA was determined by using NanoDrop ND-1000 spectrometer (PeqLab) after pipetting 1.6 μL of RNA (in RNase-free water) into the spectrometer. The spectrophotometer was blanked using RNase-free water and the concentration was determined at 260 nm wavelength (1 OD at 260 nm is equal to 40 μg RNA /mL). The quality and purity was determined by $A_{260/280}$ ratio analysis. Absorption at 280 indicates protein contamination and a ratio 260/280 of ~ 2 indicates pure RNA.

2.8.3.2 Gel electrophoresis – RNA quality and purity

The quality and purity of RNA samples prepared for gene expression analysis were additionally examined on denaturing agarose gels and ethidium bromide staining. Gel preparation: 55 mg of agarose was dissolved in a mixture of DEPC- H_2O (50 ml) and 10x MESA-Buffer (5.5 ml), boiled until clear solution was obtained. Formaldehyde (1 mL) and 0.2 μL of ethidium bromide were added (after cooling to $\sim 60^\circ\text{C}$) and mixture was poured into a gel slide. The solidified gel was placed into the electrophoresis chamber and samples prepared by mixing of 1 μL of isolated RNA with 2.5 μL of loading buffer (RNA Sample Loading Buffer, without ethidium bromide, Sigma) were loaded. RNA was separated by electrophoresis at constant electric field at 100 V for 30 min and documentation was performed with Vilber Lourmat Bio-Vision apparatus.

2.8.3.3 cDNA synthesis and Quantitative Real-Time PCR

Synthesis of cDNA, required as template for DNA polymerase, was performed from all samples by using the First Strand cDNA Synthesis Kit (Thermo Scientific) following the manufacturer's protocol. Briefly, total RNA was reverse transcribed from 1 μg of RNA in a final reaction volume of 20 μL using oligo(dT)₁₈ primer (included in kit). With the cDNA templates qPCR was performed in 384-well plate format. The qPCR reaction in 20 μL volume / well includes: 10 μL of SYBER green PCR master MIX (Applied Biosystems), 6 μL of water, 2 μL of primers pair of gene of interest or housekeeping gene (forward (1 μL) and reverse (1 μL) primer) and 2 μL of cDNA (1/10 diluted). In case of control wells 2 μL of water were added instead cDNA. Amplification and quantification of PPAR γ was

performed using primers previously described (Fu, Luo et al. 2005). All other primers were designed by using free software Primer3 (http://biotools.umassmed.edu/bioapps/primer3_www.cgi) according to parameters presented in **Table 2**. Primers used in this study were purchased from Metabion and are listed in **Table 3**. Real-time polymerase chain amplification was performed in triplicates in two independent experiments with a standard protocol presented in

Table 4, the target and housekeeping genes were always placed onto the same plate. qPCR reaction was conducted by using a TaqMan 7900HT cycler equipped with SDS2.3 software (Applied Biosystems).

Table 2 Parameters provided for primer pars design with Primer3 software * “X” denotes exon-intron boundary; number after comma (20) indicate region of 10 bp forward and 10 bp rearward the boundary which are included into amplification product.

| Parameters | Variety area |
|--------------------------------------|--------------|
| Mispriming library | Rodent |
| Targets | X,20* |
| Product size | 120 - 220 |
| Max 3' stability | 7 |
| Max mispriming | 10 |
| Pair max mispriming | 20 |
| Primer size [bp] | 18 - 20 |
| Primer melting temperature [Tm] [°C] | 58 - 61 |
| Max Tm difference | 1.5 |
| Primer GC content [%] | 45 - 55 |
| Max self complementarity | 6 |
| Max 3' self complementarity | 2 |

Table 3 Primers for qPCR. Listed genes were amplified and quantified from 3T3-L1 cells at different days of adipogenesis.

| Gene | Name/Direction | Sequence (5' --> 3') | Tm (°C) |
|---------------------------------|---------------------------|------------------------|---------|
| AUH | mAUH_215_for | GGTGCTCGGGATTAACAGAG | 60 |
| | mAUH_423_rev | TGGAGACAAAGGGACCAACT | 58 |
| C/EBPβ | mC/EBP β _762_for | GACAAGCTGAGCGACGAGTA | 60 |
| | mC/EBP β _919_rev | AGCTGCTCCACCTTCTTCTG | 60 |
| C/EBPα | mC/EBP α _962_for | TGGACAAGAACAGCAACGAGTA | 60 |
| | mC/EBP α _1082_rev | GTCAACTCCAGCACCTTCTGT | 61 |
| CHPT1 | mCHPT1_510_for | TTTATGTGCCCTGGGACTCT | 58 |
| | mCHPT1_726_rev | CATGAACATCCCAACGAAAG | 56 |
| ELOVL1 | mELOVL1_139_for | TGGAGGCTGTTGTGAACTTG | 58 |
| | mELOVL1_300_rev | GCTTCCGATTAGCCATGATT | 56 |
| ELOVL3 | mELOVL3_133_for | CCCTACCCCAAGCTCTGTAA | 60 |
| | mELOVL3_349_rev | CGCGTTCTCATGTAGGTCTG | 60 |
| ELOVL4 | mELOVL4_309_for | GATGTCCACGGCATTCAAC | 57 |
| | mELOVL4_452_rev | AGCCACACGAACAGGAGATAG | 61 |
| ELOVL5 | mELOVL5_175_for | GAACATTTGATGCGTCACT | 56 |
| | mELOVL5_363_rev | GATGCCTCGGCAAGAGAA | 56 |
| HMGCR | mHMGCR_426_for | GGTATTGCTGGCCTCTTCAC | 60 |
| | mHMGCR_562_rev | CTCGCTCTAGAAAGGTCAATCA | 60 |
| IPO8 | mIPO8_2267_for | CAGCAGGATTGCTTCGAGTA | 58 |
| | mIPO8_2434_rev | AGCATAGCACTCGGCATCTT | 58 |
| MCEE | mMCEE_457_for | CATCCACTGGGGAGTGATAGT | 61 |
| | mMCEE_648_rev | GGGATGGAGGAAAATCACAG | 58 |
| MUT | mMUT_377_for | ATTCACACGGGGACCATATC | 58 |
| | mMUT_570_rev | CACGAACTCTGGGGTTGTCT | 60 |

| | | | |
|--------------------------------|---------------------|-----------------------|----|
| MVD | mMVD_37_for | GGGACTCCAGCATCTCAGTTA | 61 |
| | mMVD_253_rev | ATGCGGTCCTCTGTGAAGTC | 60 |
| PCCb | mPCCb_284_for | CATGGAGAGCGACATGTTTG | 60 |
| | mPCCb_492_rev | TGGCCTGGTCCATGATTT | 60 |
| PPARγ | mPPAR γ _for | TTTTCAAGGGTGCCAGTTT | 53 |
| | mPPAR γ _rev | AATCCTTGGCCCTCTGAGAT | 58 |

Table 4 The amplification protocol schema

| Parameters | Temperature [°C] | Time [min] | Cycle |
|-----------------------|------------------|------------|-------|
| Denaturation | 90 | 10 | 1 |
| Annealing | 60 | 1 | 1 |
| Amplification | 95 | 0:15 | 39 |
| Melting curve program | 95 | 0:15 | 1 |
| | 60 | 0:15 | |
| | 95 | 0:15 | |

Quantification of mRNA expression was performed with a sequence - detection system of the SDS2.3 software (Applied Biosystems). Relative gene expression was calculated using the comparative $2^{-\Delta\Delta CT}$ method (Livak and Schmittgen 2001) normalized to the IPO8 (importin 8) housekeeping gene and the gene expression of samples at day zero of adipogenic cell differentiation.

2.8.4 Analysis of adipogenesis by Western Blot

2.8.4.1 Total protein extraction from 3T3-L1 cell line

Growth medium was removed, cells were washed with ice-cold PBS buffer (2 mL) and scraped off the well with 300 μ L of lysis buffer (Cell signaling) supplemented with protease and phosphatase inhibitors (Roche) as well as phenylmethanesulfonylfluoride (PMSF), a serine protease inhibitor. Samples were transferred into 1.5 mL Eppendorf tubes and immediately frozen in liquid nitrogen. Freeze-thaw cycles were repeated 3 times. The samples were always thawed on ice and frozen in liquid nitrogen. Afterwards, samples were incubated with nuclease (Benzonase, Sigma) for 30 min at RT to reduce sample viscosity. Protein denaturation was performed by incubation with 4x Laemmli buffer at 95 °C for 10 min.

2.8.4.2 SDS-PAGE and protein transfer

Denatured proteins (20 μ L) and a protein marker sample (Thermo Scientific) were loaded onto a SDS-PAGE (sodium dodecylsulfate poly acrylamide gel electrophoresis) ready gel (Bio-Rad) and separated in a constant electric field (50 mA) in a Miniprotean III apparatus (Bio-Rad). After separation gel was equilibrated for 10 min at RT in blotting buffer (containing 48 mM Tris, 33mM Tricin, 1.3 mM SDS (10%) and 20% MeOH). A polyvinylidene difluoride (PVDF) membrane (Millipore) was activated by incubation with 100% MeOH for 30 sec. The PVDF membrane and Whatman-filter papers were further soaked in blotting buffer. Protein transfer was performed in a Trans-Blot SD-Transfer Cell (Bio-Rad) after a “blot sandwich” was built in the following order: anode \rightarrow 2 pieces of filter paper, PVDF membrane, gel, 2 pieces of filter paper \leftarrow cathode. Proteins from gel were electrophoretically transferred to the PVDF membrane by the application of 85 mA for 1 h. The membrane was blocked in 5 % milk solution (dissolved in T-PBS: PBS buffer containing 0.5 % of polysorbate 20 (Tween 20)) for 1 h, washed three times with T-PBS and incubated with the first antibody (diluted in 0.5 % milk solution) overnight at 4 °C. The membrane was washed three times for 10 min with T-PBS and incubated for 1h at RT with the secondary antibody (horseradish peroxidase coupled, diluted in 0.5% milk solution). All primary and secondary antibodies are listed in **Table 5**. Protein band detection was performed by enhanced chemiluminescence (ECL) method using the SuperSignal West Pico Chemiluminescent Substrate (Thermo Scientific), which is a

substrate for the horseradish peroxidase (coupled to the second antibody). The membrane was washed three times with T-PBS and incubated with 2 mL of solution containing the chemiluminescent substrate for 5 min at RT. Excessive substrate was removed and membranes were exposed to X-ray films (Kodak) or images were captured using the Fusion FX7 apparatus (Vilber Lourmat).

Table 5 Antibodies used in this study.

| | Antibodies | Dilution | Provider (order nr) |
|-----------|--------------------------------------|----------|----------------------|
| Primary | C/EBP α rabbit polyclonal IgG | 1:500 | Santa Cruz (Sc-61) |
| | C/EBP β rabbit polyclonal IgG | 1:500 | Santa Cruz (Sc-150) |
| | PPAR γ mouse monoclonal IgG1 | 1:500 | Santa Cruz (Sc-7273) |
| | β -Actin rabbit polyclonal IgG | 1:500 | Sigma (A2066) |
| Secondary | HPR-conjugated goat anti rabbit | 1:10000 | Dianova (115035-068) |
| | HPR-conjugated goat anti rabbit | 1:10000 | Dianova (115035-068) |
| | HRP-conjugated goat anti mice | 1:5000 | Sigma (A-6154) |
| | HPR-conjugated goat anti rabbit | 1:10000 | Dianova (115035-068) |

2.8.5 Characterization of adipogenesis by metabolomics

Metabolic alterations occurring during adipogenesis were characterized by using three different assays from the company Biocrates: the Absolute IDQ p180 kit assay which was performed in-house in the Helmholtz Zentrum München (see chapter **2.6.2**) and two assays for fatty acids and prostaglandins which were measured by the company Biocrates in Innsbruck. Cells were prepared according to the description in subsection **2.5.2**. Metabolite concentrations were measured in both conditioned medium and cell homogenates. For normalization cell number was determined in a parallel assay using ImageJ software after DAPI staining (see **2.8.1**). Statistical data analysis was performed with the *metaP* server at the Helmholtz Zentrum München (<http://metabolomics.helmholtz-muenchen.de/metap2/>) providing automated and standardized data analysis for metabolomics data (Kastenmüller, Römisch-Margl et al.

2010) under the supervision of Dr. Gabriele Kastenmüller from the Institute of Bioinformatics and Systems Biology (IBIS).

2.8.6 Characterization of adipogenesis by transcriptomics

Gene expression profiling experiments were performed under the supervision of Dr. Marion Horsch from the Institute of Experimental Genetics in the Helmholtz Zentrum München. Experiments were carried out in three biologically independent replicates using the Illumina Bead Array Technology with the Illumina Mouse Ref-8 v2.0 Expression BeadChip (Illumina, San Diego, CA, USA). Samples from one experiment (covering eight different days of adipogenesis) were evaluated on one BeadChip, targeting approximately 25,600 well-annotated RefSeq transcripts for over 19,100 unique genes and enabling performance of eight samples in parallel. The total RNA hybridized to the chips was isolation in a procedure described in section **2.8.3.1**. Sample preparation including staining, hybridization and scanning were done according to the Illumina expression protocol. Briefly, total RNA was reverse transcribed from 500 ng of RNA (in 11 μ L of RNase-free water) into double-strand cDNA using oligo (dT) primer bearing a T7 promoter. *In vitro* transcription, performed to synthesize biotin-labeled cRNA was carried out on purified cDNA. Purified cRNA samples (750 ng in 5 μ L of RNase-free water) were incubated with 10 μ L of HYB buffer for 5 min at 65 °C and after chilling to RT placed onto BeadChip slides. Microarray hybridization was performed in disposable adhesive hybridization chambers at 58 °C for 16h. After hybridization arrays were stained with Streptavidin-Cy3 in darkness for 10 minutes on a shaker at medium speed. Washed and dried slides were scanned on a HiScan reader (Illumina). Data normalization (quantile algorithm) and background corrections were done with the Illumina Genomestudio 2011.1. Statistical analysis for the identification of differentially expressed genes was performed using SAM (Significant Analysis of Microarrays), a tool included in the TM4 software package (Tusher, Tibshirani et al. 2001, Saeed, Sharov et al. 2003, Horsch, Schadler et al. 2008). The selection of regulated genes with reproducible up- or down-regulation includes 0% false positives rate (FDR) in combination with mean fold changes > 2. Expression data were submitted to the GEO

database (GSE34150), a public repository that archives and freely distributes high-throughput gene expression data submitted by the scientific community (Edgar, Domrachev et al. 2002).

2.9 Pathway analysis

After having met the requirements of the selection criteria differentially expressed genes were analyzed for their global function as well as their network and canonical pathway membership with the Ingenuity Pathway Analysis System (IPA, <http://www.ingenuity.com/products/ipa>). For the analysis 1000 significantly regulated genes were imported into IPA and 932 of them were mapped to the IPA database. Although analysis was performed in mouse cell line, gene descriptions are designated for human model. Additionally, regulated metabolites were combined with transcription data for integrated pathway analyzes. The achieved networks are based on Ingenuity Knowledge Base a repository of expertly curated biological interactions and functional annotations.

3 RESULTS

3.1 Metabolite measurement in cells – protocols development

To monitor biochemical changes in cells the metabolomics approach was chosen due to its proximity to phenotype. This research area can provide information about nutrition effect, mechanism of diseases, new diagnostic markers or response to treatment. The high-throughput targeted metabolomics AbsoluteIDQ p150 assay was successfully applied for metabolite measurements in human bio fluids (Gieger, Geistlinger et al. 2008) as well as in mice tissue (Römisch-Margl, Prehn et al. 2012). Moreover, the newborn screening (NBS) assay, based on a LC/MS method is routinely used for screening infants to manage treatable genetic and endocrine diseases (Chace, Kalas et al. 2003). However, the metabolite profile of a whole organism or a tissue does not provide relevant information about a specific cell type under different conditions which though would be important for understanding cellular processes or to find characteristic metabolic biomarkers. For this reason, to approach process on the cellular level development of a simple and robust method suitable for high-throughput analysis and applicable for cell culture was performed.

3.1.1 Optimization of new born screening assay for cell culture

The NBS assay covers 42 metabolites including amino acids and acylcarnitines and has ability to screen for about 30 metabolic disorders in a single analysis from one single disk of dried blood (Chace, Kalas et al. 2003). Due to advantages of the assay like robustness and metabolite panel it was considered to adapt it for monitoring of cellular processes. Adaptation of the NBS assay for cell culture approach was started with an optimization experiment: DMEM growth medium with declared concentration of amino acids was differently applied to filter paper, extracted and measured by FIA-MS/MS. The results are presented in **Figure 6**.

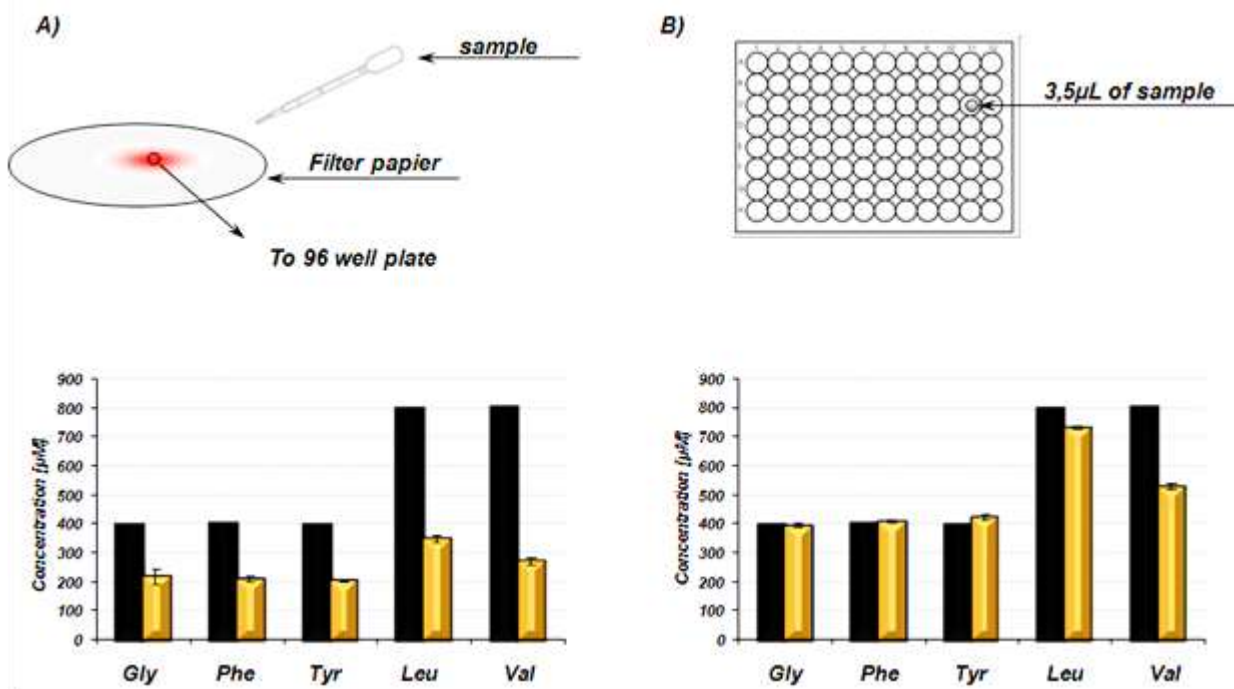


Figure 6 Optimization of NBS for cell culture approaches. **A)** Concentration of selected amino acids after sample preparation according to the standard procedure: spotting of DMEM onto filter paper and metabolite extraction out of a 3mm disk punched from the spot. **B)** Concentration of amino acids after application of 3.5 µL DMEM directly onto a 3 mm blank filter paper disk. Black bars represent metabolite concentrations declared by manufacturer and orange bars reflect metabolite concentrations after samples preparation according to NBS assay and measurements with FIA-MS/MS. Values represent the mean (\pm SD) of triplicates

In this experiment, the routine procedure, based on application of the DMEM sample onto filter paper and metabolite measurements from 3 mm disks cut out centrally of the application area (**Figure 6 A**), was compared with a modified method, where metabolites were measured after 3.5 µL of DMEM was placed direct onto 3 mm blank filter paper disks (**Figure 6 B**). Measured amino acid concentrations were compared with those declared by the manufacturer. Generally, sample preparation according to the standard procedure resulted in concentration much lower than declared for all examined metabolites. In contrast, the modified method enabled more accurate monitoring of the real metabolite concentrations (see **Figure 6**). In this case, concentrations of glycine, phenylalanine and tyrosine were very similar to those declared by the manufacturer. In turn valine, and leucine were only marginally lower. These results demonstrated that

NBS assay could be easily adapted for the cell culture approach. Moreover, the modified method was more sensitive and could be further implemented for metabolite measurements of cell extracts. In the following chapter (see **3.2**) the adapted NBS assay was applied for metabolite measurements in cancer cell lines.

3.1.2 Optimization of Absolute IDQ assay for cell culture approaches

Since metabolomics refers to the identification and quantification of ideally all small molecules in a living system (Beckonert, Keun et al. 2007), an assay like the NBS covering only 42 metabolites is limited regarding some biological questions. Thus, the targeted metabolomics assay, originally developed for plasma samples and covering 163 molecules including acylcarnitines, amino acids, glycerophospholipids, hexoses and sphingomyelins (Absolute IDQ p150 kit), was applied for metabolite measurement in cell culture. In a standard procedure the usage of 10 μL of plasma resulted in relative low matrix effects (Römisch-Margl, Prehn et al. 2012). However, metabolite concentrations and ion suppression of plasma samples are different from those of cell extracts. The intensity of internal standard (IS) is essential for data quantification and calculation of the ion suppression affected by different matrix. To elucidate the influence of cell extracts on IS signals, three different loading volumes (20, 40 and 60 μL) of supernatants from differently extracted cells (with water, 40% methanol (MeOH), or 87.5% MeOH) were analyzed. The ion suppression values shown in **Figure 7** were calculated by dividing the intensity of IS signals from cell extracts through IS signal intensity of the pure respective extraction solvent (water, 40% MeOH or 87.5% MeOH) called zero samples. The IS signals from the matrix free samples (zero samples) were set to 100%. Generally, ion suppressions of all applied cell extracts volumes were dependent on metabolite classes and were lower than those found for plasma samples. Nevertheless, both the extraction solvent and the applied volume affected the intensities of IS. The lowest matrix effect was observed for cells extracted with 87.5% MeOH. Moreover, cells extracted with 40% MeOH or even with water resulted in lower matrix effects, in almost all (except hexoses) metabolite classes, if compared to plasma

samples.

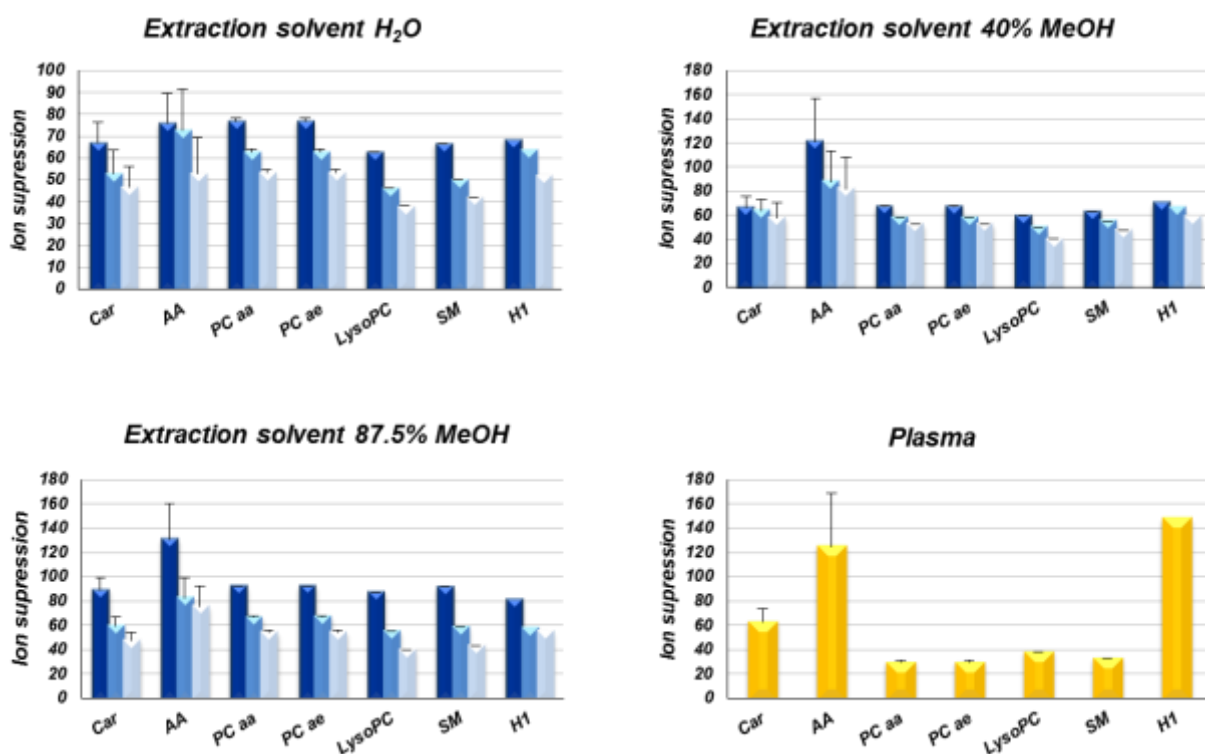


Figure 7 Matrix effects of cellular extracts characterized by ion suppression. Ion suppressions caused by plasma samples or 3T3-L1 cells extracted with: water, 40% MeOH, or 87.5% MeOH. The bar colors indicate different volumes applied onto a kit plate (dark blue - 20 μ L, light blue - 40 μ L and white - 60 μ L). Yellow bars indicate 10 μ L of plasma samples applied onto a kit plate. The influence of cell extracts on internal standard (IS) intensity was examined in the following compound groups: carnitines (Car), amino acids (AA), phosphatidylcholines (PC) with acyl (aa) or ether (ae) side chains, lysophosphatidylcholines (LysoPC), sphingomyelins (SM) and hexoses (H1). The IS signals from matrix free samples, *i.e.* extraction solvents (zero samples) were set for calculation to 100%.

In case of the cells extracted with solvents containing methanol increased ion suppression (~120) was observed. Also in plasma samples increased ion suppression of amino acids has been detected. This effect indicates potential interferences of unknown compounds in the methanol containing extracts. Among all examined extraction volumes, 20 μ L of cellular extract showed the lowest matrix effects, *i.e.* the highest IS signals and were used for further experiments.

The cell culture protocols for metabolite measurements were optimized to be compatible with the high-throughput targeted metabolomics Absolute IDQ p150 assay.

Nevertheless, at that time point the novel Absolute IDQ p180 assay, expanded by biogenic amines and some amino acids, covering a panel of 186 metabolites was developed and commercialized. Therefore, protocols established for the p150 assay were adapted for Absolute IDQ p180 assay. **Figure 8** shows the comparison in ion suppression values of the p150 and p180 assays, caused by 20 μ L of cell culture extracts from different stages of adipogenesis.

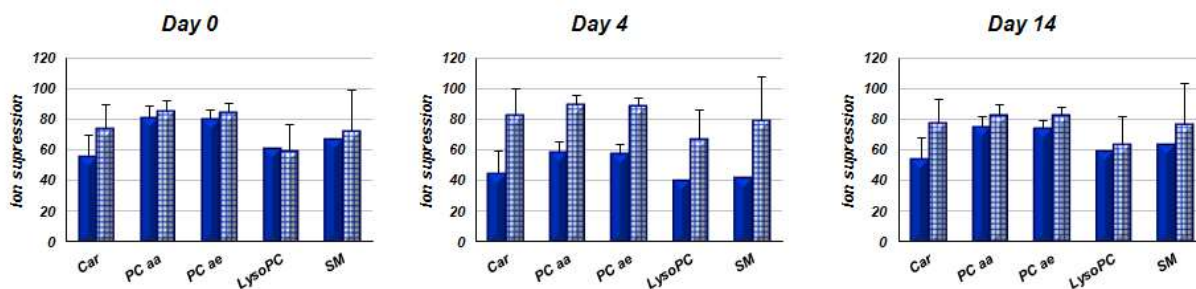


Figure 8 Comparison of p150 and p180 Absolute IDQ assays. Ion suppression caused by 3T3-L1 cells extracted with 80% MeOH at different stages of adipogenesis (preadipocytes – Day 0, differentiated adipocytes Day 4 and mature adipocytes Day 14) in metabolite groups: carnitines (Car), amino acids (AA), phosphatidylcholine (PC) with acyl (aa) or ether (ae) side chain, lysophosphatidylcholine (LysoPC), sphingomyeline (SM) and hexoses (H1). The blue bars indicate the ion suppression after measurements with absolute IDQ p 150 assay and crossbred bars indicate ion suppressions after measurements with IDQ p 180 assay. The ion suppressions were calculated by dividing the intensity of IS signal from cell extracts through IS signal intensity of the respective extraction solvent applied as zero sample. The IS signals from matrix free samples like extraction solvents (zero sample) are set for calculation to 100%.

The ion suppression of amino acids could not be directly compared due to different detection methods in assays (FIA-MS/MS in p150 and LC-MS/MS in p180 assay). The IS intensity of all metabolite classes given by the p180 assay resulted in similar or higher values if compared to the p150 assay. Importantly, in contrast to the p150 assay, ion suppressions of the p180 assay were not affected by the stage of adipogenesis.

3.1.3 Evaluation of harvesting and extraction procedures for metabolite measurements in adherent growing cells lines

The main goal of cell metabolomics is to analyze as many metabolites as possible in a defined cell status (conditions in which all enzymatic and chemical processes are

stopped by quenching procedures) as quickly as possible. Those requirements create difficulties in development of metabolite extraction procedures because every extraction method is limited by some molecule characteristics (lipophilic or hydrophilic). Moreover, quenching - necessary for the establishment of a representative cellular background (Cuperlovic-Culf, Barnett et al.), is frequently causing leakage of some intracellular metabolites (Winder, Dunn et al. 2008). The conventional method for harvesting of adherently growing cells is trypsinization to detach the cells from their growth area. Since metabolite concentrations are sensitive to any variation in the cell environment (Villas-Boas, Hojer-Pedersen et al. 2005), trypsin can completely change the cellular metabolism due to interaction with membrane proteins (Batista, Garvas et al. 2010). To determine the most efficient protocol for metabolite measurements in adherently growing cells, which are also compatible with the Absolute IDQ assay, two different harvesting methods, including trypsinization and cell scraping, combined with three extraction solvents (water, 40% MeOH, or 80% MeOH) were applied to 3T3-L1 cells. The trypsinized cell pellets were washed twice with phosphate buffer saline (PBS) to avoid contamination with external metabolites (from growth medium). The pellets were mixed with different extraction solvents and homogenized. In the second experimental setup the cells were washed twice with PBS, scrapped off the wells with different extraction solvents and homogenized. In all samples extracted with solutions containing methanol the quenching occurred simultaneously with extraction to prevent uncontrolled metabolite loss. The first objective was to determine the number of metabolites, from different metabolite classes, which can be detected in cell homogenates by the Absolute IDQ assay. The influence of different extraction solvents on metabolite quantities (detection level above LOD) in scrapped and trypsinized cells is presented in **Figure 9**.

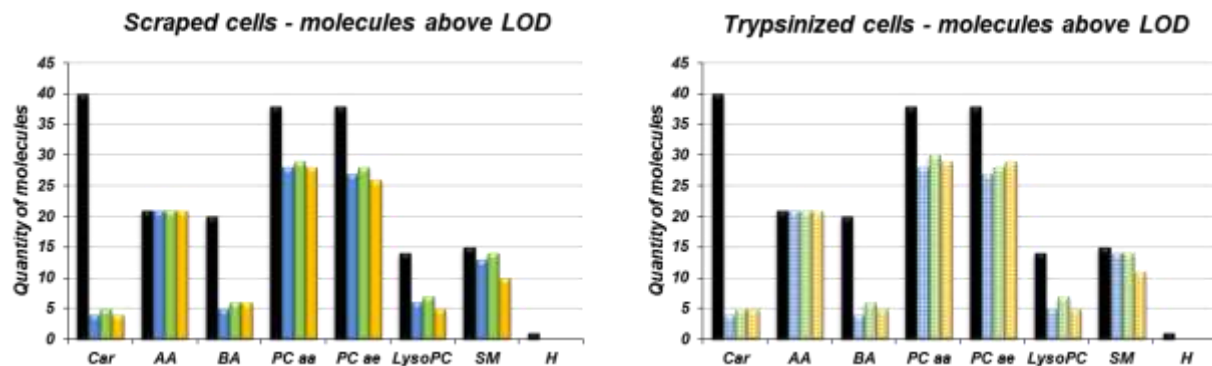


Figure 9 Effect of different harvesting method on metabolite extraction efficiency. The number of molecules with signals above LOD detected after 3T3-L1 cells harvesting by scratching (represented by solid bars) or trypsinization (represented by crossbred bars) and extracted with different solvents: blue - water, green - 40% methanol, yellow - 80% methanol. The black bars indicate total number of molecules detectable with Absolute IDQ assay for each metabolite class including carnitines (car), amino acids (AA), biogenic amines (BA), phosphatidylcholines (PC) with acyl (aa) and ether (ae) side chains, lysophosphatidylcholines (LysoPC), sphingomyelins (SM) and hexoses (H).

On the overall, independent of the used extraction solvent, the cell culture extraction/quenching assay is compatible with the Absolute IDQ p180 kit. Moreover, the number of detectable metabolites (giving signals above LOD) is neither dependent on the harvesting protocol nor on the extraction solvent. Importantly, the low number of carnitines with signals above LOD could correlate with assay sensitivity adjusted for plasma concentration of patients with metabolic disease.

A second goal of this study was to examine the influence of harvesting methods combined with different extraction solvents on the quantification of metabolites of the different metabolite classes (see **Figure 10**). As can be seen in Figure 9 remarkable differences in concentrations of carnitines, amino acids and biogenic amines were detected between harvesting procedures however, independent of the extraction solvent. In most cases the trypsinization resulted in lower metabolite concentrations except of lipids, which exhibited a marginal increase in concentration. Notably, this effect confirms the information on trypsin that might change metabolic profile of cells (Teng, Huang et al. 2009). If extraction solvents were compared, 80% MeOH resulted in the highest efficiency for lipid and biogenic amines extraction. Moreover, concentrations of acylcarnitines and amino acids of cells extracted with 80% MeOH were only slightly lower when compared to water extraction.

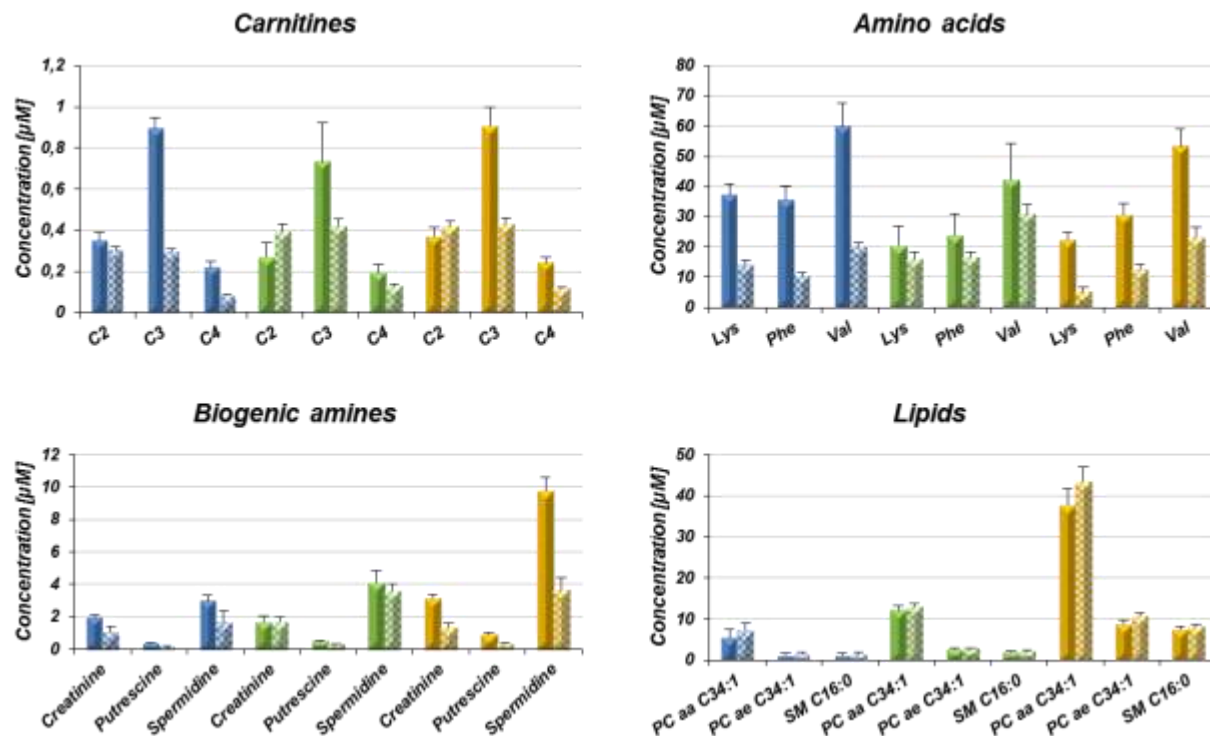


Figure 10 Effect of different harvesting method on metabolite extraction efficiency. Concentrations of molecules from different metabolic classes detected after cell scratching (solid bars) or trypsinization (crosshatched bars). Different extraction solvents are depicted in: blue - water, green - 40% MeOH, yellow - 80% MeOH. Abbreviations: C2, acetylcarnitine; C3, propionylcarnitine; C4, butyrylcarnitine, Lys, lysine; Phe, phenylalanine; Val, valine. In case of lipids, only the total compositions of the lipid species are determined. The side chain, substitution region and stereochemistry are unknown. For example PC.aa.C34:1 indicate phosphatidylcholines (PC) with acyl (aa) side chain with 34 number of carbons and single double bond in both side chains.

Taken together, the optimized protocols for metabolite measurements in cells presented in this section (3.1) were implemented to facilitate explanation of some biological phenomena like apoptosis or adipogenesis on the metabolic level. In all of those experiments cells were harvested by scrapping and extracted only with solvents containing methanol (20% MeOH for apoptosis experiments and 80% MeOH for adipogenesis).

3.2 Metabolic signatures of apoptotic human cancer cell lines

Since agents promoting apoptosis in tumors are considered as powerful tools for cancer therapeutics (Call, Eckhardt et al. 2008), the efficient monitoring of this biological phenomenon is urgently required. The present study aimed to identify apoptosis in cancer cell lines on the targeted metabolic level to find novel biomarkers for this cellular process. Amino acids and carnitines were quantified by the NBS assay, which was adapted for metabolite measurements in cells (see **Chapter 3.1.1**). Following different treatment schedules, including cell viability, caspase 3/7 expression together with metabolic studies, were evaluated in HepG2 (human hepatocellular carcinoma), HEK 293 (human embryonic kidney), PC3 (human prostate adenocarcinoma) and human breast adenocarcinoma – MCF7 cells.

3.2.1 Staurosporine as apoptotic agent

Triggering of apoptosis by staurosporine has been reported to be effective in HEK 293, HepG2 and MCF7 cells ((Miyamoto, Takikawa et al. 2004), (Nagata, Luo et al. 2005), (Xue, Chiu et al. 2003)). The unique property of staurosporine is its ability to rapidly and completely drive virtually all mammalian cells into apoptosis (Bertrand, Solary et al. 1994); (Stepczynska, Lauber et al. 2001). Furthermore, the staurosporine induced apoptosis involves mitochondrial caspase activation (Caballero-Benitez and Moran 2003), which can be easily detected by caspase 3/7 assay. Moreover, staurosporine and its derivatives have been used in clinical trials for cancer therapies (Edelman, Bauer et al. 2007); (Perez, Lewis et al. 2006).

3.2.1.1 Cell viability after staurosporine treatment or heating

Prior to metabolite analyzes the sensitivity of four cell lines (HEK 293, HepG2, PC3, and MCF7) to staurosporine (inducer of apoptosis (Alberici, Moratto et al. 1999)) or heating (induction of necrosis (Proskuryakov, Konoplyannikov et al. 2003)) by MTT assay was

examined. Necrotic cells were analyzed in parallel as alternative way of cell death (for a control). **Figure 11** shows the influence of vehicle (DMSO), staurosporine (2 and 4 μM in DMSO), and the heating on cell viability. Values were normalized to the viability of untreated cells. Generally, vehicle (DMSO) had no influence on cell viability.

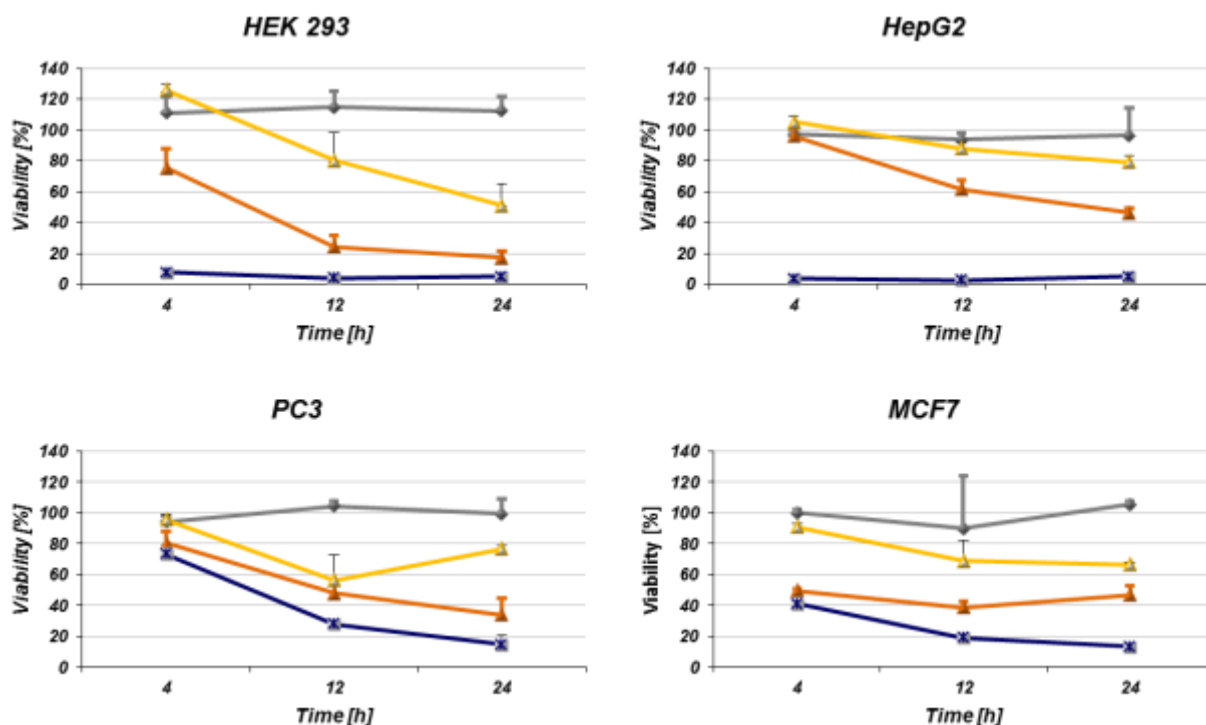


Figure 11 Cell viability after staurosporine treatment or heating. Viability of HEK 293, HepG2, PC3 and MCF7 cells was determined with the MTT assay after cells treatment with vehicle DMSO (grey line), 2 μM or 4 μM of staurosporine in DMSO (yellow and orange line respectively), or by heating (blue line) followed over time (4, 12 and 24 hours). Values were normalized to the viability of untreated cells (taken as 100%) and represent the mean (\pm SD) of triplicates from three independent experiments.

Staurosporine treatment caused a time and dose dependent decrease in cell viability in all examined cell lines with the strongest effect after 24h at 4 μM concentration. In MCF7 cells a marked decrease in the number of viable cells was apparent already after 4h of treatment with 4 μM of staurosporine. A higher sensitivity to this pro-apoptotic agent was also found in HEK 293 and PC3 cells, where after 12h of treatment viability decreased dramatically to 20% and 40%, respectively. Viability of HepG2 cells treated with 4 μM staurosporine decreased up to 60%, compared to the control group (untreated

cells) after 12h. Furthermore, the viability of all heated (necrotic) cells decreased already after 4h of incubation and went down to 0 – 10% after 24h. Notably, this effect was more pronounced for HEK 293 and HepG2 cells resulting in a dramatic decrease in cell viability already early after treatment (below 20% compared to the control group). In contrast, necrotic PC3 and MCF7 cells showed a decrease in cell viability of around 80% and 40%, 4 h after induction and the stronger effects only later after thermal treatment.

3.2.1.2 Apoptosis validation

To estimate the extent of apoptosis induced by different treatment schedules in the four cell lines, the activity of caspase 3 and 7 was analyzed. **Figure 12** shows the time course of caspase 3/7 activity after treatment of cells with staurosporine (2 and 4 μM) or heating at 57 °C for 20 min. Cells incubated with DMSO were followed over time as control and values were normalized to the caspase 3/7 activity of non-treated ones. The four cell lines showed different response to staurosporine, however this was dependent on agent concentration and incubation time. Treatment of PC3 cells with 4 μM staurosporine resulted in a time dependent, step by step elevated caspase 3/7 activity visible already 4h after treatment. The caspase 3/7 activity of pro-apoptotic treated HEK 293 and HepG2 cells reached a maximum after 12h and decreased after that. Distinct changes were observed for the MCF7 cells. In this cell line the activity of caspase 3 and 7 reached its maximum already after 4h and dramatically decreased afterwards (these effects were most pronounced at 4 μM staurosporine concentration). In none of the cell lines when treated only with vehicle an activation of caspase 3 and 7 has been observed. Heated cells showed decrease of caspase 3/7 activity when compared to non-treated cells. Such a decrease can be connected to the necrotic processes occurring in the heated cells.

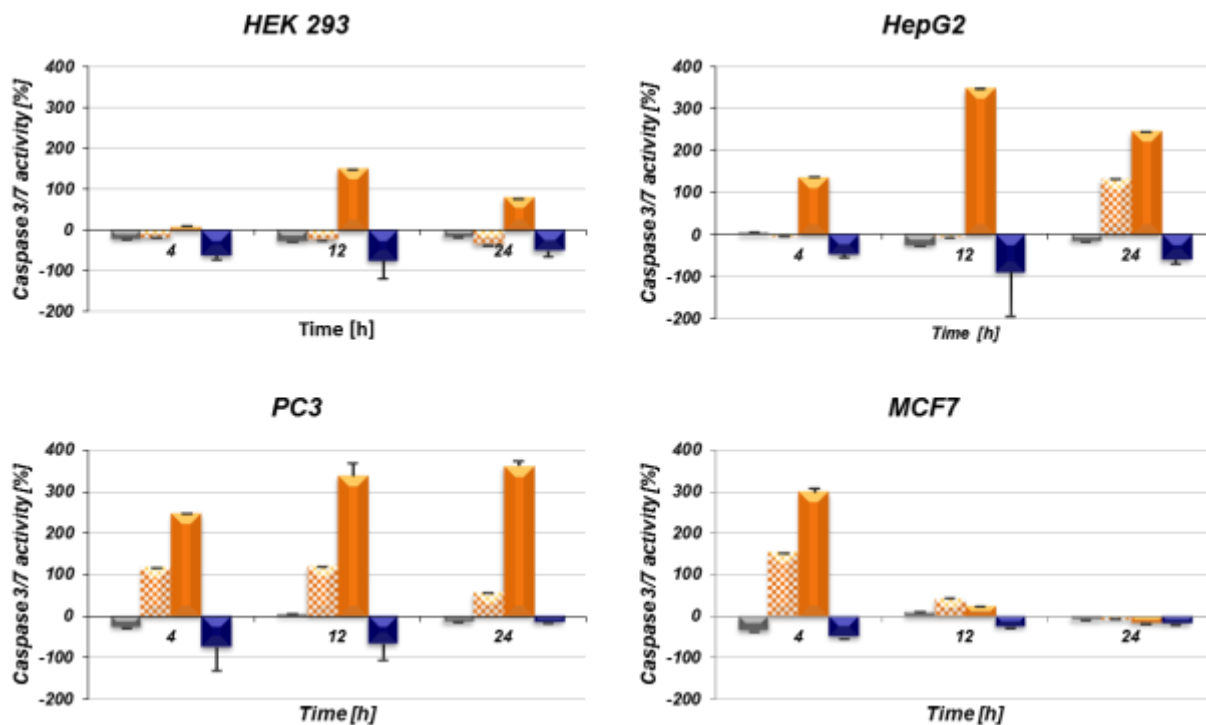


Figure 12 Apoptosis validation in HEK293, HepG2, PC3 and MCF7 cells. The effect of staurosporine or heating on the caspase 3/7 activity was measured by using the Caspase-Glo 3/7 kit after cell treatment with DMSO [gray bars], 2 μM [orange crossbred bars] or 4 μM [orange bars] staurosporine, or by heating [blue bars] at indicated time points. The data were normalized to the caspase 3/7 activity of untreated cells and are expressed as mean values (\pm SD) out of three independent experiments each performed in triplicates.

3.2.1.3 Distinct metabolic signatures of non-treated cancer cell lines

To investigate differences in the metabolite profile between cancer cell lines, metabolite concentration of HEK 293, HepG2, PC3 and MCF7 cells were examined at zero time point (24h after cells were seeded) with the NBS assay and were normalized to cell number (4×10^5). Statistical evaluation of the results was performed using Kruskal-Wallis analysis and **Table 6** summarizes metabolites that were found to be significantly different between those cells lines. Distinctions in the concentrations of alanine (Ala), glutamic acid (Glu), phenylalanine (Phe), methionine (Met), glycine (Gly), free carnitine (C0-carnitine), acetylcarnitine (C2-carnitine) and propionylcarnitine (C3-carnitine) were observed.

Table 6 Metabolic diversity of untreated cancer cell lines HEK293, HepG2, PC3 and MCF7.

The concentrations of metabolites were normalized to the number of 4×10^5 cells and expressed as mean values out of two independent experiments each performed in triplicates (\pm SD). The statistical data evaluation of the four control groups (untreated HEK293, HepG2, PC3 and MCF7 cells) was performed with *metaP* server. Significant differences between cell lines were found in alanine (Ala), glutamate (Glu), phenylalanine (Phe), glycine (Gly), propionylcarnitine (C3-carnitine), acetylcarnitine (C2-carnitine) and isovalerylcarnitine (C5-carnitine) concentrations. The p-values were calculated according to Kruskal-Wallis: (*) denotes a significance level of 5% and (**) a significance level of 1% after Bonferroni correction.

| | Cells | | | | | p-value |
|--|--------------|---------|-------|-------|-------|---------------------------|
| | Metabolites | HEK 293 | HepG2 | PC3 | MCF7 | |
| Metabolite concentrations [μM] | Ala | 27.74 | 24.57 | 4.11 | 8.49 | (*) 3.6×10^{-4} |
| | Glu | 29.27 | 65.86 | 14.07 | 22.96 | (**) 7.9×10^{-5} |
| | Phe | 3.24 | 5.59 | 1.58 | 1.90 | (*) 8.0×10^{-4} |
| | Met | 1.87 | 2.53 | 1.13 | 1.07 | (*) 7.5×10^{-4} |
| | Gly | 42.88 | 76.60 | 17.36 | 20.63 | (*) 2.9×10^{-4} |
| | C3-carnitine | 0.17 | 0.03 | 0.06 | 0.09 | (**) 1.6×10^{-4} |
| | C2-carnitine | 0.34 | 1.14 | 0.26 | 0.56 | (*) 2.8×10^{-4} |
| | C5-carnitine | 0.01 | 0.04 | 0.03 | 0.2 | (*) 6.9×10^{-4} |

To better illustrate these differences, the concentrations of Glu and C3-carnitine are presented in form of box-plots (**Figure 13**).

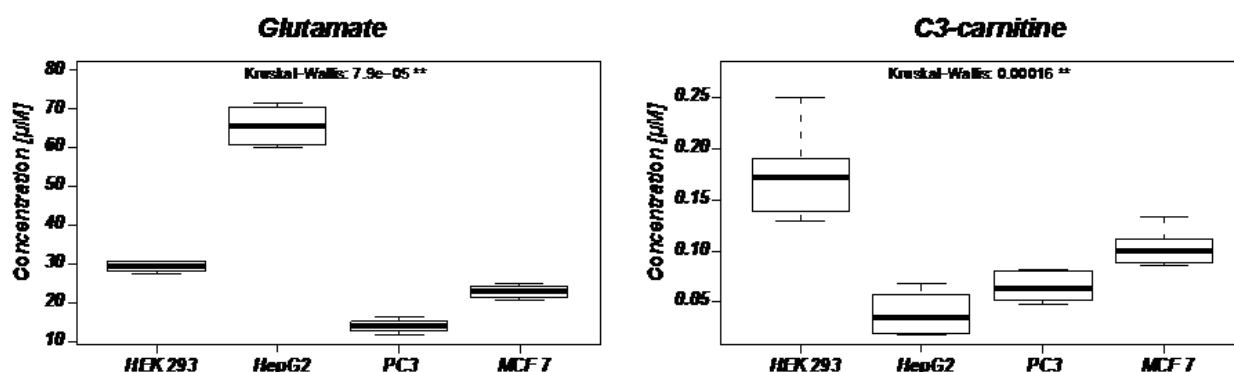


Figure 13 Difference in glutamate and propionylcarnitine (C3-carnitine) concentrations of untreated HEK 293, HepG2, PC3 and MCF7 cell lines. Box-plots, obtained after statistical data analysis with the *metaP* server demonstrate the medians out of two independent experiments carried out in triplicates. The p-values calculated by using Kruskal-Wallis, “**” denotes a significance level of 1% after Bonferroni correction. Metabolite concentration values were normalized to the number of 4×10^5 cells.

The highest concentrations of Glu, Phe, Met, Gly and C2-carnitine of all four analyzed cell lines have been found in HepG2. Furthermore, Ala and C3-carnitine reached the highest level in HEK 293 cells. The PC3 cells distinguished from the other cells by having the lowest concentration of Ala, Glu, Phe, Gly and C2-carnitine. The lowest concentration of Met was specific for MCF7 cells.

3.2.1.4 Staurosporine or heating resulted in characteristic metabolic patterns

A major potential of metabolomics involves either definition of pathways that contribute to a biological process or identification of characteristic metabolic signatures, which could be used for a novel drug testing. Apoptosis is an important phenomenon in cancer therapy and represents a common mechanism of drug activity (Salomons, Smets et al. 1999). Therefore, introduction of early apoptosis biomarkers in theranostics (Picard and Bergeron 2002) of cancer therapies is required. For that reason, in HEK 293 and in three different cancer cell lines HepG2, PC 3 and MCF7 apoptosis was induced with 4 μ M staurosporine (this concentration resulted in highest sensitivity in all examined cell lines in MTT and Caspase 3/7 assays), and metabolite concentrations were measured using the NBS assay. Time and dose dependent influence of staurosporine on apoptosis progression in those cell lines was already described in **Chapter 3.2.1.2**. In the experiment setup metabolite levels of apoptotic cells were compared with those of control (non-treated) and necrotic (heated) cells. Consequently, any changes that occurred in apoptotic, but not in both necrotic and control cells, should be specifically related to apoptosis and could be considered as biomarkers. For the identification of early biomarkers of apoptosis, metabolite concentrations of four groups including staurosporine treated (apoptosis induced), heat-treated (necrosis induced), vehicle treated (control), and non-treated cells were normalized to the number of cells (4×10^5). Statistical data evaluation was performed using Kruskal-Wallis analyzes. Metabolic patterns are summarized in **Table 7**.

Table 7 Metabolic changes of HEK 293, HepG2, PC3 and MCF7 cells undergoing apoptosis or necrosis – time course. The changes in metabolite concentrations after cell treatment with staurosporine (for apoptosis) or by heating (for necrosis) were measured by using NBS assay based FIA/MS-MS method. The statistical analysis of data including 4 groups (controls, vehicle treated, apoptotic “A_” and necrotic “N_” cells, was performed with the *metaP* server. Increase in metabolite concentration is labeled red, decrease and no change are shown as green and gray, respectively.

| Time [h] | Aspartate | | | Glutamate | | | Methionine | | | Glycine | | | Alanine | | | C3-carnitine | | | C3DC-carnitine | | |
|----------|-----------|-------|-------|-----------|-------|-------|------------|-------|-------|---------|-------|-------|---------|------|------|--------------|-------|-------|----------------|------|-------|
| | 4 | 12 | 24 | 4 | 12 | 24 | 4 | 12 | 24 | 4 | 12 | 24 | 4 | 12 | 24 | 4 | 12 | 24 | 4 | 12 | 24 |
| A_HEK293 | Red | Red | Red | Gray | Gray | Gray | Red | Gray | Red | Gray | Green | Red | Gray | Gray | Red | Green | Gray | Gray | Red | Gray | Red |
| N_HEK293 | Red | Red | Green | Green | Green | Green | Green | Green | Green | Green | Green | Green | Gray | Gray | Gray | Green | Green | Green | Gray | Gray | Green |
| A_HepG2 | Red | Red | Red | Red | Red | Red | Red | Red | Red | Red | Red | Red | Gray | Gray | Red | Green | Green | Green | Gray | Gray | Red |
| N_HepG2 | Green | Green | Green | Green | Green | Green | Green | Green | Green | Green | Green | Green | Gray | Gray | Gray | Green | Green | Green | Gray | Gray | Green |
| A_PC3 | Red | Red | Green | Red | Gray | Gray | Red | Red | Red | Red | Green | Green | Red | Red | Red | Red | Gray | Gray | Red | Gray | Gray |
| N_PC3 | Gray | Green | Green | Gray | Gray | Gray | Red | Green | Green | Green | Green | Green | Red | Red | Red | Green | Green | Green | Red | Gray | Gray |
| A_MCF7 | Gray | Green | Green | Gray | Green | Green | Red | Red | Gray | Gray | Gray | Gray | Red | Red | Red | Green | Green | Green | Gray | Gray | Green |
| N_MCF7 | Gray | Green | Green | Gray | Green | Green | Red | Green | Gray | Gray | Gray | Gray | Red | Red | Red | Green | Green | Green | Gray | Gray | Red |

Treatment resulted in all cell lines in significant changes in seven (5 amino acids and 2 acylcarnitines) of the 42 analyzed metabolites including Asp, Glu, Met, Ala and Gly as well as C3-carnitine and malonylcarnitine (C3DC-carnitine). However, each cell line showed different, characteristic pattern of metabolic changes according to treatment and exposure time. Concentrations of aspartate, glutamate, methionine, and C3DC carnitine increased in apoptotic HEK 293 cells (A_HEK293) already after 4h of treatment. Furthermore, alanine and glycine concentrations increased first after 24h of treatment. In contrary, the metabolic pattern of the necrotic HEK 293 (N_HEK 293) cells showed a decrease in aspartate, glutamate, methionine glycine and C3DC carnitine concentrations already after 4h incubation. The HepG2 cells compared with HEK 293 exhibited similar metabolic patterns after induction of apoptosis or necrosis. Elevated already 4h after treatment the high levels of aspartate, glutamate, methionine and glycine concentrations seems to remain up during the 24 h of the experiment in HepG2. Notably, a similar effect with increased aspartate concentration in A_HEK 293 cells has been observed. The C3-carnitine was the only metabolite that was significantly down regulated in both HEK293 and HepG2, independent of the kind of treatment. PC3 and MCF7 revealed different signatures to that of HEK 293 and HepG2 cells as well as among each other. In both cell lines, many from those seven metabolites were either up

or down regulated regardless of the different treatments. In the PC3 cells all seven metabolites were up-regulated after 4 h. However apoptosis could be distinguished from necrosis only with Asp and C3-carnitine. At later time points this effect was no longer observed. In case of Asp the difference between apoptotic and necrotic PC3 cells was still visible 12 h after treatment, but not detected later on. Met and Ala varied between apoptotic and necrotic PC3 cells only at the later time points (12 and 24 h). In MCF7 cells unique metabolic signatures were observed. The majority of regulated metabolites was either down- or up-regulated in comparison to controls but independent of treatment. Only Met and C3DC-carnitine showed a difference according to the nature of treatment, but at diverse time points, after 12 h and 24 h, respectively. To determine candidates for early apoptotic biomarkers metabolic alterations occurring after 4 h of treatment were further analyzed and visualized in form of box-plots. **Figure 14** shows the concentration patterns of aspartate, glutamate, methionine, glycine, alanine, C3-carnitine and C3DC-carnitine found in all four examined cell lines. Indeed, distinct values become already apparent at this time and are depicted for the most significant metabolites. Generally, both examined mechanisms regulating cell death (apoptosis and necrosis) resulted in diverse concentrations of Asp, Glu, Met, Gly, Ala, C3-carnitine, and C3DC-carnitine **Figure 14** in three (HEK 293, HepG2, and PC3) from four examined cell lines. In contrast, no significant changes differentiating apoptosis from necrosis in MCF7 cells in the analyzed time window has been observed.

Moreover, apoptotic HEK 293, HepG2 and PC3 cells differed from necrotic and control groups in some metabolite concentrations. An increased concentration of alanine and C3-carnitine has been observed only in HepG2 and PC3 cell, respectively. Elevated glycine and C3DC-carnitine levels were detected in both HepG2 and PC3 apoptotic cells. Furthermore, aspartate and methionine has been found as hallmark of apoptosis in all of those three cell lines.

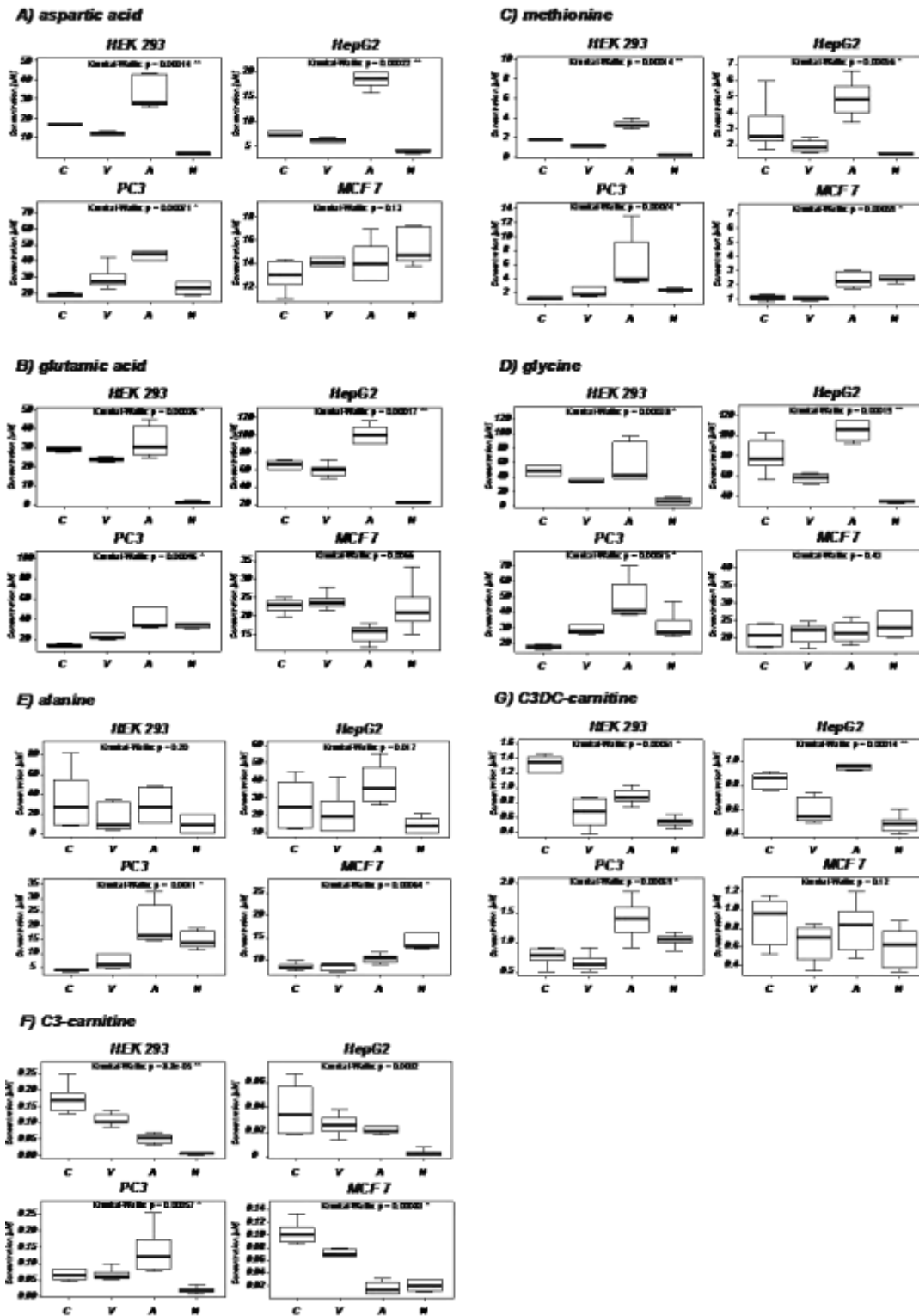


Figure 14 Metabolomics of the cellular response to staurosporine treatment or heating 4 h after incubation. Differences in metabolite concentrations of treated with DMSO (V), 4 µM staurosporine (A) and heated (N) HEK293, HepG2, PC3, and MCF7 cells when compared with control cells (C). The box-plots demonstrate the medians out of two independent experiments carried out in triplicates. The p-value calculated by using Kruskal-Wallis are given in each diagram, “*” denotes a significance level of 5% and “**” a significance level of 1% after Bonferroni correction.

3.2.2 Etoposide and 5-Fluorouracil as proapoptotic agents

Since metabolic alteration observed in staurosporine treated cells may reflect a characteristic of the pro-apoptotic agent (staurosporine) but not of the biological process (apoptosis), complementary experiments were required. Hence, apoptosis was further characterized after implementation of two others pro-apoptotic agents etoposide and 5-fluorouracil (5-Fu) in HEK293 and HepG2 cell lines. Etoposide is a commonly used drug in therapy of small lung cancer or lymphomas (de Jong, Mulder et al. 1995) and has been described as a pro-apoptotic agent (Okamoto-Kubo, Nishio et al. 1994). 5-Fu is like etoposide an inducer of apoptosis in cancer cell lines (Osaki, Tatebe et al. 1997) and is widely used (since 20 years) in colorectal and breast cancer therapy (Longley, Harkin et al. 2003).

3.2.2.1 Cell viability and apoptosis validation after etoposide or 5-Fu treatment

Prior to metabolite analyzes the sensitivity of two cell lines (HEK 293 and HepG2) to etoposide and 5-fluorouracil (5-Fu) was tested to find the optimal dosage and incubation time to effectively induce apoptosis. Viability of HEK 293 and HepG2 cells exposed to two different concentrations (100 μ M and 500 μ M) of etoposide or 5-Fu in the time course of 18, 24, 48 and 72 hours is shown in **Figure 15 A**. Values were corrected to the viability of vehicle (DMSO) treated cells (taken as 100%). Generally, etoposide and 5-Fu treatment affected cell viability in time- and dose-dependent manner. Higher sensitivity to etoposide has been observed in both cell lines. Etoposide treated HEK 293 and HepG2 resulted in a stepwise decrease of viability after 18 h and 24 h which was continued within the following hours. Cells treated with 5-Fu resulted in a decrease of viability to up to 60% after 48 h and 72 h in HepG2 and HEK293 cells, respectively. **Figure 15 B** presents apoptosis progression evaluated with the Caspase3/7. Generally, in both examined cell lines, etoposide had the strongest impact on caspase 3/7 activity. However, the cell lines showed a time- and dose- dependent response pattern. Caspase 3/7 activity of HepG2 cells reached a maximum after 24 h exposure to 500 μ M

etoposide. In contrast, HEK293 cells resulted in highest caspase activity after 72h incubation with 100 μ M of etoposide. Furthermore, for 5-Fu-treated HepG2 cells a noteworthy caspase 3/7 activity was detected first after 48h and only with higher concentration (500 μ M) of 5-Fu. For following metabolic analysis only treatments which effectively induces apoptosis were applied.

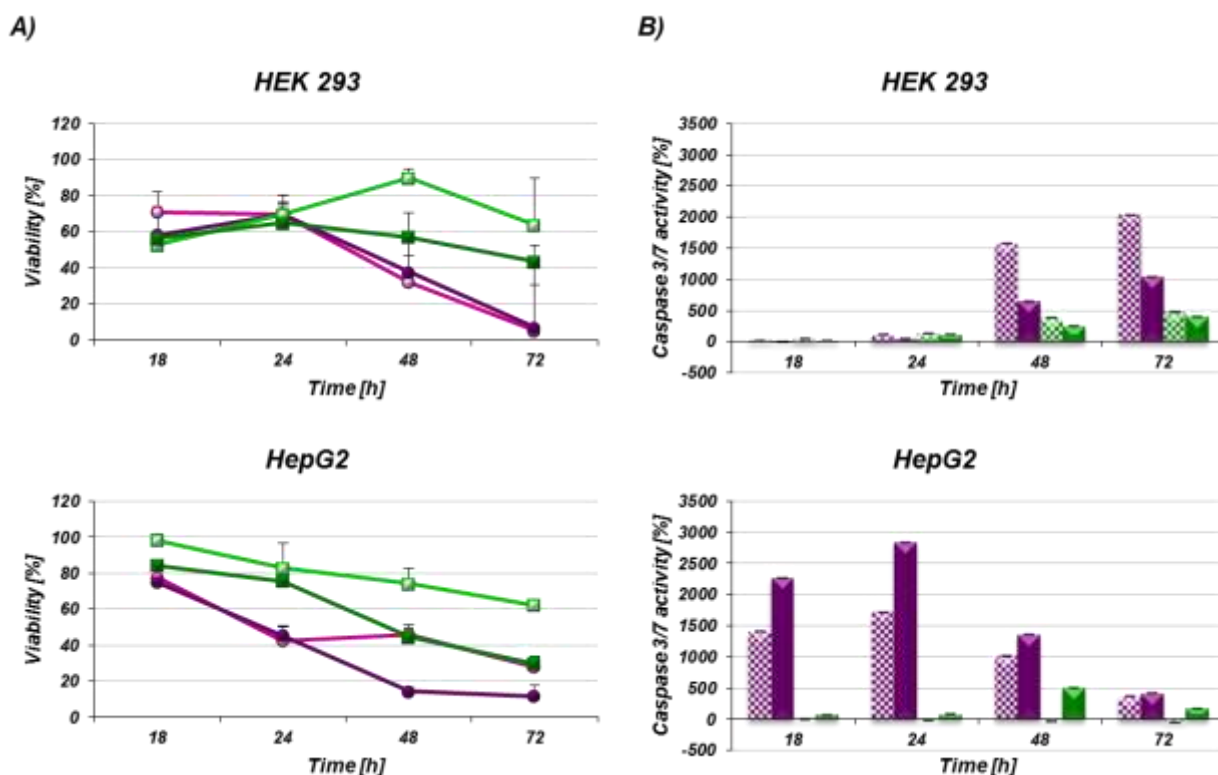


Figure 15 Cell viability and apoptosis validation after etoposide or 5-Fu treatment. A) Viability of HEK 293 and HepG2 cells after treatment with etoposide (100 μ M (pink) or 500 μ M (violet)), or 5-Fu (100 μ M (light green) or 500 μ M (dark green)) at different time points (18, 24, 48 and 72h) was determined by using MTT assay. Values were normalized to the viability of vehicle (DMSO) treated cells (taken as 100%) and represent the mean (\pm SD) of triplicates from three independent experiments. **B)** Effect of etoposide or 5-Fu on the caspase 3/7 activity in HEK 293 and HepG2 cell measured after incubation with 100 μ M [violet crossbred bars] or 500 μ M [violet bars] etoposide, or 100 μ M [green crossbred bars] or 500 μ M [green bars] at indicated time points. The data were normalized to the caspase 3/7 activity of vehicle treated cells and are expressed as mean values (\pm SD) out of three independent experiments each performed in triplicates.

3.2.2.2 Metabolic signatures of etoposide or 5-Fu treated cells

Characteristic patterns of elevated levels of amino acids and acylcarnitines in staurosporine induced apoptosis in cells were already described in **chapter 3.2.1** as well as already published (Halama, Moller et al. 2011). However, those changes could be characteristic for staurosporine but not for apoptosis itself. For that reason further examination of apoptotic biomarkers was performed after HEK 293 and HepG2 cell lines were treated with further pro-apoptotic agents including etoposide or 5-Fu. Notably, both etoposide and 5-Fu were shown to affect cell viability and induced apoptosis in those cell lines (see **3.2.2.1** and **3.2.2.2**). Amino acid and acylcarnitines quantification was performed with the adapted NBS assay on the three groups of cells: control – cells incubated with vehicle (DMSO), apoptotic cells (HEK 293 cells incubated with 100 μ M etoposide or 100 μ M 5-Fu for 72 h; HepG2 cells incubated with 100 μ M etoposide for 24 h or 500 μ M 5-Fu for 48 h) and necrotic cells (cells cultivated in medium containing and vehicle heated at 57°C for 20 min). Metabolite concentrations were normalized to total protein level examined in the parallel experiment. In the experimental setup the metabolite levels of apoptotic cells were compared with those of control and necrotic cells. Consequently, any changes that occurred in apoptotic, but not in necrotic and control cells, were specifically related to apoptosis. Data evaluation was performed with the *metaP* server using Kruskal-Wallis analyzes. **Table 8** summarizes the changes observed after HEK 293 and HepG2 treatment. Among 11 metabolites only alanine (Ala), arginine (Arg), aspartate (Asp), glutamate (Glu) and acetylcarnitine (C2) were particular for apoptotic HEK 293 and HepG2 independent of the apoptotic-agent. Moreover, both cell lines also showed cell specific responses to treatment. For example increase in propionylcarnitine (C3) and isovalerylcarnitine (C5) was observed only in HEK 293 cells treated with 5-Fu and up-regulation in methionine leucine and phenylalanine was characteristic for apoptotic HepG2 cells. In case of the HEK 293 cell line clear differences between apoptotic and necrotic cells were observed. In contrast apoptotic and necrotic HepG2 cells exhibited similar metabolic patterns.

Table 8 Metabolic signatures of HEK293 and HepG2 cells treated with etoposide, 5-Fu or heat. Changes in metabolite concentrations of cells after heating (“N_”) or incubation with etoposide (Eto) or 5-fluorouracil (5-Fu) (“A_”) for indicated periods (HEK 293 cells were incubated with 100 μ M etoposide or 100 μ M 5-Fu and HepG2 cells were incubated with 100 μ M etoposide or 500 μ M 5-Fu). The statistical data analysis of 3 groups, includes vehicle treated, apoptotic and necrotic cells, was performed with the *metaP* server. Red indicates increase, green decrease and gray no changes in metabolite concentrations in comparison to vehicle treated cells. Name of abbreviated metabolites are given in the body text.

| | | <i>Ala</i> | <i>Arg</i> | <i>Asp</i> | <i>Glu</i> | <i>Gly</i> | <i>Leu</i> | <i>Met</i> | <i>Phe</i> | <i>C2</i> | <i>C3</i> | <i>C5</i> |
|-----------------|----------------|------------|------------|------------|------------|------------|------------|------------|------------|-----------|-----------|-----------|
| 72h_Eto | A_HEK | Red | Red | Red | Red | Green | Gray | Gray | Gray | Red | Gray | Gray |
| | N_HEK | Gray | Red | Red | Green | Green | Green | Green | Green | Green | Green | Green |
| 72h_5-Fu | A_HEK | Red | Red | Red | Red | Green | Gray | Green | Green | Red | Red | Red |
| | N_HEK | Gray | Red | Red | Green | Green | Green | Green | Green | Green | Green | Gray |
| 24h_Eto | A_HepG2 | Red | Red | Red | Gray |
| | N_HepG2 | Red | Red | Gray | Gray |
| 48h_5-Fu | A_HepG2 | Red | Red | Gray | Gray |
| | N_HepG2 | Red | Red | Red | Green | Green | Red | Red | Red | Gray | Gray | Gray |

The metabolites showing the same trend in both cell lines regardless of the used apoptotic agent were broader analyzed. Changes occurred in concentrations of alanine, arginine, glutamate and acetylcarnitine are presented in **Figure 16**. The differences in metabolite concentrations in control, apoptotic and necrotic cells were tested for significance by Kruskal-Wallis analysis on the *metaP* server and the p-value (*) denote significance levels of 5% after Bonferroni correction. Apoptotic HEK 293 exhibited a trend clearly distinguishing them from necrotic and control cells in all four metabolites. In contrast, characteristic patterns of apoptotic HepG2 cells were found only after 5-Fu treatment in the alanine and glutamate concentrations. The etoposide treated HepG2 cells can be discriminated from the necrotic only by metabolite concentrations but not by patterns.

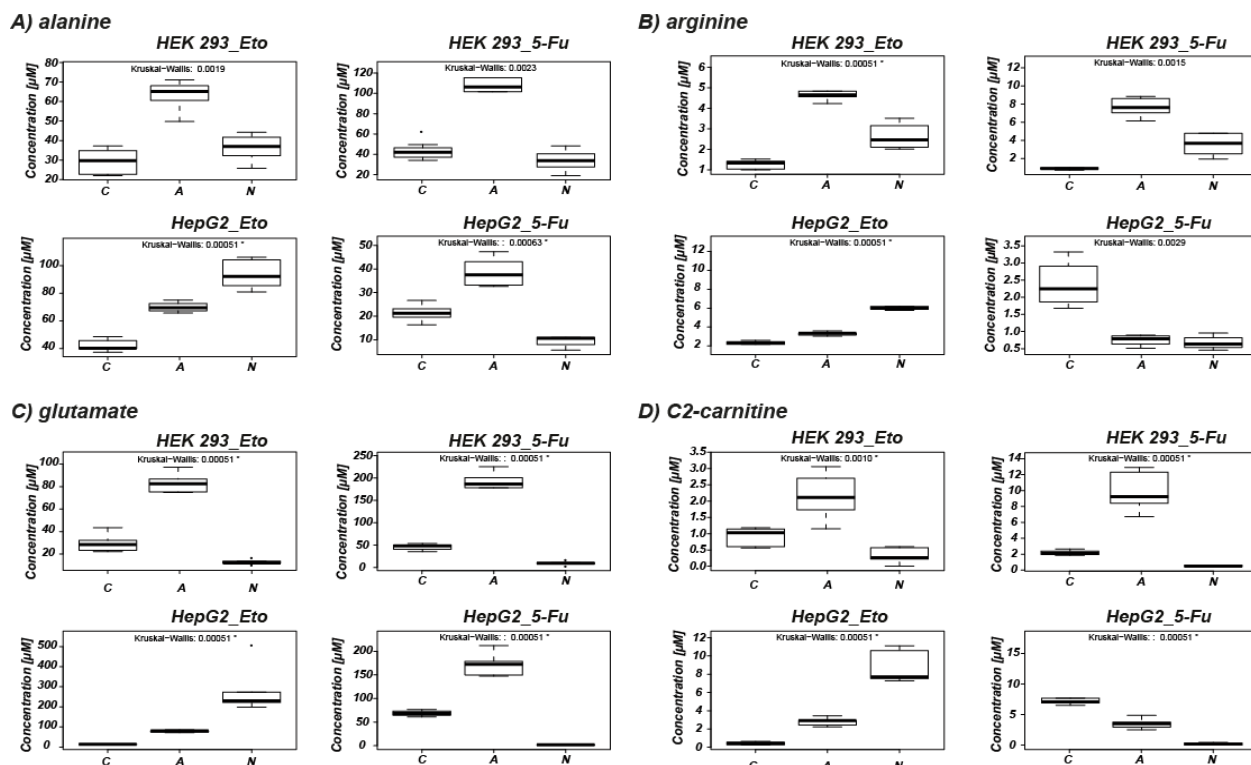


Figure 16 Metabolite concentrations of HEK 293 and HepG2 cells after heating or treatment with etoposide or 5-Fu. Metabolite concentrations of HEK293 and HepG2 cells: heated (N), treated with DMSO (C) or pro-apoptotic agents (etoposide – Eto or 5-Fluorouracil – 5-Fu) were compared. HEK 293 cells were incubated for 72 h independent on pro-apoptotic agent and etoposide or 5-Fu treated HepG2 cells for 24 h and 48 h, respectively. The box-plots, obtained after statistical data analysis with the *metaP* server demonstrate the medians out of two independent experiments carried out in triplicates. The p-value calculated by using Kruskal-Wallis are given in each diagram, “*” denotes a significance level of 5% after Bonferroni correction.

3.2.3 Alanine and glutamate distinguish apoptotic cells regardless of treatment

To find biomarkers of apoptosis independently of the treatment, the metabolic patterns occurring in HEK 293 and HepG2 cell lines after treatment with staurosporine were compared to those obtain after etoposide or 5-Fu treatment. Only alanine and glutamate out of measured 42 metabolites could be considered as metabolic biomarkers of apoptosis. The alanine, a non-essential amino acid which can be produced by reductive amination of pyruvate, was detected as significantly up-regulated in apoptotic HEK293 and HepG2 cells after cells were incubated either with staurosporine or etoposide or 5-

Fu. Furthermore, in both cell lines regardless of the used apoptotic agent a significant increase in glutamate, a key component in cellular metabolism, has been observed.

3.3 Adipogenesis “pathfinding” - first step toward novel biomarkers in development of obesity

The ongoing explosion in the incidence of obesity (Rosen, Walkey et al. 2000), has focused attention on adipose tissue - emerging in the last two decades as key endocrine and regulatory organ of integrated fuel homeostasis (Herman, She et al. 2010). However, the mechanisms and involved metabolic pathways regulating adipogenesis – development of a fat cell from preadipocytes - still remain elusive. The murine preadipocyte cell line 3T3-L1, originally generated in the 1970's by Green and colleagues (Green and Meuth 1974), has been used in studies of adipogenesis, obesity and insulin resistance (Williams and Mitchell 2012); (Sakoda, Ogihara et al. 2000) over the last 35 years. The 3T3-L1 can be easily differentiated into adipocyte after treatment with hormonal mixture. (Green and Kehinde 1975) and have all three attributes of *in vivo* adipocytes including lipid storage, insulin sensitivity and endocrine properties (White and Stephens 2010). For that reason the 3T3-L1 cell line was used to uncover the biochemical processes of adipogenic cell differentiation and to find novel relevant biomarkers. **Figure 17** illustrates the experimental design and all sampling procedures applied at different days of adipogenic 3T3-L1 differentiation. Cells were cultivated from preadipocytes to adipocytes during 18 days and samples were collected at different stages of adipogenesis. Post-confluence, labeled 0 (depicted in white) indicates post-confluent adipocytes cultivated in unmodified DMEM medium for 96 hours (with medium exchange every 48 hours) – this stage is called day zero. Differentiation, labeled 2 and 4 (depicted in light yellow) indicates cells treated with a hormonal mixture (insulin, dexamethasone (DEX) and 3-isobutyl-1 methyl xanthine (IBMX)) inducing adipogenic cell differentiation (treatment inducing differentiation started at day zero). Maturation, labeled 6, 8, 10, 14 and 18 (depicted in dark yellow) indicates cells stimulated only by insulin (treatment for maturation started at day 4).

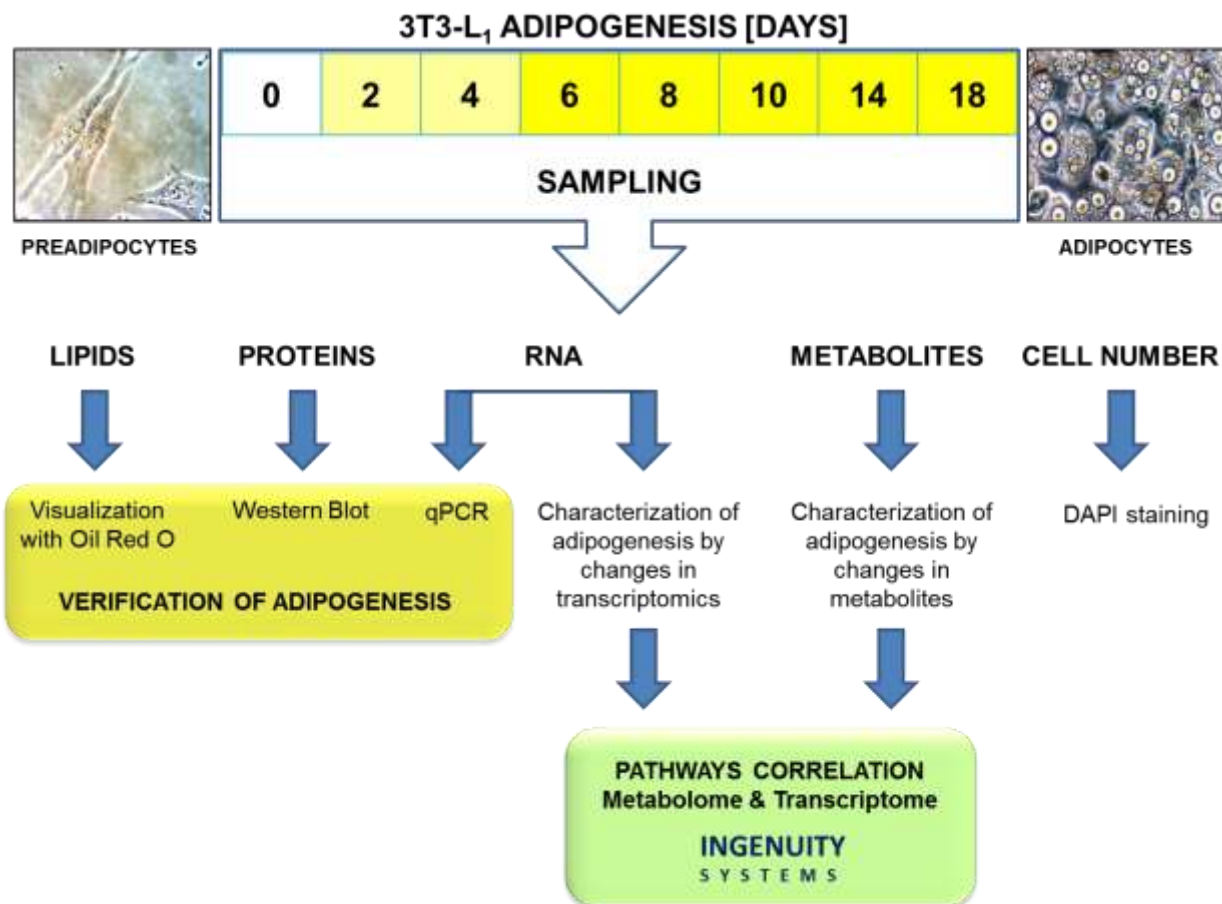


Figure 17 Illustration of the experimental work flow to monitor adipogenesis. The 3T3-L1 cell line preadipocytes were differentiated into adipocytes during 18 days. The cell differentiation, induced by insulin (10 $\mu\text{g/ml}$), dexamethasone (1 μM) and IBMX (0.5 mM), started at day 0, corresponding to the preadipocytes in post-confluent phase, and was ongoing until day 4. The maturation started at day 4 by cell treatment with insulin (10 $\mu\text{g/ml}$) only. At each given day progression in cell differentiation was documented by Oil Red O assay and cells were collected for Western blot analysis, qPCR, transcriptomics and metabolomics study. DAPI staining was implemented to monitor cell proliferation. Metabolites measurements were performed with the Absolute IDQ assay and transcriptomics with the Illumina BeadChip technology. The conditioned medium was changed every 48 h.

3T3-L1 adipogenesis was verified by Oil Red O assay, directly monitoring lipid accumulation, as well as by expression analysis of known regulated during adipogenesis molecules (White and Stephens 2010), on transcriptional (quantitative PCR) and translational (Western blot) level. To understand adipogenesis on the metabolite level, high-throughput targeted metabolomics was used to analyze acylcarnitines, amino acids, biogenic amines, hexoses, sphingomyelins, glycerophospholipids, fatty acids and prostaglandines in conditioned medium and cells. Cell homogenates were prepared for

metabolite measurement according to the novel protocol described in **chapter 3.1.3**. DAPI staining was carried out in parallel experiments to determine cell proliferation during adipogenesis and for normalization purposes. Gene expression profiling, based on Illumina Bead Array Technology, was carried out after total RNA extraction. This Bead Chip allows for parallel examination of over 19,100 unique genes. Transcriptomics and metabolomics data sets were combined to study crucial pathways and to find novel metabolic biomarkers of adipogenesis. The data sets were analyzed using Ingenuity Systems IPA software for pathway analysis. Detailed results are presented in the following chapters.

3.3.1 Monitoring of adipogenesis by Oil Red O assay

Adipogenesis progression, represented by increasing fat accumulation in cell liposomes, was monitored in the 3T3-L1 cell line by Oil Red O staining. **Figure 18 A** demonstrate the changes in cell morphology from preadipocytes, having fibroblast characteristics with branched cytoplasm surrounding and elliptical blotchy nucleus, into mature adipocytes, spherical cells containing lipid droplets. In the post-confluence phase described as day 0 the cellular growth is repressed, cells formed a monolayer but accumulation of fat droplets was not detected. Cells incubated for 48 hours with differentiation mixture exhibited a different morphology from post-confluent cells. Nevertheless, cells at day 2 were similar to fibroblasts but fat accumulation could not yet be observed. In contrast, at day four cells acquired the morphological characteristics of adipocytes, by showing up with an enlarged, rounded cell shape with accumulation of small lipid droplet. Those early steps are usually followed by the appearance of PPAR γ , C/EBP α and C/EBP β activating *de novo* or enhanced expression of genes that are characteristic for the adipocyte phenotype (MacDougald and Lane 1995), (Linhart, Ishimura-Oka et al. 2001) (also observed in this study see **chapter 3.3.2**). The stepwise increase of lipid accumulation detected first at day 4 was continued within the following days. Noteworthy, between day 6 and day 10 cells contained many small lipid droplets, which reconfigured to one or two big ones at day 14 and day 18. Quantification of Oil Red O staining was examined by absorbance measurements after the dye was dissolved in

isopropanol. **Figure 18 B** shows a step by step increase of the Oil Red O accumulation, starting after day 4 and reaching a maximum at day 18.

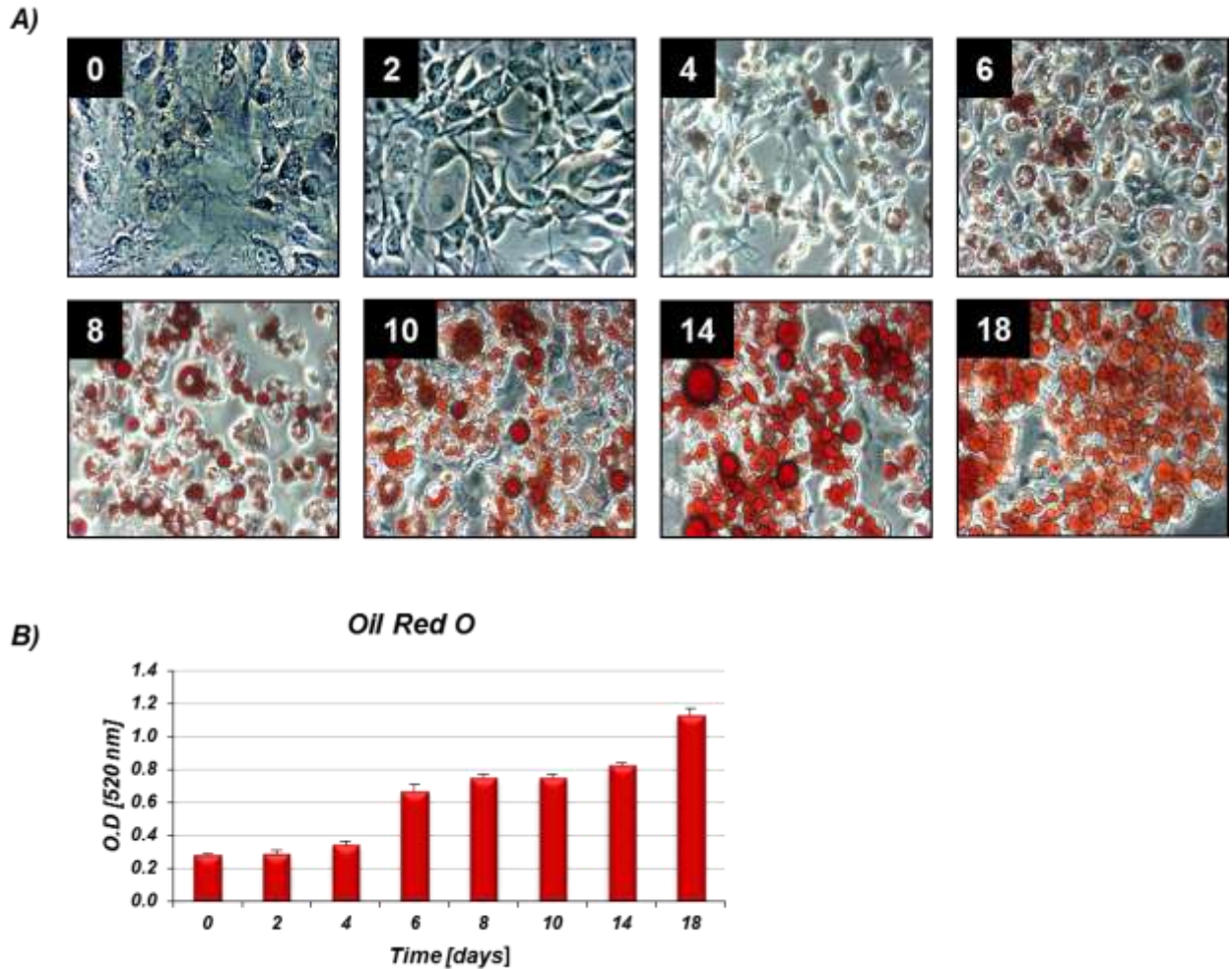


Figure 18 Monitoring of adipogenesis with Oil Red O assay. A) Cells were fixed and stained with Oil Red O at different days of 3T3-L1 differentiation. Photos were taken at initial magnifications $\times 200$. The red spots indicate triglyceride droplets. **B)** Quantification of accumulated lipids based on absorbance measurements (O.D. values at 520 nm) after Oil Red O was eluted from cells by isopropanol. Data are expressed as mean values (\pm SD) out of three independent experiments performed in triplicates.

3.3.2 Verification of adipogenesis by monitoring of crucial transcription factors promoting adipogenesis

Morphological transformation of fibroblasts to spherical, lipid droplets containing cells is caused by molecular changes during adipogenesis. Crucial transcription factors, which promote adipogenic differentiation are well characterized (Rosen and MacDougald 2006) and were used here for the verification of adipogenesis on the gene and protein level. The amounts of C/EBP α , C/EBP β and PPAR γ were determined by real-time quantitative PCR with SYBER Green detection and relative amounts of those genes were calculated using the $2^{-\Delta\Delta CT}$ equations. C/EBP β , C/EBP α and PPAR γ (1 and 2) protein concentrations in cell homogenates were measured by Western blot analysis. **Figure 19** shows changes in gene expression and protein level of peroxisome proliferator-activated receptor γ (PPAR γ) and the CCAAT/enhancer binding proteins (C/EBP) β and α during 3T3-L1 cell differentiation.

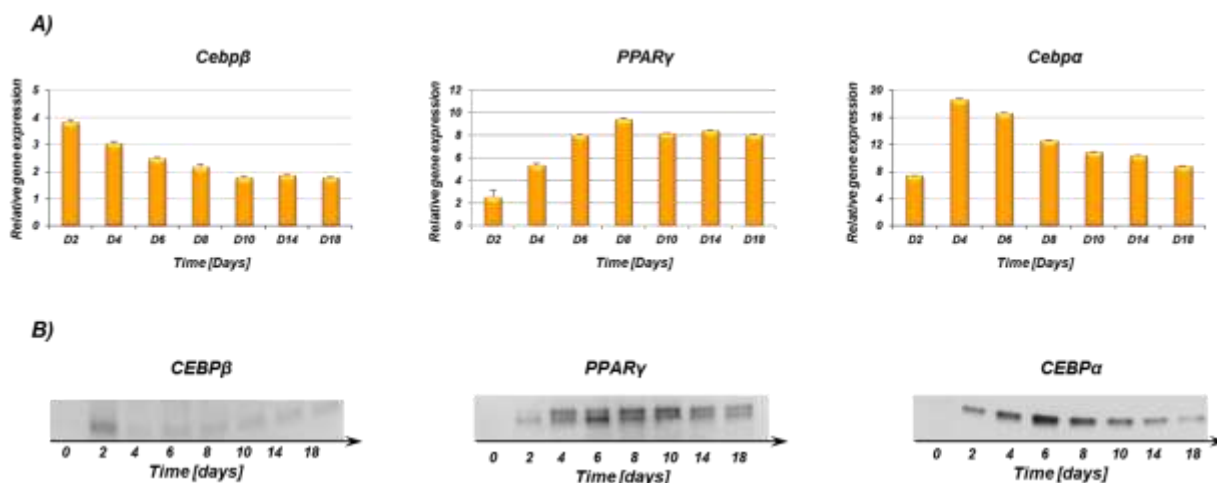


Figure 19 Adipogenesis verification: regulation of C/EBP β , PPAR γ and C/EBP α expression. **A)** qPCR was performed on cDNA generated by using RNA isolated from cell pellets. The relative gene expression was calculated by using the $2^{-\Delta\Delta CT}$ method. **B)** Western Blots were performed after protein isolation from cell pellets at different days of adipogenesis. β -actin was used as a loading control (data not shown).

As expected, after exposure of confluent preadipocytes to the “hormonal cocktail”, regulation of C/EBP β , C/EBP α and PPAR γ on transcriptional and translational level was

observed. The C/EBP β , primarily responding to DEX (Ntambi and Young-Cheul 2000), reached maximum at day two of differentiation and decreased after removal of differentiation mixture to less than two of $2^{-\Delta\Delta CT}$. The expression of PPAR γ thought to be mediated by C/EBP β (Clarke, Robinson et al. 1997), was found to be transcriptionally induced after D2 post treatment, reached a maximum at day 8 and stayed highly up-regulated until D18 of adipogenesis. Furthermore, C/EBP α increased from undetectable levels in preadipocytes to detectable at D2 and reached full expression at D4 post-stimulation. Expression on the protein level followed the same pattern as the on the transcript level.

3.3.3 Monitoring of adipogenesis by metabolomics

Characterization of adipogenesis in 3T3-L1 cell line on the metabolite level was performed using the high-throughput targeted metabolomics Absolute IDQ p180 kit in conditioned medium and cells from three independent experiments carried out in triplicates. Statistical calculations of normalized data were performed using the *metaP* server. At first, a Kendall analysis, tests the correlation between two quantities (Kastenmüller, Römisch-Margl et al. 2010), visualized in heat maps, was used to examine the relationship between changes in metabolite concentrations and the time course of adipogenesis or experimental procedure (sample replication) in both medium **Figure 20 A** and cells **Figure 20 B**. Correlations between variables are represented by gradient of color intensities. A positive relation in the plots, indicating increase, is shown in green, a negative relation (decrease) is depicted in red and not related variables are represented by black. Generally, changes in metabolite concentrations were mostly dependent on the adipogenic cell differentiation and not on the experimental procedure. Adipogenesis strongly affected metabolite concentrations in conditioned medium as well as in cell lysates resulting in characteristic patterns, however with some similarities. For example, some glycerophospholipids, like phosphatidylcholines, PC ae C34 with several saturation variants, and lysophosphatidylcholines in particular those containing palmitic acid (C16:0), palmitoleic acid (C16:1) or heptadecanoic acid (C17:0) as well as amino acids like serine and branched chain amino acids, exhibited similar trends in conditioned

medium and in cell lysates. In contrast, opposite patterns of alanine, acetylcarnitine (C2), butyrylcarnitine (C4) or alpha-aminoadipic acid (alpha-AAA) between conditioned medium and cell lysate have been observed. Correlation between adipogenesis and arachidonic acid, mead acid and lysophosphatidylcholines in particular containing eighteen-carbon fatty acid chain with two different saturation variants (C18:1 and C18:2) were found only in cells. In turn, strong correlation of hexoses and aspartate with adipogenesis was observed only in case of medium samples.

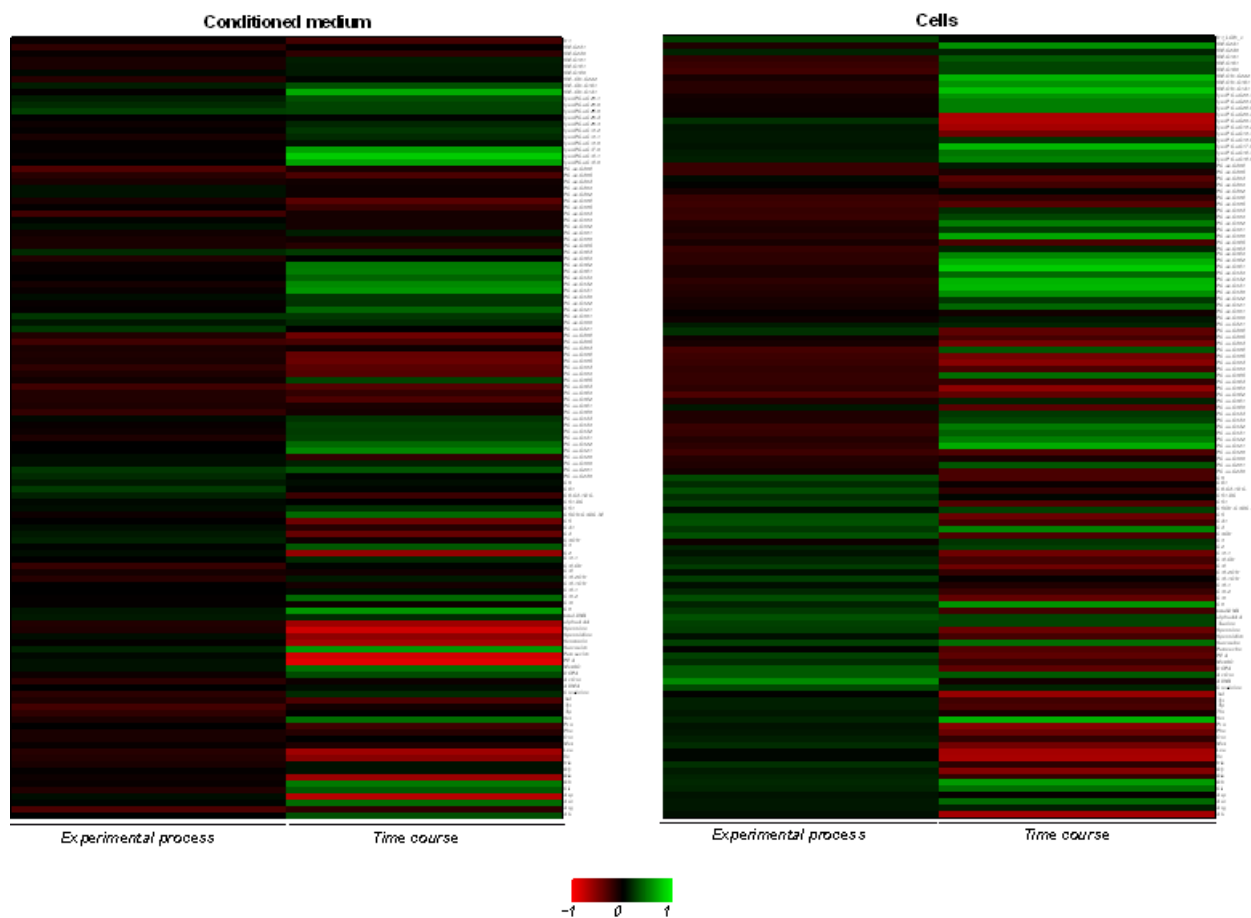


Figure 20 Correlation between metabolite concentration and adipogenesis progression (time course) or correlation between changes in metabolite concentration and experimental procedure. The Kendall correlation between each metabolite concentration and adipogenic cell differentiation or experimental procedure in medium and cells was determined by the *metaP* server. The Kendall's tau values were visualized in the heat maps. The colors and their intensities are linked to the correlation: green indicate positive, red negative and black no correlation.

However, Kendall correlation assay showed only a trend but did not provide information about the differences in metabolite composition at different stages of adipogenesis. For

that reason, principle component analysis (PCA) has been applied. **Figure 21** shows medium and cell samples at different days of adipogenesis (colored dots) after PCA analysis represented by scatterplots of principal compound (PC) 1 vs. 3. Separation among days of adipogenesis with tight clustering of biological replicates could be observed, which is in good agreement to the Kendall correlation results. Thus, metabolites can clearly reflect adipogenesis development with firmly separated stages: not differentiated, adipogenic differentiated and matured adipocytes. The PCA represents combinations of the original dimensions (metabolites), whose contributions to the component can give hints which metabolites separate the intrinsic groups (Kastenmuller, Romisch-Margl et al. 2011). **Figure 22** presents metabolites, after PCA analysis of PC1, with the highest contribution to adipogenesis in form of box-plots.

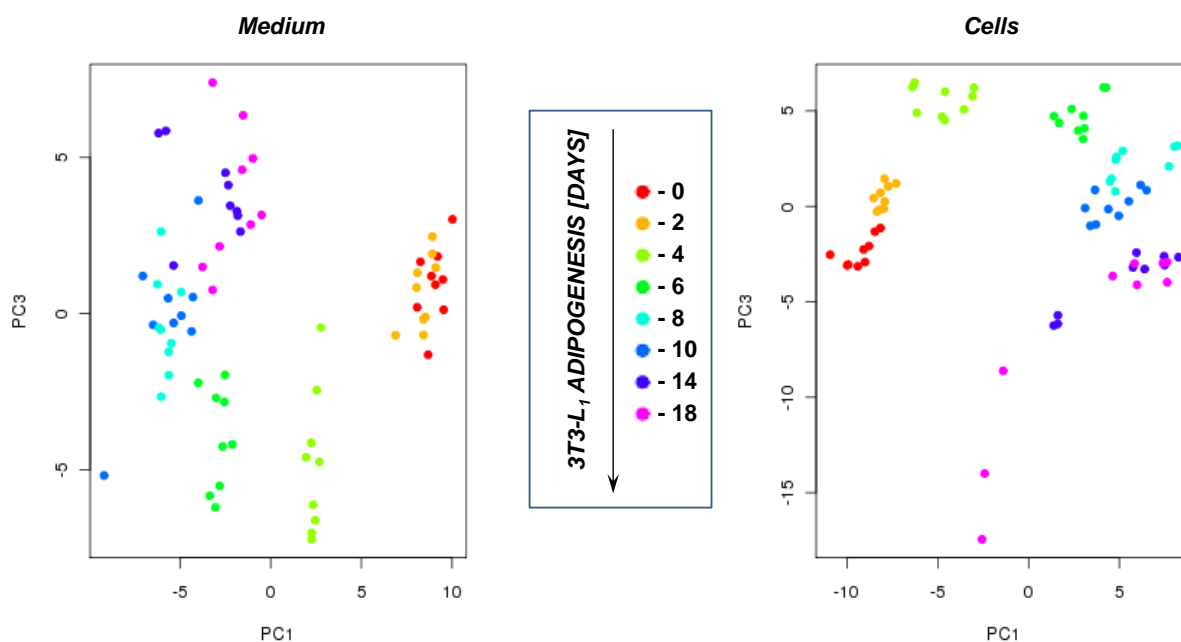


Figure 21 Different stages of adipogenesis distinguished by metabolite patterns. The PCA score plots determined by the *metaP* server showed distinct clustering between stages of adipogenesis in conditioned medium and cells. Colored dots in the PCA plots representing metabolite profiles observed at different days of differentiation: red – day 0, orange – day 2, light green – day 4, dark green day 6, light blue - day 8, dark blue – day 10, violet – day 14 and pink – day 18.

Generally, significantly regulated metabolites which were found in condition medium and cells represented different metabolic classes. The strongest changes in metabolite

concentrations were observed in cells switching from differentiation to maturation (between day 4 and 6) stage. Adipogenesis progression resulted in increased concentration of asparagine, glutamine, lysophosphatidylcholine (LysoPC a C16:0) and phosphatidylcholine (PC aa C32:1) in medium and aspartate and phosphatidylcholine (PC aa C32:2 and PC aa C34:2) in cells.

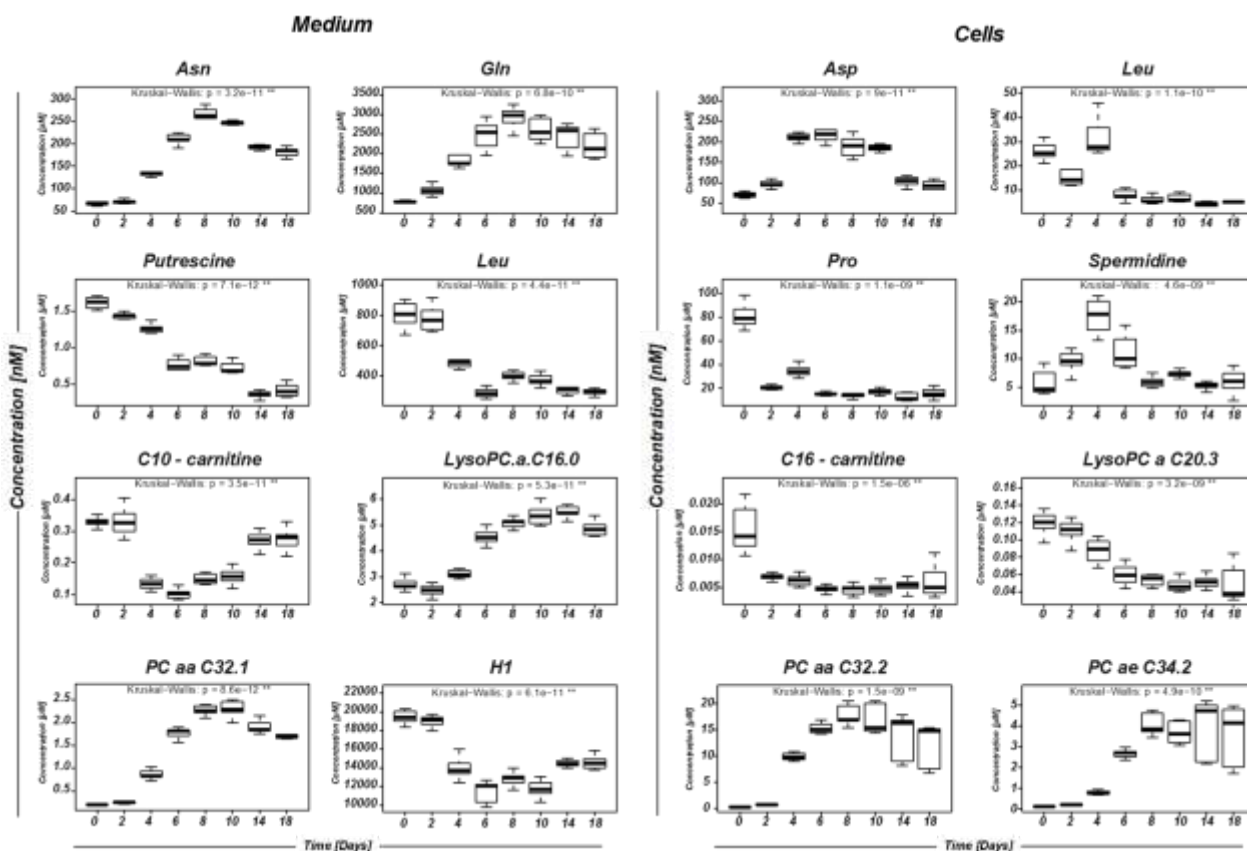


Figure 22 Metabolites regulated during adipogenesis highlighted by PCA analysis. The specific metabolites for adipogenesis progression in conditioned medium and cells determined by PCA analysis include asparagine (Asn), glutamine (Gln), leucine (Leu), putrescine, decadienyl-L-carnitine (C10-carnitine), glycerophospholipids like LysoPC a C16:0 or PC aa C32:1 and hexoses in medium and aspartate (Asp), leucine (Leu), proline (Pro), spermidine, hexadecanoylcarnitine (C16-carnitine) and glycerophospholipids include LysoPC a C20:3, PC aa C32:2 and PC ae C34:2 in cells. The box-plots, obtained after statistical data analysis with the *metaP* server demonstrate the medians out of two independent experiments carried out in triplicates. The p-value calculated by using Kruskal-Wallis are given in each diagram, “*” denotes a significance level of 5% and “***” a significance level of 1% after Bonferroni correction.

Moreover, in conditioned medium significant decreases of putrescine, leucine, decanoylcarnitine (C10) and hexoses (H1) were detected. Furthermore, in intracellular

extracts significant decreases of proline, palmitoylcarnitine (C16) and lysophosphatidylcholines (LysoPC a 20:4) were found. The patterns displayed by leucine during adipogenesis were remarkable. The cells entering the differentiation phase (at day 2) exhibited significant decrease in leucine (only in cells).

Further differentiation (at day 4) in turn, resulted in leucine increase in cells (to control level) but a significant decrease in conditioned medium. In the maturation phase both cells and conditioned medium showed a significant decrease in the leucine level. Those observations suggest efforts of the cell to preserve a constant leucine concentration.

3.3.4 Monitoring of adipogenesis by transcriptomics

3.3.4.1 RNA concentration and integrity

To analyze expression profiling of the 3T3-L1 cell line during adipogenesis, samples were collected in three biologically independent replicates and total RNA of all samples were isolated using RNeasy Kit. Prior to expression profiling the concentrations of total RNA from all samples were measured with NanoDrop spectrometer (**Table 9**) and integrity was assayed by denaturing gel electrophoresis and ethidium bromide staining (**Figure 23**). The RNA obtained in the concentration range of 260 to 1300 ng/ μ L was diluted for further experiments.

Table 9 RNA concentration and absorption ratios OD_{260}/OD_{280} of 3T3-L1 cells during adipogenesis. Total RNA concentration expressed in ng/mL was determined by spectrophotometric absorbance measurements at 260 nm and the ratio of absorbance at 260 nm and 280 nm (OD_{260}/OD_{280}) was used to assay the RNA purity.

| Time [days] | Experiments | | | | | |
|-------------|---------------------------------|------------|---------------------------------|------------|---------------------------------|------------|
| | 1 | | 2 | | 3 | |
| | RNA concentration [ng/ μ L] | OD 260/280 | RNA concentration [ng/ μ L] | OD 260/280 | RNA concentration [ng/ μ L] | OD 260/280 |
| 0 | 260 | 2.14 | 288 | 2.13 | 319 | 2.12 |
| 2 | 680 | 2.11 | 531 | 2.12 | 678 | 2.14 |
| 4 | 1116 | 2.13 | 1008 | 2.13 | 1304 | 2.14 |
| 6 | 1004 | 2.13 | 994 | 2.13 | 1077 | 2.12 |
| 8 | 972 | 2.14 | 1018 | 2.14 | 961,2 | 2.14 |
| 10 | 808 | 2.14 | 762 | 2.13 | 908,9 | 2.13 |
| 14 | 638 | 2.13 | 626 | 2.13 | 660 | 2.12 |
| 18 | 754 | 2.12 | 719 | 2.12 | 676,9 | 2.12 |

The ratios of absorbance (260 and 280) used to assess the RNA purity, were comparable with 2.1, the OD 260/280 ratio of pure RNA. Furthermore, the RNA integrity assay showed sharp, distinct bands corresponding to 28S and 18S ribosomal RNA and little smear indicating an intact RNA. As desired, the 28S band was approximately twice as intense as that of 18S RNA. Gene expression profiling was performed by using the Illumina Bead Array Technology. The resulting subset consisted of 1000 significantly regulated genes. Before further analysis, the data set was screened for previously described transcription factors promoting adipogenesis, to verify transcriptomics results (Rosen and MacDougald 2006).

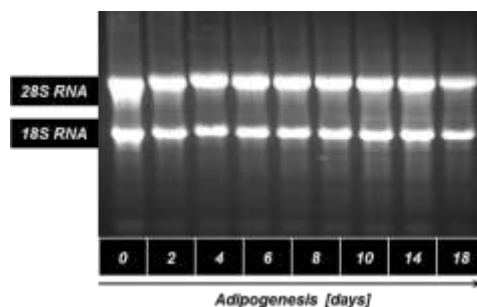


Figure 23 Electrophoresis of total RNA from 3T3-L1 cells during adipogenesis. The RNA integrity was confirmed by running the RNA on a denaturing gel and staining by ethidium bromid. Each number indicates the respective day of adipogenesis. The bands as indicated show 28S and 18S RNA. The band intensity of the 28S is twice that of 18S suggesting good quality and integrity of RNA.

A complex transcriptional cascade is shown in **Figure 24 A**, representing gene products and their known interactions (Rosen and MacDougald 2006), during adipogenesis and includes C/EBP α , C/EBP β and PPAR γ , Kruppel-like factors (KLF5 and KLF15), insulin-sensitive glucose transporter (GLUT4), GATA binding protein 2 (GATA2) and transcription factor homologous to CCAAT – enhancer binding protein (CHOP). Indeed, six of these eight transcription factors, namely PPAR γ , KLF5, KLF15, GATA2, CHOP and GLUT4, were found in the set of 1000 significantly regulated genes. The main direction of regulation is shown in **Figure 24 A**: the red color indicates up-regulation and the green down-regulation of these genes. When looking closer at the regulation during the time course of adipogenesis (**Figure 24 B**), KLF5, stimulated by C/EBP β (Oishi, Manabe et al. 2005), was as expected strongly expressed in the first days of adipogenic cell

differentiation. Moreover, KLF15, involved in stimulation of lipid accumulation (Mori, Sakaue et al. 2005), (Banerjee, Feinberg et al. 2003) due to PPAR γ induction and regulation of GLUT4 (Gray, Feinberg et al. 2002) was up-regulated at day 4 and continuously within the following days. PPAR γ , plays an important role in converting preadipocytes into adipocytes (Rosen, Walkey et al. 2000), as well as GLUT4 having energetic/metabolic functions in adipocytes by allowing glucose transportation into the cell (Shepherd and Kahn 1999). These genes were highly expressed from day 2 and 4 on, respectively. The anti-adipogenic factors like GATA2 or CHOP, able to inhibit cell differentiation by binding to C/EBP α or PPAR γ (Tong, Tsai et al. 2005), (Ron and Habener 1992), were down-regulated.

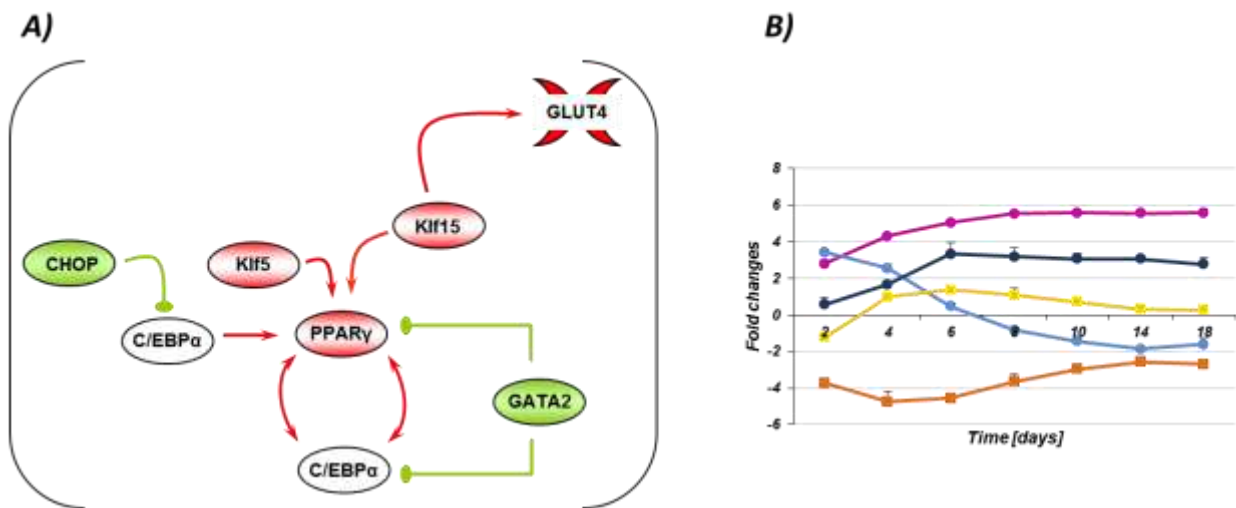


Figure 24 Identification and monitoring of genes known to be involved in adipogenesis – verification of transcriptomics data. A)

Genes and their interactions during cell differentiation from preadipocytes into adipocytes are shown and stimulatory (red) as well as inhibitory (green) interactions are indicated. The green colored genes GATA2 and CHOP refer to decrease and the red colored genes KLF5, KLF15, PPAR γ and insulin-sensitive glucose transporter (GLUT4) indicate increase in expression during the adipogenesis in my experimental setup. **B)** Gene expression values of KLF 5 (light blue), KLF 15 (dark blue), PPAR γ (violet), GATA2 (orange) and CHOP (yellow) presented as fold changes relative to the gene expression of untreated cells (preadipocytes in postconfluent phase). Pro-adipogenic genes are represented by colored circles and anti-adipogenic by colored squares. Data are expressed as mean values of three independent experiments (\pm SD).

In the next step clustering of the ~1000 significantly regulated genes was performed according to functional genomics: genes which shows similar expression profiles (co-expressed genes) are mostly regulated by the same mechanism (co-regulated genes)

(Eisen, Spellman et al. 1998, Lubovac and Olsson 2003). The associated gene transcripts were organized in 6 clusters including 3 with differentially up-regulated and 3 with down-regulated genes (**Figure 25**).

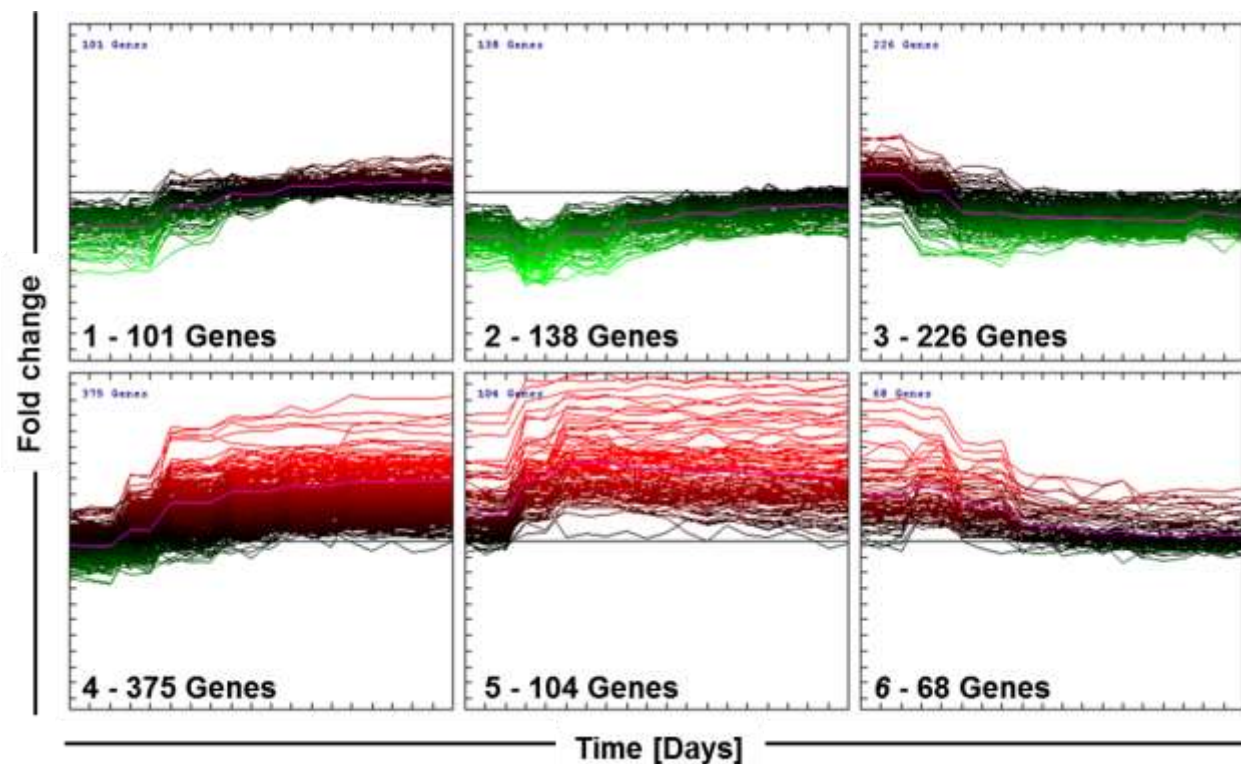


Figure 25 Expression patterns of differently regulated genes. Significantly regulated genes (1012) were clustered into 6 groups. Green color depicted down-regulation, red up-regulation and black no regulation. The magenta colored lines denote regulation trend.

Separately assigned clusters were classified into functional categories with Ingenuity Pathways Analysis (IPA) (**Figure 26**). Cluster 1 contains genes down-regulated mostly at day 2 and day 4 of differentiation and referred to molecules observed in several cancer categories, like adenocarcinoma, head and neck cancer or nervous system tumor. Genes falling into the cluster 2 and 3 were found to be down-regulated at day 2 and increased then until day 14 or were slowly down-regulated until day 6 and remained down until day 18, respectively. Those transcripts are mostly related to decreased proliferation (caused by cell to cell contact effects (MacDougald and Lane 1995) or decreased organization of cytoplasm and cytoskeleton (Smas and Sul 1995), (Kubo, Kaidzu et al. 2000). Analysis of clusters 4 and 5, include mostly up-regulated genes with

several important biological functions involved in adipogenic cells differentiation.

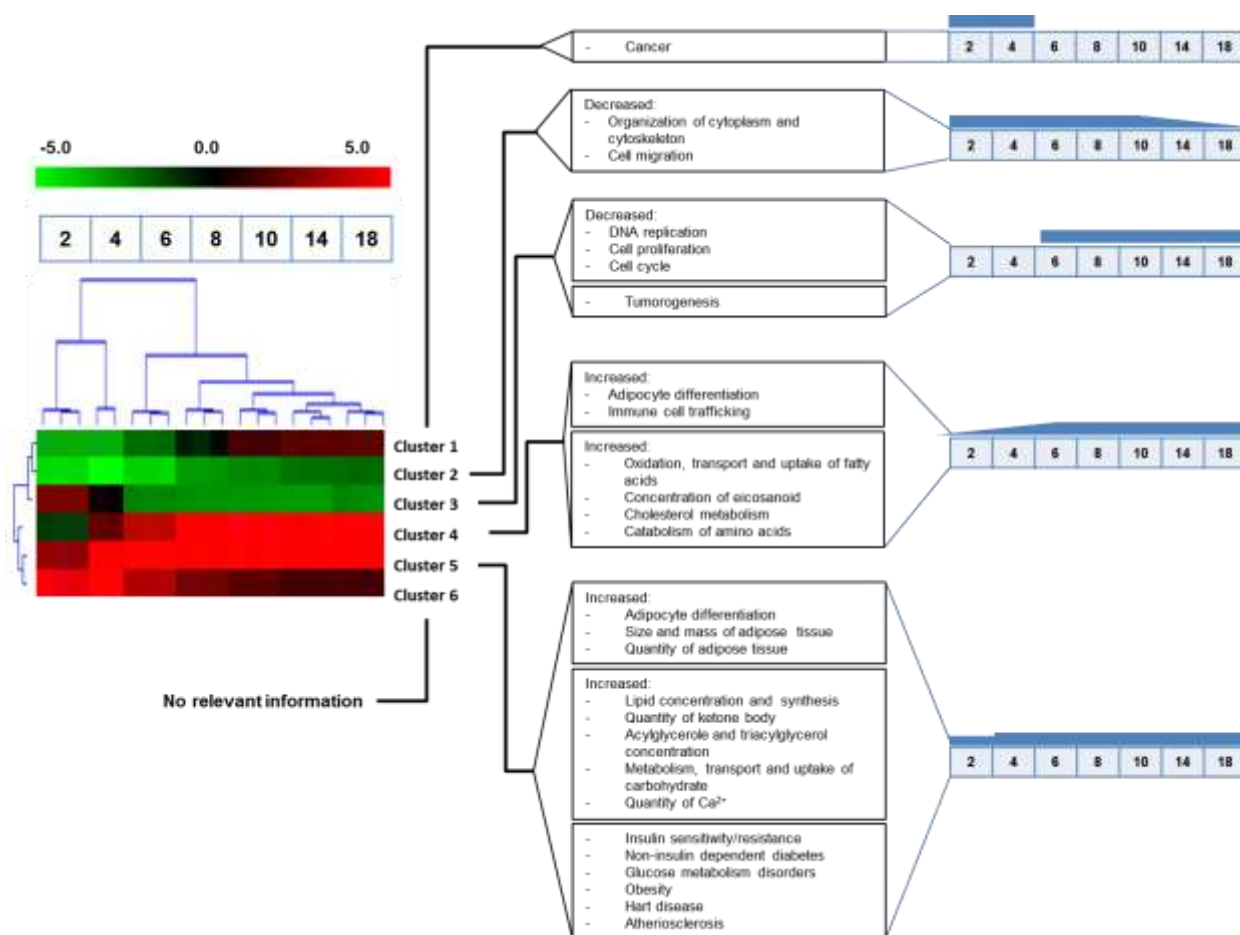


Figure 26 Functional classifications of gene clusters. Classification of genes was performed by using Ingenuity Pathways Analysis (IPA). Left panel: partial hierarchical clustering of gene expression profiles of differentiated 3T3-L1 cells. Numbers in squares denote days of adipogenesis. Right panel: The blue bars above differentiation days illustrate level of gene regulation at the different days of adipogenesis. For example: Cluster 1 contains genes mostly regulated at day 2 and 4 involved in different cancer types.

Cluster 5 contains crucial transcription factors and genes participating in early adipogenesis like PPAR γ , or stearyl-CoA 9-desaturase (SCD) (Casimir and Ntambi 1996) in contrast to cluster 4 in which the up-regulated genes mostly participate in cell maturation, like glycogen phosphorylase kinase (PHK) (Ross, Erickson et al. 2002) or ATP binding cassette subfamily G (ABCD2) (Liu, Sabeva et al. 2010). Furthermore, both clusters show the abundance of genes involved in basic metabolic pathways: especially genes linked to fatty acid and cholesterol metabolism were found in cluster 4 and genes involved in lipid synthesis (acylglycerol and triacylglycerol) as well as carbohydrate

uptake, transport and metabolism in cluster 5. Moreover, genes linked to insulin resistance, non-insulin dependent diabetes, atherosclerosis and obesity were detected in cluster 5. However, regulation of these latter genes was remarkable, according to contrary expression patterns observed in type 2 diabetes patients and obese individuals (Shepherd, Gnudi et al. 1993, Fasshauer, Klein et al. 2002).

Table 10 Shift of functional networks during adipogenesis. Impact of adipogenesis on the functional networks, created with regard to all significantly regulated genes, was analyzed with IPA. The height of the blue bar at the bottom of the table reflects which of the referred pathways are effected to which extend on the different days of adipogenesis.

ASSOCIATED NETWORK FUNCTIONS

| | | | | | |
|----|--|---|--|---|---|
| 2 | Cell-To-Cell Signaling and Interaction, Tissue Development, Cellular movement | Cancer, Cellular growth and Proliferation, Gastrointestinal disease | Cellular Development, DNA replication, Recombination and Repair, Cellular Movement | Energy Production, Lipid Metabolism, Small Molecule Biochemistry | Lipid Metabolism, Small Molecule Biochemistry, Vitamin and Mineral Metabolism |
| 4 | Cardiovascular System development and Function, Organismal Development, Tissue Development | Cellular Development, Cellular growth and Proliferation, Gene Expression | Cellular Movement, Immune Cell Trafficking, Hematological System Development | Cellular Movement, Immune Cell Trafficking, Organismal Injury and Abnormalities | Inflammatory Response, Cellular Movement, Hematological System Development |
| 6 | Carbohydrate Metabolism, Molecular Transport, Small Molecule Biochemistry | Cellular Movement, Immune Cell Trafficking, Hematological System Development | Cellular Movement, Cell-To-Cell Signaling and Interaction, Tissue Development | Nutritional Disease, Connective Tissue Disorders, Genetic Disorders | Energy Production, Lipid Metabolism, Small Molecule Biochemistry |
| 8 | Cellular Development, Connective Tissue Development, Lipid Metabolism | Organismal Development, Developmental Disorder, Sceletal and Muscular Disorders | Cellular Movement, Hematological System Development, Immune Cell Trafficking | Lipid Metabolism, Small Molecule Biochemistry, Molecular Transport | Cancer, Cellular growth and Proliferation, Cellular Movement, Cell Death |
| 10 | Lipid Metabolism, Small Molecule Biochemistry, Vitamin and Mineral Metabolism | Endocrine System Disorders, Metabolic Disease, Carbohydrate Metabolism | Cellular Movement, Hematological System Development, Immune Cell Trafficking | Lipid Metabolism, Small Molecule Biochemistry, Molecular Transport | Cellular growth and Proliferation, Cellular Movement, Cell Death |
| 14 | Lipid Metabolism, Small Molecule Biochemistry, Vitamin and Mineral Metabolism | Energy Production, Lipid Metabolism, Small Molecule Biochemistry | Cellular Movement, Hematological System Development, Immune Cell Trafficking | Embrionic Development, Organismal Development, Tissue Development | Lipid Metabolism, Molecular Transport, Small Molecule Biochemistry |
| 18 | Lipid Metabolism, Small Molecule Biochemistry, Vitamin and Mineral Metabolism | Carbohydrate Metabolism, Molecular Transport, Small Molecule Biochemistry | Lipid Metabolism, Small Molecule Biochemistry, Organ Morphology | Energy Production, Lipid Metabolism, Small Molecule Biochemistry | Lipid Metabolism, Small Molecule Biochemistry, Molecular Transport |

Genes from cluster 6, after IPA analysis, could not be assigned to any functional category or canonical pathway. Additionally to cluster analysis, the complete data (including all clusters) were analyzed in context of transcriptomics changes associated with functional networks occurring at different stages of adipogenesis. The top hit networks (5 networks for each day of adipogenesis) are shown in

Table 10 and indicate the importance of cellular signaling and development in the first day of differentiation (day 2 and 4). Nevertheless, molecules linked to energy production and lipid metabolism networks were also present at those days. Noticeable, a major shift in functional networks started at day 6, with the highest impact of carbohydrate metabolism, molecular transport and small molecule biochemistry. In mature adipocytes (day 10 to day 18) mostly lipid metabolism related networks were observed.

3.3.5 Pathway interferences: where metabolomics meet transcriptomics

Combining gene expression microarray and high-throughput targeted metabolomics technologies allows for comparison of the transcriptional and metabolic profiles, which can lead to the discovery of new pathways and key molecules of the cellular processes. For that reason, metabolomics and transcriptomics data sets were connected in that changes during adipogenesis on the metabolic level were reassessed by transcriptomics data. The first objective was to uncover global changes including alteration of essential pathways regulated during adipogenesis. Here, overlapping regulated molecules (metabolites and genes) were mostly linked to glycolysis, citrate cycle (TCA) or fat metabolism. A scheme presented in **Figure 18** was prepared according to IPA knowledge base, showing the relations between molecules and affected pathways. A dramatic decrease of hexoses in conditioned medium was detected at day 4 and could be associated with the simultaneous up-regulation of insulin-regulated glucose transporter type 4 (GLUT4) and glucokinase (GCK), which plays an important role in the carbohydrate metabolism by catalyzing the conversion of glucose into glucose 6-phosphate. The glycolytic pathway can supply the citrate cycle and lipid metabolism with acetyl-CoA, a product of acetate-CoA synthase short chain family member 2 (ACSS2). This enzyme was up-regulated at the second day of adipogenic cell differentiation. The concentrations of amino acids like aspartate, glutamate, proline or branched chain amino acids (BCAA) decreased in conditioned medium and were associated with regulation of enzymes catalyzing the formation of citrate cycle intermediates. Glutamate

can be converted by aldehyde dehydrogenase (ALDH5A1) to succinate and aspartate by D-aspartate oxidase (DDO) to oxaloacetate.

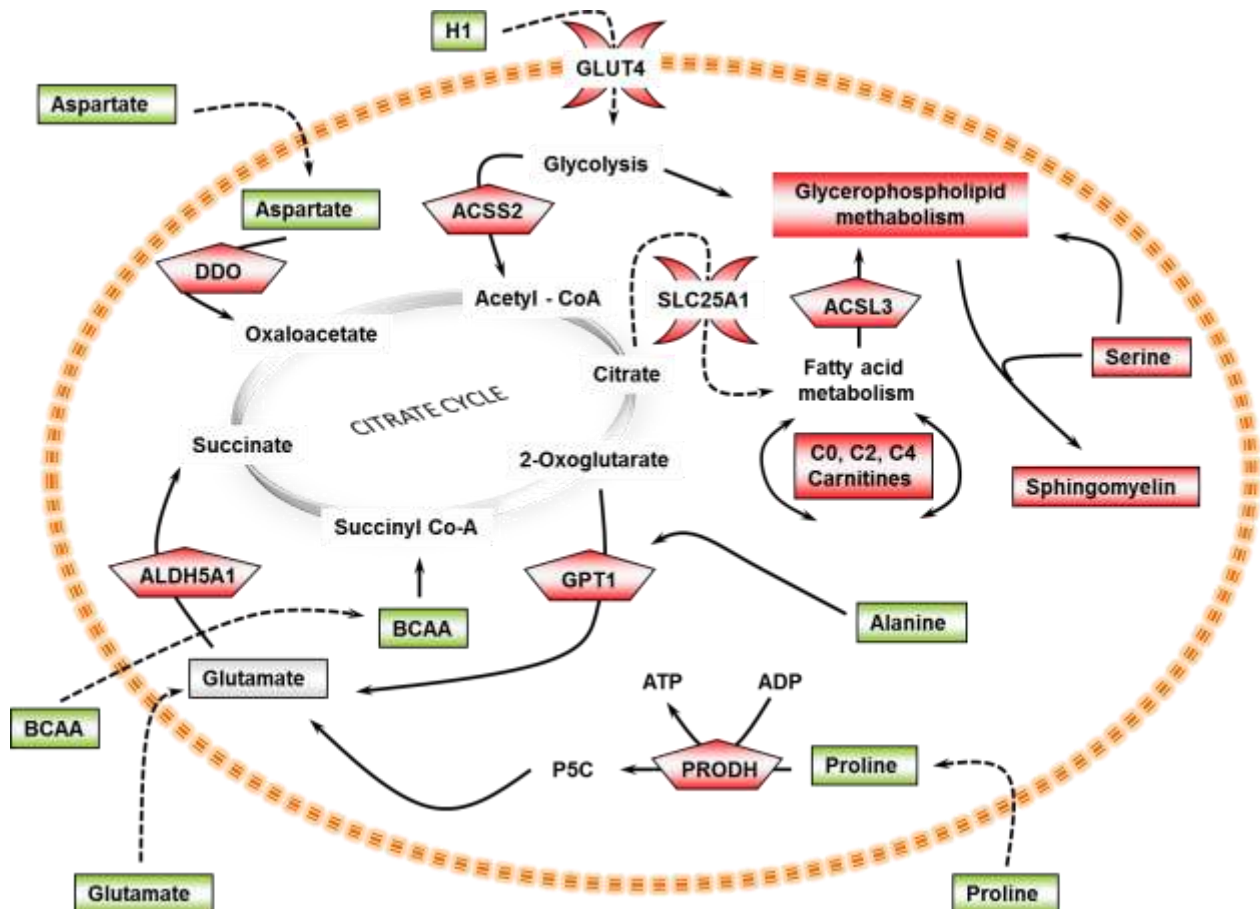


Figure 27 Schematic representation of global changes occurring during adipogenesis.

Transcriptomic and metabolomic data were together evaluated. All molecules (genes and metabolites) inside the orange circle refer to processes observed inside the cell. The molecules outside indicate metabolites observed in conditioned medium. Green and red colored molecules refer to concentration or gene expression decrease and increase, respectively. All enzymes are represented by pentagons, metabolites by rectangle, transporters by two half-moons and all molecules without frames have not been observed in measured data sets. All colored molecules are significantly regulated during adipogenesis. Affected by adipogenesis pathways includes: glycolysis, citrate cycle and glycerophospholipids metabolism. Abbreviations: H1, hexoses; GLUT4, insulin-sensitive glucose transporter 4; ACSS2, acetate-CoA synthase short chain family member 2; SLC25A1, citrate transporter; GPT1, glutamic pyruvic transaminase; BCAA, branched chain amino acids (isoleucine, leucine, valine); ALDH5A1, aldehyde dehydrogenase 5A1; DDO, D-aspartate oxidase; ACSL3, acetyl-CoA synthase long-chain family member and PRODH, proline dehydrogenase.

Both of the enzymes were found to be up-regulated during adipogenesis. A slight increase in the level of glutamate in cells could be explained by increased expression of glutamic pyruvic transaminase (GPT1) catalyzing the synthesis of glutamate and pyruvate from 2-oxoglutarate and alanine, which strongly decreased in cell homogenates. A significant decrease of proline concentration in cell lysates and conditioned medium, detected already at the second day of differentiation with a constant trend until day 18, was related to increased proline dehydrogenase expression (PRODH) which ensures the conversion of proline to proline-5-carboxylase, involved in glutamate and urea cycle metabolism. Furthermore, the TCA cycle intermediate citrate is transported across the mitochondrial inner membrane by SLC25A1 (a citrate transporter). This enzyme, essential for supplying the cytoplasm with a carbon source for the fatty acid metabolism, showed increased expression at day 4 with constant trend up until day 18, is. Moreover, other essential compounds for the fatty acid metabolism, like short-chain carnitines (carnitine (C0), acylcarnitines (C2) or butyrylcarnitine (C4), were up-regulated during adipogenesis. The fatty acids, basically increased over adipogenesis development, are easily metabolized into glycerophospholipids (phosphahtidylcholines or lysophosphatidylcholines) or sphingomyelins through acetyl-CoA synthase long-chain family member (ACSL3), which was up-regulated from day six. A detailed analysis of the metabolism of BCAAs, biogenic amines and glycerophospholipids is presented in following subsections.

3.3.5.1 Characterization of branched chain amino acid metabolism during adipogenesis

A significant decrease of all three branched chain amino acids (isoleucine, leucine and valine) in both cell lysates and conditioned medium **Figure 28** was observed. These alterations were associated with up-regulated expression of enzymes involved in BCAA degradation, namely mitochondrial BCAA transaminase (BCAT1), dihydrolipoamid branched chain transacylase (DBT), acyl-CoA dehydrogenase (ACADS), acetyl-CoA acyltransferase 2 (ACAA2) and propionyl-CoA carboxylase (PCCB) (**Figure 29**).

Although the pathway build from transcriptomics and metabolomics data already elucidated the first steps of BCAA breakdown (**Figure 29**), the involvement of BCAAs in adipogenesis still remains elusive. To gain additional insight into the BCAA metabolism combined with transcriptomics and metabolomics data sets, BCAA degradation pathways were further verified by qPCR.

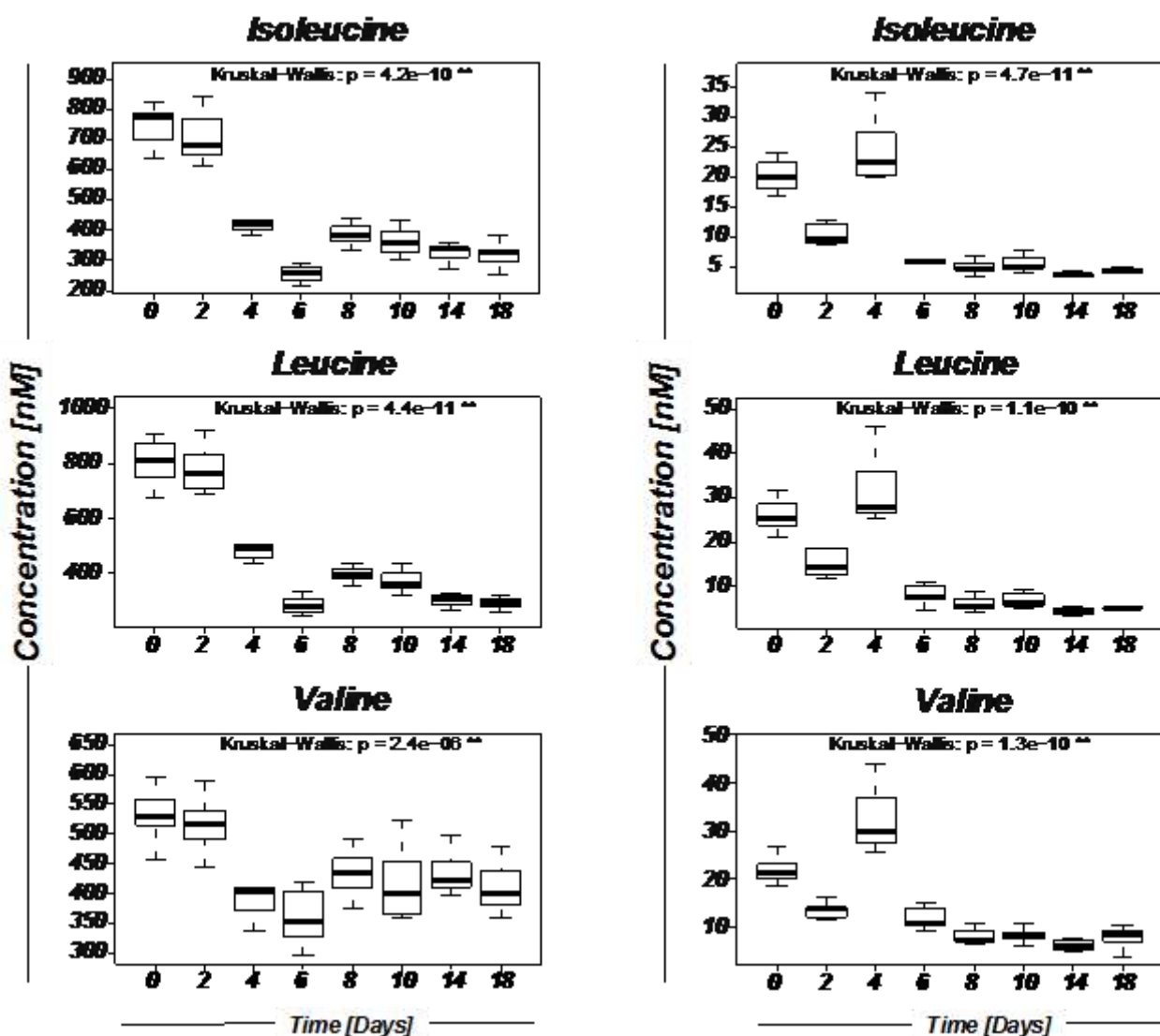


Figure 28 Changes in branched chain amino acid concentrations during adipogenesis. Changes in isoleucine, leucine and valine concentrations in conditioned medium and cells were monitored by the high-throughput targeted metabolomics Absolute IDQ p180 assay. The p-values were calculated according to Kruskal-Wallis: (**) denotes a significance level of 1% after Bonferroni correction. Data are expressed as mean value out of three independent experiments each performed in triplicates.

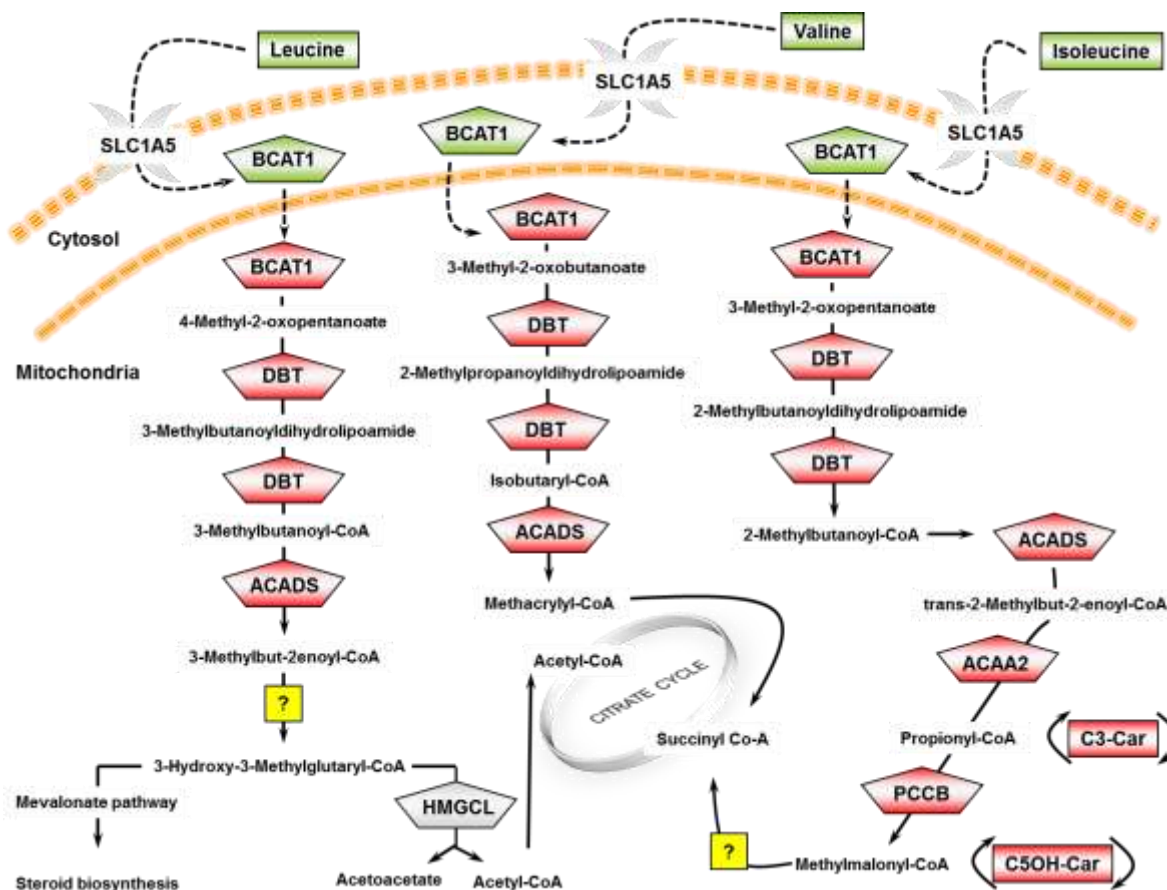


Figure 29 Schematic illustration of BCAA catabolism during adipogenesis. Significant decrease in BCAA concentrations (metabolites colored green) was linked to increased expression of genes involved in BCAA catabolism (colored red), molecules without frames have not been observed in the measured data sets. Molecules above the orange lines, representing the cellular membrane (leucine, valine and isoleucine), were detected in conditioned medium. Abbreviations: SLC1A5, amino acid transporter; BCAT1/2, BCAA transaminase (cytosol/mitochondria); DBT, dihydrolipoyl transacetylase BC transacylase; ACADS, acyl-CoA dehydrogenase; ACAA2, acetyl-CoA acyltransferase; PCCB, propionyl CoA carboxylase; C3-car, propionyl carnitine; C5(OH)-car, methylmalonylcarnitine and HMGCS, 3-hydroxy-3-methylglutaryl-CoA synthase.

3.3.5.2 Leucine degradation

Presented in **Figure 30** the illustration suggests the participation of leucine in cholesterol synthesis as precursor of cholesterol, a molecule involved in the constitution of membranes, steroid synthesis, and signaling processes. As shown in **Figure 29** leucine is known to be degraded in several steps to 3-hydroxy-3-methylglutaryl-CoA, the starting of cholesterol synthesis. Indeed, Leucine was found to be down-regulated during

adipogenesis and. enoyl-CoA-hydratase (AUH) catalyzing the synthesis of 3-hydroxy-3-methylglutaryl-CoA was up-regulated from day 6 on.

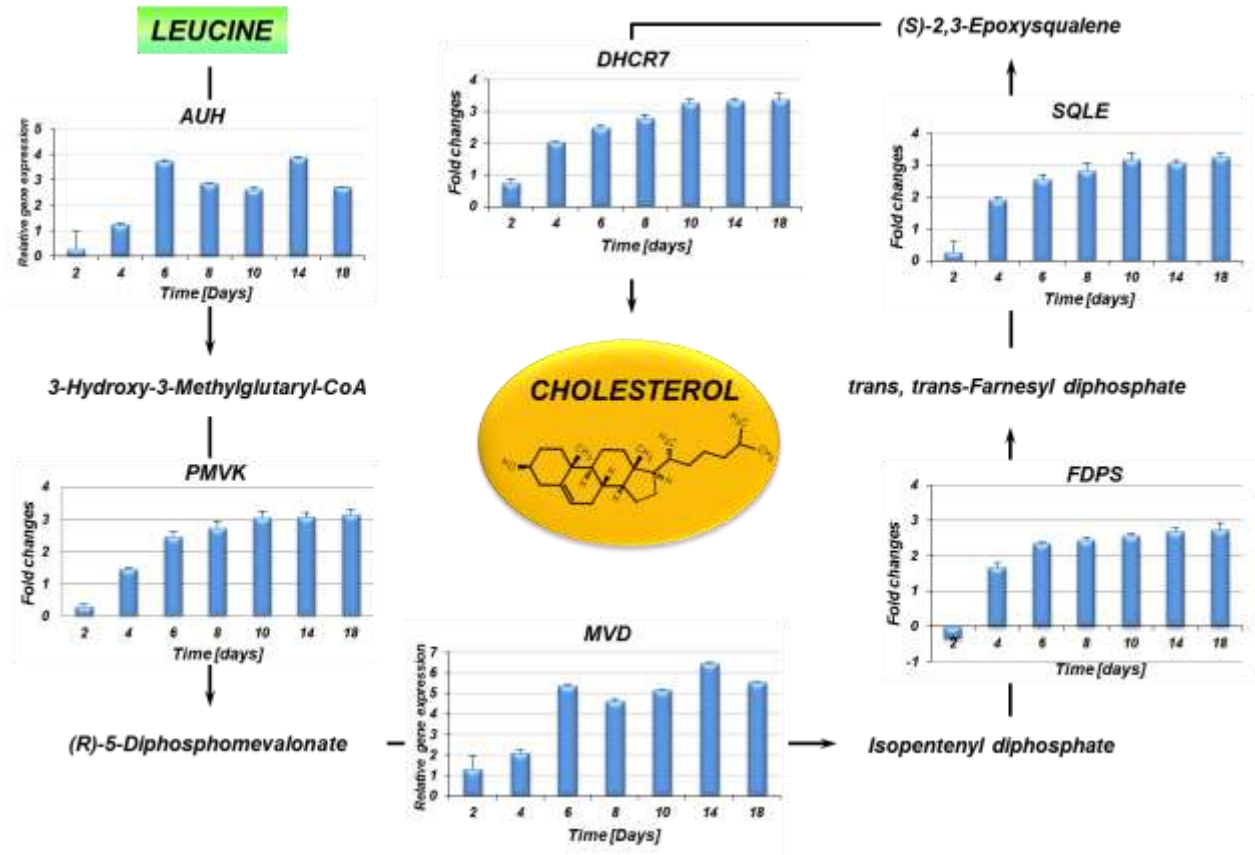


Figure 30 Leucine may serve as precursor of cholesterol biosynthesis. The leucine degradation/cholesterol synthesis pathway was examined with combined qPCR and microarray tools. The qPCR was performed on cDNA generated using RNA isolated from cell pellets at different days of adipogenic cell differentiations. The relative gene expression of AUH (enoyl-CoA-hydratase) and MVD (mevalonate diphosphate decarboxylase) was calculate by using the $2^{-\Delta\Delta CT}$ method. Data are representative of two experiments performed in triplicates (\pm SD). The PMVK (phosphomevalonate kinase), FDPS (farnesyl diphosphate synthase), SQLE (squalene epoxidase) and DHCR7 7-dehydrocholesterol reductase were found in transcriptomics data set and are expressed as fold changes relative to the gene expression of untreated cells (preadipocytes in post-confluent phase). Data represent a mean (\pm SD) from three independent experiments.

The phosphomevalonate kinase (PMVK) catalyzing the fifth reaction of the cholesterol biosynthetic pathway (conversion of mevalonate-5-phosphate into mevalonate-5-diphosphate) was up-regulated from day 4 on. Furthermore, increased expression of

MVD (mevalonate diphosphate decarboxylase) and FDPS (farnesyl diphosphate synthase), catalyzing the formation of key intermediate in cholesterol and sterol biosynthesis (Hinson, Chambliss et al. 1997), was observed from day 4 on. Elevated levels of squalene epoxidase (SQLE), catalyzing the first oxygenation step in the sterol biosynthesis (Sakakibara, Watanabe et al. 1995), was detected from day four of adipogenesis on followed by further increase until day eighteen. The same expression pattern was observed for 7-dehydrocholesterol reductase (DHCR7) which through elimination of the double C(7-8) bond in the B ring of sterols is catalyzing the final conversion of 7-dehydrocholesterol to (Honda, Tint et al. 1995, Tint, Seller et al. 1995).

3.3.5.3 Isoleucine and Valine degradation

Isoleucine and valine were strongly down-regulated in conditioned medium and cells during adipogenesis (**Figure 28**) and degradation products as well as involved enzymes found in the metabolomics and transcriptomics data (**Figure 29**). The degradation pathway was further analyzed by qPCR. **Figure 31** shows the possible further degradation pathways of isoleucine and valine, suggesting an involvement of these metabolites in citrate cycle. Propionyl-CoA, the product of isoleucine degradation (**Figure 29**), can be transformed into (S)-methylmalonyl-CoA by propionyl-CoA carboxylase (PCCB), highly expressed from day 4 of adipogenic differentiation on. (S)-methylmalonyl-CoA is interconverted to (R)-methylmalonyl-CoA form by methylmalonyl-CoA epimerase (MCEE) up-regulated from day 4 on. Further methylmalonyl-CoA mutase (increase starting at day six) can catalyze the synthesis of succinyl-CoA, an intermediate of the TCA cycle, from (R)-methylmalonyl-CoA. Moreover, metabolites of valine degradation could be incorporated into mentioned pathway due to aldehyde dehydrogenase (Aldh1A7), converting (S)-methylmalonate semialdehyde into methylmalonate, which can be further converted into (R)-methylmalonyl-CoA by spontaneous insertion of coenzyme A.

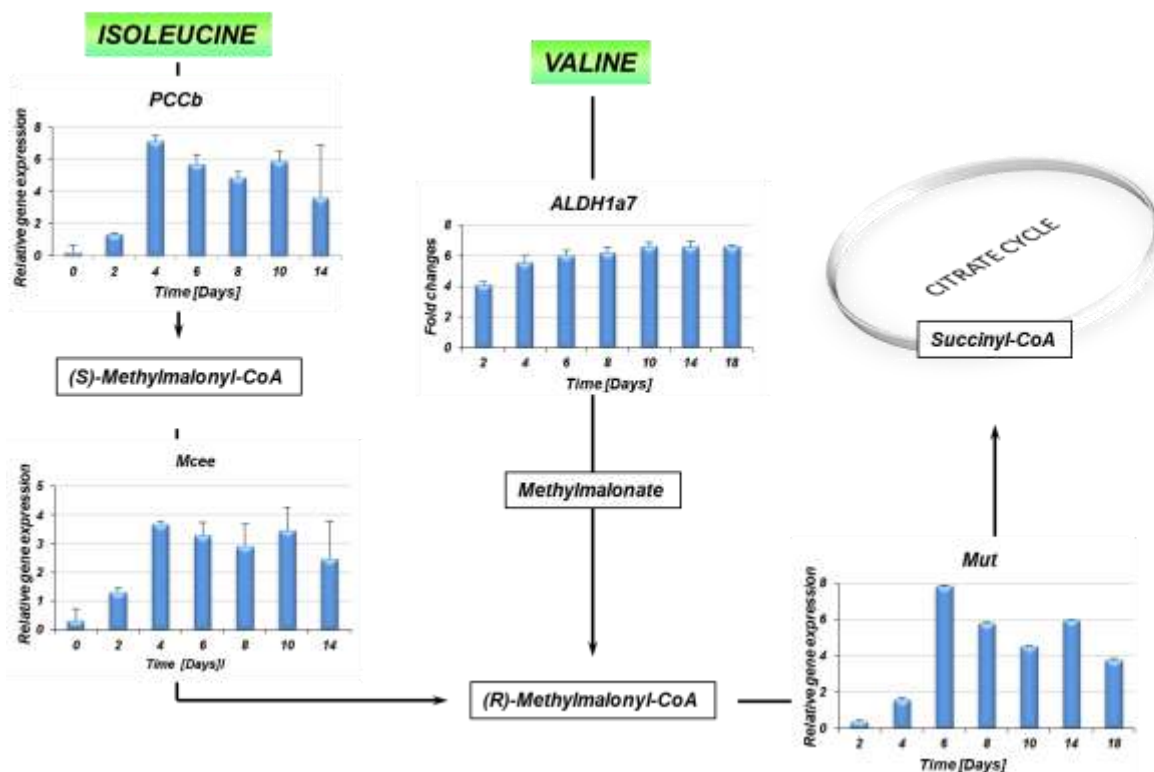


Figure 31 Incorporation of isoleucine and valine degradation products and involved enzymes in the citrate cycle. The catabolism of isoleucine and valine was examined by qPCR. Metabolites were linked to the citrate cycle due to PCCB (propionyl-CoA carboxylase), MCEE (methylmalonyl-CoA epimerase) and MUT (methylmalonylCoA mutase). Relative gene expression was calculated by using the $2^{-\Delta\Delta CT}$ method. Data represent the mean (\pm SD) from three independent experiments.

3.3.5.4 Polyamine metabolism in adipogenesis

The polyamines like putrescine (diamine), spermidine (triamine) and spermine (tetraamine), involved in several cellular processes including cell growth and proliferation (Agostinelli, Marques et al. 2010), were altered in the cells during adipogenesis (**Figure 32**). The metabolic pattern shows that putrescine reached a maximum concentration at the second day of differentiation to then decrease, probably due to further conversion to spermidine, which indeed was strongly up-regulated at day 4. In addition, spermine, which can be synthesized from spermidine remained unchanged until it decreased at day eight with the constant trend until day 18. However, the decrease in putrescine concentration could be also associated with elevated expression of amine oxidase (AOC3), up-regulated at day six, and aldehyde dehydrogenase (ALDH1A7), up-regulated already at the second day of adipogenic cell differentiation.

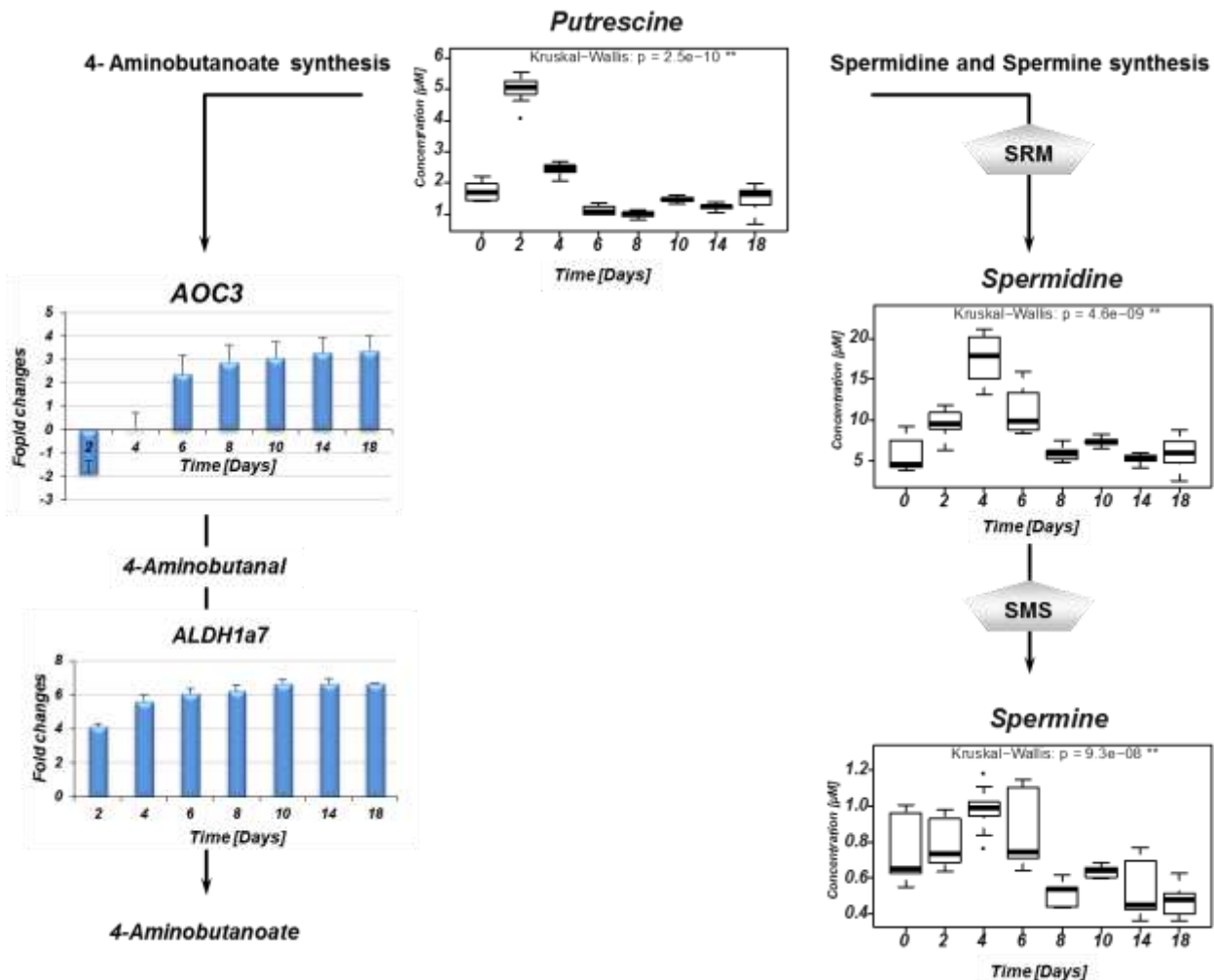


Figure 32 Metabolism of biogenic amines. Changes in putrescine, spermidine and spermine concentrations were visualized in form of box-plots, showing the medians from three independent experiments carried out in triplicates, after metabolic data analysis with the *metaP* server. The p-values calculated by using Kruskal-Wallis are given in each diagram, “***” denotes a significance level of 1% after Bonferroni correction. The AOC3 (amine oxidase) and Aldh1A7 (aldehyde dehydrogenase) gene expression values are expressed as fold changes relative to the gene expression of untreated cells (preadipocytes in post-confluent phase). Data are representative of three independent experiments (\pm SD). Gray colored pentagons SRM (spermidine synthase) and SRS (spermine synthase) indicate genes participating in the putrescine metabolism which had not been observed in 1000 significantly regulated genes from the transcriptomics data set.

Both enzymes are involved in formation of 4-aminobutanal and 4-aminobutanoate, which were previously described as up-regulated during adipogenesis (Roberts, Virtue

et al. 2009). The 4-aminobutanoate could be incorporated into citrate cycle or glutamate metabolism (Bessman, Rossen et al. 1953, Roberts and Bregoff 1953). Nevertheless, genes catalyzing conversion of 4-aminobutanoate either into succinate semialdehyd or glutamate have not been detected. Moreover, genes involved in putrescine transformation into spermidine or spermine had not been detected in top 1000 significantly regulated genes. Although alteration in the polyamine patterns still remain unclear, characteristic patterns were detected for each stage of adipogenesis, which makes polyamines potential candidates for novel biomarkers of adipogenesis development.

3.3.6 Changes in glycerophospholipids metabolism as consequence of adipogenesis

3.3.6.1 Up-regulation in the Kennedy pathway

The phosphatidylcholines, the most abundant phospholipid species in eukaryotic cells (Gibellini and Smith 2010), were the strongest regulated group of metabolites during adipogenesis. A significant increase of 21 and decrease of 12 from 76 measured phosphatidylcholines was detected and therefore the transcriptomics data set was screen with respect to regulated genes involved in glycerophospholipids metabolism. The elevated phosphatidylcholines levels were directly related to the Kennedy pathway, the *de novo* synthesis of phosphatidylcholine (PC) and phosphatidylethanolamine (PE). **Figure 33** schematically shows the biosynthesis of those glycerolipids, originally described in 1956 by Kennedy (Kennedy and Weiss 1956). In the transcriptomics data sets, gene expression associated with PC and PE synthesis consists of three enzymatic steps. Colored symbols indicate up- (red) or down- (green) regulated molecules: pentagram - enzymes and rectangle - metabolites. Ethanolamine kinase (EK) and choline kinase (CK) catalyzing the formation of ethanolamine-phosphate (Etn-P) and cholinephosphate (Cho-P), respectively did not occur in the top 1000 significantly regulated genes and are colorless. In the second, rate-limiting step phosphoethanolamine cytidyltransferase (PCYT2), catalyzing the formation of the high-

energy donor cytidinediphosphate-ethanolamine (CDP-Etn) was up-regulated from day 4. The expression of choline-phosphate cytidyltransferase (PCYT1), catalyzing the formation of cytidinediphosphate-choline has not been observed in the top 1000 significantly regulated genes. Finally, stepwise increase in expression of cholinephosphotransferase (CHPT1), catalyzing the last phase of the PC biosynthesis from CDP-choline and 1,2-diacylglycerol (1,2-DG), was observed from day 4 of adipogenesis on.

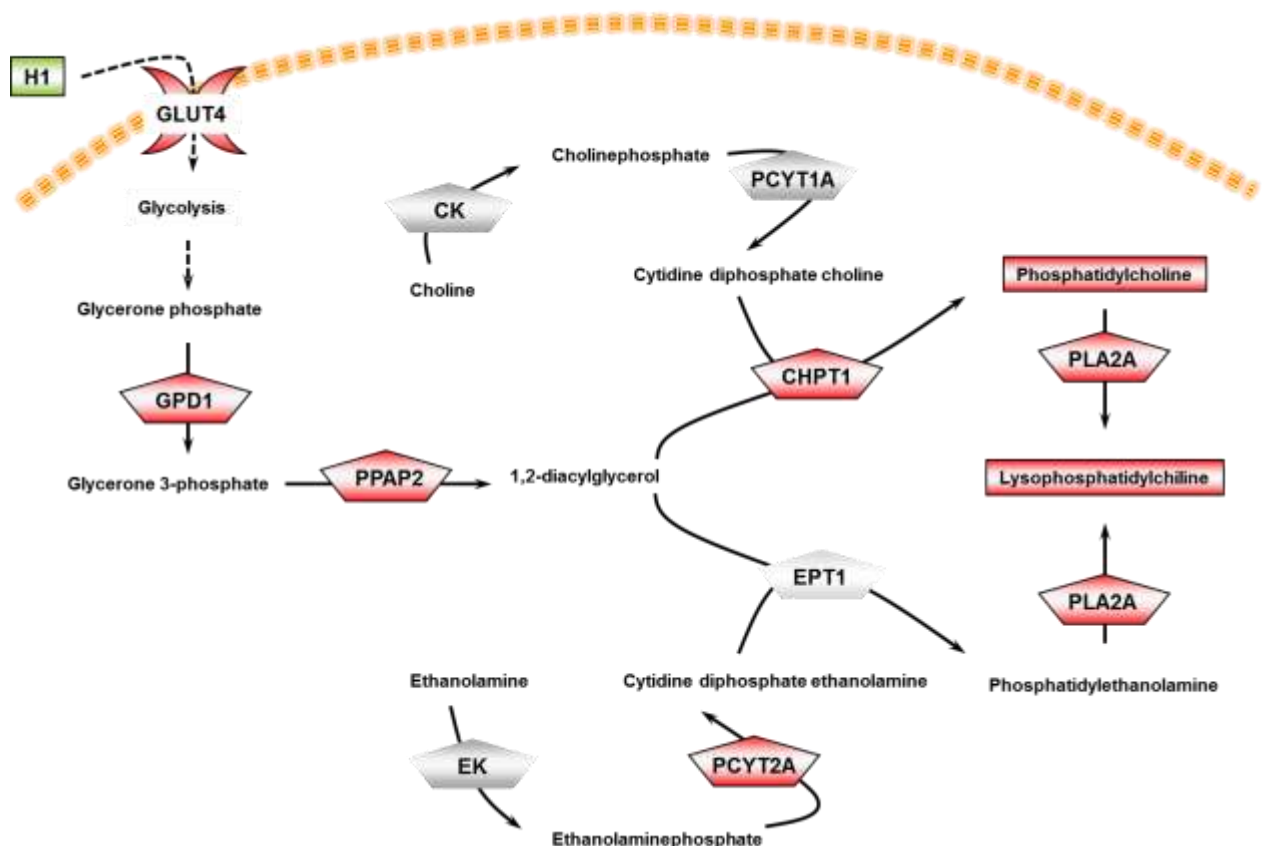


Figure 33 Kennedy pathway up-regulated during adipogenesis of 3T3-L1 cells. Significant increase in phosphatidylcholines and lysophosphatidylcholines was connected to the Kennedy pathway *de novo* synthesis of phosphatidylethanolamine and phosphatidylcholine. Significantly up-regulated molecules are colored red, down regulated green, and molecules without frames and colored gray have not been observed in the measured data sets. Abbreviations: GPD1, (glycerol-3-phosphate dehydrogenase); PPAP2, phosphatidate phosphatase; E/C K, ethanolamine/choline kinase; PCYT1, choline-phosphate cytidyltransferase; PCYT2, phosphoethanolamine cytidyltransferase; EPT1/CHPT, ethanolaminephosphotransferase/cholinephosphotransferase; PLA2, phospholipase A2.

Furthermore, adipogenic cell differentiation resulting in significant decrease of hexoses in conditioned medium at day 4 was connected with increased, expression of GLUT4 from day 4 on. Notably, glycerol-3-phosphate dehydrogenase (GPD1), strongly expressed already at day 2 with a continuous upward trend within the following days of adipogenesis, serves as a major link between carbohydrate and lipid metabolism through converting of glycerone phosphate (GP) to glycerone 3 phosphate (G3-P) (Mayes and Botham 1993), a substrate for 1,2-DG.

3.3.6.2 Lipid accumulation

An increase observed in phosphatidylcholine concentrations reflects particular patterns for different stages of adipogenesis. Accumulation of phosphatidylcholines containing fatty acids with distinct chain lengths or saturation levels suggests their remodelling during adipogenic cell differentiation. Potential composition of phosphatidylcholine chains and schematic reactions occurring on the fatty acid chains, like elongation and desaturation is presented in **Figure 34** and

Figure 35, respectively. Metabolic patterns of acyl-acyl phosphatidylcholines could be linked to desaturation of fatty acid (hydrogen removal resulting in double bonds), and the preferable incorporations of those into acyl-acyl PCs. Oxidative desaturation of saturated fatty acids is predominantly catalyzed by Δ 9 desaturase (SCD1) (Cook and McMaster 2002) in Δ 9 position (Cook and McMaster 2002). This enzyme was strongly expressed in the second day of cell differentiation followed by further increase up to day 18. Thus, a dramatic decrease of PC aa C32:0 at day 4 could be linked to the strong increase of PC aa C32:1 at day 4 with the constant trend up to day eighteen. An increase in PC aa C32:2 concentration, observed at day 4 was associated with further desaturation of monounsaturated fatty acids, catalyzed by fatty acid desaturase 2 (FADS2) up regulated at day 6. On the other hand, phosphatidylcholines with an ether side chain exhibited a simultaneous decrease in molecules consisting of short chain fatty acids and increase in molecules with longer fatty acid chains (see **Figure 35**). Elongation of the fatty acid chain could be associated with increased gene expression of elongase family members.

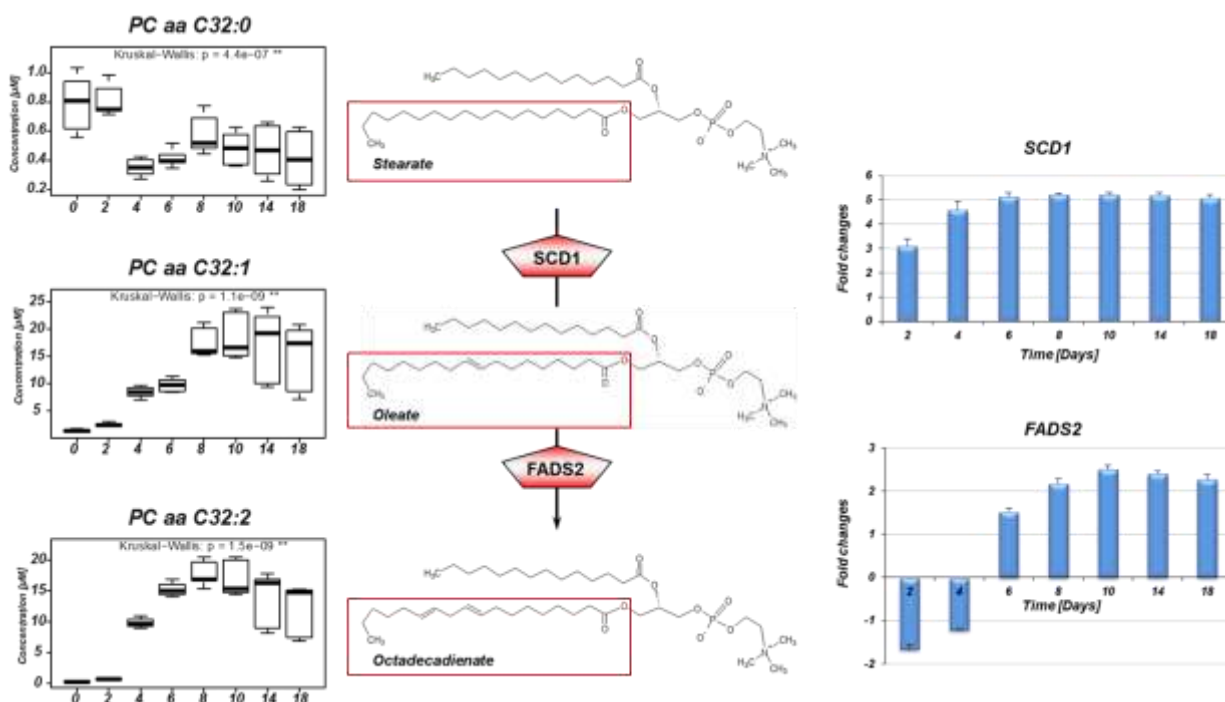


Figure 34 Adipogenesis resulted in increased accumulation of unsaturated fatty acid chain in acyl-acyl PCs. The PC aa concentrations (PC aa C32:0; PC aa C32:1 and PC aa C32:2) were determined with targeted metabolomics using the Absolute IDQ p180 kit. The p-values were calculated according to Kruskal-Wallis: (**) denotes a significance level of 1% after Bonferroni correction. Data is expressed as mean value out of three independent experiments each performed in triplicates. Illustration shows potential fatty acid chain compositions and their desaturation from saturated - stearic, monounsaturated - oleic and to polyunsaturated - linoleic acid. Molecules involved in fatty acid desaturation including SCD1 ($\Delta 9$ desaturase) and FADS2 (fatty acid desaturase 2) are presented in fold changes (from transcriptomics experiments) relative to the gene expression of untreated cells (preadipocytes in post-confluent phase). Data are representative of three independent experiments (\pm SD).

Results from transcriptomics study, indicating up-regulated expression of fatty acid elongase 3 (ELOVL3), were complemented with quantitative PCR data, which confirmed the increase in ELOVL3 and additionally showed increased expression of ELOVL1 or ELOVL4 at day 4 and ELOVL5 at day 8.

The increase in concentration of PC ae C34.1 could be explained by elongation of palmitoleic acid (structural part of product molecule of decreased PC ae C30.1 at day six) to oleic acid (component of PC ae C32.1 reaching a maximum at day eight) and further to eicosenoic acid (

Figure 35). It can be catalyzed by ELOVL3 which has a putative role in elongation of

saturated and monounsaturated fatty acids with up to 24 carbons in length (Tvrdik, Westerberg et al. 2000).

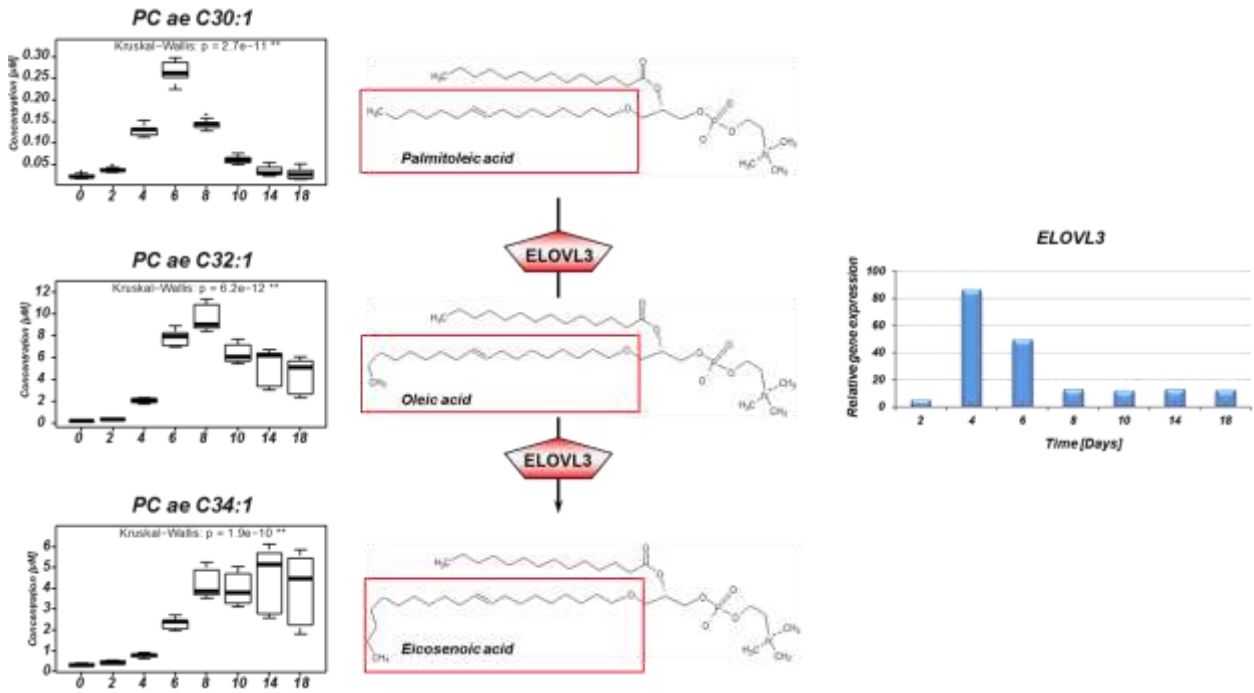


Figure 35 Adipogenesis resulted in increased accumulation of long chain fatty acid in ether lipid PCs. The PC ae concentrations (PC ae C30:1; PC ae C32:1 and PC ae C34:1) were determined with the targeted metabolomics Absolute IDQ p180 kit. The p-values were calculated according to Kruskal-Wallis: (**) denotes a significance level of 1% after Bonferroni correction. Data is expressed as mean value out of three independent experiments each performed in triplicates. Illustration shows potential fatty acid chain compositions and their elongation. Elongation could be catalyzed by ELOVL3 denoted by fold changes (from transcriptomics experiments) relative to the gene expression of untreated cells (preadipocytes in post-confluent phase). Data are representative of three independent experiments (\pm SD).

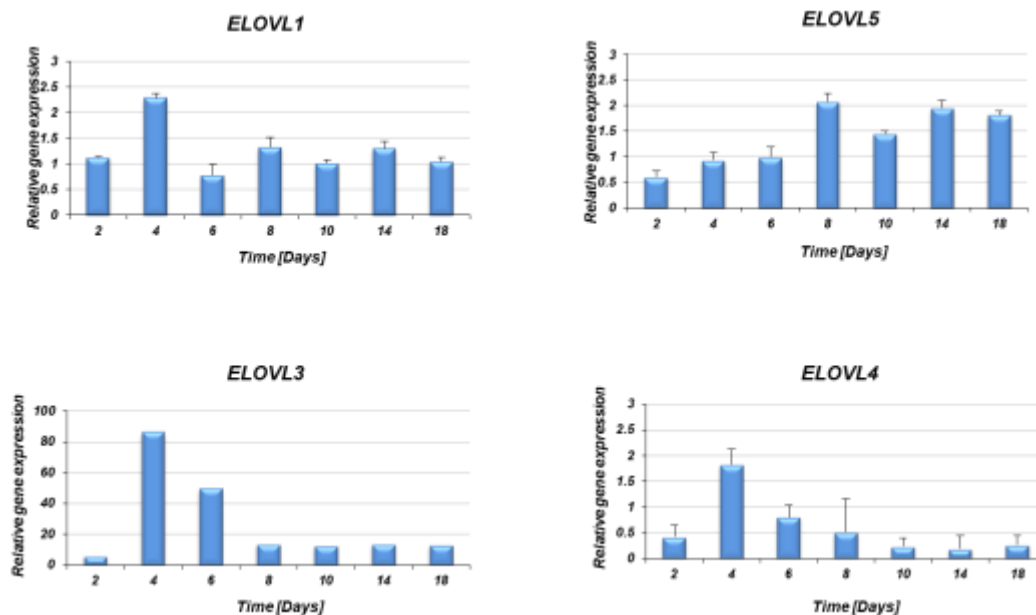


Figure 36 Gene expression patterns of elongase family members determined by qPCR. The relative gene expression of the elongase family members ELOVL1, ELOVL3, ELOVL4, and ELOVL5 was calculated by using the $2^{-\Delta\Delta CT}$ method. Data are representative of two experiments performed in triplicates (\pm SD).

3.3.6.3 Changes in fatty acid metabolism during adipogenesis

The information provided by the Absolute IDQ p180 assay regarding PC is limited to the total number of carbons of the two fatty acid side chains and chain compositions cannot be determined. However, to get this desired information, changes in total fatty acids concentrations occurring during adipogenesis were quantified out of three independent experiments using the external services of the Biocrates Life Science AG. Among all 62 examined fatty acids only 5 in medium and 6 in cells exhibited clear regulation patterns during adipogenesis (see **Figure 37**). Furthermore, four of them including myristic, myristoleic, palmitoleic, and oleic acid belong to the even chain fatty family. All others, like tridecanoic, pentadecanoic, or heptadecanoic acid containing uneven number of carbons in chain belonged to the odd chain fatty acid family. Hence, the in **Figure 34** and

Figure 35 presented hypothetical composition of fatty acid chains in phosphatidylcholines and their desaturations and elongations could be changed to those shown in **Figure 38**, though the tendency to accumulate PC aa with increased number

of double bonds and PC ae with increased number of carbons in their fatty acid chains holds still true and is strongly suggested due to the patterns exhibited by the phosphatidylcholines. The involvement of SCD1 in odd chain fatty acid desaturation was recently reported (Su, Han et al. 2004).

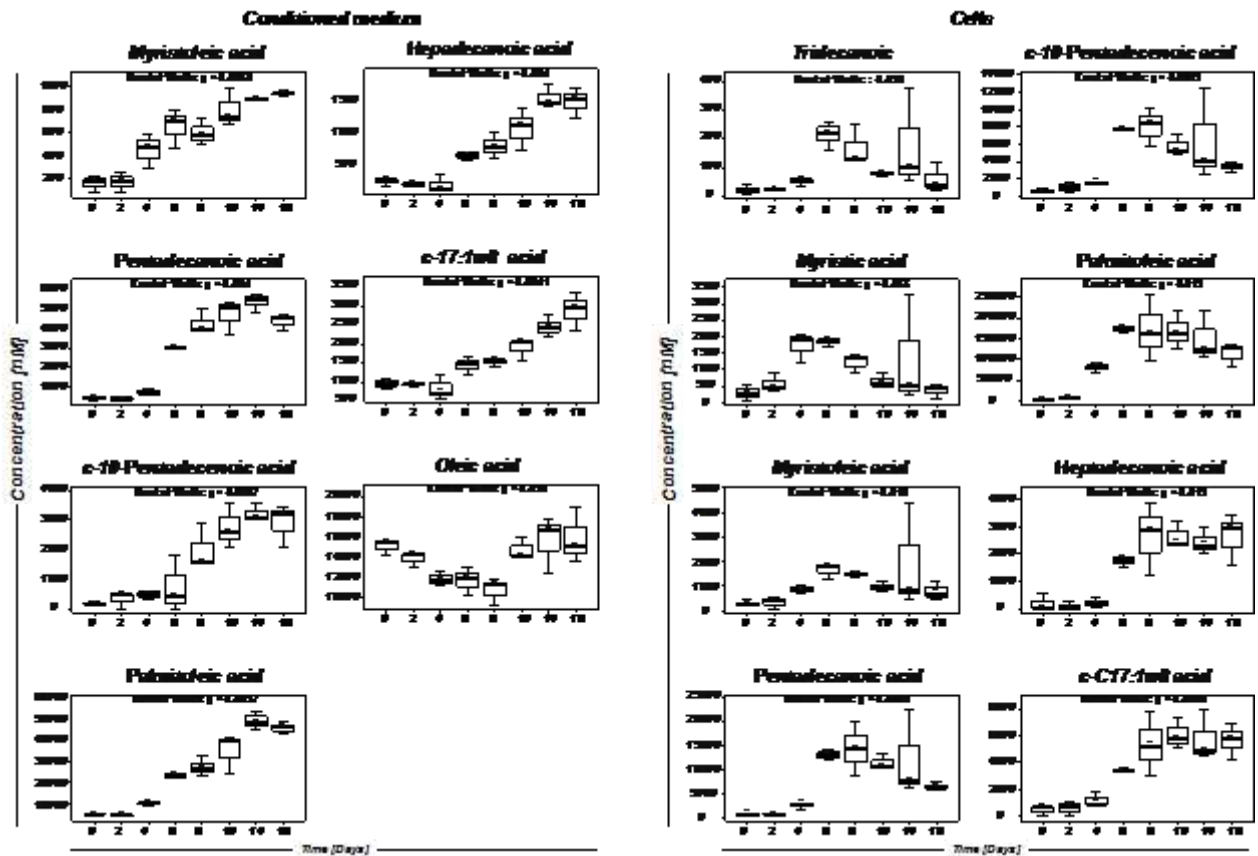


Figure 37 Changes in total fatty acid concentrations during adipogenesis. Significant alteration in the concentrations of 5 fatty acids in medium and 6 inside cells were observed ($p < 0.05$). The p-values were calculated according to Kruskal-Wallis. Data is expressed as mean value out of three independent experiments.

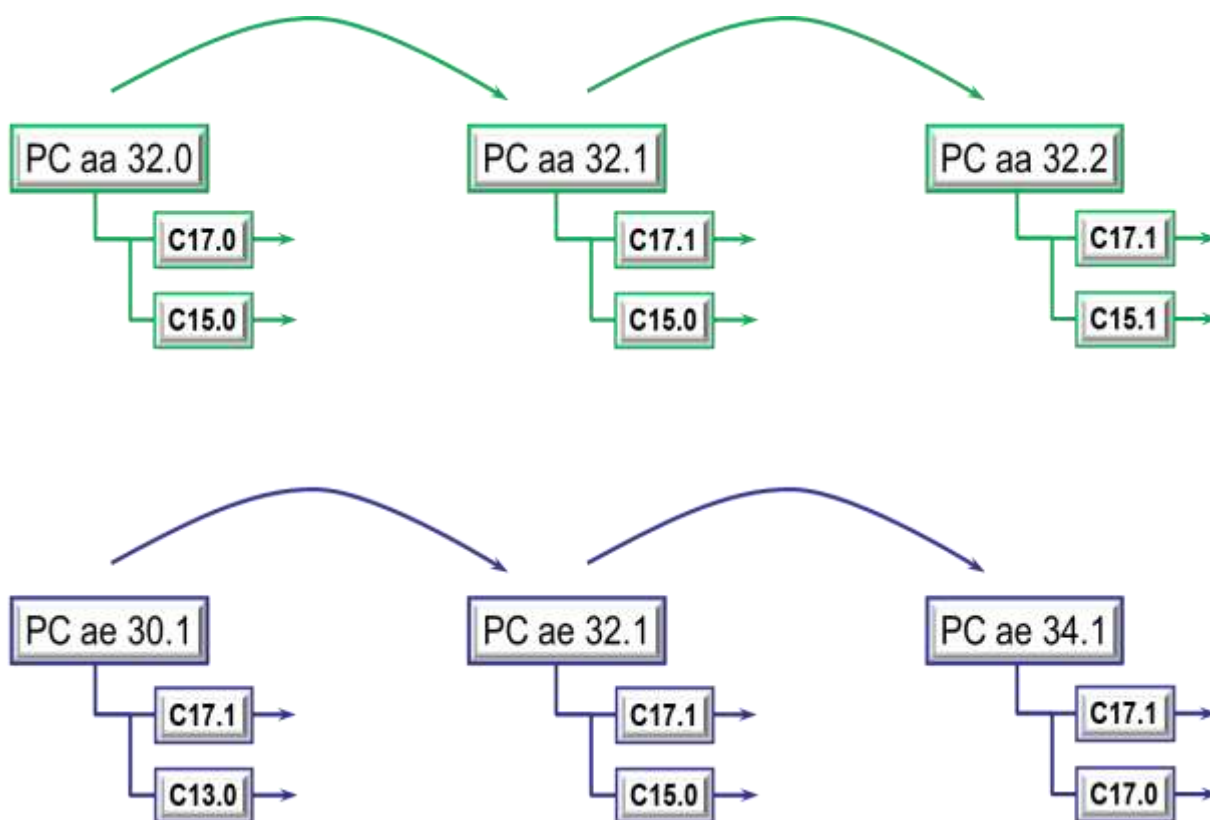


Figure 38 Changes in phosphatidylcholine composition may occur during adipogenesis.

Patterns of phosphatidylcholines concentration changes suggest that during adipogenesis PC aa fatty acid chains with increasing number of double bonds (increase of desaturation) and PC ae containing fatty acids with increasing chain length are accumulating. Putative composition of depicted PCs is based on results of odd chain fatty acid accumulation (**Figure 37**) during adipogenesis

3.3.6.4 Lipid degradation

Unexpectedly, a dramatic decrease in the concentrations of some phosphatidylcholines and lysophosphatidylcholines (specified in **Table 11**), occurring throughout adipogenic differentiation was observed already at day four. Since the regulated LysoPCs contain only one fatty acid chain, an assignment of those side chains in the down-regulated LysoPCs was easily possible: the 20-carbon fatty acids with different number of double bonds (3, 4 and 5) could be linked to mead acid, arachidonic acid and eicosapentaenoic acid, respectively. As LysoPCs and PCs are inter-converted they might contain the same side chain fatty acids. **Figure 39** visualizes the decrease in concentration of

representative phosphatidylcholines (PC aa) and lysophosphatidylcholines (LysoPC a) with acyl side chains (**Figure 39 A**) and the fatty acids probably present in the depicted phospholipids (**Figure 39 B**). To find genes involved in glycerophospholipid degradation and long chain fatty acid metabolism, transcriptomics data were screened.

Table 11 Significantly down-regulated phospholipids during adipogenesis. Phospholipid concentrations at different days of adipogenesis were determined with the targeted metabolomics Absolute IDQ p180 kit. The p-values were calculated according to Kruskal-Wallis: (**) denotes a significance level of 1% after Bonferroni correction.

| Metabolites | p - value |
|----------------|------------------------|
| PC aa C38:3 | 2.4 e ^{-07**} |
| PC aa C38:4 | 2.7 e ^{-08**} |
| PC aa C38:5 | 8.0 e ^{-09**} |
| PC aa C40:4 | 8.7 e ^{-06**} |
| PC ae C40:3 | 3.2 e ^{-09**} |
| LysoPC a C20:3 | 3.2 e ^{-09**} |
| LysoPC a C20:4 | 6.7 e ^{-11**} |

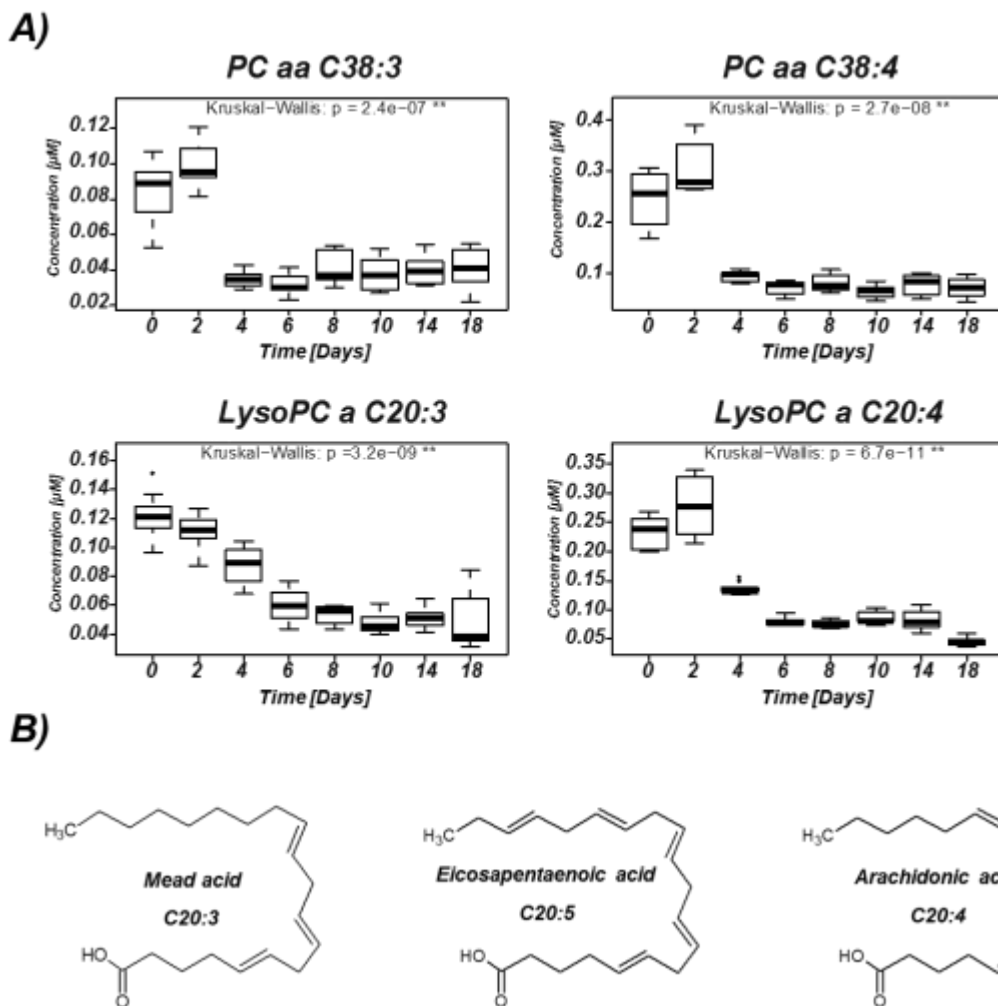


Figure 39 Down-regulated glycerophospholipids. **A)** Alteration patterns exhibited by exemplary down-regulated phospholipids. Molecule concentrations were visualized in form of box-plots. The p-values were calculated according to Kruskal-Wallis: (**) denotes a significance level of 1% after Bonferroni correction. **B)** Schematic structure of differently un-saturated 20-carbon fatty acids which can be connected to the down-regulated phospholipids.

Figure 40 shows possible mechanism of lysophosphatidylcholines (LysoPC a C20:4) degradation, catalyzed by monoglyceride lipase (MGLL), hydrolyzing monoacylglycerols into fatty acids and glycerol (Taschler, Radner et al. 2011), which indeed is 3-fold increased at day 4 and continuously up-regulated in following days of adipogenesis. Thus, the LysoPCs a C20:3 and a C20:4 could be metabolized to glycerol-3-phosphocholine with the release of mead acid or arachidonic acid, respectively.

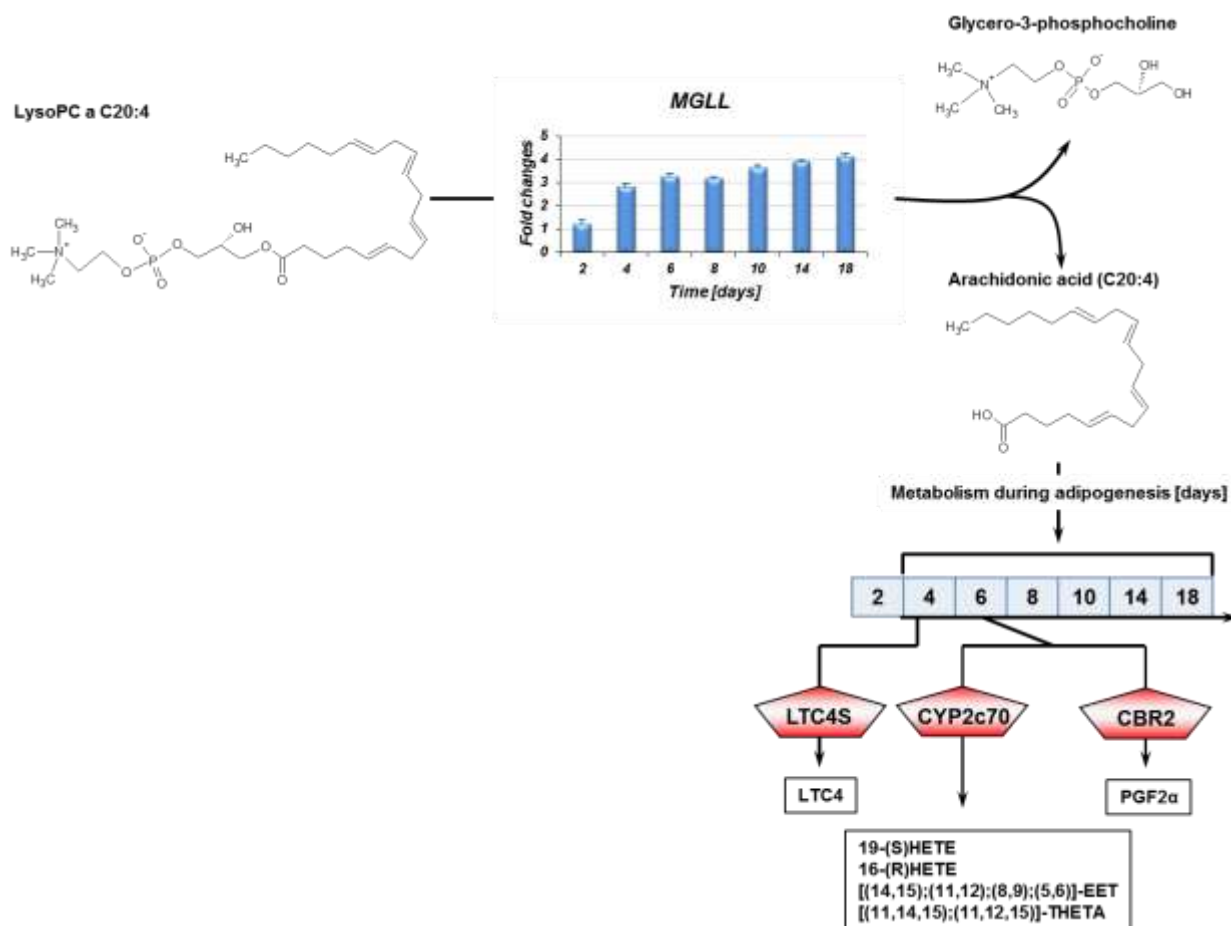


Figure 40 Possible mechanisms of LysoPC degradation to arachidonic acid and its catabolism. Strongly up-regulated MGLL may be involved in the degradation of phospholipids containing arachidonate molecules. The arachidonate degradation started at day 4 and 6 of adipogenesis and can be catalyzed by leukotriene C4 synthase (LTC4S), microsomal monooxygenase Cyp2c70 and carbonyl reductase 2 (CBR2).

Besides, genes involved in the metabolism of arachidonic acid like LTC4S, CYP2c70 and CBR2 were found to be strongly up-regulated from day 4 and 6 on. The LTC4S is involved in the synthesis of leukotriene C4 (LTC4) and CYP2c70 can catalyze the conversion of arachidonate into epoxyeicosatrienoic acids (EETs), hydroxyeicosatetraenoic acids (HETEs) or trihydroxyeicosatrienoic acids (THETAs). The CBR2 is involved in the synthesis of prostaglandin-2F alpha (PGF2α) (Samuelsson 1991).

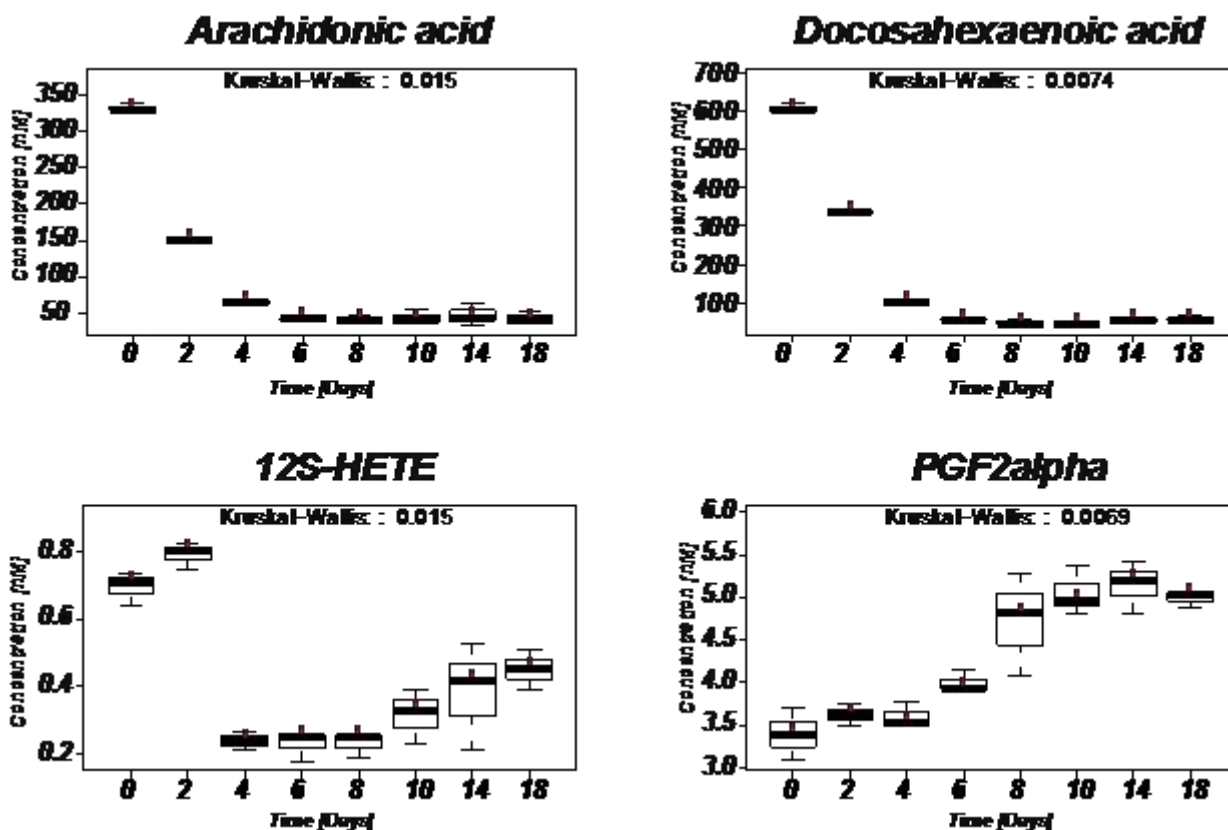


Figure 41 Changes in eicosanoid concentrations in conditioned medium during adipogenesis. Alteration in concentrations of 4 eicosanoids including arachidonate, docosahexaenoic acid, 12-S-HETE and PGF2alpha was detected. The p-values were calculated according to Kruskal-Wallis. Data is expressed as mean value out of three independent experiments.

To verify the results presented in **Figure 40** and examine the possible connection between adipocytes and inflammation in obesity the eicosanoids concentration in medium and cells was determined using the external services of the Biocrates Life Science AG. Interestingly, alterations in prostaglandin concentrations were observed only in conditioned medium in 4 out of 17 examined prostaglandins (**Figure 41**). Strong decrease of arachidonic, docosahexaenoic and 12S-HETE, and an increase in PGF2 α has been detected. Down-regulation of arachidonic acid in parallel to up-regulation of PGF2 α concentrations is in good accordance to the simultaneous up-regulated genes involved simultaneously in arachidonate catabolism and prostaglandins synthesis presented in **Figure 40**. Furthermore, increased concentration of PGF2 α in conditioned medium suggests its excretion by adipocytes.

4 DISCUSSION

4.1 Metabolomics for cell culture approach – assay development and optimization

Implementation of metabolomics in human studies enabled the detection of several biomarkers for various diseases (Tukiainen, Tynkkynen et al. 2008, Sreekumar, Poisson et al. 2009, Misek and Kim 2011, Ferrannini, Natali et al. 2012, Wang-Sattler, Yu et al. 2012). This omics can be used in early diagnosis or in monitoring responses after treatment (Spratlin, Serkova et al. 2009, Hyotylainen 2012). The metabolic profiles of whole organisms is highly complex and their molecule compositions are strongly affected by several factors including gender, age (Yu, Zhai et al. 2012), daily habits (diet, nicotine (Wang-Sattler, Yu et al. 2008), coffee consumption (Altmaier, Kastenmüller et al. 2009)) or environment (Rezzi, Martin et al. 2009). Metabolic profiles of biofluids and tissues reflect those factors, nevertheless, they cannot provide relevant information regarding cellular processes of their biological properties and functions which are fundamental for drug and markers development for specific cellular phenotype (Cuperlovic-Culf, Barnett et al. 2010). Therefore, in this work, metabolomics in cell cultures was applied to complement human studies of complex diseases including cancer and obesity.

4.1.1 Adaptation of human targeted metabolomics assays for cell culture approaches

There is no single analytical technique that completely meets metabolomics guidelines (Griffiths and Wang 2009) to depict the whole metabolome (Adamski and Suhre 2013). In this study, two targeted metabolomics assays, the newborn screening modification of

(NBS) and the Absolute IDQ assay were optimized and applied for metabolite measurements in cells. Selection of these high throughput technologies (NBS assay and Absolute IDQ) was not incidental. Since both are frequently used in human studies, their application for the cell culture approach may be beneficial regarding early phase of drug development or complementation of those studies. By that, cellular metabolomics can provide more detailed data otherwise not discernible in human studies.

4.1.1.1 New born screening assay suitable for metabolomics in cell culture

The NBS assay is a LC-MS/MS based targeted metabolomics approach. This method is originally applied for dry blood spots screening of infants to monitor and to diagnose treatable inborn errors, e.g. phenylketonuria (PKU), propionic acidemia (PROP), or carnitine uptake defect (CUD) (Couce, Castineiras et al. 2011). More than 30 multiple metabolite disorders can be detected in a single analysis out of dried blood spot (Chace, Kalas et al. 2003, Baumgartner, Bohm et al. 2004). Because all disorders detectable by NBS are associated with amino acids, carnitines and fatty acid metabolism, molecules crucial for cellular functions, this tool was newly adapted for cell culture approaches, a work already published recently (Halama, Moller et al. 2011). In the first step growth medium DMEM, routinely used for cell cultivation, with declared amino acids concentrations was used as a control to examine two different preparation procedures. Decrease in concentration of DMEM samples, prepared according to the original method, obviously demonstrated some limitations of the procedure. It is likely that this effect can be explained by the sample composition and ingredient concentrations may lead to strong diffusion and irregular migration of molecules through the filter paper. In consequence, metabolite composition of the disks punched from spotted DMEM did not represent the whole sample on the filter paper (see **3.1.1**). In contrast, the modified application procedure resulted in DMEM concentration compatible with that declared by the manufacturer (see **3.1.1**). In this case, the whole applied sample volume (3.5 μ l) was further processed for analysis and therefore obtained metabolite concentration is representative for the source material.

4.1.1.2 Absolute IDQ p150 and p180 Biocrates assays are suitable for metabolomics in cell culture

Although the NBS assay enables the monitoring of disorders in amino acid and fatty acid metabolism as a result of disrupted carnitine pathways (Chace, Kalas et al. 2003), some metabolic processes, e.g. fat metabolism, remain out of the analysis. However, monitoring of the lipid metabolism is fundamental to gain a broader picture of the cellular processes. Therefore, assays with a widespread metabolite spectrum, i.e. the Absolute IDQ p150 and p180 kits, were implemented for cell culture approaches. The assays cover 163 and 186 metabolites for the p150 and p180 kit, respectively, including acyl carnitines, amino acids, biogenic amines, lipids (phosphatidylcholines, lysophosphatidylcholines, and sphingomyelins) and hexoses, and were earlier used in analyses of human biofluids (Gieger, Geistlinger et al. 2008, Illig, Gieger et al. 2010) and tissue samples (Römisch-Margl, Prehn et al. 2012). Considering different metabolite concentrations and matrix effects, application of this analytical tool for cell culture required some optimization tests. Labeled internal standards (IS) (integrated in the kit) are essential for metabolite quantification. By assessing the recovery of the ISs, the influence of different methanol/water ratios as extraction solvents was examined to achieve an optimum analysis. The optimum method should exhibit minimum ion suppression of IS signals. Ion suppression was not higher than reported for plasma, the matrix for which the Absolute IDQ kits were developed. Thus, the kit assays were shown to be suitable for analyzes of cell culture samples. Since application of 20 μ L resulted in the highest response of ISs, this volume was used in further experiments. Interestingly, cellular extracts with high methanol concentrations resulted in higher intensities of amino acid ISs in comparison with zero samples (samples with ISs in different ratios of methanol/water without biological matrices). This effect was previously observed for free carnitine and amino acids in tissue extracts (liver, muscle, adipose tissue) and was connected to interferences of unknown compounds in this samples (Römisch-Margl, Prehn et al. 2012).

4.1.2 Harvesting and extraction protocols for adherently growing cells – in search for golden standard

Recently, some investigators attempted to develop harvesting and extraction protocols for metabolomics in cell culture (Teng, Huang et al. 2009, Danielsson, Moritz et al. 2010, Dietmair, Timmins et al. 2010, Dettmer, Nurnberger et al. 2011, Van Gulik, Canelas et al. 2012). A number of factors including cell type, growth conditions (adherent, suspension) as well as the applied analytical methods have to be considered for that attempt. Sample harvesting and extraction protocols have to be developed to be particularly suitable for adherently growing cells and for applicable analytical tools. In this study two harvesting protocols, *i.e.* scrapping and trypsinization combined with three extraction solvents (water and direct quenching with 40% MeOH and 80% MeOH) were examined in adherently growing 3T3-L1 cells (see 3.1.3). Overall, the developed procedure independent of the harvesting process and extraction solvents matched well with the Absolute IDQ assays. Nevertheless, among all metabolite classes, acyl carnitines (5 out of 40), biogenic amines (5 out of 20) and hexoses (0 out of 1) were poorly detected. Because the number of extracted molecules of those metabolite classes remained the same regardless of the application of different extraction solvents, the low number of metabolites detected can be explained by assay sensitivity: Ion suppression was not higher than reported for plasma, the matrix for which the Absolute IDQ kits were developed. Thus, the kit assays were shown to be suitable for analyzes of cell culture samples. Furthermore, metabolite concentrations were strongly affected by harvesting and extraction procedures. Cells harvested by trypsinization exhibited lower metabolite concentration in almost all metabolic classes except lipids, which is in good agreement to previous studies on adherently growing cells analyzed with NMR and GC-MS (Teng, Huang et al. 2009, Dettmer, Nurnberger et al. 2011). Trypsinization may contribute to cell membrane damage (Batista, Garvas et al. 2010) and metabolite leakage. Moreover, considering the number of wash/centrifugation steps, small molecules can diffuse outside the cells even though trypsin had no influence on the cellular membrane (Teng, Huang et al. 2009). Since changes in metabolite concentrations can represent a systemic response on environmental stimuli (Fiehn 2002), trypsin by modifying the

physiological state of cells (Teng, Huang et al. 2009), may also be responsible for marginal alteration in lipids. To avoid the above mentioned disadvantage of trypsinization scrapping as harvesting method was chosen for all further experiments in this study. Various ratios of methanol/water as extraction solvents were investigated to determine the optimum conditions, which would give the highest metabolite concentrations among all metabolite classes. As expected, cells extracted with water showed highest concentrations for amino acids but not the optimum for other metabolic classes, whereas cell samples directly quenched and extracted with 80% MeOH achieved highest concentrations for lipids and was still in good agreement to solvent selectivity toward other classes of metabolites. The cells extracted with 80% methanol exhibited only 10% loss in amino acid concentrations compared to those extracted with water. In contrast, lipid concentrations of water-extracted cells were about 87% lower than those extracted with 80% methanol. Consequently, extraction solvents, limited toward molecular characteristic, have significant influence on metabolite profile and therefore should be carefully selected (Cuperlovic-Culf, Barnett et al. 2010). Among all examined extraction solvents, 80% methanol resulted in relatively good extraction efficiency which correlate to metabolic studies in human fibroblasts (Bennett, Yuan et al. 2008) and adherently growing human colon adenocarcinoma (SW480) cells (Dettmer, Nurnberger et al. 2011). Besides, solvents containing 80% methanol are recommended for cell quenching due to enzyme denaturation and precipitation of proteins and lipids (Williams 2011) and preferred to other solvents. Hence, combined cell scrapping with direct quenching/extraction with 80% methanol method is far better than the other protocols as this combined method enables a snapshot taking of the intracellular metabolites status.

4.2 Novel biomarkers of apoptosis depicted by metabolomics – a step towards personalized medicine

Since novel drug development for clinical trials in oncology reached slow success rate, programs aiming to optimize drug discovery based on integration research become an emerging subject (Kamb, Wee et al. 2006). Recently, targeted induction of apoptosis in cancer cells appeared to be a successful strategy in cancer treatment (Gerl and Vaux

2005, Cai, Sun et al. 2011). Hence, a robust detection of apoptosis is urgently required in drug development toward personalized medicine to monitor responses on treatment. Recently, oncology research is strongly facilitated by all omics technologies (genomics, transcriptomics, proteomics and metabolomics) that enabled the detection of characteristic patterns for several cancer types (Spratlin, Serkova et al. 2009). The analytical system suitable for metabolomics in drug development should be robust, highly sensitive, and rapid to enable identification of therapeutic agents and targets, determination of drug mechanism and actions, and monitoring of treatment efficiency (Park, Kerbel et al. 2004). Metabolomics is reflecting the sum of genetic features, regulation of gene expression, protein abundance and environmental influence (Artati, Prehn et al. 2012). Therefore, it is closer to phenotype functions than other omics. Recently, metabolomics was implemented in oncology to characterize cancer metabolome (Mazurek and Eigenbrodt 2003, Falus 2005, Bathen, Jensen et al. 2007) and to determine biomarkers that enable diagnosis (Cheng, Wu et al. 2001, Glunde, Jie et al. 2004) and increase treatment efficiency (El-Deredy, Ashmore et al. 1997, Griffin, Pole et al. 2003, Serkova and Boros 2005). The aim of this part of the thesis was to determine novel biomarkers of apoptosis in cancer cell lines by using metabolomics to facilitate screening and development of anti-cancer drugs.

4.2.1 Staurosporine, 5-Fluorouracil and Etoposide – representatives for pro-apoptotic agents in cancer treatment

In order to obtain biomarkers of apoptosis, three different substances, previously reported as pro-apoptotic agents, were tested in this thesis: staurosporine (Bertrand, Solary et al. 1994); (Stepczynska, Lauber et al. 2001), 5-Fluorouracil (5-Fu) (Osaki, Tatebe et al. 1997) and etoposide (Okamoto-Kubo, Nishio et al. 1994). Those drugs were implemented in clinical trials already. For example, etoposide was used for small cell lung cancer or lymphomas (de Jong, Mulder et al. 1995) treatment, staurosporine for solid tumor therapy (Edelman, Bauer et al. 2007) and 5-Fu is applied since at least 20 years in colorectal and breast cancer therapies (Longley, Harkin et al. 2003). Since various stimuli can cause both apoptosis and necrosis in the same cell population, and

the transformation between them can occur (Proskuryakov, Konoplyannikov et al. 2003), the necrosis was inserted into the experimental design. In this course of this experiment, necrosis was induced by thermal treatment according to previously published study by (Proskuryakov, Konoplyannikov et al. 2003, Rainaldi, Romano et al. 2008). Hence, metabolic alternation occurring only in apoptotic (but not in necrotic and control) cells, regardless of the pro-apoptotic agents applied, are considered as apoptotic biomarkers.

4.2.2 Staurosporine, 5-Fluorouracil and Etoposide affect cell viability by apoptosis induction

Apoptosis was verified by using cell viability assay (MTT) and caspase 3/7 assay. In the first experimental trial, 4 different cell lines, i.e. PC3, MCF7, HepG2 and HEK293 were examined. Although the strength of the response to the treatment was dependent on the cell line, all cell lines exhibited a decrease in cell viability and an increase in caspase 3/7 activity after treatment with 4 μ M staurosporine. Since the PC3 cell line was reported to be a staurosporine-insensitive (Marcelli, Marani et al. 2000), detected caspase 3/7 activities were unexpected and considered as a consequence of a mutation, which however was not further investigated in this study. In this first trial, only HEK293 and HepG2 exhibited similarities of cell viability, caspase 3/7 activity and metabolomics changes. Therefore, in the second trial, only those cell lines were further examined with 2 other pro-apoptotic drugs, i.e. 5-Fu and etoposide. Such experimental design eliminates factors like false response on treatment (like in case of PC3) or improper adjustment of incubation time (like in case of MCF7 cells) which may overshadow the metabolic results. HepG2 and HEK293 cell lines in second experimental trial exhibited different cell viability and caspase 3/7 activity patterns. Therefore, the metabolic changes of those cell lines treated only with optimum etoposide and 5-Fu concentrations and with optimum incubation time were examined. Decrease in viability of thermally treated cells was not a result of apoptosis. This was clearly demonstrated by caspase 3/7 assay that showed no increase in enzyme activities.

4.2.3 Newborn screening assay promising tool for metabolomics study in cancer cell line

Recently, several groups reported the implementation of the $^1\text{H-NMR}$ technique for metabolic studies in cancer cell lines (El-Deredy, Ashmore et al. 1997, Griffin, Pole et al. 2003, Rainaldi, Romano et al. 2008, Zhou, Xu et al. 2009, Bayet-Robert, Loiseau et al. 2010). However, the sensitivity of this technique is considerably low, in comparison with MS based approaches such as FIA-MS or LC-MS (Pan and Raftery 2007). The MS-methods enable the detection of metabolites in concentrations two orders of magnitude below that of NMR (Griffin and Shockcor 2004). Hence, low metabolite concentrations in cells convinced to the implementation of MS based analyzes. In this apoptosis study, the NBS assay was implemented. Although only limited 42 targeted metabolites can be quantified, this assay covers amino acids and carnitines which were previously reported as important metabolite groups in cancer biology. Several decades ago, some amino acids including valine, isoleucine and glutamine were reported as preferentially metabolized by tumor cells (Wagle, Morris et al. 1963, Kovacevic and Morris 1972). Moreover, carnitines have been shown to reveal a protective effect on cisplatin-mediated toxicity (Altun, Gunes et al. 2009) as well as to be involved in intracellular transport during apoptosis (Mazzarelli, Pucci et al. 2007). Other advantages of this assay are the low sample amount requirement and its previous achievement in the clinic routine (Stadler, Polanetz et al. 2006, Spiekerkoetter, Haussmann et al. 2010, Weisfeld-Adams, Morrissey et al. 2010), what demonstrates that it is highly suitable for cell culture study and can be easily adapted for validation in bio fluids of patients in context of early diagnostic markers.

4.2.3.1 Metabolic diversity in cancer cell lines

Characterization of the metabolite profiles of different cancer cells is required for a proper diagnosis, the development of novel therapeutics (for targeting metabolic pathways to undermine the bioenergetic status of the tumor) and monitoring functions of gene products (Griffin and Shockcor 2004). As an example, for the diagnosis of brain

tumor lineage, metabolomics based on the $^1\text{H-NMR}$ technique has already been successfully applied to distinguish three different human brain tumors (Usenius, Tuohimetsa et al. 1996). Moreover, the metabolic profiles of cell and tumors were collected to design pattern-recognition software beneficial for the diagnosis (Usenius, Tuohimetsa et al. 1996, Hagberg 1998, Griffin and Shockcor 2004). In the present study metabolic diversity between four cell lines was observed. Increased concentration of glutamate in HepG2 cells could be connected with increased proliferation of this cell line. It is in good agreement to previous studies which demonstrated that glutamate and glutathione, products of the glutamine metabolism, are molecules which play a crucial role in tumor proliferation, invasiveness and resistance to therapy (Szeliga and Obara-Michlewska 2009). A low concentration of methionine detected in breast cancer cell line (MCF7) may be another important factor playing a role in breast tumor, beside the previously reported low glucose and choline concentrations detected by NMR (Gribbestad, Sitter et al. 1999).

4.2.3.2 Metabolomics can distinguish apoptotic from necrotic cells

Metabolomics studies based on the $^1\text{H-NMR}$ technique were implemented for monitoring of alteration in cell metabolic profiles after pro-apoptotic treatment to determine biomarkers of apoptosis (Williams, Anthony et al. 1998, Griffin, Lehtimaki et al. 2003, Rainaldi, Romano et al. 2008, Mirbahai, Wilson et al. 2010). In the mentioned reports apoptosis was mostly characterized by alteration in the lipid metabolism which is inconsistent with cancer biology studies the reported the importance of amino acid and carnitine in cancer metabolism (Wagle, Morris et al. 1963, Kovacevic and Morris 1972, Altun, Gunes et al. 2009). It is likely that this effect can be explained by cell line specificity or improper sensitivity of $^1\text{H-NMR}$ for the quantification of amino acid and carnitines changes in cells. In contrast, the present study uncovers strong diversity in the concentration of amino acid and carnitines among apoptotic and necrotic cells in all examined cell line. However, in case of the MCF7 cell line a variance between apoptotic and necrotic cell was limited only to methionine and malonylcarnitine (C3D3 carnitine). It may correlate to the recently reported ability of staurosporine to induce necroptotic cell

death (Dunai, Imre et al. 2012) or possibility to switch between both cell death pathways (Proskuryakov, Konoplyannikov et al. 2003). In contrast the necrotic cells, of all other examined cell lines (HEK293, HepG2, PC3), exhibited a decrease in aspartate, glutamate, methionine, glycine and propionylcarnitine levels. This is in good accordance to the results reported by Mirbahai *et al.* who observed a decrease in glycine and glutamate levels in cells which were triggered to necrosis by starvation (Mirbahai, Wilson et al. 2010). Moreover, the “metabolic loss” in necrotic cells could be connected to low structural integrity resulting in metabolite dissipation. All these facts indicate that the NBS assay is highly suitable for monitoring and distinguishing of cellular process.

4.2.3.3 Pro-apoptotic agents display characteristic metabolic patterns

Considering the number and the variety of therapeutic agents currently present in the early clinical development, robust assay to determine their mechanism of action or therapeutic targets is urgently required (Spratlin, Serkova et al. 2009). Clinical studies on pro-apoptotic drugs are facilitated by the detection of molecules specific for apoptosis (biomarkers) including e.g. caspase (2, 3, 7, 8, 9), cytochrome c, bcl-2, by using ELISA, DNA array or PCR analysis (Ward, Cummings et al. 2008). However, assays detecting single biomarkers, are often to inaccurate to predict proof of concept or monitor responses to therapeutics (Ward, Cummings et al. 2008). Hence, in the present studies, aimed to determine novel biomarkers of programmed cell death, 42 molecules were monitored in a single screen after apoptosis validation with a standard caspase 3/7 assay. The metabolite alterations found in the first experimental trial, applying staurosporine as apoptosis inducer, were cell line specific. Similar metabolic patterns were observed only in case of HEK293 and HepG2 cells, which is in good agreement with results of caspase 3/7 assay. This effect may be explained by possible different mechanism induced by staurosporine in MCF7 and PC3 cell lines. In case of PC3 cells staurosporine-induce apoptosis was unexpected (Marcelli, Marani et al. 2000) and can be a consequence of mutations, which however was not further analyzed. Similar metabolic patterns of apoptotic and necrotic MCF7 cells can be a result of improper adjustment of the staurosporine treatment, which was not further investigated.

Implementation of additional pro-apoptotic agents resulted in the detection of metabolic patterns specific for the different drugs (staurosporine or 5-Fu) as well as identical patterns, independent of treatment. The metabolites including aspartate, methionine, and glycine and malonylcarnitine may be potential biomarkers of staurosporine treatment. Moreover the alteration in aspartate levels can be explained by the discorded energy metabolism (Rainaldi, Romano et al. 2008). In turn, changes in carnitine concentrations (C3 (propionylcarnitine) and (C5 (isovalerylcarnitine)) specific for 5-Fu may be linked to the intracellular transport occurring during apoptosis (Mazzarelli, Pucci et al. 2007). It could be suspected that the lack in characteristic metabolic patterns, as found in case of etoposide, can be a result of the limitation in the number of metabolites measured by the NBS assay. Only alanine and glutamate, among all 42 monitored metabolites, increased in apoptotic cells independently of the kind of pro-apoptotic agent. Nevertheless, presented results are inconsistent with those reported by Rainaldi *et al.* (Rainaldi, Romano et al. 2008). HL60 cells triggered to apoptosis by ionizing radiation or doxorubicin exhibited, in a metabolic study based on $^1\text{H-NMR}$, a decrease in glutamate levels (Rainaldi, Romano et al. 2008). In contrast, a recent metabolic study, based on LC-MS, on gastric cancer patients treated with 5-Fu, known to induce apoptosis in gastric cancer cells (Osaki, Tatebe et al. 1997), demonstrated a significant increase in glutamate after treatment (Sasada, Miyata et al. 2013) which is in good agreement with the results presented in the current thesis. Moreover, among examined patients with or without a drug (5-Fu) resistance only those patients had an increased glutamate level which were not resistant (Sasada, Miyata et al. 2013). The contradictory reports can be explained by the use of different analytical methods and cell types in the studies.

4.2.3.4 Alanine and glutamate are potential novel biomarkers of apoptosis

Validation of a biomarker into a clinical trial is a long process in which reliable connection of biomarkers to disorders or biological processes as well as pharmacodynamics or clinical end points should be determined (Wagner 2002, Ward, Cummings et al. 2008). Moreover, each biomarker validation procedure requires

retrospective and prospective clinical trials as well as large population screening (Ward, Cummings et al. 2008). However, the requirements for the early-phase drug discovery are not that restricted (Lee, Weiner et al. 2005). As described by Lee *et al.* an ideal biomarker supporting drug development would be biologically and clinically relevant, analytically and operationally practical, timely, interpretable and cost effective (Lee, Weiner et al. 2005). Currently, reported alanine and glutamate, depicted from 42 metabolites and measured with a robust assay in less than 3 minutes, achieved almost all features of ideal biomarker for pro-apoptotic drug development. Nevertheless, the biological relevance remains unclear and was further elucidated. It is hypothesized that the simultaneous increase of alanine, a non-essential amino acid produced by reductive amination of pyruvate, and glutamate, the key component in the cellular metabolism, is connected with taurine metabolism. Taurine can be metabolized to alanine and glutamate due to taurine pyruvate aminotransferase (EC.2.6.1.77) and taurine 2-oxoglutarate transaminase (EC.2.6.1.55), respectively (see **Figure 42**). During apoptosis the conversion of taurine is probably strongly up-regulated, but unfortunately, taurine could not be assessed directly in this study as it is not in the panel of the NBS assay. The importance of taurine in apoptotic processes is however supported by two recent publications. In the taurine receptor knockout mouse model a strong correlation between low taurine concentrations and an increased number of apoptotic cells was clearly demonstrated (Warskulat, Borsch et al. 2007). In an earlier report the authors showed that taurine treatment suppressed apoptosis in cardiomyocytes by targeting the apoptotic protease activity factor-1 (Apaf-1)/ caspase 9 apoptosome – complex (Takatani, Takahashi et al. 2004). In conclusion it can be assumed that the adaptation of the NBS assay for metabolomics studies in cells may provide promising strategies to improve drug screening and development, especially regarding its easy further application in human biofluids. Alanine and glutamate, detected by NBS assay to be up-regulated specifically in apoptotic cells independent of the pro-apoptotic agent, meet all requirements pointed out by Lee *et al.*, to support early-phase drug development in cell culture (Lee, Weiner et al. 2005)

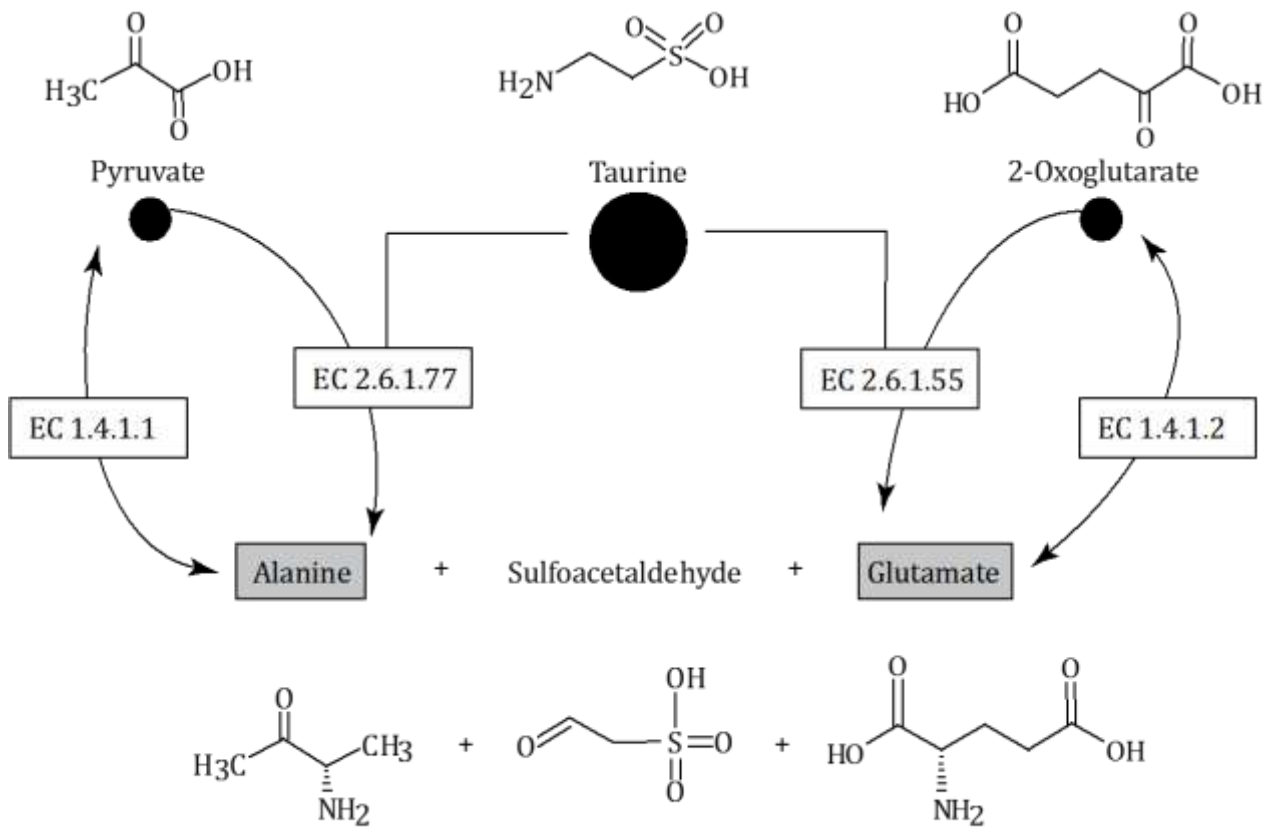


Figure 42 Connection between alanine, glutamate, and taurine metabolism. The metabolism of the two metabolites alanine and glutamate (presented in grey) which were found to be up-regulated in apoptotic cells can be connected to taurine. Both, alanine and glutamate might be synthesized from taurine via reactions catalyzed by taurine pyruvate aminotransferase (EC. 2.6.1.77) and taurine 2-oxoglutarate transaminase (EC. 2.6.1.55), respectively.

4.3 Facing adipogenesis – a step forward in obesity prevention. (Adipogenesis blamed for obesity – would metabolomics be a judge?)

Obesity, characterized as an excess of adipose tissue (Yang, Kelly et al. 2007), is a major risk factor of several diseases e.g. cardiovascular disease, insulin resistance, type 2 diabetes, hypertension or metabolic syndrome. Recently, these complex diseases arising from the interaction of multiple genes with environmental and behavioral factors, reach worldwide epidemic level (Rossner 2002, Flier 2004). Considering the multifactorial etiology of obesity its prevention and management is especially challenging (Yang, Kelly et al. 2007). Recently, new emerging high throughput technologies like e.g. metabolomics, based on the metabolic profiling of human individuals in large population studies, enables the prediction of metabolic diseases before become clinically apparent (Wang, Larson et al. 2011, Ferrannini, Natali et al. 2012, Wang-Sattler, Yu et al. 2012, Floegel, Stefan et al. 2013). Although metabolic studies regarding human obesity have been performed in obese individuals (in children (Wahl, Yu et al. 2012) or adults (Newgard, An et al. 2009)), metabolomics of obesity development remains open. The aim of this part of the thesis was thus to characterize adipogenesis by transcriptomics and metabolomics to uncover biologically relevant metabolic pathways and molecules which are related to obesity development (biomarkers) and do detect putative biomarkers for early detection of obesity risk.

4.3.1 3T3-L1 cell culture model for the study of obesity development on the metabolic level

White adipose tissue serves as energy reservoir (Rosen and Spiegelman 2006) as well as an endocrine organ (Kershaw and Flier 2004). In conditions of disrupted energy balance (energy overload), excess energy is stored in adipocyte tissue, which as a result increases in cell size or/ and number. In consequence, the number of adipokines, free fatty acids and inflammatory mediators, produced by adipocytes, increase and affect

other tissue, e.g. liver, muscle, or neural connections, which leads to obesity and its co-mortalities (de Ferranti and Mozaffarian 2008, Guilherme, Virbasius et al. 2008). To determine the metabolic profile of patients with risk of obesity, lengthy processes requiring large population screenings are needed. Besides, with evaluation of large human population studies, several influencing factors have to be taken into account, including overall health, gender, environmental exposure, age (Cuperlovic-Culf, Barnett et al. 2010) which may overshadow the metabolic profile underlying to obesity development. Since the metabolic profile of whole organisms may not provide relevant information about the subjects (molecular mechanisms in adipogenesis), studies were performed in a suited cell culture model. The murine preadipocyte cell line 3T3-L1, originally generated in 1970's by Green and colleagues (Green and Meuth 1974), have all three attributes of *in vivo* adipocytes including lipid storage, insulin sensitivity and endocrine properties (White and Stephens 2010). Furthermore, electron micrographic analysis demonstrated that 3T3-L1 cells are identical to *in vivo* adipocytes (Novikoff, Novikoff et al. 1980, MacDougald and Lane 1995). In contrast to human cell culture model 3T3-L1 cells are easily differentiated into adipocytes after treatment with a hormonal mixture (Green and Kehinde 1975). Over the last 35 years, 3T3-L1 has been used for studies on adipogenesis, obesity and insulin resistance (Williams and Mitchell 2012); (Sakoda, Ogihara et al. 2000), and therefore was applied in current pioneer analysis. Cells were cultivated and differentiated with a hormonal mixture containing insulin, IBMX and dexamethasone in accordance to previously described protocols (Green and Kehinde 1975, Student, Hsu et al. 1980). The experimental setup of this study enabled monitoring of different stages of adipogenesis and due to a fixed time frame for exchanging conditioned medium (every 48 h), prevented accidental metabolite alteration (**Figure 16**). Adipogenesis progression was verified in respect of morphological modifications, resulting in lipid accumulation in form of liposomes (Oil Red O assay), and changes of gene expression and protein levels of molecules fundamental for adipogenesis (Rosen and Spiegelman 2000), including C/EBP β (Cao, Umek et al. 1991), PPAR γ (Tontonoz, Hu et al. 1994), C/EBP α (Lin and Lane 1994). Cell numbers were monitored and used for normalization to exclude false metabolite alteration which may have occurred due to changes in cell number. For metabolomics studies, targeted

high-throughput Absolute IDQ assays, optimized for cell culture approaches, were applied because they enable for monitoring of different metabolite classes including amino acids, biogenic amines, carnitines, hexoses and lipids (Floegel, Stefan et al. 2013). Metabolomics studies were supported by transcriptomics experiments to puzzle out the metabolic pathways relevant for adipogenesis. Similar strategies were recently applied in human population studies in which metabolomics was complementing the limitations of genome wide association studies (GWAS) (Gieger, Geistlinger et al. 2008, Illig, Gieger et al. 2010, Suhre, Shin et al. 2011, Adamski 2012, Adamski and Suhre 2013). For the first time combined GWAS and targeted metabolomics, performed in small scale pilot project, clearly demonstrated a correlation between four genetic variants in genes coding for enzymes (FADS1, LIPC, SCAD, MCAD) and the metabolic phenotype, which clearly matched the biochemical pathways in which these enzymes are active (Gieger, Geistlinger et al. 2008). Pathway analysis of combined metabolomics and transcriptomics data sets was performed by using the Ingenuity Pathway Analysis (IPA) tool which was previously reported as powerful tool for identification of biological pathways that influence disease outcomes (Ngwa, Manning et al. 2011).

4.3.2 Adipogenesis validation

Cell differentiation was verified in the first place by monitoring lipid accumulation in liposomes which is directly proportional to the development of adipogenesis (Kuri-Harcuch and Green 1978, Kuri-Harcuch, Wise et al. 1978). A suitable and fast method for lipid visualization and quantification is the Oil Red O assay (Ramirez-Zacarias, Castro-Munozledo et al. 1992) which uses a colored substance that is soluble in lipids (Kasturi and Joshi 1982, Kruth 1984). Adipogenic cell differentiation resulted in loss of fibroblastic cell morphology toward round containing lipid droplet adipocytes started at day 4 which is in good accordance to previous reports, applied same differentiation protocols (Student, Hsu et al. 1980). The morphological changes may occur due to alterations in the expression of cytoskeletal and extracellular molecules which strongly decrease, like β and γ - actin or α - and β tubulin, or increase, like different types of collagen (Spiegelman and Farmer 1982, MacDougald and Lane 1995). Nevertheless, it

has to be taken into account and clarified that changes in cell phenotype, occurring during adipogenesis, are a consequence of a transcriptional cascade, as previously described (Bernlohr, Bolanowski et al. 1985, Cook, Hunt et al. 1985, Christy, Yang et al. 1989). Therefore, patterns presented during adipogenesis by key molecules (C/EBP β , PPAR γ , C/EBP α) involved in the transcriptional cascade were examined by qPCR and Western blot. In the current study gene expression profiles correlated with protein level in all examined molecules. The C/EBP β was strongly up-regulated from day 2 of cell differentiation on and decreased afterwards which is in good accordance to results reported by other groups where studies showed sensitivity of C/EBP β to dexamethasone treatment, reaching a maximum in the first 2 days and decreased before C/EBP α occurred (Cao, Umek et al. 1991, Ntambi and Young-Cheul 2000). The C/EBP β is a known activator of PPAR γ (Wu, Bucher et al. 1996) which reached its maximum at day 8 of the differentiation. The Western blot results presented for PPAR γ , exhibit two bands which may reflect its two isoforms (γ 1 and γ 2) (Tontonoz, Hu et al. 1994, Vidal-Puig, Jimenez-Linan et al. 1996) occurring in adipocytes. Furthermore the activity of PPAR γ thought to mediate the expression of C/EBP α (Rosen and Spiegelman 2000) reached its maximum at day 4, which is similar with previous studies (Christy, Kaestner et al. 1991, Lin and Lane 1994). This indicates that obviously a well-regulated adipogenesis had been induced in 3T3-L1 by giving a hormonal cocktail, which was desirable for the further study on the metabolomics and transcriptomics level.

4.3.3 Metabolomics reflect different stages of adipogenesis

In contrast to obesity or type 2 diabetes, frequently studied by metabolomics, changes in small molecule composition of cells undergoing adipogenesis were only once reported (Roberts, Virtue et al. 2009). Noteworthy, in this study only intracellular metabolites were monitored and trypsin, reported to change the metabolite profile (Teng, Huang et al. 2009, Batista, Garvas et al. 2010, Dettmer, Nurnberger et al. 2011), was applied for cell harvesting. The current study applied targeted metabolomics to examine metabolite alteration in both cell extracts and conditioned medium to get a global view on pathways underlying adipogenesis. Statistical data analysis was performed by using the *metaP*

server providing automated and standardized data analysis for quantitative metabolomics data (Kastenmuller, Romisch-Margl et al. 2011). Besides, for quality checks and estimation of reproducibility the *metaP* server enables the calculation of correlations of the metabolite concentration with given phenotypes (Kendall correlation test), the visualization of similarities or differences among generated intrinsic groups in the data (PCA) or testing the association of metabolites concentrations with categorical phenotypes (hypothesis test). In the current case, the metabolite alterations correlated well with adipocyte differentiation progress but not with the experimental procedure (no systemic mistake throughout sample replication) (**Figure 20**). Furthermore, different groups observed in cells and in conditioned medium, as highlighted by PCA, correspond to particular stages as well as days of ongoing adipogenesis, what clearly demonstrates that metabolomics is a suitable tool to study this process. Metabolites depicted by PCA as the mostly contributing to adipogenesis (**Figure 22**) belonged to different metabolite classes and exhibited variable patterns in the course of adipogenesis. Considering the fat cells function regarding the energy reservoir (Rosen and Spiegelman 2006), the increased level of phosphatidylcholines in the medium and the cells was connected to lipid metabolism. It is in good accordance to the results presented by Roberts *et al.* a study on metabolic phenotyping of adipogenesis (Roberts, Virtue et al. 2009). Furthermore, elevated levels of glutamine and asparagine in conditioned medium can be in direct correlation to the metabolic patterns of obese individuals reported to have increased serum level of those metabolites (Newgard, An et al. 2009). However, when leucine patterns from the current study were compared with those of a metabolic study in obese humans, contradictory results were found (decrease in adipogenesis and increase in human study) (Newgard, An et al. 2009). Hence, it has to be taken into account and clarified that profiles presented by metabolites in cells may not be always in direct correlation to the those presented by systemic body fluids, as previously described (Cuperlovic-Culf, Barnett et al. 2010). The metabolic patterns observed in case of spermidine and putrescine may support results presented by Ishii et al. who demonstrated the involvement of polyamines in adipogenesis (Ishii, Ikeguchi et al. 2012). Furthermore, the decrease in palmitoylcarnitine (C16) concentrations in cells is in good accordance to the previous study that reported a decrease in carnitine

concentrations (nonesterified carnitine, acid-soluble acylcarnitines and acid-insoluble acylcarnitines) during adipogenesis (Cha, Eun et al. 2003). Although metabolic alterations are target-oriented and reflect biological processes the origins and mechanisms causing the changes are often non-specific. Hence, to elucidate the gene expression profiling was implemented in the next step.

4.3.4 Transcriptomics reflect adipogenesis progression

In contrast to the poorly explored metabolomics of adipogenesis, gene expression profiling was more often investigated (Guo and Liao 2000, Ross, Erickson et al. 2002, Cheng, Lee et al. 2008, Billon, Kolde et al. 2010). The here performed transcriptomics study revealed 1000 significantly regulated genes among which GLUT4, KLF5, KLF15, PPAR γ , CHOP and GATA2 (known genes involved in adipogenesis) exhibit expression patterns which correlated with those previously reported (Rosen and MacDougald 2006) and served as positive control. Further analysis was performed by the clustering the genes because those genes, which exhibit similar expression patterns, may be regulated by the same mechanisms (Eisen, Spellman et al. 1998, Lubovac and Olsson 2003). The IPA analysis of cluster 1 highlighted genes involved in cancer biology which can be related to the previous finding suggesting relation between obesity and cancer (Spiegelman, Choy et al. 1993), an issue that was however not further investigated. The morphological transformation of examined cells, besides using cell imaging, can be also monitored through the expression patterns of genes responsible for morphology of filaments and fibrils affecting the cytoskeleton. For example, genes presented in cluster 2 including among others γ -actin and β -tubulin, known as concomitants of loss of the preadipocyte phenotype (Spiegelman and Farmer 1982), or decorin, recently reported as key molecule in the formation of collagen fibers (Danielson, Baribault et al. 1997) reflected morphological changes during adipogenesis. In turn, patterns exhibited by genes from cluster 3 were correlated with growth-arrest and a decrease in cell proliferation, which is a known event of adipogenesis (Ross, Erickson et al. 2002). Finally, genes which are known attributes of the adipocyte phenotype including among others lipid-droplet associated protein CIDEC (Puri, Konda et al. 2007), adipogenin,

adipocyte-specific membrane protein (Hong, Hishikawa et al. 2005), adiponectin, expressed exclusively in adipocytes (Scherer, Williams et al. 1995, Haluzik, Parizkova et al. 2004), PPAR γ , and stearoyl-CoA 9-desaturase (SCD) (Casimir and Ntambi 1996) occurred in cluster 4 and 5. Moreover, those clusters are highly interesting since they contain genes involved in lipid synthesis like PCYT2, a key player in phospholipid synthesis (Bladergroen and van Golde 1997, Nakashima, Hosaka et al. 1997), FDPS, involved in cholesterol biosynthesis (Spear, Kutsunai et al. 1992), or BCAT2, participating in the branched chain amino acid (BCAA) catabolism (Torres, Vargas et al. 2001). Nevertheless, genes grouped in cluster 5, related to several diseases, exhibited remarkable patterns which are not always similar to those described for human obesity or diabetes. For example, adiponectin, up-regulated during adipogenesis and in mature adipocytes in the current study, has been previously described as being down-regulated in obese individuals and strongly expressed by leanness (Fasshauer, Klein et al. 2002, Makimura, Mizuno et al. 2002, Haluzik, Parizkova et al. 2004). Furthermore, the glucose transporter GLUT4 was, like adiponectin, up-regulated in adipocytes and adipogenesis in the current study but down-regulated in adipose tissue of obese individuals suffering from type 2 diabetes (Shepherd, Gnudi et al. 1993). Similar effects, referring to opposite expression patterns, in adipocytes and obese type 2 diabetes patients, has been previously described for SREBP1 (sterol regulatory element binding transcription factor 1) involved in sterol biosynthesis (Nadler, Stoehr et al. 2000). In turn, gene expression profiles of CIDEC, exhibited during adipogenesis and in mature adipocytes, are in good accordance to strongly up-regulated CIDEC patterns in omental and subcutaneous adipose tissue in obese individuals (Puri, Ranjit et al. 2008). Although the knowledge on adipogenesis related molecules has recently strongly increased and can be even connected to several metabolic pathways (see

Table 10), their real connection to obesity and type 2 diabetes remain unclear. This issue was broadly discussed by Flier *et al.* in his review (Flier 2004). Hence, determination of the role played by adipogenesis and mature adipocytes in the mechanisms underlying the development of those complex diseases is the great interest of the current study referring to early diagnosis of obesity development.

4.3.5 Global metabolic pathways are regulated during adipogenesis – highlighted after merging metabolomics and transcriptomics data.

Integrated metabolomics and transcriptomics studies were recently applied in a mouse model to discover novel biomarkers of diabetes (Connor, Hansen et al. 2010). In the current analysis of integrated data the first objective was to uncover global metabolic differences between adipocytes and preadipocytes. The molecules found to be regulated during adipogenesis were preliminary linked to increase rates of glycolysis, citrate cycle, amino acid catabolism (BCAAs, proline, aspartate, glutamate and alanine) and lipid metabolism (see

Figure 27). The changes in the glycolytic pathway, characterized by a decrease of hexoses in conditioned medium and an increase of several genes involved in carbohydrate metabolism including e.g. glucokinase (GCK), increasing the glycolysis rate (Aiston, Peak et al. 2000) or MLX interacting protein-like(MLXIPL), reported as mediator of glycolysis (Begrache, Igoudjil et al. 2006), was connected to the citrate cycle through acetyl-CoA (product of e.g. glycolysis). This findings supplement studies on the metabolic phenotyping of adipogenesis in which a rise of glucose utilization was connected with fatty acid synthesis through the TCA cycle, a process monitored with ¹³C-labeled glucose tracing (Roberts, Virtue et al. 2009). Furthermore, findings related to up-regulation in the citrate cycle, through the intermediates like citrate, succinate, fumarate, malate and oxaloacetate were not measurable due to the targeted metabolomics assay applied in this study. However, the proof of TCA up-regulation is indirectly supported by the increased glycolysis, supplying the TCA with acetyl-CoA, an increased expression of the citrate transporter SLC25A1 and a decrease in the concentrations of aspartate, glutamate (decreased only in medium), proline and BCAAs which can be incorporated into the TCA by appropriate enzymes (also detected in the course of this study). Notably, the BCAA patterns were not consistent with previous reports and therefore the analysis was extended and will be further discussed in the next subset (see **Figure 28**). Moreover, a previous report regarding a metabolomics study in a mouse model with chronic obesity, insulin resistance, and hyperglycemia showed an increase in TCA cycle

components in obese animals (Connor, Hansen et al. 2010). The glutamate level in cells, which slightly increased during adipogenesis, can be connected to proline and alanine, which may be metabolized to glutamate. This effect is in good accordance to the increased glutamate concentrations reported by Roberts *et al.* (Roberts, Virtue et al. 2009). Moreover, highlighted by Newgard *et al.* increased pyruvate levels in plasma of obese individuals (Newgard, An et al. 2009), facilitates the in the current study presented hypothesis, suggesting the synthesis of glutamate and pyruvate from 2-oxoglutarate and alanine. However, the alanine level, strongly decreased in the current study, was up-regulated in above referred plasma samples which may be related to other metabolic events occurring in a complex system like the human body. Furthermore, carnitines playing a crucial role in fatty acid transport (Xie, Waters et al. 2012), were connected to obesity in several reports, however with contradictory results (Newgard, An et al. 2009, Kim, Park et al. 2010, Wahl, Yu et al. 2012). On the one hand, elevated carnitine levels were connected to increased free fatty acid (FFA) metabolism requiring carnitines for β -oxidation, or to the BCAA catabolic pathway in which carnitines may occur as products (Newgard, An et al. 2009, Xie, Waters et al. 2012). On the other hand, decreased carnitine levels in obese individuals may be reasonable due to the previous study reporting supplementation of carnitine being beneficial for weight loss supplementation of carnitine (Mun, Soh et al. 2007). In the current thesis, variable carnitines patterns were observed: short chain carnitines were up-regulated, which is in good accordance to the Newgard *et al.* study; in contrast, long chain carnitines, like C16, were strongly down-regulated which can be supported by the previous study monitoring carnitine levels during adipogenesis (Cha, Eun et al. 2003).

Hence, metabolic patterns exhibited by carnitines during adipogenesis are strongly dependent on their chain length.

4.3.6 BCAA degradation is crucial for adipogenesis progression – in searching for a link to obesity

Recent studies (Newgard, An et al. 2009) revealed the BCAA metabolism as important subject in obesity due to the strong increase of BCAAs in the plasma of obese

individuals. Nevertheless, in the current study BCAA concentrations strongly decreased during adipogenesis and remained down-regulated in mature adipocytes (see **Figure 28**). The metabolomics results were supported by transcriptomics data exhibiting increased expression patterns of genes involved in the catabolism of those metabolites (see **Figure 29**). Furthermore, the current results are in good accordance to previous reports which showed correlation between decreased BCAA and obese children (Wahl, Yu et al. 2012) or obese adolescent and adolescent with type 2 diabetes (Mihalik, Michalyszyn et al. 2012). Remarkably, even in the past, BCAA metabolism in adipocytes was a controversial subject. Already in the 1974 Rosenthal et al. reported that leucine can serve as a precursor for the sterol biosynthesis and showed its increased conversion rate into the lipids and sterols in adipose tissue (Rosenthal, Angel et al. 1974). This effect was supported by Tischler *et al.* demonstrating rapid degradation of leucine as well as isoleucine and valine in adipocytes from fat rats which was stimulated by glucose and insulin (Tischler and Goldberg 1980). However, other study revealed low activity of enzymes involved in the BCAA catabolism in adipose tissue (Suryawan, Hawes et al. 1998). Hence, the mechanism of BCAA metabolism in adipocytes and its role in the whole metabolic system has to be clarified. The metabolomics and transcriptomics study were supplemented with qPCR experiments essential to close gaps for pathways reconstruction. The leucine catabolic pathway was connected to cholesterol synthesis, due to 3-hydroxy-3-methylglutaryl-CoA, which is known molecule in cholesterol biosynthesis and a product of leucine degradation (Thomas, Shentu et al.). Although cholesterol is not measurable by the here applied targeted metabolomics, it can be monitored indirectly by the Oil Red O assay (Ramirez-Zacarias, Castro-Munozledo et al. 1992) which in this studies showed a high increase in lipid accumulation (**Figure 18**). Moreover, enzymes involved in cholesterol synthesis were up-regulated. Hence, it is considered that during adipogenesis cholesterol synthesis require leucine as a substrate. This findings is supported by a previous report (Rosenthal, Angel et al. 1974). Furthermore, a “leucine deficiency” study on fat pads found decreased glutamine and alanine concentrations in medium which may suggest that these molecules are metabolized subsidiary (Tischler and Goldberg 1980). In turn, leucine and valine were connected to increased citrate cycle metabolism and may serve

as substrates for fatty acid metabolism. However, only experiments applying labeled BCAAs may provide evidence, which can facilitate or dismiss the proposed hypothesis, however it was not further investigated. Noteworthy, the currently presented BCAA patterns are in good agreement only to those presented for obese children or adolescent which may be related to the dynamics of fat cell turnover during human life. Although the major factor determining fat mass in human adults is the adipocyte number, the quantity of fat cells remains constant in adults (Spalding, Arner et al. 2008) and is established during childhood and adolescent. Hence, decreased BCAA concentrations should be further investigated toward their potential as novel biomarkers determining human obesity development already in children.

4.3.7 Biogenic amines as potential biomarkers of different stages of adipogenesis

The alteration in polyamines, key players in adipogenesis (Bethell and Pegg 1981, Ishii, Ikeguchi et al. 2012), in the current study reflect different stages of adipogenesis. Patterns exhibited by putrescine which increased in the early phase of differentiation and shortly after decreased is in good accordance to the previous study on adipogenic cell differentiation (Roberts, Virtue et al. 2009). The metabolic patterns in cells as well as in conditioned medium showing only a decrease in putrescine and spermine may suggest that putrescine and spermine are metabolized to spermidine. However, transcriptomics data do not support this finding and suggest that putrescine is metabolized into 4-aminobutanoate which is good correlation to a previous study (Roberts, Virtue et al. 2009). Although the regulation of spermine and spermidine was not further investigated, the metabolic signatures presented by polyamines in the course of adipogenesis may be applied for standardized monitoring of adipogenic cell differentiation.

4.3.8 Lipid metabolism and adipogenesis

Previously, the role of lipids in organisms was thought to be limited only to the structural.

However, recent studies clearly demonstrate that lipids are second messengers in signaling pathways stimulating cell survival or proliferation and are involved in pathophysiological disease states including inflammation, obesity (Shimizu 2009), coronary heart disease (Khaw, Friesen et al. 2012), diabetes (Jones and Varela-Nieto 1999) and cancer (Mills and Moolenaar 2003). Thereby, monitoring the lipid metabolism during adipogenesis can be applied to determine lipid involvement in obesity development and characterization at an early stage enabling the detection of patients with obesity risk as well as connections to other complex diseases like diabetes or cancer.

4.3.8.1 Phosphatidylcholine synthesis, remodelling and accumulation of odd chain fatty acid are consequences of adipogenesis

A direct correlation between the increased concentration of phosphatidylcholines and an up-regulation of the Kennedy pathway, the *de novo* biosynthesis of PCs, can obviously be drawn (**Chapter 3.3.6.1**). However, the regulation patterns of PCs are strongly dependent on the type of their fatty acid side chains e.g. position (acyl, acyl or acyl, ether), length or saturation level. Since the metabolic approach used in the current study is incapable to provide information about chain composition, possible reactions on fatty acid chain hypothesized as presented in **Figure 34** and

Figure 35. Patterns exhibited by PCs aa and PCs ae during adipogenesis suggest incorporation of fatty acids chain with increasing saturation levels or increasing length, respectively. Moreover, genes involved in fatty acid desaturation (SCD1, FADS 2) and elongation (ELOVL 3) were found to be up-regulated which is in good accordance to previous studies (Christy, Yang et al. 1989) (Kobayashi and Fujimori 2012). SCD1, catalyzing the biosynthesis of $\Delta 9$ monounsaturated fatty acid oleate, from the saturated fatty acid stearate, has been highlighted as target molecule to prevent or treat obesity (Warensjo, Ingelsson et al. 2007). Furthermore, FADS2 involved in second desaturation of oleate to octadecadienate, is known to play role in inflammatory diseases (Obukowicz, Raz et al. 1998). The reorganization of phosphatidylcholine composition may be connected to modifications in cellular membranes necessary to meet

requirements for specific signals transduction. As it was already reported, the fatty acid chain composition has physiological consequences regarding membrane fluidity, permeability and stability (Vance and Vance 2002). Hence, the properties of the cellular membrane in young and mature adipocytes can be characterized by increased fluidity and decreased rigidity and solubility as consequence of increased desaturation and elongation (Vance and Vance 2008). An indirect determination of the composition of chains incorporated into PCs has been performed in this study by the measurement of fatty acid concentrations with a different metabolic approach. The altered patterns of only three molecules with even numbers of carbons and of the majority of uneven (odd) fatty acid chains were unexpected. Whereas elevated levels of myristic, myristoleic, and palmitoleic as well as stearic, oleic, linoleic, and arachidonic acids were previously observed in obese individuals (Newgard, An et al. 2009), changes in odd chain fatty acid concentrations have not been reported. In turn, the odd chain fatty acids have been previously determined as biomarkers of dairy consumption, as measured in subcutaneous adipose tissue and in serum of male individuals (Wolk, Furuheim et al. 2001). Moreover, the authors suggest that odd chain fatty acids cannot be metabolized in the human body and are delivered with diet (Wolk, Furuheim et al. 2001). Nevertheless, in the current study the odd chain fatty acid accumulation correlated with adipogenesis progression in both cells and conditioned medium. Remarkable, in this case condition medium is not the source of odd chain fatty acids for cells. Moreover, current studies are in good accordance to previous reports showing an increased odd chain fatty acid level during adipogenesis (Su, Han et al. 2004, Roberts, Virtue et al. 2009). Furthermore, enhanced synthesis of odd-number long chain fatty acids, stimulated by an excess of propionyl-CoA, has been reported in red cell membrane lipids of patients with propionic acidemia and methylmalonic aciduria, disorders of the propionate catabolism (Wendel 1989). Noteworthy, in the current thesis an increased catabolism of BCAA, resulting in propionyl-CoA excess was demonstrated. It can thus be suggested that the excessive BCAA catabolism stimulated odd chain fatty acid synthesis. However, some reports suggest α -oxidation of even chain fatty acids as possible pathway for odd chain fatty synthesis (Su, Han et al. 2004). Hence, the ancestry of odd chain fatty acids in mammals is unclear and reports are inconsistent. On

the one hand it was reported that only branched chain fatty acids (like phytanoyl-CoA) can undergo α -oxidation (Wanders, Jansen et al. 2003), on the other hand it has been shown that purified peroxisomal phytanoyl-CoA alpha hydroxylase can use un-branched long chain fatty acids as substrate (Mukherji, Kershaw et al. 2002). Recently, accumulation of odd chain fatty acids was reported in human with coronary heart diseases (Khaw, Friesen et al. 2012), one of the major risk factors of obesity. However, in this case the milk consumption can probably not be used as explanation since the dairy products are known to correlate to lower risk of heart diseases (Elwood, Pickering et al. 2004) and hypertension (Wang, Manson et al. 2008). However, the BMI between cases and controls was significantly different what suggests involvement of fat cells in the odd chain fatty acid synthesis. Furthermore, as presented by Wolk *et al.* a correlation between dairy intake and odd chain fatty acid increase in male serum does not provide information on the BMI of proband (Wolk, Gridley et al. 2001). Moreover, since in the current study, adipocytes were involved in synthesis and secretion of odd chain fatty acids, which is in good line to previous reports (Pike, Han et al. 2002, Roberts, Virtue et al. 2009), determination of odd chain fatty acids as biomarkers of dairy consumption should be reconsidered.

4.3.8.2 Phosphatidylcholine degradation can have impact on low-grade chronic inflammatory state in obesity

Recently, obesity and metabolic dysfunctions were associated with a low-grade chronic inflammatory state (Das 2001, Shimizu 2009) and frequently linked to adipose tissue and fatty acid composition (Garaulet, Perez-Llamas et al. 2001, Wahl, Yu et al. 2012). Therefore, the unexpected decrease in phosphatidylcholines and lysophosphatidylcholines containing very long unsaturated fatty acids can be connected to the formation of subunits like mead, arachidonic, and eicosapentaenoic acid, which are known as precursors of fatty acids that mediate inflammatory response (Iyer, Fairlie et al. 2010). Besides, arachidonate is strongly up-regulated in human obesity (Williams, Baylin et al. 2007, Newgard, An et al. 2009). Hence, it was thought that released arachidonate would be increased in conditioned medium or in cells. In contrast, after

implementation of different targeted metabolomics approaches, a strong decrease of arachidonic acid and docosahexaenoic acid in conditioned medium and no changes in cells were detected which is in opposition to previously reported human study in obese individuals (Williams, Baylin et al. 2007, Newgard, An et al. 2009). However, the effect can be supported by the recently presented survey in which lysophosphatidylcholines (LysoPC a C20:4) were shown to be decreased in plasma samples of obese children (Wahl, Yu et al. 2012). Hence, the release of arachidonate from the cellular membrane and its increased absorption from conditioned medium suggests that arachidonic acid and other very long chain un-saturated fatty acids are highly required for adipogenesis. These findings could be facilitated by the transcriptomics data uncovering a strong increase in genes involved in arachidonic acid catabolism towards prostaglandins synthesis. Nevertheless, the expression pattern of phospholipase A2, preliminary involved in the release of arachidonate from the cellular membrane (actually from phosphatidylcholines) (Jaworski, Ahmadian et al. 2009) was up-regulated first at day eight, although the decrease of phospholipids visible already at day 4 of differentiation. For this reason, monoglycerol lipase (MGLL) strongly, up-regulated already from day 4 on, was proposed as candidate responsible for arachidonate release (see Figure 40). Monoglycerol lipase is known to play a role in the degradation of monoacylglycerols like 2-arachidonyl into arachidonate and glycerol, which is a part of the endocannabinoid signaling involved in several neuronal process including the regulation of food intake and lipid metabolism (Dinh, Carpenter et al. 2002, Chon, Zhou et al. 2007). On the one hand, MGLL is involved in triacylglycerol degradation (in brain), on the other hand its overexpression in the small intestine of mutant mice resulted in significant body mass gain and body fat accumulation (Chon, Douglass et al. 2012). Moreover MGLL-KO mice receiving a high fat diet exhibited significantly improved glucose tolerance and insulin sensitivity, and lower weight than controls (Taschler, Radner et al. 2011). Furthermore, it has been reported that human adipose and liver tissue are structurally comparable and in close proximity to the composition of immune-regulatory cells, like Kupffer cells, macrophages, and T cells and therefore are involved in dynamic interactions between immune and metabolic processes crucial to regulate signaling networks (Hotamisligil 2006, Iyer, Fairlie et al. 2010). Moreover, the increased level of PGF2 α in conditioned

medium of young and mature adipocytes suggest that adipocytes are capable of exporting prostaglandins into the system which is in good accordance to a previous study where increased PGF2 α levels were detected in plasma of obese children (Giannini, de Giorgis et al. 2008). Hence, referring to the increased arachidonate and prostaglandin metabolism in fat cells, it can be concluded that adipocytes may be responsible for the low-grade chronic inflammatory state in individuals with obesity which presumably have impact on the development of other chronic diseases like cancer or type 2 diabetes.

Taken together, presented results showing down-regulation in the BCCAs level and up-regulation of PGF2 α correlate with the studies on children obesity (Mihalik, Michaliszyn et al. 2012, Wahl, Yu et al. 2012). This phenotype can be explained by findings suggesting that adipogenic cell differentiation occurs only in children and adolescents (Spalding, Arner et al. 2008). In conclusion, metabolic pathways and molecules highlighted in this thesis, as characteristic for adipogenesis, are potential biomarkers for obesity development and drug targets for its prevention. Moreover, identification of obesity risk in early stages of human life and its effective treatment may reduce related health complications.

5 APPENDIX

5.1 Abbreviations

| | |
|-----------|--|
| SD | standard deviation |
| 1,2-DG | 1,2-Diacylglycerol |
| 5-Fu | 5-Fluoruracil |
| ABCD2 | ATP binding cassette subfamily G |
| ACAA2 | acetyl-CoA acyltransferase |
| ACADS | acyl-CoA dehydrogenase |
| ACSL3 | acetyl-CoA synthase long-chain family member |
| ACSS2 | acetate-CoA synthase short chain family member |
| Ala | alanine |
| ALDH | aldehyde dehydrogenase |
| alpha-AAA | alpha-amino adipic acid |
| AOC3 | amine oxidase |
| Arg | arginine |
| Asp | aspartate |
| AUH | enoyl-CoA-hydratase |
| BCA | bovine serum albumin |
| BCAA | branched chain amino acids |
| BCAT | branched chain amino acids transaminase |
| Bcl-2 | b-cell lymphoma 2 |
| BMI | body mass index |
| BSA | bovine serum albumin |
| C/EBP | CCAAT-enhancer-binding proteins |
| C0 | free carnitine |
| C16 | palmitoyl carnitine |
| C2 | acetylcarnitine |
| C3 | propionylcarnitine |
| C3DC | malonylcarnitine |
| C5 | isovaleryl carnitine |
| CBR | carbonyl reductase |
| cDNA | complementary DNA |
| CETP | cholesterol ester transfer protein |
| CHOP | CCAAT – enhancer binding protein |
| Cho-P | cholinephosphate |
| CHPT | cholinephosphotransferase |
| CK | choline kinase |
| cps | counts per second |
| CUD | carnitine uptake defect |

| | |
|-------|---|
| CYP | cytochrome |
| DAPI | 4',6-diamidino-2-phenylindole |
| DBT | dihydrolipoamid branched chain transacylase |
| DDO | D-aspartate oxidase |
| DEPC | diethyl pyrocarbonate |
| Dex | dexamethasone |
| DHCR | dehydrocholesterol reductase |
| DMEM | dulbecco's modified eagle medium |
| DMSO | dimethyl sulfoxide |
| DNA | deoxyribonucleic acid |
| ECL | enzymatic chemiluminescence |
| EETs | epoxyeicosatrienoic acids |
| EK | ethanolamine kinase |
| ELOVL | fatty acid elongase |
| EPT | ethanolaminephosphotransferase |
| Etn-P | ethanolamine-phosphate |
| Eto | etoposide |
| FADS | fatty acid desaturase |
| FBS | fetal bovine serum |
| FDPS | farnesyl diphosphate synthase |
| FIA | flow injection analysis |
| FT-IR | Fourier transform infrared |
| GATA2 | GATA binding protein 2 |
| GC | gas chromatography |
| GCK | glucokinase |
| Glu | glutamate |
| GLUT4 | insulin- sensitive glucose transporter type 4 |
| Gly | glycine |
| GP | glycerone phosphate |
| GPD1 | glycerol-3-phosphate dehydrogenase 1 |
| GPT1 | glutamic pyruvic transaminase 1 |
| GWAS | genome wide association studies |
| H1 | hexosose |
| HETEs | hydroxyeicosatetraenoic acids |
| HMGCL | 3-hydroxymethyl-3-methylglutaryl-CoA lyase |
| HMGCS | 3-hydroxy-3-methylglutaryl-CoA synthase |
| HPLC | high performance liquid chromatography |
| HSD | hydroxysteroid dehydrogenase |
| IBMX | 1-Methyl-3-isobutylxanthine |
| IL-6 | interleukin-6 |
| IPA | Ingenuity Pathway Analysis System |
| IS | internal standard |
| KLF | Kruppel-like factor |

| | |
|---------------|---|
| LC | liquid chromatography |
| Leu | leucine |
| LOD | limit of detection |
| LPL | lipoprotein lipase |
| LTC | leukotriene |
| MCEE | methylmalonyl-CoA epimerase |
| MeOH | methanol |
| MESA | buffer |
| Met | methionine |
| MGLL | monoglyceride lipase |
| MRM | multiple reaction monitoring |
| mRNA | messenger RNA |
| MTT | dimethyl thiazolyl diphenyl tetrazolium salt |
| MUT | methylmalonylCoA mutase |
| MVD | mevalonate diphosphate decarboxylase |
| NBS | newborn screening |
| NMR | nuclear magnetic resonance |
| O.D | optical density |
| PBS | phosphate buffered saline |
| PC | phosphatidylcholine or principal component |
| PC aa | phosphatidylcholine with acyl-acyl side chain |
| PC ae | phosphatidylcholine with acyl-ether side chain |
| PCA | principle component analysis |
| PCCB | propionyl-CoA carboxylase |
| PCD | programmed cell death |
| PCYT | choline-phosphate cytidyltransferase |
| PE | phosphatidylethanolamine |
| PGF2 α | prostaglandin-2F alpha |
| Phe | phenylalanine |
| PHK | glycogen phosphorylase kinase |
| PITC | phenylisothiocyanate |
| PKU | phenylketonuria |
| PLA2 | Phospholipase A2 |
| PMSF | phenylmethylsulfonyl fluoride |
| PMVK | phosphomevalonate kinase |
| PPAR γ | peroxisome proliferator-activated receptor γ |
| PRODH | proline dehydrogenase. |
| PROP | propionic acidemia |
| PVDF | polyvinylidene fluoride |
| qPCR | quantitative real-time polymerase chain reaction |
| RNA | ribonucleic acid |
| rpm | rotations per minute |
| RPMI | Roswell Park Memorial Institute Medium |

| | |
|--------------|---|
| RT | room temperature |
| SCD | stearoyl-CoA 9-desaturase |
| SDS-page | sodium dodecyl sulfate polyacrylamide gel electrophoresis |
| SLC1A5 | amino acid transporter |
| SLC25A1 | citrate transporter |
| SM | sphingolipids |
| SNP's | single nucleotide polymorphisms |
| SQLE | squalene epoxidase |
| SREBP1 | sterol regulatory element binding transcription factor 1 |
| SRM | spermidine synthase |
| SRS | spermine synthase |
| Stauro | staurosporine |
| TCA | citrate cycle |
| TEMED | tetramethylethylenediamine |
| THETAs | trihydroxyeicosatrienoic acids |
| TNF α | tumor necrosis factor |
| UPLC | ultra-high performance liquid chromatography |
| WHO | world health organization |

5.2 Publications and presentations

5.2.1 Original papers

Halama A.,_Riesen N., Moller G., Adamski J. : " Identification of biomarkers for apoptosis in cancer cell lines using metabolomics: tools for individualized medicine." J Intern Med. in second revision

Peter C., Waibel M., Keppeler H., Lehmann R., Xu G., **Halama A.**, Adamski J., Schulze-Osthoff K., Wesselborg S., Lauber K. : "Release of lysophospholipid 'find-me' signals during apoptosis requires the ATP-binding cassette transporter A1.", 2012, Autoimmunity **45**(8): 568-573.

Halama A., Moller G., Adamski J. : "Metabolic signatures in apoptotic human cancer cell lines.", 2011, OMICS **15**(5): 325-335.

Russ V, Fröhlich T, Li Y, **Halama A**, Ogris M, Wagner E. „Improved in vivo gene transfer into tumor tissue by stabilization of pseudodendritic oligoethylenimine-based polyplexes.” , 2010, J Gene Med. **12**(2):180-93.

Russ V, Günther M, **Halama A**, Ogris M, Wagner E. “Oligoethylenimine-grafted polypropylenimine dendrimers as degradable and biocompatible synthetic vectors for

gene delivery.”, 2008, J Control Release. 132(2):131-40.

5.2.2 Manuscripts in preparation

Halama A., Horsch M, Kastenmüller G., Artati A., Möller G., Beckers J., Suhre K., Adamski J.: Facing adipogenesis – step forward in obesity prevention. - Adipogenesis blamed for obesity – would metabolomics be a judge? – in preparation

Boehm A., **Halama A.**, Meile T., Zdichavsky M., Lehmann R., Weigert C., Fritsche A., Stefan N., Haering H, Hrabe de Angelis M., Adamski J., Staiger H.: “Metabolic profiling of cultured human adipocytes from metabolically melign versus benign obese individuals” – in preparation

5.2.3 Reviews

Halama A., Kuliński M., Librowski T., Lochyński S.: "Polymer based non-viral gene delivery - concept for a cancer treatment.”, 2009, Pharmacol Rep. **61**(6):993-9.

5.2.4 Poster presentations

Halama A., Horsch M., Kastenmüller G., Möller G., Hrabe de Angelis M., Beckers J., Adamski J.: Leucine Degradation Correlates with Cholesterol Biosynthesis During Adipogenic Differentiation In 3T3-L1 Cells – Potential early biomarkers for obesity development, Congress on Steroid Research, 2013, Chicago, USA

Halama A., Horsch M, Kastenmüller G, Möller G., Hrabe de Angelis M, Beckers J, Adamski J.: Metabolic pathways regulated during adipogenesis - potential novel biomarkers for obesity, European Association for the Study of Diabetes, 2012, Berlin, Germany

Halama A., Horsch M., Artati A., Möller G., Hrabe de Angelis M., Beckers J., Adamski J.: Metabolomics of Adipogenesis - in Search for Obesity and Diabetes Biomarkers, American Diabetes Association, 2012, Philadelphia, USA

Halama A., Zieglmeier G., Möller G., Adamski J.: Metabolite Signatures of Apoptotic Human Cancer Cell Lines, Congress on Steroid Research, 2011, Chicago, USA

Halama A., Prehn C., Möller G., Adamski J.: Metabolomics of apoptotic cancer cell lines analyzed by newborn screen, Congress on ...2010, Erice, Italy

Halama A., Prehn C., Möller G., Adamski J.: Changes in metabolite profile during cell

differentiation measured with the newborn screening assay adapted for cell culture, Metabolomics & More, 2010, Freising, Germany

5.2.5 Oral presentations

Halama A., Horsch M., Kastenmüller G., Möller G., Hrabe de Angelis M., Beckers J., Adamski J.: Leucine Degradation Correlates with Cholesterol Biosynthesis During Adipogenic Differentiation In 3T3-L1 Cells – Potential early biomarkers for obesity development. Congress on Steroid Research, 2013, Chicago, USA

Halama A., Prehn C., Möller G., Adamski J.: Metabolomics of apoptotic cancer cell lines analyzed by newborn screen. Advanced Meeting on Cancer omics, 2010, Erice, Italy

6 REFERENCES

- Adamski, J. (2012). "Genome-wide association studies with metabolomics." Genome Med **4**(4): 34.
- Adamski, J. and K. Suhre (2013). "Metabolomics platforms for genome wide association studies-linking the genome to the metabolome." Curr Opin Biotechnol **24**(1): 39-47.
- Agostinelli, E., M. P. Marques, R. Calheiros, F. P. Gil, G. Tempera, N. Viceconte, V. Battaglia, S. Grancara and A. Toninello (2010). "Polyamines: fundamental characters in chemistry and biology." Amino Acids **38**(2): 393-403.
- Aiston, S., M. Peak and L. Agius (2000). "Impaired glycogen synthesis in hepatocytes from Zucker fatty fa/fa rats: the role of increased phosphorylase activity." Diabetologia **43**(5): 589-597.
- Ajit, V., C. Richard, E. Jeffrey, F. Hudson, H. Gerald and M. Jamey (2009). Essentials of glycobiology. Glycomics, Cold Spring Harbor Laboratory Press, New York.
- Alberg, A. J. and J. M. Samet (2003). "Epidemiology of lung cancer." Chest **123**(1 Suppl): 21S-49S.
- Alberici, A., D. Moratto, L. Benussi, L. Gasparini, R. Ghidoni, L. B. Gatta, D. Finazzi, G. B. Frisoni, M. Trabucchi, J. H. Growdon, R. M. Nitsch and G. Binetti (1999). "Presenilin 1 protein directly interacts with Bcl-2." J Biol Chem **274**(43): 30764-30769.
- Alberts, B. (2008). Molecular biology of the cell. New York, Garland Science.
- Altmaier, E., G. Kastenmüller, W. Römisch-Margl, B. Thorand, K. M. Weinberger, J. Adamski, T. Illig, A. Döring and K. Suhre (2009). "Variation in the human lipidome associated with coffee consumption as revealed by quantitative targeted metabolomics." Molecular nutrition & food research **53**(11): 1357-1365.
- Altmaier, E., S. L. Ramsay, A. Graber, H. W. Mewes, K. M. Weinberger and K. Suhre (2008). "Bioinformatics analysis of targeted metabolomics--uncovering old and new tales of diabetic mice under medication." Endocrinology **149**(7): 3478-3489.
- Altshuler, D., M. J. Daly and E. S. Lander (2008). "Genetic mapping in human disease." science **322**(5903): 881-888.
- Altun, Z. S., D. Gunes, S. Aktas, Z. Erbayraktar and N. Olgun (2009). "Protective effects of acetyl-L-carnitine on cisplatin cytotoxicity and oxidative stress in neuroblastoma." Neurochem Res **35**(3): 437-443.
- Amling, C. L. (2005). "Relationship between obesity and prostate cancer." Curr Opin Urol **15**(3): 167-171.
- Artati, A., C. Prehn, G. Möller and J. Adamski (2012). Assay Tools for Metabolomics. Genetics Meets Metabolomics. K. Suhre, Springer New York: 13-38.
- Asyali, M. H., D. Colak, O. Demirkaya and M. S. Inan (2006). "Gene expression profile classification: a review." Current Bioinformatics **1**(1): 55-73.
- Banerjee, S. S., M. W. Feinberg, M. Watanabe, S. Gray, R. L. Haspel, D. J. Denking, R. Kawahara, H. Hauner and M. K. Jain (2003). "The Kruppel-like factor KLF2 inhibits peroxisome proliferator-activated receptor-gamma expression and adipogenesis." J Biol

Chem **278**(4): 2581-2584.

Bathen, T. F., L. R. Jensen, B. Sitter, H. E. Fjosne, J. Halgunset, D. E. Axelson, I. S. Gribbestad and S. Lundgren (2007). "MR-determined metabolic phenotype of breast cancer in prediction of lymphatic spread, grade, and hormone status." Breast Cancer Res Treat **104**(2): 181-189.

Batista, U., M. Garvas, M. Nemeč, M. Schara, P. Veranic and T. Koklic (2010). "Effects of different detachment procedures on viability, nitroxide reduction kinetics and plasma membrane heterogeneity of V-79 cells." Cell Biol Int **34**(6): 663-668.

Baumgartner, C., C. Bohm, D. Baumgartner, G. Marini, K. Weinberger, B. Olgemoller, B. Liebl and A. A. Roscher (2004). "Supervised machine learning techniques for the classification of metabolic disorders in newborns." Bioinformatics **20**(17): 2985-2996.

Bayet-Robert, M., D. Loiseau, P. Rio, A. Demidem, C. Barthomeuf, G. Stepien and D. Morvan (2010). "Quantitative two-dimensional HRMAS 1H-NMR spectroscopy-based metabolite profiling of human cancer cell lines and response to chemotherapy." Magn Reson Med **63**(5): 1172-1183.

Beckonert, O., H. C. Keun, T. M. Ebbels, J. Bundy, E. Holmes, J. C. Lindon and J. K. Nicholson (2007). "Metabolic profiling, metabolomic and metabonomic procedures for NMR spectroscopy of urine, plasma, serum and tissue extracts." Nat Protoc **2**(11): 2692-2703.

Begrache, K., A. Igoudjil, D. Pessayre and B. Fromenty (2006). "Mitochondrial dysfunction in NASH: causes, consequences and possible means to prevent it." Mitochondrion **6**(1): 1-28.

Bell, C. G., S. Finer, C. M. Lindgren, G. A. Wilson, V. K. Rakyan, A. E. Teschendorff, P. Akan, E. Stupka, T. A. Down, I. Prokopenko, I. M. Morison, J. Mill, R. Pidsley, C. International Type 2 Diabetes 1q, P. Deloukas, T. M. Frayling, A. T. Hattersley, M. I. McCarthy, S. Beck and G. A. Hitman (2010). "Integrated genetic and epigenetic analysis identifies haplotype-specific methylation in the FTO type 2 diabetes and obesity susceptibility locus." PLoS One **5**(11): e14040.

Bennett, B. D., J. Yuan, E. H. Kimball and J. D. Rabinowitz (2008). "Absolute quantitation of intracellular metabolite concentrations by an isotope ratio-based approach." Nat Protoc **3**(8): 1299-1311.

Bernlöh, D. A., M. A. Bolanowski, T. J. Kelly, Jr. and M. D. Lane (1985). "Evidence for an increase in transcription of specific mRNAs during differentiation of 3T3-L1 preadipocytes." J Biol Chem **260**(9): 5563-5567.

Bertrand, R., E. Solary, P. O'Connor, K. W. Kohn and Y. Pommier (1994). "Induction of a common pathway of apoptosis by staurosporine." Exp Cell Res **211**(2): 314-321.

Bessman, S. P., J. Rossen and E. C. Layne (1953). "Gamma-Aminobutyric acid-glutamic acid transamination in brain." J Biol Chem **201**(1): 385-391.

Bethell, D. R. and A. E. Pegg (1981). "Polyamines are needed for the differentiation of 3T3-L1 fibroblasts into adipose cells." Biochem Biophys Res Commun **102**(1): 272-278.

Billon, N., R. Kolde, J. Reimand, M. C. Monteiro, M. Kull, H. Peterson, K. Tretyakov, P. Adler, B. Wdziekonski, J. Vilo and C. Dani (2010). "Comprehensive transcriptome analysis of mouse embryonic stem cell adipogenesis unravels new processes of adipocyte development." Genome Biol **11**(8): R80.

Bladergroen, B. A. and L. M. van Golde (1997). "CTP:phosphoethanolamine cytidyltransferase." Biochim Biophys Acta **1348**(1-2): 91-99.

Bogumil, R., T. Koal, K. M. Weinberger and D. S. (2008). "Massenspektrometrische

- Analyse von Blutplasma im Kitformat " Laborwelt **2**: 17-23.
- Caballero-Benitez, A. and J. Moran (2003). "Caspase activation pathways induced by staurosporine and low potassium: role of caspase-2." J Neurosci Res **71**(3): 383-396.
- Cai, Q., H. Sun, Y. Peng, J. Lu, Z. Nikolovska-Coleska, D. McEachern, L. Liu, S. Qiu, C. Y. Yang, R. Miller, H. Yi, T. Zhang, D. Sun, S. Kang, M. Guo, L. Leopold, D. Yang and S. Wang (2011). "A potent and orally active antagonist (SM-406/AT-406) of multiple inhibitor of apoptosis proteins (IAPs) in clinical development for cancer treatment." J Med Chem **54**(8): 2714-2726.
- Call, J. A., S. G. Eckhardt and D. R. Camidge (2008). "Targeted manipulation of apoptosis in cancer treatment." Lancet Oncol **9**(10): 1002-1011.
- Calle, E. E. and M. J. Thun (2004). "Obesity and cancer." Oncogene **23**(38): 6365-6378.
- Calle, E. E., M. J. Thun, J. M. Petrelli, C. Rodriguez and C. W. Heath, Jr. (1999). "Body-mass index and mortality in a prospective cohort of U.S. adults." N Engl J Med **341**(15): 1097-1105.
- Camp, H. S., D. Ren and T. Leff (2002). "Adipogenesis and fat-cell function in obesity and diabetes." Trends Mol Med **8**(9): 442-447.
- Cao, Z., R. M. Umek and S. L. McKnight (1991). "Regulated expression of three C/EBP isoforms during adipose conversion of 3T3-L1 cells." Genes Dev **5**(9): 1538-1552.
- Casimir, D. A., C. W. Miller and J. M. Ntambi (1996). "Preadipocyte differentiation blocked by prostaglandin stimulation of prostanoid FP2 receptor in murine 3T3-L1 cells." Differentiation **60**(4): 203-210.
- Casimir, D. A. and J. M. Ntambi (1996). "cAMP activates the expression of stearoyl-CoA desaturase gene 1 during early preadipocyte differentiation." J Biol Chem **271**(47): 29847-29853.
- Ceglarek, U., C. Shackleton, F. Z. Stanczyk and J. Adamski (2010). "Steroid profiling and analytics: going towards sterome." J Steroid Biochem Mol Biol **121**(3-5): 479-480.
- Cha, Y. S., J. S. Eun and S. H. Oh (2003). "Carnitine profiles during differentiation and effects of carnitine on differentiation of 3T3-L1 cells." J Med Food **6**(3): 163-167.
- Chace, D. H., T. A. Kalas and E. W. Naylor (2003). "Use of tandem mass spectrometry for multianalyte screening of dried blood specimens from newborns." Clin Chem **49**(11): 1797-1817.
- Cheng, L. L., C. Wu, M. R. Smith and R. G. Gonzalez (2001). "Non-destructive quantitation of spermine in human prostate tissue samples using HRMAS 1H NMR spectroscopy at 9.4 T." FEBS Lett **494**(1-2): 112-116.
- Cheng, Y. S., T. S. Lee, H. C. Hsu, Y. R. Kou and Y. L. Wu (2008). "Characterization of the transcriptional regulation of the regulator of G protein signaling 2 (RGS2) gene during 3T3-L1 preadipocyte differentiation." J Cell Biochem **105**(3): 922-930.
- Chon, S. H., J. D. Douglass, Y. X. Zhou, N. Malik, J. L. Dixon, A. Brinker, L. Quadro and J. Storch (2012). "Over-expression of monoacylglycerol lipase (MGL) in small intestine alters endocannabinoid levels and whole body energy balance, resulting in obesity." PLoS One **7**(8): e43962.
- Chon, S. H., Y. X. Zhou, J. L. Dixon and J. Storch (2007). "Intestinal monoacylglycerol metabolism: developmental and nutritional regulation of monoacylglycerol lipase and monoacylglycerol acyltransferase." J Biol Chem **282**(46): 33346-33357.
- Christy, R. J., K. H. Kaestner, D. E. Geiman and M. D. Lane (1991). "CCAAT/enhancer binding protein gene promoter: binding of nuclear factors during differentiation of 3T3-L1 preadipocytes." Proc Natl Acad Sci U S A **88**(6): 2593-2597.

- Christy, R. J., V. W. Yang, J. M. Ntambi, D. E. Geiman, W. H. Landschulz, A. D. Friedman, Y. Nakabeppu, T. J. Kelly and M. D. Lane (1989). "Differentiation-induced gene expression in 3T3-L1 preadipocytes: CCAAT/enhancer binding protein interacts with and activates the promoters of two adipocyte-specific genes." Genes Dev **3**(9): 1323-1335.
- Clarke, S. L., C. E. Robinson and J. M. Gimble (1997). "CAAT/enhancer binding proteins directly modulate transcription from the peroxisome proliferator-activated receptor gamma 2 promoter." Biochem Biophys Res Commun **240**(1): 99-103.
- Connor, S. C., M. K. Hansen, A. Corner, R. F. Smith and T. E. Ryan (2010). "Integration of metabolomics and transcriptomics data to aid biomarker discovery in type 2 diabetes." Mol Biosyst **6**(5): 909-921.
- Consultation, W. (2000). "Obesity: preventing and managing the global epidemic." World Health Organization technical report series(894).
- Cook, H. W. and C. R. McMaster (2002). "Fatty acid desaturation and chain elongation in eukaryotes." New comprehensive biochemistry **36**: 181-204.
- Cook, K. S., C. R. Hunt and B. M. Spiegelman (1985). "Developmentally regulated mRNAs in 3T3-adipocytes: analysis of transcriptional control." J Cell Biol **100**(2): 514-520.
- Couce, M. L., D. E. Castineiras, M. D. Boveda, A. Bana, J. A. Cocho, A. J. Iglesias, C. Colon, J. R. Alonso-Fernandez and J. M. Fraga (2011). "Evaluation and long-term follow-up of infants with inborn errors of metabolism identified in an expanded screening programme." Mol Genet Metab **104**(4): 470-475.
- Cuperlovic-Culf, M., D. A. Barnett, A. S. Culf and I. Chute "Cell culture metabolomics: applications and future directions." Drug Discov Today **15**(15-16): 610-621.
- Cuperlovic-Culf, M., D. A. Barnett, A. S. Culf and I. Chute (2010). "Cell culture metabolomics: applications and future directions." Drug Discov Today **15**(15-16): 610-621.
- Danielson, K. G., H. Baribault, D. F. Holmes, H. Graham, K. E. Kadler and R. V. Iozzo (1997). "Targeted disruption of decorin leads to abnormal collagen fibril morphology and skin fragility." J Cell Biol **136**(3): 729-743.
- Danielsson, A. P., T. Moritz, H. Mulder and P. Spegel (2010). "Development and optimization of a metabolomic method for analysis of adherent cell cultures." Anal Biochem **404**(1): 30-39.
- Das, U. (2001). "Is obesity an inflammatory condition?" Nutrition **17**(11): 953-966.
- de Ferranti, S. and D. Mozaffarian (2008). "The perfect storm: obesity, adipocyte dysfunction, and metabolic consequences." Clin Chem **54**(6): 945-955.
- de Jong, R. S., N. H. Mulder, D. Dijksterhuis and E. G. de Vries (1995). "Review of current clinical experience with prolonged (oral) etoposide in cancer treatment." Anticancer Res **15**(5B): 2319-2330.
- Desai, M., M. Beall and M. G. Ross (2013). "Developmental origins of obesity: programmed adipogenesis." Curr Diab Rep **13**(1): 27-33.
- Dettmer, K., N. Nurnberger, H. Kaspar, M. A. Gruber, M. F. Almstetter and P. J. Oefner (2011). "Metabolite extraction from adherently growing mammalian cells for metabolomics studies: optimization of harvesting and extraction protocols." Anal Bioanal Chem **399**(3): 1127-1139.
- Dietmair, S., N. E. Timmins, P. P. Gray, L. K. Nielsen and J. O. Kromer (2010). "Towards quantitative metabolomics of mammalian cells: development of a metabolite

- extraction protocol." *Anal Biochem* **404**(2): 155-164.
- Dinh, T. P., D. Carpenter, F. M. Leslie, T. F. Freund, I. Katona, S. L. Sensi, S. Kathuria and D. Piomelli (2002). "Brain monoglyceride lipase participating in endocannabinoid inactivation." *Proc Natl Acad Sci U S A* **99**(16): 10819-10824.
- Dunai, Z. A., G. Imre, G. Barna, T. Korcsmaros, I. Petak, P. I. Bauer and R. Mihalik (2012). "Staurosporine induces necroptotic cell death under caspase-compromised conditions in U937 cells." *PLoS One* **7**(7): e41945.
- Edelman, M. J., K. S. Bauer, Jr., S. Wu, R. Smith, S. Bisacia and J. Dancey (2007). "Phase I and pharmacokinetic study of 7-hydroxystaurosporine and carboplatin in advanced solid tumors." *Clin Cancer Res* **13**(9): 2667-2674.
- Edgar, R., M. Domrachev and A. E. Lash (2002). "Gene Expression Omnibus: NCBI gene expression and hybridization array data repository." *Nucleic acids research* **30**(1): 207-210.
- Eisen, M. B., P. T. Spellman, P. O. Brown and D. Botstein (1998). "Cluster analysis and display of genome-wide expression patterns." *Proc Natl Acad Sci U S A* **95**(25): 14863-14868.
- El-Deredy, W., S. M. Ashmore, N. M. Branston, J. L. Darling, S. R. Williams and D. G. Thomas (1997). "Pretreatment prediction of the chemotherapeutic response of human glioma cell cultures using nuclear magnetic resonance spectroscopy and artificial neural networks." *Cancer Res* **57**(19): 4196-4199.
- Elwood, P. C., J. E. Pickering, J. Hughes, A. M. Fehily and A. R. Ness (2004). "Milk drinking, ischaemic heart disease and ischaemic stroke II. Evidence from cohort studies." *Eur J Clin Nutr* **58**(5): 718-724.
- Fahy, E., M. Sud, D. Cotter and S. Subramaniam (2007). "LIPID MAPS online tools for lipid research." *Nucleic Acids Res* **35**(Web Server issue): W606-612.
- Falus, A. (2005). "'Tumor metabolome": a post-modern genomic view on the role of low molecular weight substances in cancerous cell growth:an introduction." *Semin Cancer Biol* **15**(4): 245-246.
- Fasshauer, M., J. Klein, S. Neumann, M. Eszlinger and R. Paschke (2002). "Hormonal regulation of adiponectin gene expression in 3T3-L1 adipocytes." *Biochem Biophys Res Commun* **290**(3): 1084-1089.
- Ferrannini, E., A. Natali, S. Camastra, M. Nannipieri, A. Mari, K. P. Adam, M. V. Milburn, G. Kastenmuller, J. Adamski, T. Tuomi, V. Lyssenko, L. Groop and W. E. Gall (2012). "Early Metabolic Markers of the Development of Dysglycemia and Type 2 Diabetes and Their Physiological Significance." *Diabetes*.
- Fiehn, O. (2002). "Metabolomics--the link between genotypes and phenotypes." *Plant Mol Biol* **48**(1-2): 155-171.
- Fiehn, O., J. Kopka, P. Dormann, T. Altmann, R. N. Trethewey and L. Willmitzer (2000). "Metabolite profiling for plant functional genomics." *Nat Biotechnol* **18**(11): 1157-1161.
- Flier, J. S. (2004). "Obesity wars: molecular progress confronts an expanding epidemic." *Cell* **116**(2): 337-350.
- Floegel, A., N. Stefan, Z. Yu, K. Muhlenbruch, D. Drogan, H. G. Joost, A. Fritsche, H. U. Haring, M. Hrabe de Angelis, A. Peters, M. Roden, C. Prehn, R. Wang-Sattler, T. Illig, M. B. Schulze, J. Adamski, H. Boeing and T. Pischon (2013). "Identification of serum metabolites associated with risk of type 2 diabetes using a targeted metabolomic approach." *Diabetes* **62**(2): 639-648.
- Fu, Y., N. Luo, R. L. Klein and W. T. Garvey (2005). "Adiponectin promotes adipocyte

- differentiation, insulin sensitivity, and lipid accumulation." *J Lipid Res* **46**(7): 1369-1379.
- Fujitani, N., J. Furukawa, K. Araki, T. Fujioka, Y. Takegawa, J. Piao, T. Nishioka, T. Tamura, T. Nikaido, M. Ito, Y. Nakamura and Y. Shinohara (2013). "Total cellular glycomics allows characterizing cells and streamlining the discovery process for cellular biomarkers." *Proc Natl Acad Sci U S A* **110**(6): 2105-2110.
- Garaulet, M., F. Perez-Llamas, M. Perez-Ayala, P. Martinez, F. S. de Medina, F. J. Tebar and S. Zamora (2001). "Site-specific differences in the fatty acid composition of abdominal adipose tissue in an obese population from a Mediterranean area: relation with dietary fatty acids, plasma lipid profile, serum insulin, and central obesity." *Am J Clin Nutr* **74**(5): 585-591.
- Gerl, R. and D. L. Vaux (2005). "Apoptosis in the development and treatment of cancer." *Carcinogenesis* **26**(2): 263-270.
- Giannini, C., T. de Giorgis, A. Scarinci, M. Ciampani, M. L. Marcovecchio, F. Chiarelli and A. Mohn (2008). "Obese related effects of inflammatory markers and insulin resistance on increased carotid intima media thickness in pre-pubertal children." *Atherosclerosis* **197**(1): 448-456.
- Gibellini, F. and T. K. Smith (2010). "The Kennedy pathway—De novo synthesis of phosphatidylethanolamine and phosphatidylcholine." *IUBMB life* **62**(6): 414-428.
- Gieger, C., L. Geistlinger, E. Altmaier, M. Hrabce de Angelis, F. Kronenberg, T. Meitinger, H. W. Mewes, H. E. Wichmann, K. M. Weinberger, J. Adamski, T. Illig and K. Suhre (2008). "Genetics meets metabolomics: a genome-wide association study of metabolite profiles in human serum." *PLoS Genet* **4**(11): e1000282.
- Glunde, K., C. Jie and Z. M. Bhujwalla (2004). "Molecular causes of the aberrant choline phospholipid metabolism in breast cancer." *Cancer Res* **64**(12): 4270-4276.
- Goodacre, R. (2005). "Metabolomics—the way forward." *Metabolomics* **1**(1): 1-2.
- Gray, S., M. W. Feinberg, S. Hull, C. T. Kuo, M. Watanabe, S. Sen-Banerjee, A. DePina, R. Haspel and M. K. Jain (2002). "The Kruppel-like factor KLF15 regulates the insulin-sensitive glucose transporter GLUT4." *J Biol Chem* **277**(37): 34322-34328.
- Green, H. and O. Kehinde (1975). "An established preadipose cell line and its differentiation in culture. II. Factors affecting the adipose conversion." *Cell* **5**(1): 19-27.
- Green, H. and M. Meuth (1974). "An established pre-adipose cell line and its differentiation in culture." *Cell* **3**(2): 127-133.
- Gribbestad, I. S., B. Sitter, S. Lundgren, J. Krane and D. Axelson (1999). "Metabolite composition in breast tumors examined by proton nuclear magnetic resonance spectroscopy." *Anticancer Res* **19**(3A): 1737-1746.
- Griffin, J. L. and R. A. Kauppinen (2007). "A metabolomics perspective of human brain tumours." *FEBS J* **274**(5): 1132-1139.
- Griffin, J. L., K. K. Lehtimäki, P. K. Valonen, O. H. Grohn, M. I. Kettunen, S. Ylä-Herttuala, A. Pitkanen, J. K. Nicholson and R. A. Kauppinen (2003). "Assignment of ¹H nuclear magnetic resonance visible polyunsaturated fatty acids in BT4C gliomas undergoing ganciclovir-thymidine kinase gene therapy-induced programmed cell death." *Cancer Res* **63**(12): 3195-3201.
- Griffin, J. L., J. C. Pole, J. K. Nicholson and P. L. Carmichael (2003). "Cellular environment of metabolites and a metabolomic study of tamoxifen in endometrial cells using gradient high resolution magic angle spinning ¹H NMR spectroscopy." *Biochim Biophys Acta* **1619**(2): 151-158.
- Griffin, J. L. and J. P. Shockcor (2004). "Metabolic profiles of cancer cells." *Nat Rev*
-

Cancer **4**(7): 551-561.

Griffiths, A. J. F. (2000). An introduction to genetic analysis. New York, W.H. Freeman.

Griffiths, W. J., K. Karu, M. Hornshaw, G. Woffendin and Y. Wang (2007). "Metabolomics and metabolite profiling: past heroes and future developments." Eur J Mass Spectrom (Chichester, Eng) **13**(1): 45-50.

Griffiths, W. J., T. Koal, Y. Wang, M. Kohl, D. P. Enot and H. P. Deigner (2010). "Targeted metabolomics for biomarker discovery." Angew Chem Int Ed Engl **49**(32): 5426-5445.

Griffiths, W. J. and Y. Wang (2009). "Mass spectrometry: from proteomics to metabolomics and lipidomics." Chem Soc Rev **38**(7): 1882-1896.

Guilherme, A., J. V. Virbasius, V. Puri and M. P. Czech (2008). "Adipocyte dysfunctions linking obesity to insulin resistance and type 2 diabetes." Nat Rev Mol Cell Biol **9**(5): 367-377.

Guo, X. and K. Liao (2000). "Analysis of gene expression profile during 3T3-L1 preadipocyte differentiation." Gene **251**(1): 45-53.

Hagberg, G. (1998). "From magnetic resonance spectroscopy to classification of tumors. A review of pattern recognition methods." NMR Biomed **11**(4-5): 148-156.

Halama, A., G. Moller and J. Adamski (2011). "Metabolic Signatures in Apoptotic Human Cancer Cell Lines." OMICS **15**(5): 325-335.

Haluzik, M., J. Parizkova and M. M. Haluzik (2004). "Adiponectin and its role in the obesity-induced insulin resistance and related complications." Physiol Res **53**(2): 123-129.

Hanahan, D. and R. A. Weinberg (2011). "Hallmarks of cancer: the next generation." Cell **144**(5): 646-674.

Herman, M. A., P. She, O. D. Peroni, C. J. Lynch and B. B. Kahn (2010). "Adipose tissue branched chain amino acid (BCAA) metabolism modulates circulating BCAA levels." J Biol Chem **285**(15): 11348-11356.

Hindorff, L. A., P. Sethupathy, H. A. Junkins, E. M. Ramos, J. P. Mehta, F. S. Collins and T. A. Manolio (2009). "Potential etiologic and functional implications of genome-wide association loci for human diseases and traits." Proc Natl Acad Sci U S A **106**(23): 9362-9367.

Hirsch, J. and B. Batchelor (1976). "Adipose tissue cellularity in human obesity." Clin Endocrinol Metab **5**(2): 299-311.

Honda, A., G. S. Tint, G. Salen, A. K. Batta, T. S. Chen and S. Shefer (1995). "Defective conversion of 7-dehydrocholesterol to cholesterol in cultured skin fibroblasts from Smith-Lemli-Opitz syndrome homozygotes." J Lipid Res **36**(7): 1595-1601.

Hong, Y. H., D. Hishikawa, H. Miyahara, H. Tsuzuki, Y. Nishimura, C. Gotoh, K. C. Choi, Y. Hokari, Y. Takagi, H. G. Lee, K. K. Cho, S. G. Roh and S. Sasaki (2005). "Up-regulation of adipogenin, an adipocyte plasma transmembrane protein, during adipogenesis." Mol Cell Biochem **276**(1-2): 133-141.

Horsch, M., S. Schadler, V. Gailus-Durner, H. Fuchs, H. Meyer, M. H. de Angelis and J. Beckers (2008). "Systematic gene expression profiling of mouse model series reveals coexpressed genes." Proteomics **8**(6): 1248-1256.

Hotamisligil, G. S. (2006). "Inflammation and metabolic disorders." Nature **444**(7121): 860-867.

Hunter, P. (2009). "Reading the metabolic fine print." EMBO reports **10**(1): 20-23.

Hyotylainen, T. (2012). "Novel methodologies in metabolic profiling with a focus on

- molecular diagnostic applications." Expert Rev Mol Diagn **12**(5): 527-538.
- Illig, T., C. Gieger, G. Zhai, W. Romisch-Margl, R. Wang-Sattler, C. Prehn, E. Altmaier, G. Kastenmuller, B. S. Kato, H. W. Mewes, T. Meitinger, M. H. de Angelis, F. Kronenberg, N. Soranzo, H. E. Wichmann, T. D. Spector, J. Adamski and K. Suhre (2010). "A genome-wide perspective of genetic variation in human metabolism." Nat Genet **42**(2): 137-141.
- Imaizumi, A. (February 10, 2012). Biochemistry, Genetics and Molecular Biology. Clinical Implementation of Metabolomics. U. Roessner.
- Ishii, I., Y. Ikeguchi, H. Mano, M. Wada, A. E. Pegg and A. Shirahata (2012). "Polyamine metabolism is involved in adipogenesis of 3T3-L1 cells." Amino Acids **42**(2-3): 619-626.
- Iyer, A., D. P. Fairlie, J. B. Prins, B. D. Hammock and L. Brown (2010). "Inflammatory lipid mediators in adipocyte function and obesity." Nat Rev Endocrinol **6**(2): 71-82.
- Jaworski, K., M. Ahmadian, R. E. Duncan, E. Sarkadi-Nagy, K. A. Varady, M. K. Hellerstein, H. Y. Lee, V. T. Samuel, G. I. Shulman, K. H. Kim, S. de Val, C. Kang and H. S. Sul (2009). "AdPLA ablation increases lipolysis and prevents obesity induced by high-fat feeding or leptin deficiency." Nat Med **15**(2): 159-168.
- Jones, D. R. and I. Varela-Nieto (1999). "Diabetes and the role of inositol-containing lipids in insulin signaling." Mol Med **5**(8): 505-514.
- Kamb, A., S. Wee and C. Lengauer (2006). "Why is cancer drug discovery so difficult?" Nature Reviews Drug Discovery **6**(2): 115-120.
- Kang, M. H. and C. P. Reynolds (2009). "Bcl-2 inhibitors: targeting mitochondrial apoptotic pathways in cancer therapy." Clin Cancer Res **15**(4): 1126-1132.
- Kastenmuller, G., W. Romisch-Margl, B. Wagele, E. Altmaier and K. Suhre (2011). "metaP-server: a web-based metabolomics data analysis tool." Journal of biomedicine & biotechnology **2011**.
- Kastenmüller, G., W. Römisch-Margl, B. Wägele, E. Altmaier and K. Suhre (2010). "metaP-Server: a web-based metabolomics data analysis tool." Journal of Biomedicine and Biotechnology **2011**.
- Kastenmüller, G., W. Römisch-Margl, B. Wägele, E. Altmaier and K. Suhre (2010). "metaP-Server: A Web-Based Metabolomics Data Analysis Tool." Journal of Biomedicine and Biotechnology **2011**: ID839862.
- Kasturi, R. and V. C. Joshi (1982). "Hormonal regulation of stearoyl coenzyme A desaturase activity and lipogenesis during adipose conversion of 3T3-L1 cells." J Biol Chem **257**(20): 12224-12230.
- Kennedy, E. P. and S. B. Weiss (1956). "The function of cytidine coenzymes in the biosynthesis of phospholipides." J Biol Chem **222**(1): 193-214.
- Kershaw, E. E. and J. S. Flier (2004). "Adipose tissue as an endocrine organ." Journal of Clinical Endocrinology & Metabolism **89**(6): 2548-2556.
- Khaw, K. T., M. D. Friesen, E. Riboli, R. Luben and N. Wareham (2012). "Plasma phospholipid fatty acid concentration and incident coronary heart disease in men and women: the EPIC-Norfolk prospective study." PLoS Med **9**(7): e1001255.
- Khoo, S. H. and M. Al-Rubeai (2007). "Metabolomics as a complementary tool in cell culture." Biotechnol Appl Biochem **47**(Pt 2): 71-84.
- Kim, J. Y., J. Y. Park, O. Y. Kim, B. M. Ham, H. J. Kim, D. Y. Kwon, Y. Jang and J. H. Lee (2010). "Metabolic profiling of plasma in overweight/obese and lean men using ultra performance liquid chromatography and Q-TOF mass spectrometry (UPLC-Q-TOF MS)." J Proteome Res **9**(9): 4368-4375.
-

- Knox, S. S. (2010). "From 'omics' to complex disease: a systems biology approach to gene-environment interactions in cancer." Cancer Cell Int **10**: 11.
- Kobayashi, T. and K. Fujimori (2012). "Very long-chain-fatty acids enhance adipogenesis through coregulation of Elovl3 and PPARgamma in 3T3-L1 cells." Am J Physiol Endocrinol Metab **302**(12): E1461-1471.
- Kovacevic, Z. and H. P. Morris (1972). "The role of glutamine in the oxidative metabolism of malignant cells." Cancer Res **32**(2): 326-333.
- Kruth, H. S. (1984). "Filipin-positive, oil red O-negative particles in atherosclerotic lesions induced by cholesterol feeding." Lab Invest **50**(1): 87-93.
- Ku, C. S., E. Y. Loy, Y. Pawitan and K. S. Chia (2010). "The pursuit of genome-wide association studies: where are we now?" J Hum Genet **55**(4): 195-206.
- Kubo, Y., S. Kaidzu, I. Nakajima, K. Takenouchi and F. Nakamura (2000). "Organization of extracellular matrix components during differentiation of adipocytes in long-term culture." In Vitro Cellular & Developmental Biology-Animal **36**(1): 38-44.
- Kuri-Harcuch, W. and H. Green (1978). "Adipose conversion of 3T3 cells depends on a serum factor." Proc Natl Acad Sci U S A **75**(12): 6107-6109.
- Kuri-Harcuch, W., L. S. Wise and H. Green (1978). "Interruption of the adipose conversion of 3T3 cells by biotin deficiency: differentiation without triglyceride accumulation." Cell **14**(1): 53-59.
- Lavie, C. J., R. V. Milani and H. O. Ventura (2009). "Obesity and cardiovascular disease: risk factor, paradox, and impact of weight loss." J Am Coll Cardiol **53**(21): 1925-1932.
- Lee, J. W., R. S. Weiner, J. M. Sailstad, R. R. Bowsher, D. W. Knuth, P. J. O'Brien, J. L. Fourcroy, R. Dixit, L. Pandite, R. G. Pietrusko, H. D. Soares, V. Quarmby, O. L. Vesterqvist, D. M. Potter, J. L. Witliff, H. A. Fritche, T. O'Leary, L. Perlee, S. Kadam and J. A. Wagner (2005). "Method validation and measurement of biomarkers in nonclinical and clinical samples in drug development: a conference report." Pharm Res **22**(4): 499-511.
- Li, Y. and R. G. Martin (2009). Apoptosis in Carcinogenesis and Chemotherapy – Esophageal Cancer. Apoptosis in Carcinogenesis and Chemotherapy. G. Chen and P. S. Lai, Springer Netherlands: 127-156.
- Liebler, D. C. (2002). Introduction to proteomics : tools for the new biology. Totowa, NJ, Humana Press.
- Ligibel, J. (2011). "Obesity and breast cancer." Oncology (Williston Park) **25**(11): 994-1000.
- Lin, F. T. and M. D. Lane (1994). "CCAAT/enhancer binding protein alpha is sufficient to initiate the 3T3-L1 adipocyte differentiation program." Proc Natl Acad Sci U S A **91**(19): 8757-8761.
- Linhart, H. G., K. Ishimura-Oka, F. DeMayo, T. Kibe, D. Repka, B. Poindexter, R. J. Bick and G. J. Darlington (2001). "C/EBPalpha is required for differentiation of white, but not brown, adipose tissue." Proc Natl Acad Sci U S A **98**(22): 12532-12537.
- Liu, J., N. S. Sabeva, S. Bhatnagar, X. A. Li, A. Pujol and G. A. Graf (2010). "ABCD2 is abundant in adipose tissue and opposes the accumulation of dietary erucic acid (C22:1) in fat." J Lipid Res **51**(1): 162-168.
- Liu, Y., D. A. Peterson, H. Kimura and D. Schubert (1997). "Mechanism of cellular 3-(4,5-dimethylthiazol-2-yl)-2,5-diphenyltetrazolium bromide (MTT) reduction." J Neurochem **69**(2): 581-593.
- Livak, K. J. and T. D. Schmittgen (2001). "Analysis of relative gene expression data

- using real-time quantitative PCR and the 2(-Delta Delta C(T)) Method." Methods **25**(4): 402-408.
- Longley, D. B., D. P. Harkin and P. G. Johnston (2003). "5-fluorouracil: mechanisms of action and clinical strategies." Nat Rev Cancer **3**(5): 330-338.
- Lubovac, Z. and B. Olsson (2003). "Towards Reverse Engineering of Genetic Regulatory Networks."
- Ma, Y., Y. Yang, F. Wang, P. Zhang, C. Shi, Y. Zou and H. Qin (2013). "Obesity and risk of colorectal cancer: a systematic review of prospective studies." PLoS One **8**(1): e53916.
- MacDougald, O. A. and M. D. Lane (1995). "Adipocyte differentiation. When precursors are also regulators." Curr Biol **5**(6): 618-621.
- MacDougald, O. A. and M. D. Lane (1995). "Transcriptional regulation of gene expression during adipocyte differentiation." Annu Rev Biochem **64**: 345-373.
- Makimura, H., T. M. Mizuno, H. Bergen and C. V. Mobbs (2002). "Adiponectin is stimulated by adrenalectomy in ob/ob mice and is highly correlated with resistin mRNA." Am J Physiol Endocrinol Metab **283**(6): E1266-1271.
- Malvezzi, M., P. Bertuccio, F. Levi, C. La Vecchia and E. Negri (2012). "European cancer mortality predictions for the year 2012." Ann Oncol **23**(4): 1044-1052.
- Marcelli, M., M. Marani, X. Li, L. Sturgis, S. J. Haidacher, J. A. Trial, R. Mannucci, I. Nicoletti and L. Denner (2000). "Heterogeneous apoptotic responses of prostate cancer cell lines identify an association between sensitivity to staurosporine-induced apoptosis, expression of Bcl-2 family members, and caspase activation." Prostate **42**(4): 260-273.
- Mayes, P. A. and K. M. Botham (1993). "Metabolism of acylglycerols and sphingolipids." 1993 Harper's Biochemistry, 23rd edn. Appleton & Lange, Norwalk, CT: 241-249.
- Mazurek, S. and E. Eigenbrodt (2003). "The tumor metabolome." Anticancer Res **23**(2A): 1149-1154.
- Mazzarelli, P., S. Pucci, E. Bonanno, F. Sesti, M. Calvani and L. G. Spagnoli (2007). "Carnitine palmitoyltransferase I in human carcinomas: a novel role in histone deacetylation?" Cancer Biol Ther **6**(10): 1606-1613.
- Mihalik, S. J., S. F. Michalyszyn, J. de las Heras, F. Bacha, S. Lee, D. H. Chace, V. R. DeJesus, J. Vockley and S. A. Arslanian (2012). "Metabolomic profiling of fatty acid and amino acid metabolism in youth with obesity and type 2 diabetes: evidence for enhanced mitochondrial oxidation." Diabetes Care **35**(3): 605-611.
- Mills, G. B. and W. H. Moolenaar (2003). "The emerging role of lysophosphatidic acid in cancer." Nat Rev Cancer **3**(8): 582-591.
- Mirbahai, L., M. Wilson, C. S. Shaw, C. McConville, R. D. Malcomson, J. L. Griffin, R. A. Kauppinen and A. C. Peet (2010). "(1)H magnetic resonance spectroscopy metabolites as biomarkers for cell cycle arrest and cell death in rat glioma cells." Int J Biochem Cell Biol.
- Misek, D. E. and E. H. Kim (2011). "Protein biomarkers for the early detection of breast cancer." Int J Proteomics **2011**: 343582.
- Miyamoto, Y., Y. Takikawa, S. De Lin, S. Sato and K. Suzuki (2004). "Apoptotic hepatocellular carcinoma HepG2 cells accelerate blood coagulation." Hepatol Res **29**(3): 167-172.
- Mori, T., H. Sakaue, H. Iguchi, H. Gomi, Y. Okada, Y. Takashima, K. Nakamura, T. Nakamura, T. Yamauchi, N. Kubota, T. Kadowaki, Y. Matsuki, W. Ogawa, R. Hiramatsu and M. Kasuga (2005). "Role of Kruppel-like factor 15 (KLF15) in transcriptional

- regulation of adipogenesis." J Biol Chem **280**(13): 12867-12875.
- Mosmann, T. (1983). "Rapid colorimetric assay for cellular growth and survival: application to proliferation and cytotoxicity assays." J Immunol Methods **65**(1-2): 55-63.
- Mukherji, M., N. J. Kershaw, C. J. Schofield, A. S. Wierzbicki and M. D. Lloyd (2002). "Utilization of sterol carrier protein-2 by phytanoyl-CoA 2-hydroxylase in the peroxisomal alpha oxidation of phytanic acid." Chem Biol **9**(5): 597-605.
- Mun, E.-G., J.-R. Soh and Y.-S. Cha (2007). "L-Carnitine reduces obesity caused by high-fat diet in C57BL/6J mice." Food Science and Biotechnology **16**.
- Nadler, S. T., J. P. Stoehr, K. L. Schueler, G. Tanimoto, B. S. Yandell and A. D. Attie (2000). "The expression of adipogenic genes is decreased in obesity and diabetes mellitus." Proc Natl Acad Sci U S A **97**(21): 11371-11376.
- Nagata, E., H. R. Luo, A. Saiardi, B. I. Bae, N. Suzuki and S. H. Snyder (2005). "Inositol hexakisphosphate kinase-2, a physiologic mediator of cell death." J Biol Chem **280**(2): 1634-1640.
- Nakashima, A., K. Hosaka and J. Nikawa (1997). "Cloning of a human cDNA for CTP-phosphoethanolamine cytidyltransferase by complementation in vivo of a yeast mutant." J Biol Chem **272**(14): 9567-9572.
- Newgard, C. B., J. An, J. R. Bain, M. J. Muehlbauer, R. D. Stevens, L. F. Lien, A. M. Haqq, S. H. Shah, M. Arlotto, C. A. Slentz, J. Rochon, D. Gallup, O. Ilkayeva, B. R. Wenner, W. S. Yancy, Jr., H. Eisenson, G. Musante, R. S. Surwit, D. S. Millington, M. D. Butler and L. P. Svetkey (2009). "A branched-chain amino acid-related metabolic signature that differentiates obese and lean humans and contributes to insulin resistance." Cell Metab **9**(4): 311-326.
- Ngwa, J. S., A. K. Manning, J. L. Grimsby, C. Lu, W. V. Zhuang and A. L. Destefano (2011). "Pathway analysis following association study." BMC Proc **5 Suppl 9**: S18.
- Novikoff, A. B., P. M. Novikoff, O. M. Rosen and C. S. Rubin (1980). "Organelle relationships in cultured 3T3-L1 preadipocytes." J Cell Biol **87**(1): 180-196.
- Ntambi, J. M. and K. Young-Cheul (2000). "Adipocyte differentiation and gene expression." J Nutr **130**(12): 3122S-3126S.
- Obukowicz, M. G., A. Raz, P. D. Pyla, J. G. Rico, J. M. Wendling and P. Needleman (1998). "Identification and characterization of a novel delta6/delta5 fatty acid desaturase inhibitor as a potential anti-inflammatory agent." Biochem Pharmacol **55**(7): 1045-1058.
- Oishi, Y., I. Manabe, K. Tobe, K. Tsushima, T. Shindo, K. Fujiu, G. Nishimura, K. Maemura, T. Yamauchi, N. Kubota, R. Suzuki, T. Kitamura, S. Akira, T. Kadowaki and R. Nagai (2005). "Kruppel-like transcription factor KLF5 is a key regulator of adipocyte differentiation." Cell Metab **1**(1): 27-39.
- Okamoto-Kubo, S., K. Nishio, Y. Heike, M. Yoshida, T. Ohmori and N. Saijo (1994). "Apoptosis induced by etoposide in small-cell lung cancer cell lines." Cancer Chemother Pharmacol **33**(5): 385-390.
- Oliver, S. G., M. K. Winson, D. B. Kell and F. Baganz (1998). "Systematic functional analysis of the yeast genome." Trends Biotechnol **16**(9): 373-378.
- Osaki, M., S. Tatebe, A. Goto, H. Hayashi, M. Oshimura and H. Ito (1997). "5-Fluorouracil (5-FU) induced apoptosis in gastric cancer cell lines: role of the p53 gene." Apoptosis **2**(2): 221-226.
- Pan, Z. and D. Raftery (2007). "Comparing and combining NMR spectroscopy and mass spectrometry in metabolomics." Anal Bioanal Chem **387**(2): 525-527.
- Park, J. W., R. S. Kerbel, G. J. Kelloff, J. C. Barrett, B. A. Chabner, D. R. Parkinson, J.
-

- Peck, R. W. Ruddon, C. C. Sigman and D. J. Slamon (2004). "Rationale for biomarkers and surrogate end points in mechanism-driven oncology drug development." Clin Cancer Res **10**(11): 3885-3896.
- Perez, R. P., L. D. Lewis, A. P. Beelen, A. J. Olszanski, N. Johnston, C. H. Rhodes, B. Beaulieu, M. S. Ernstoff and A. Eastman (2006). "Modulation of cell cycle progression in human tumors: a pharmacokinetic and tumor molecular pharmacodynamic study of cisplatin plus the Chk1 inhibitor UCN-01 (NSC 638850)." Clin Cancer Res **12**(23): 7079-7085.
- Picard, F. J. and M. G. Bergeron (2002). "Rapid molecular theranostics in infectious diseases." Drug Discov Today **7**(21): 1092-1101.
- Pike, L. J., X. Han, K. N. Chung and R. W. Gross (2002). "Lipid rafts are enriched in arachidonic acid and plasmenylethanolamine and their composition is independent of caveolin-1 expression: a quantitative electrospray ionization/mass spectrometric analysis." Biochemistry **41**(6): 2075-2088.
- Proskuryakov, S. Y., A. G. Konoplyannikov and V. L. Gabai (2003). "Necrosis: a specific form of programmed cell death?" Exp Cell Res **283**(1): 1-16.
- Puri, V., S. Konda, S. Ranjit, M. Aouadi, A. Chawla, M. Chouinard, A. Chakladar and M. P. Czech (2007). "Fat-specific protein 27, a novel lipid droplet protein that enhances triglyceride storage." J Biol Chem **282**(47): 34213-34218.
- Puri, V., S. Ranjit, S. Konda, S. M. Nicoloso, J. Straubhaar, A. Chawla, M. Chouinard, C. Lin, A. Burkart, S. Corvera, R. A. Perugini and M. P. Czech (2008). "Cidea is associated with lipid droplets and insulin sensitivity in humans." Proc Natl Acad Sci U S A **105**(22): 7833-7838.
- Rainaldi, G., R. Romano, P. Indovina, A. Ferrante, A. Motta, P. L. Indovina and M. T. Santini (2008). "Metabolomics using ¹H-NMR of apoptosis and Necrosis in HL60 leukemia cells: differences between the two types of cell death and independence from the stimulus of apoptosis used." Radiat Res **169**(2): 170-180.
- Ramirez-Zacarias, J. L., F. Castro-Munozledo and W. Kuri-Harcuch (1992). "Quantitation of adipose conversion and triglycerides by staining intracytoplasmic lipids with Oil red O." Histochemistry **97**(6): 493-497.
- Rashed, M. S., M. P. Bucknall, D. Little, A. Awad, M. Jacob, M. Alamoudi, M. Alwattar and P. T. Ozand (1997). "Screening blood spots for inborn errors of metabolism by electrospray tandem mass spectrometry with a microplate batch process and a computer algorithm for automated flagging of abnormal profiles." Clin Chem **43**(7): 1129-1141.
- Rastogi, R. P. and R. P. Sinha (2010). "Apoptosis: molecular mechanisms and pathogenicity."
- Rezzi, S., F. P. Martin, C. Alonso, M. Guilarte, M. Vicario, L. Ramos, C. Martínez, B. Lobo, E. Saperas and J. R. Malagelada (2009). "Metabotyping of biofluids reveals stress-based differences in gut permeability in healthy individuals." Journal of Proteome Research **8**(10): 4799-4809.
- Ritter, J. B., Y. Genzel and U. Reichl (2008). "Simultaneous extraction of several metabolites of energy metabolism and related substances in mammalian cells: optimization using experimental design." Anal Biochem **373**(2): 349-369.
- Roberts, E. and H. M. Bregoff (1953). "Transamination of gamma-aminobutyric acid and beta-alanine in brain and liver." J Biol Chem **201**(1): 393-398.
- Roberts, L. D., S. Virtue, A. Vidal-Puig, A. W. Nicholls and J. L. Griffin (2009). "Metabolic

- phenotyping of a model of adipocyte differentiation." *Physiol Genomics* **39**(2): 109-119.
- Rodolfo, C., F. Ciccocanti, G. D. Giacomo, M. Piacentini and G. M. Fimia (2010). "Proteomic analysis of mitochondrial dysfunction in neurodegenerative diseases." *Expert Rev Proteomics* **7**(4): 519-542.
- Römisch-Margl, W., C. Prehn, R. Bogumil, C. Röhring, K. Suhre and J. Adamski (2012). "Procedure for tissue sample preparation and metabolite extraction for high-throughput targeted metabolomics." *Metabolomics* **8**: 133-142.
- Ron, D. and J. F. Habener (1992). "CHOP, a novel developmentally regulated nuclear protein that dimerizes with transcription factors C/EBP and LAP and functions as a dominant-negative inhibitor of gene transcription." *Genes Dev* **6**(3): 439-453.
- Rosen, E. D. and O. A. MacDougald (2006). "Adipocyte differentiation from the inside out." *Nat Rev Mol Cell Biol* **7**(12): 885-896.
- Rosen, E. D. and B. M. Spiegelman (2000). "Molecular regulation of adipogenesis." *Annu Rev Cell Dev Biol* **16**: 145-171.
- Rosen, E. D. and B. M. Spiegelman (2006). "Adipocytes as regulators of energy balance and glucose homeostasis." *Nature* **444**(7121): 847-853.
- Rosen, E. D., C. J. Walkey, P. Puigserver and B. M. Spiegelman (2000). "Transcriptional regulation of adipogenesis." *Genes Dev* **14**(11): 1293-1307.
- Rosenthal, J., A. Angel and J. Farkas (1974). "Metabolic fate of leucine: a significant sterol precursor in adipose tissue and muscle." *Am J Physiol* **226**(2): 411-418.
- Ross, S. E., R. L. Erickson, I. Gerin, P. M. DeRose, L. Bajnok, K. A. Longo, D. E. Misek, R. Kuick, S. M. Hanash, K. B. Atkins, S. M. Andresen, H. I. Nebb, L. Madsen, K. Kristiansen and O. A. MacDougald (2002). "Microarray analyses during adipogenesis: understanding the effects of Wnt signaling on adipogenesis and the roles of liver X receptor alpha in adipocyte metabolism." *Mol Cell Biol* **22**(16): 5989-5999.
- Rossner, S. (2002). "Obesity: the disease of the twenty-first century." *Int J Obes Relat Metab Disord* **26 Suppl 4**: S2-4.
- Roux, A., D. Lison, C. Junot and J. F. Heilier (2011). "Applications of liquid chromatography coupled to mass spectrometry-based metabolomics in clinical chemistry and toxicology: A review." *Clin Biochem* **44**(1): 119-135.
- Saeed, A. I., V. Sharov, J. White, J. Li, W. Liang, N. Bhagabati, J. Braisted, M. Klapa, T. Currier, M. Thiagarajan, A. Sturn, M. Snuffin, A. Rezantsev, D. Popov, A. Ryltsov, E. Kostukovich, I. Borisovsky, Z. Liu, A. Vinsavich, V. Trush and J. Quackenbush (2003). "TM4: a free, open-source system for microarray data management and analysis." *Biotechniques* **34**(2): 374-378.
- Sakakibara, J., R. Watanabe, Y. Kanai and T. Ono (1995). "Molecular cloning and expression of rat squalene epoxidase." *J Biol Chem* **270**(1): 17-20.
- Sakoda, H., T. Ogihara, M. Anai, M. Funaki, K. Inukai, H. Katagiri, Y. Fukushima, Y. Onishi, H. Ono, M. Fujishiro, M. Kikuchi, Y. Oka and T. Asano (2000). "Dexamethasone-induced insulin resistance in 3T3-L1 adipocytes is due to inhibition of glucose transport rather than insulin signal transduction." *Diabetes* **49**(10): 1700-1708.
- Salomons, G. S., L. A. Smets, M. Verwijs-Janssen, A. A. Hart, E. G. Haarman, G. J. Kaspers, E. V. Wering, A. V. Der Does-Van Den Berg and W. A. Kamps (1999). "Bcl-2 family members in childhood acute lymphoblastic leukemia: relationships with features at presentation, in vitro and in vivo drug response and long-term clinical outcome." *Leukemia* **13**(10): 1574-1580.
- Saltiel, A. R. (2001). "You are what you secrete." *Nature medicine* **7**(8): 887-888.

- Samuelsson, B. (1991). "Arachidonic acid metabolism: role in inflammation." Z Rheumatol **50 Suppl 1**: 3-6.
- Sasada, S., Y. Miyata, Y. Tsutani, N. Tsuyama, T. Masujima, J. Hihara and M. Okada (2013). "Metabolomic analysis of dynamic response and drug resistance of gastric cancer cells to 5-fluorouracil." Oncol Rep **29**(3): 925-931.
- Schena, M., D. Shalon, R. W. Davis and P. O. Brown (1995). "Quantitative monitoring of gene expression patterns with a complementary DNA microarray." Science **270**(5235): 467-470.
- Scherer, P. E., S. Williams, M. Fogliano, G. Baldini and H. F. Lodish (1995). "A novel serum protein similar to C1q, produced exclusively in adipocytes." J Biol Chem **270**(45): 26746-26749.
- Schork, N. J. (1997). "Genetics of complex disease: approaches, problems, and solutions." Am J Respir Crit Care Med **156**(4 Pt 2): S103-109.
- Sellick, C. A., R. Hansen, A. R. Maqsood, W. B. Dunn, G. M. Stephens, R. Goodacre and A. J. Dickson (2009). "Effective quenching processes for physiologically valid metabolite profiling of suspension cultured Mammalian cells." Anal Chem **81**(1): 174-183.
- Serkova, N. and L. G. Boros (2005). "Detection of resistance to imatinib by metabolic profiling: clinical and drug development implications." Am J Pharmacogenomics **5**(5): 293-302.
- Service, R. F. (2012). "Cell biology. Looking for a sugar rush." Science **338**(6105): 321-323.
- Shastri, B. S. (2002). "SNP alleles in human disease and evolution." J Hum Genet **47**(11): 561-566.
- Shepherd, P. R., L. Gnudi, E. Tozzo, H. Yang, F. Leach and B. B. Kahn (1993). "Adipose cell hyperplasia and enhanced glucose disposal in transgenic mice overexpressing GLUT4 selectively in adipose tissue." J Biol Chem **268**(30): 22243-22246.
- Shepherd, P. R. and B. B. Kahn (1999). "Glucose transporters and insulin action--implications for insulin resistance and diabetes mellitus." N Engl J Med **341**(4): 248-257.
- Shimizu, T. (2009). "Lipid mediators in health and disease: enzymes and receptors as therapeutic targets for the regulation of immunity and inflammation." Annu Rev Pharmacol Toxicol **49**: 123-150.
- Smas, C. M. and H. S. Sul (1995). "Control of adipocyte differentiation." Biochem J **309** (Pt 3): 697-710.
- Spalding, K. L., E. Arner, P. O. Westermark, S. Bernard, B. A. Buchholz, O. Bergmann, L. Blomqvist, J. Hoffstedt, E. Naslund, T. Britton, H. Concha, M. Hassan, M. Ryden, J. Frisen and P. Arner (2008). "Dynamics of fat cell turnover in humans." Nature **453**(7196): 783-787.
- Spear, D. H., S. Y. Kutsunai, C. C. Correll and P. A. Edwards (1992). "Molecular cloning and promoter analysis of the rat liver farnesyl diphosphate synthase gene." J Biol Chem **267**(20): 14462-14469.
- Spiegelman, B. M., L. Choy, G. S. Hotamisligil, R. A. Graves and P. Tontonoz (1993). "Regulation of adipocyte gene expression in differentiation and syndromes of obesity/diabetes." J Biol Chem **268**(10): 6823-6826.
- Spiegelman, B. M. and S. R. Farmer (1982). "Decreases in tubulin and actin gene expression prior to morphological differentiation of 3T3 adipocytes." Cell **29**(1): 53-60.
-

- Spiekerkoetter, U., U. Haussmann, M. Mueller, F. ter Veld, M. Stehn, R. Santer and Z. Lukacs (2010). "Tandem mass spectrometry screening for very long-chain acyl-CoA dehydrogenase deficiency: the value of second-tier enzyme testing." J Pediatr **157**(4): 668-673.
- Spratlin, J. L., N. J. Serkova and S. G. Eckhardt (2009). "Clinical applications of metabolomics in oncology: a review." Clin Cancer Res **15**(2): 431-440.
- Sreekumar, A., L. M. Poisson, T. M. Rajendiran, A. P. Khan, Q. Cao, J. Yu, B. Laxman, R. Mehra, R. J. Lonigro, Y. Li, M. K. Nyati, A. Ahsan, S. Kalyana-Sundaram, B. Han, X. Cao, J. Byun, G. S. Omenn, D. Ghosh, S. Pennathur, D. C. Alexander, A. Berger, J. R. Shuster, J. T. Wei, S. Varambally, C. Beecher and A. M. Chinnaiyan (2009). "Metabolomic profiles delineate potential role for sarcosine in prostate cancer progression." Nature **457**(7231): 910-914.
- Stadler, S. C., R. Polanetz, E. M. Maier, S. C. Heidenreich, B. Niederer, P. U. Mayerhofer, F. Lagler, H. G. Koch, R. Santer, J. M. Fletcher, E. Ranieri, A. M. Das, U. Spiekerkotter, K. O. Schwab, S. Potzsch, I. Marquardt, J. B. Hennermann, I. Knerr, S. Mercimek-Mahmutoglu, N. Kohlschmidt, B. Liebl, R. Fingerhut, B. Olgemoller, A. C. Muntau, A. A. Roscher and W. Roschinger (2006). "Newborn screening for 3-methylcrotonyl-CoA carboxylase deficiency: population heterogeneity of MCCA and MCCB mutations and impact on risk assessment." Hum Mutat **27**(8): 748-759.
- Stepczynska, A., K. Lauber, I. H. Engels, O. Janssen, D. Kabelitz, S. Wesselborg and K. Schulze-Osthoff (2001). "Staurosporine and conventional anticancer drugs induce overlapping, yet distinct pathways of apoptosis and caspase activation." Oncogene **20**(10): 1193-1202.
- Steppan, C. M., S. T. Bailey, S. Bhat, E. J. Brown, R. R. Banerjee, C. M. Wright, H. R. Patel, R. S. Ahima and M. A. Lazar (2001). "The hormone resistin links obesity to diabetes." Nature **409**(6818): 307-312.
- Student, A. K., R. Y. Hsu and M. D. Lane (1980). "Induction of fatty acid synthetase synthesis in differentiating 3T3-L1 preadipocytes." J Biol Chem **255**(10): 4745-4750.
- Stunkard, A. J., T. T. Foch and Z. Hrubec (1986). "A twin study of human obesity." JAMA **256**(1): 51-54.
- Stunkard, A. J., T. I. Sorensen, C. Hanis, T. W. Teasdale, R. Chakraborty, W. J. Schull and F. Schulsinger (1986). "An adoption study of human obesity." N Engl J Med **314**(4): 193-198.
- Su, X., X. Han, J. Yang, D. J. Mancuso, J. Chen, P. E. Bickel and R. W. Gross (2004). "Sequential ordered fatty acid alpha oxidation and Delta9 desaturation are major determinants of lipid storage and utilization in differentiating adipocytes." Biochemistry **43**(17): 5033-5044.
- Suhre, K., C. Meisinger, A. Doring, E. Altmaier, P. Belcredi, C. Gieger, D. Chang, M. V. Milburn, W. E. Gall, K. M. Weinberger, H. W. Mewes, M. Hrabce de Angelis, H. E. Wichmann, F. Kronenberg, J. Adamski and T. Illig (2010). "Metabolic footprint of diabetes: a multiplatform metabolomics study in an epidemiological setting." PLoS One **5**(11): e13953.
- Suhre, K., S. Y. Shin, A. K. Petersen, R. P. Mohny, D. Meredith, B. Wagele, E. Altmaier, CardioGram, P. Deloukas, J. Erdmann, E. Grundberg, C. J. Hammond, M. H. de Angelis, G. Kastenmuller, A. Kottgen, F. Kronenberg, M. Mangino, C. Meisinger, T. Meitinger, H. W. Mewes, M. V. Milburn, C. Prehn, J. Raffler, J. S. Ried, W. Romisch-Margl, N. J. Samani, K. S. Small, H. E. Wichmann, G. Zhai, T. Illig, T. D. Spector, J.

- Adamski, N. Soranzo and C. Gieger (2011). "Human metabolic individuality in biomedical and pharmaceutical research." Nature **477**(7362): 54-60.
- Suryawan, A., J. W. Hawes, R. A. Harris, Y. Shimomura, A. E. Jenkins and S. M. Hutson (1998). "A molecular model of human branched-chain amino acid metabolism." Am J Clin Nutr **68**(1): 72-81.
- Szeliga, M. and M. Obara-Michlewska (2009). "Glutamine in neoplastic cells: focus on the expression and roles of glutaminases." Neurochem Int **55**(1-3): 71-75.
- Takatani, T., K. Takahashi, Y. Uozumi, E. Shikata, Y. Yamamoto, T. Ito, T. Matsuda, S. W. Schaffer, Y. Fujio and J. Azuma (2004). "Taurine inhibits apoptosis by preventing formation of the Apaf-1/caspase-9 apoptosome." Am J Physiol Cell Physiol **287**(4): C949-953.
- Taschler, U., F. P. Radner, C. Heier, R. Schreiber, M. Schweiger, G. Schoiswohl, K. Preiss-Landl, D. Jaeger, B. Reiter, H. C. Koefeler, J. Wojciechowski, C. Theussl, J. M. Penninger, A. Lass, G. Haemmerle, R. Zechner and R. Zimmermann (2011). "Monoglyceride lipase deficiency in mice impairs lipolysis and attenuates diet-induced insulin resistance." J Biol Chem **286**(20): 17467-17477.
- Teng, Q., W. Huang, T. Collette, D. Ekman and C. Tan (2009). "A direct cell quenching method for cell-culture based metabolomics." Metabolomics **5**(2): 199-208.
- Teng, Q., W. Huang, T. W. Collette, D. R. Ekman and C. Tan (2009). "A direct cell quenching method for cell-culture based metabolomics." Metabolomics **5**(2): 199-208.
- Thomas, J., T. Shentu and D. K. Singh Cholesterol: Biosynthesis, Functional Diversity, Homeostasis and Regulation by Natural Products. D. Ekin.
- Tint, G. S., M. Seller, R. Hughes-Benzie, A. K. Batta, S. Shefer, D. Genest, M. Irons, E. Elias and G. Salen (1995). "Markedly increased tissue concentrations of 7-dehydrocholesterol combined with low levels of cholesterol are characteristic of the Smith-Lemli-Opitz syndrome." J Lipid Res **36**(1): 89-95.
- Tischler, M. E. and A. L. Goldberg (1980). "Amino acid degradation and effect of leucine on pyruvate oxidation in rat atrial muscle." Am J Physiol **238**(5): E480-486.
- Tischler, M. E. and A. L. Goldberg (1980). "Leucine degradation and release of glutamine and alanine by adipose tissue." J Biol Chem **255**(17): 8074-8081.
- Tong, Q., J. Tsai, G. Tan, G. Dalgin and G. S. Hotamisligil (2005). "Interaction between GATA and the C/EBP family of transcription factors is critical in GATA-mediated suppression of adipocyte differentiation." Mol Cell Biol **25**(2): 706-715.
- Tontonoz, P., E. Hu and B. M. Spiegelman (1994). "Stimulation of adipogenesis in fibroblasts by PPAR gamma 2, a lipid-activated transcription factor." Cell **79**(7): 1147-1156.
- Torres, N., C. Vargas, R. Hernandez-Pando, H. Orozco, S. M. Hutson and A. R. Tovar (2001). "Ontogeny and subcellular localization of rat liver mitochondrial branched chain amino-acid aminotransferase." Eur J Biochem **268**(23): 6132-6139.
- Tukiainen, T., T. Tynkkynen, V. P. Makinen, P. Jylanki, A. Kangas, J. Hokkanen, A. Vehtari, O. Grohn, M. Hallikainen, H. Soininen, M. Kivipelto, P. H. Groop, K. Kaski, R. Laatikainen, P. Soininen, T. Pirttila and M. Ala-Korpela (2008). "A multi-metabolite analysis of serum by 1H NMR spectroscopy: early systemic signs of Alzheimer's disease." Biochem Biophys Res Commun **375**(3): 356-361.
- Tusher, V. G., R. Tibshirani and G. Chu (2001). "Significance analysis of microarrays applied to the ionizing radiation response." Proc Natl Acad Sci U S A **98**(9): 5116-5121.
- Tvrđik, P., R. Westerberg, S. Silve, A. Asadi, A. Jakobsson, B. Cannon, G. Loison and

- A. Jacobsson (2000). "Role of a new mammalian gene family in the biosynthesis of very long chain fatty acids and sphingolipids." The Journal of cell biology **149**(3): 707-718.
- Usenius, J. P., S. Tuohimetsa, P. Vainio, M. Ala-Korpela, Y. Hiltunen and R. A. Kauppinen (1996). "Automated classification of human brain tumours by neural network analysis using in vivo ¹H magnetic resonance spectroscopic metabolite phenotypes." Neuroreport **7**(10): 1597-1600.
- Van Gulik, W. M., A. B. Canelas, H. Taymaz-Nikerel, R. D. Douma, L. P. de Jonge and J. J. Heijnen (2012). "Fast sampling of the cellular metabolome." Methods Mol Biol **881**: 279-306.
- Vance, D. E. and J. E. Vance (2002). Biochemistry of lipids, lipoproteins, and membranes. Amsterdam ; Boston, Elsevier.
- Vance, D. E. and J. E. Vance (2008). Biochemistry of lipids, lipoproteins and membranes. Amsterdam ; Boston, Elsevier.
- Vidal-Puig, A., M. Jimenez-Linan, B. B. Lowell, A. Hamann, E. Hu, B. Spiegelman, J. S. Flier and D. E. Moller (1996). "Regulation of PPAR gamma gene expression by nutrition and obesity in rodents." J Clin Invest **97**(11): 2553-2561.
- Villas-Boas, S. G., J. Hojer-Pedersen, M. Akesson, J. Smedsgaard and J. Nielsen (2005). "Global metabolite analysis of yeast: evaluation of sample preparation methods." Yeast **22**(14): 1155-1169.
- Wagle, S. R., H. P. Morris and G. Weber (1963). "Comparative Biochemistry of Hepatomas. V. Studies on Amino Acid Incorporation in Liver Tumors of Different Growth Rates." Cancer Res **23**: 1003-1007.
- Wagner, J. A. (2002). "Overview of biomarkers and surrogate endpoints in drug development." Dis Markers **18**(2): 41-46.
- Wahl, S., Z. Yu, M. Kleber, P. Singmann, C. Holzapfel, Y. He, K. Mittelstrass, A. Polonikov, C. Prehn, W. Romisch-Margl, J. Adamski, K. Suhre, H. Grallert, T. Illig, R. Wang-Sattler and T. Reinehr (2012). "Childhood obesity is associated with changes in the serum metabolite profile." Obes Facts **5**(5): 660-670.
- Wanders, R. J., G. A. Jansen and M. D. Lloyd (2003). "Phytanic acid alpha-oxidation, new insights into an old problem: a review." Biochim Biophys Acta **1631**(2): 119-135.
- Wang-Sattler, R., Y. Yu, K. Mittelstrass, E. Lattka, E. Altmaier, C. Gieger, K. H. Ladwig, N. Dahmen, K. M. Weinberger and P. Hao (2008). "Metabolic profiling reveals distinct variations linked to nicotine consumption in humans—First results from the KORA study." PLoS One **3**(12): e3863.
- Wang-Sattler, R., Y. Yu, K. Mittelstrass, E. Lattka, E. Altmaier, C. Gieger, K. H. Ladwig, N. Dahmen, K. M. Weinberger, P. Hao, L. Liu, Y. Li, H. E. Wichmann, J. Adamski, K. Suhre and T. Illig (2008). "Metabolic profiling reveals distinct variations linked to nicotine consumption in humans--first results from the KORA study." PLoS One **3**(12): e3863.
- Wang-Sattler, R., Z. Yu, C. Herder, A. C. Messias, A. Floegel, Y. He, K. Heim, M. Campillos, C. Holzapfel, B. Thorand, H. Grallert, T. Xu, E. Bader, C. Huth, K. Mittelstrass, A. Doring, C. Meisinger, C. Gieger, C. Prehn, W. Roemisch-Margl, M. Carstensen, L. Xie, H. Yamanaka-Okumura, G. Xing, U. Ceglarek, J. Thiery, G. Giani, H. Lickert, X. Lin, Y. Li, H. Boeing, H. G. Joost, M. H. de Angelis, W. Rathmann, K. Suhre, H. Prokisch, A. Peters, T. Meitinger, M. Roden, H. E. Wichmann, T. Pischon, J. Adamski and T. Illig (2012). "Novel biomarkers for pre-diabetes identified by metabolomics." Mol Syst Biol **8**: 615.
- Wang, L., J. E. Manson, J. E. Buring, I. M. Lee and H. D. Sesso (2008). "Dietary intake

- of dairy products, calcium, and vitamin D and the risk of hypertension in middle-aged and older women." Hypertension **51**(4): 1073-1079.
- Wang, T. J., M. G. Larson, R. S. Vasan, S. Cheng, E. P. Rhee, E. McCabe, G. D. Lewis, C. S. Fox, P. F. Jacques, C. Fernandez, C. J. O'Donnell, S. A. Carr, V. K. Mootha, J. C. Florez, A. Souza, O. Melander, C. B. Clish and R. E. Gerszten (2011). "Metabolite profiles and the risk of developing diabetes." Nat Med **17**(4): 448-453.
- Ward, T. H., J. Cummings, E. Dean, A. Greystoke, J. M. Hou, A. Backen, M. Ranson and C. Dive (2008). "Biomarkers of apoptosis." Br J Cancer.
- Warensjo, E., E. Ingelsson, P. Lundmark, L. Lannfelt, A. C. Syvanen, B. Vessby and U. Riserus (2007). "Polymorphisms in the SCD1 gene: associations with body fat distribution and insulin sensitivity." Obesity (Silver Spring) **15**(7): 1732-1740.
- Warskulat, U., E. Borsch, R. Reinehr, B. Heller-Stilb, C. Roth, M. Witt and D. Haussinger (2007). "Taurine deficiency and apoptosis: findings from the taurine transporter knockout mouse." Arch Biochem Biophys **462**(2): 202-209.
- Weisfeld-Adams, J. D., M. A. Morrissey, B. M. Kirmse, B. R. Salveson, M. P. Wasserstein, P. J. McGuire, S. Sunny, J. L. Cohen-Pfeffer, C. Yu, M. Caggana and G. A. Diaz (2010). "Newborn screening and early biochemical follow-up in combined methylmalonic aciduria and homocystinuria, cblC type, and utility of methionine as a secondary screening analyte." Mol Genet Metab **99**(2): 116-123.
- Weljie, A. M., J. Newton, P. Mercier, E. Carlson and C. M. Slupsky (2006). "Targeted profiling: quantitative analysis of 1H NMR metabolomics data." Anal Chem **78**(13): 4430-4442.
- Wendel, U. (1989). "Abnormality of odd-numbered long-chain fatty acids in erythrocyte membrane lipids from patients with disorders of propionate metabolism." Pediatr Res **25**(2): 147-150.
- Wenk, M. R. (2005). "The emerging field of lipidomics." Nat Rev Drug Discov **4**(7): 594-610.
- White, U. A. and J. M. Stephens (2010). "Transcriptional factors that promote formation of white adipose tissue." Mol Cell Endocrinol **318**(1-2): 10-14.
- White, U. A. and J. M. Stephens (2010). "Transcriptional factors that promote formation of white adipose tissue." Molecular and cellular endocrinology **318**(1): 10-14.
- Williams, E. S., A. Baylin and H. Campos (2007). "Adipose tissue arachidonic acid and the metabolic syndrome in Costa Rican adults." Clin Nutr **26**(4): 474-482.
- Williams, J. A. (2011). Predictive approaches in drug discovery and development : biomarkers and in vitro/in vivo correlations. Hoboken, N.J., Wiley.
- Williams, M. D. and G. M. Mitchell (2012). "MicroRNAs in insulin resistance and obesity." Exp Diabetes Res **2012**: 484696.
- Williams, S. N., M. L. Anthony and K. M. Brindle (1998). "Induction of apoptosis in two mammalian cell lines results in increased levels of fructose-1,6-bisphosphate and CDP-choline as determined by 31P MRS." Magn Reson Med **40**(3): 411-420.
- Williamson, J., J. Goldman and K. S. Marder (2009). "Genetic aspects of Alzheimer disease." Neurologist **15**(2): 80-86.
- Winder, C. L., W. B. Dunn, S. Schuler, D. Broadhurst, R. Jarvis, G. M. Stephens and R. Goodacre (2008). "Global metabolic profiling of Escherichia coli cultures: an evaluation of methods for quenching and extraction of intracellular metabolites." Anal Chem **80**(8): 2939-2948.
- Wolk, A., M. Furuheim and B. Vessby (2001). "Fatty acid composition of adipose tissue

- and serum lipids are valid biological markers of dairy fat intake in men." J Nutr **131**(3): 828-833.
- Wolk, A., G. Gridley, M. Svensson, O. Nyren, J. K. McLaughlin, J. F. Fraumeni and H. O. Adam (2001). "A prospective study of obesity and cancer risk (Sweden)." Cancer Causes Control **12**(1): 13-21.
- Wu, Z., N. L. Bucher and S. R. Farmer (1996). "Induction of peroxisome proliferator-activated receptor gamma during the conversion of 3T3 fibroblasts into adipocytes is mediated by C/EBPbeta, C/EBPdelta, and glucocorticoids." Mol Cell Biol **16**(8): 4128-4136.
- Xie, B., M. J. Waters and H. J. Schirra (2012). "Investigating potential mechanisms of obesity by metabolomics." J Biomed Biotechnol **2012**: 805683.
- Xue, L. Y., S. M. Chiu and N. L. Oleinick (2003). "Staurosporine-induced death of MCF-7 human breast cancer cells: a distinction between caspase-3-dependent steps of apoptosis and the critical lethal lesions." Exp Cell Res **283**(2): 135-145.
- Yanagida, M. (2002). "Functional proteomics; current achievements." J Chromatogr B Analyt Technol Biomed Life Sci **771**(1-2): 89-106.
- Yang, W., T. Kelly and J. He (2007). "Genetic epidemiology of obesity." Epidemiol Rev **29**: 49-61.
- Yu, Z., G. Zhai, P. Singmann, Y. He, T. Xu, C. Prehn, W. Romisch-Margl, E. Lattka, C. Gieger, N. Soranzo, J. Heinrich, M. Standl, E. Thiering, K. Mittelstrass, H. E. Wichmann, A. Peters, K. Suhre, Y. Li, J. Adamski, T. D. Spector, T. Illig and R. Wang-Sattler (2012). "Human serum metabolic profiles are age dependent." Aging Cell **11**(6): 960-967.
- Zhou, J., B. Xu, J. Huang, X. Jia, J. Xue, X. Shi, L. Xiao and W. Li (2009). "1H NMR-based metabolomic and pattern recognition analysis for detection of oral squamous cell carcinoma." Clin Chim Acta **401**(1-2): 8-13.
- Zimmet, P., K. G. Alberti and J. Shaw (2001). "Global and societal implications of the diabetes epidemic." Nature **414**(6865): 782-787.

7 ACKNOWLEDGEMENTS

A lot of people had a direct and indirect impact on this work. I would like to take this opportunity to thank all of them for their assistance, effort and cooperation, which made the completion of this work possible.

Foremost, I would like to thank Prof. Jerzy Adamski for giving me the opportunity to perform this work in his laboratories. Thank you for the scientific support, fruitful and helpful discussion, which were essential for the success of this thesis. Dziękuję Profesorze za udzielone zaufanie, dużą wolność w prowadzeniu badań, a także za dodawanie otuchy wtedy kiedy wszystko wydawało się czarne.

Special thanks to Prof. Karsten Suhre for his scientific support: for listening to all problems, fruitful discussions and giving helpful advises.

I would like to thank Prof. Hans Hauner for supervising this thesis in the Center of Life and Food Sciences, Weihenstephan TUM.

I am very grateful to Dr. Gabriele Möller for her continuous advice and discussion, esp. that she never gave up during reading and correcting of my abstracts, manuscripts and finally my PhD work - thank you a lot!

The completion of my thesis work would not have been possible without cooperation. I am deeply grateful to Dr. Johannes Beckers for providing access to his facilities for transcriptomics study. Dr. Marion Horsch I would like to acknowledge for her great assistance during transcriptomics experiments and precious elaboration of those data sets. A great thank to Gabi Kastenmüller for her huge involvement in the statistical analysis of metabolomics data and explaining me what the PCA actually is 😊.

I want to thank Dr. Anna Artati for being a friend and a teacher. I would like to thank Dr. Cornelia Prehn for the initiation into the world of mass spectrometry. Thanks to Julia Scarpa for always finding a place and made measurements of my samples on the kit plates possible. To Katarina Sckell, I am grateful for her excellent support during preparation of thousands of samples and for each “coffee” breaks ;) A great thank to Gabi Zieglmeier being very supportive during my experimental work and also for

continuously listening, reading my mind or “just” being there if something went wrong. A big thank to Marion Schieweg for coffee support and coffee breaks. I am also grateful to Bianca Schmick and Andrea Nefzger for their ... technical assistance.

Many thanks to Caro, Ferdi, Janina, Mark, Susane and Tobi for all the fun we had and so much more. Special Thank to Sven Zukunft for being the best sparring partner in Kung Fu ;) I ever had. Najserdeczniejsze podziękowania dla Pauliny Banachowicz za współpracę przy projekcie HSD17B1, cierpliwość do mojego pesymizmu oraz za wiele wyjątkowo miłych i zabawnych momentów! Special thanks to Markus for Tea time☺

I would like to thank all my friends for their support and never ending encouragement. Many thanks to the “SestoSenso crew” for each Saturday! A big thank to Dr. Marianna Lucio for believing in me and for the many precious memories. Special thanks to Dr. Verena Russ for being supportive and for always listening - thank you for so many reasons! Many thanks to Helmut, Rosi and Winfried for their support.

Serdecznie dziękuję mojej rodzinie za obecność podczas mojej drogi. Dziękuję moim ukochanym rodzicom, którzy pięknie pokazali mi świat i nauczyli mnie marzyć. Serdecznie dziękuję Ani i Andrzejowi za szczerą wiarę w powodzenie wtedy kiedy mi jej brakowało. Mojej ukochanej Babci Zosi i Babci Halince za troskę. Mojemu Bratu, Mariannie i Selinie za nieocenioną pomoc podczas mojego przyjazdu i pobytu w Monachium.

Serdecznie dziękuję Michałowi, który jest niezwykłym towarzyszem podróży. Dziękuję Ci za Twój spokój podczas mojego niepokoju, za cierpliwość do sprawdzania i naprawiania błędów, które popełniłam we wszystkich do tej pory napisanych pracach!

8 LEBENS LAUF

Persönliche Angaben

- | | |
|------------------------|------------|
| 1. Nachname | Halama |
| 2. Vorname | Anna |
| 3. Geburtsdatum | 19.09.1984 |
| 4. Staatsangehörigkeit | Polnisch |
| 5. Ausbildung | |

- | | |
|----------------------------|---|
| ab 2009 | Promotionsstudium TU München |
| 05.2009 – 05.2013 | Wissenschaftlicher Mitarbeiter an der Helmholtz Zentrum München |
| 10.2008 | Abschluss Diplom, Ingenieur-Biotechnologie of Technische Universität Breslau, Polen; Studium der Biotechnologie |
| 10.2007 – 10.2008 | Ludwig-Maximilians-Universität, München; Pharmazeutische Biologie - Biotechnologie (Exchange Student) |
| 10.2003 – 10.2008 | Technische Universität Breslau, Polen; Studium der Biotechnologie Schwerpunkt Pharmazeutische Biotechnologie und der Nebenfächer Biochemie, organische Chemie, Zellbiologie |
| 6. Titel der Dissertation: | Analysen metabolischer Stoffwechselwege von zellulären Prozessen in Apoptose und Adipogenese |
| 7. Betreuung | Prof. Dr. Jerzy Adamski |